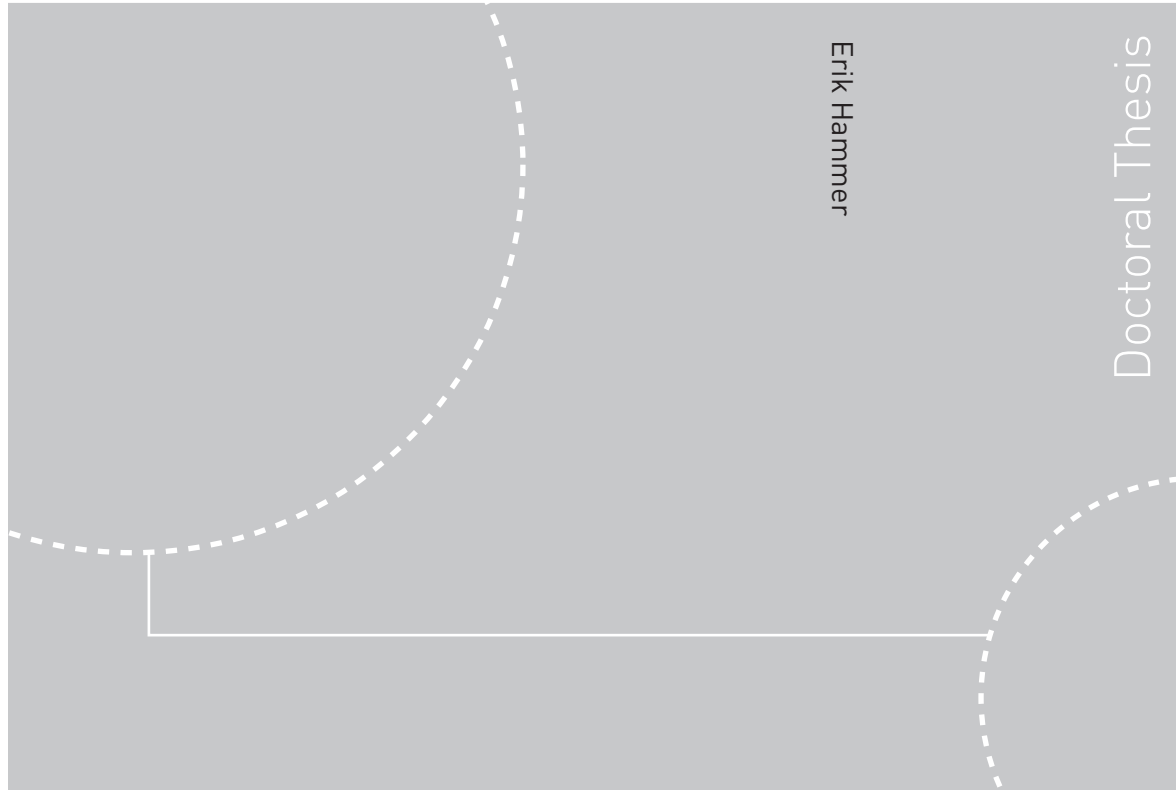


Doctoral theses at NTNU, 2010.242

Erik Hammer

Sedimentological Correlation of Heterogeneous Reservoir Rocks: Effects of Lithology, Differential Compaction and Diagenetic Processes



ISBN 978-82-471-2478-9 (printed ver.)
ISBN 978-82-471-2478-9 (electronic ver.)
ISSN 1503-8181

Doctoral theses at NTNU, 2010.242

NTNU
Norwegian University of
Science and Technology
Thesis for the degree of
philosophiae doctor
Faculty of Engineering Science and Technology
Department of Geology and Mineral Resources Engineering

 **NTNU**
Norwegian University of
Science and Technology

 **NTNU**

 **NTNU**
Norwegian University of
Science and Technology

Erik Hammer

Sedimentological Correlation of Heterogeneous Reservoir Rocks: Effects of Lithology, Differential Compaction and Diagenetic Processes

Thesis for the degree of philosophiae doctor

Trondheim, December 2010

Norwegian University of
Science and Technology
Faculty of Engineering Science and Technology
Department of Geology and Mineral Resources Engineering



NTNU

Norwegian University of
Science and Technology

NTNU

Norwegian University of Science and Technology

Thesis for the degree of philosophiae doctor

Faculty of Engineering Science and Technology
Department of Geology and Mineral Resources Engineering

©Erik Hammer

ISBN 978-82-471-2478-9 (printed ver.)

ISBN 978-82-471-2478-9 (electronic ver.)

ISSN 1503-8181

Doctoral Theses at NTNU, 2010.242

Printed by Tapir Uttrykk

Sedimentological Correlation of Heterogeneous Reservoir
Rocks: Effects of Lithology, Differential Compaction and
Diagenetic Processes

Erik Hammer

December 13, 2010

To my late brother

Preface

The work presented in this thesis was conducted at the Department of Geology and Mineral Resources Engineering (IGB) at the University of Science and Technology (NTNU) in Trondheim during the period 2003-2010. The supervisors for the project was Professor Mai Britt E. Mørk and Associate Professor Sverre Ola Johnsen at IGB and Dr. Arve Næss at Statoil E&P Norway, Stjørdal. The project was initiated by Dr. Arve Næss as a part of a large reservoir characterization project in Statoil where they wanted to elucidate the effects of differential compaction in heterogeneous fluviodeltaic reservoir rocks. The following chapters and papers are the result of collaboration between myself and several contributors and I especially want to express my gratitude to the following persons, companies and partners for their support, guidance, funding and fruitful discussions during the course of this research project: First and foremost, thanks to my supervisor Mai Britt E. Mørk for her invaluable support, both personal and professional. She has shown patience, as well as contributed actively in discussions, scientific research, article writing and document perusals. I also want to thank Arve Næss who has been my contact person to Statoil. His ability to see the industrial benefits and usefulness of the research results has been of great importance. Thanks also to Sverre Ola Johnsen for fruitful discussions and for the valuable field experience I have received during many of our field excursions. Last but not least my Ph.D.-colleagues for fruitful discussions around the coffee table.

Erik Hammer

Abstract

Correlation of reservoir rocks is a challenge in many types of reservoirs around the world today. In a time where the focus has slowly shifted away from the giant fields, towards development of smaller, more marginal fields, the importance of addressing these challenges is increasing. The purpose of the thesis is to investigate the effects of lithology, diagenesis and differential compaction on correlation of reservoir architecture in a fluvio-deltaic reservoir. To be able to address these issues several types of data, including seismic, core sections and petrophysical wireline logs, have been subjected to measurements, calculations and interpretations to be able to construct a sedimentological and sequence stratigraphic framework based on a reservoir reconstruction workflow.

First, the regional and local (field wide) geological evolution for the Åre Formation in the Heidrun Field, offshore Mid-Norway, is elucidated, including evolution of the palaeo-depositional environment and the prevailing depositional controlling factors. These studies included a facies description of studied wells based on core and wireline log data, and description/interpretation of the reservoir sequence stratigraphy. From these studies eight facies associations have been identified and described, indicating a fluvial-deltaic depositional environment. A sequence stratigraphic model based on these facies associations is suggested for the studied well data and includes five candidate sequence boundaries and eight flooding surfaces, including a marine flooding surface. Four of these surfaces are interpreted as allogenic, suggesting regional base level change, whereas the remaining nine surfaces are suggested as resulting from local, autogenic factors.

Next, the compactability of the identified facies associations was quantified in a diage-

nesis study using optical microscopy, SEM micro-probe measurements and XRD analyses. The paragenetic sequence proposed suggests that abundant early siderite cement has influenced the compactability of fine-grained deltaic siltstones. Eogenetic meteoric flushing led to leaching of detrital feldspar and precipitation of authigenic kaolinite in the fluvial part of the succession. Other cements include calcite, ankerite and Fe-dolomite which are interpreted as predominantly mesogenetic and of less importance regarding compaction. However, a persistent calcite cemented interval is suggested to be related to a flooding regional event and may therefore have sequence stratigraphic significance.

In a reservoir reconstruction study, data on lithofacies compactability and sequence stratigraphic surfaces (i.e. flooding surfaces) were combined to perform differential decompaction of the reservoir in a sequential re-burial exercise. A methodology for reservoir reconstruction is proposed based on porosity reduction vs burial for identified lithofacies classes and the application of flooding surfaces as backstripping surfaces. Based on correlation on decompacted sediment cross-sections, new horizons are identified within the lower part of the Åre Fm. (Åre 1-3.3), an interval suggested to have been subjected to large differential compaction effects due to abundant coals. These surfaces includes several local flooding surfaces related to coals, in addition to laterally correlatable channel sandstone units. The method is flexible and performed for each depth interval (15cm resolution) throughout the well.

As the proposed method is applied on real wireline log data, some sources of error are related to the manual interpretation of lithofacies classes, constituting the building blocks for the proposed model. An attempt is therefore made to interpret within lithological heterogeneities based on multivariate statistical techniques. Unstructured and structured principal component analysis has been applied to five wireline log variables (GR, NPFI, RHOB, RT, DT). The results indicate a clear beneficial potential of improving the differentiation between different lithological and depositional units by extracting small scale heterogeneities.

Contents

Preface	iii
Abstract	iv
Contribution to articles	xii
Paper I	xii
Paper II	xii
Paper III	xii
I Prelude	1
1 General introduction	3
1.1 Rationale	3
1.1.1 Hydrocarbon account	5
1.2 Objectives and approach	6
1.3 Research methods	9
1.4 Funding	12
1.5 Outline of the thesis	12
1.6 Summary of main results	13
1.6.1 Chapters 2 to 4	13
1.6.2 Paper I - Facies controls on the distribution of diagenesis and com- paction in fluviodeltaic deposits.	14

1.6.3	Paper II - Reconstruction of Heterogeneous Reservoir Architecture based on Differential Decompaction in Sequential Re-burial modelling.	16
1.6.4	Paper III - A comparison of unstructured and structured principal component analyses and their interpretation.	17
II The geology of the Haltenbanken region, the Heidrun Field and the Åre Formation		19
2	Regional geological evolution	21
2.1	Introduction	21
2.2	Tectonic evolution of Haltenbanken region	21
2.3	Sedimentological and paleogeographic evolution	28
3	Sedimentological interpretation of the Åre Fm.	35
3.1	Introduction	35
3.2	Previous work on the Åre Fm., Heidrun Field	36
3.3	Comments regarding chronostratigraphy and ichnofacies.	37
3.4	Present study; identified facies associations	38
3.4.1	Stacked, multi-storey channel facies association (MFCH)	41
3.4.2	Single storey channel facies association (SFCH)	43
3.4.3	Floodplain fines facies association (FF)	45
3.4.4	Crevasse facies association (CCH)	49
3.4.5	Bay fill facies association (SBF/MBF)	50
3.4.6	Tidally influenced distributary channel facies association (TCH)	52
3.4.7	Transgressive shallow marine shoreface facies association (TSMS)	55
3.5	Discussion on MFCH and their driving mechanisms	55
4	Stratigraphy in fluvial deposits	71
4.1	Base level changes and their controlling factors	72
4.1.1	Controlling factors; allogenic vs. autogenic	73

4.1.2	Allogenic factors	73
4.1.3	Autogenic factors	76
4.1.4	Summary	79
4.2	Compaction controls on autocyclisity	79
4.3	Sequence stratigraphic analysis of the Åre Fm.	82
4.3.1	Åre 1	83
4.3.2	Åre 2	84
4.3.3	Åre 3	90
4.3.4	Åre 4	93
4.3.5	Åre 5.1	96
4.3.6	Åre 5.2 - 6	96
4.3.7	Åre 7	98
4.4	Summary	100
References		119
III Papers		137
	Paper I	
	Paper II	
	Paper III	
IV Appendices		i
A Conference Contributions		
B Methods and Material		

List of Figures

1.1	Location of study area	7
1.2	Fields on the Halten Terrace	8
1.3	Thesis outline	11
2.1	Structural elements of the Haltenbanken region and the Heidrun Field . . .	23
2.2	Cross-section of the Mid-Norwegian continental shelf.	24
2.3	Top Åre reservoir structure	25
2.4	Seismic cross-section	26
2.5	Calculated burial curve	28
2.6	Stratigraphic compilation of the Mid-Norwegian continental shelf	29
2.7	Schematic Rhaetian-Early Jurassic reconstruction	30
2.8	Palaeolatitudinal drift of the Heidrun Field	32
3.1	Core coverage of the Åre Fm.	40
3.2	Log signatures and core examples of multi-storey channel (MFCH)	43
3.3	Channel aggradation due to peat compaction	44
3.4	Log signatures and core examples of single-storey channel (SFCH)	46
3.5	Log signatures and core examples of floodplain fines (FF)	48
3.6	Log signatures and core examples of sandy (SBF) and muddy (MBF)	53
3.7	Log signatures and core examples of tidally influenced channel (TCH)	54
3.8	Log signatures and core examples of transgressive shallow marine shoreface deposits (TSMS)	56
3.9	Decompacted sand coal relationships	58

3.10	Anastomosing river deposits	60
3.11	Core photos	62
3.12	Core photos	63
3.13	Core photos	64
3.14	Core photos	65
3.15	Core photos	66
3.16	Core photos	67
3.17	Core photos	68
3.18	Core photos	69
3.19	Sedimentological core description	70
4.1	Time-lines in fluvial deposits	80
4.2	Nature and variability of coal marker	85
4.3	Bubble maps of Åre 1 and 2.1 facies distribution	86
4.4	Base level change	88
4.5	Nature and signature of interpreted flooding surface	90
4.6	Bubblemap of zones 4.1-4.4	94
4.7	Bubble maps of Åre facies distribution	100
4.8	Stacked palaeogeography of the Åre Fm.	103
4.9	NS correlation panel	104
4.10	NS correlation panel	105
4.11	Cross-section legend	106
4.12	Cross-section 1	107
4.13	Cross-section 2	108
4.14	Cross-section 3	109
4.15	Cross-section 4	110
4.16	Cross-section 5	111
4.17	Cross-section 6	112
4.18	Cross-section 7	113

4.19	Cross-section 8	114
4.20	Cross-section 9	115
4.21	Cross-section 10	116
4.22	Cross-section 11	117
4.23	Cross-section 12	118
25	XRD diffractograms	xviii

List of Tables

3.1	Biostratigraphy	39
4.1	Effects of autogenic and allogenic factors	77
2	Wells and well coverage	vi
3	Modal analysis	viii
4	SEM standards	xiii
5	SEM Microprobe measurements	xiv
6	Well Log properties	xxii
7	Well depth and thickness definitions	xxii

Contribution to articles

The presented papers are based on projects that have involved collaboration with other people. The contributions to the papers are therefore given below:

Paper I

Facies controls on the distribution of diagenesis and compaction in fluvial-deltaic deposits. HAMMER E., MØRK, M.B.E. AND NÆSS, A. 2010. Hammer carried out the experimental work, described and interpreted the results and wrote the paper. Mørk provided guidance with the approach to the topic and discussion of diagenetic processes. She also contributed in the experimental work and assisted in the writing of the paper. Næss provided background information regarding the study area and studied interval (Åre Fm.) and helped in the acquisition of data and sample material. He also organized for the use of Statoil facilities and software.

Paper II

Reconstruction of Heterogeneous Reservoir Architecture based on Differential Decompaction in Sequential Re-burial modelling. HAMMER E., BRANDSEGG K.B., MØRK, M.B.E. AND NÆSS, A 2010. Hammer performed the review of the methodology, wrote the paper and performed the geological interpretations. Brandsegg performed all the programming. He also carried out perusals of the paper and contributed with general comments and discussion of the results. Næss defined the problem of the study and assisted with ideas for the backstripping methodology. Mørk performed perusals and comments of the paper.

Paper III

A comparison of unstructured and structured principal component analyses and their interpretation. BRANDSEGG K.B., HAMMER E. AND SINDING-LARSEN, R. 2009. Brandsegg wrote the paper and performed the calculations. He also carried out the

review of the methodology. Hammer carried out the preliminary interpretation of the data for application in the calculations. He also performed perusals of the paper and contributed with interpretations and discussions of the results. Sinding-Larsen defined/identified the approach and performed perusals of the paper, and contributed with ideas and discussions.

Part I

Prelude

Chapter 1

General introduction

1.1 Rationale

Heterogeneous sandstone formations are important petroleum reservoirs offshore Norway both in the North Sea and in the Norwegian Sea. Such reservoirs will be of increasing economic importance in the future as the focus will shift from the giant fields and large continuous reservoirs to the smaller more complex reservoirs comprising heterogeneous reservoir intervals. Heterogeneous sandstone formations are sandstone-dominated successions interbedded with other lithologies such as silt, clay and coal in various scales and spatial relations. In addition, diagenetic processes acting on the sediments from the time of transport and deposition to the consecutive burial have altered the original deposits by dissolution of framework grains and precipitation of pore filling and/or replacive authigenic minerals. Such effects further amplify the variability in reservoir properties and therefore offer particular challenges for optimal petroleum production, such as quantifying in-place petroleum resources, predicting fluid flow units, locating barriers to fluid migration in addition to well configuration.

The petroleum reservoirs offshore Norway are located subsurface commonly at 2-5km burial depth, and knowledge of their internal structure and complexity relies on geological interpretations based on advanced geophysical tools as well as petrophysical data, geologi-

cal descriptions from wells and core materials, and onshore analogue outcrops. As the well data cover very limited volumes (~ 15 cm diameter boreholes located hundreds of meters or kilometers apart), data interpretation and upscaling based on geological/sedimentological knowledge are important tasks. This is further emphasized when conventional seismics also fail to portray the intervals of interest with respect to correlation. Examples of complex heterogeneous siliciclastic reservoirs are the continental-paralic deposits of Triassic and Lower Jurassic ages that are producing both in the North Sea (e.g. Statfjord Fm. Snorre Field) and in the Norwegian Sea at Haltenbanken (e.g. Åre Fm. Heidrun Field).

Due to limited seismic resolution (10-100m scale), in addition to complex density (impedance) variations, due to e.g. coal and cemented intervals, conventional seismic techniques fail to provide the detailed reservoir architecture necessary for reservoir scale correlation.

Sandstone correlation is crucial when concerning the understanding of siliciclastic reservoir flow properties and reservoir architecture description. In heterogeneous reservoir cases, such correlation relies on detailed sedimentological facies interpretation and stratigraphic analysis (e.g. Pedersen et al., 1989). In addition, reservoir properties of deeply buried sediments have also been modified by processes taking place after deposition, during burial of the sediments. These processes cause sediment compaction and chemical diagenesis, leading to consolidation and reduction in porosity and permeability, or to chemical dissolution, influencing reservoir properties in various ways (e.g. Aplin et al., 1993; Fisher et al., 1999; Bjørlykke, 1998; Bjørlykke and Høeg, 1997; Bjørlykke et al., 1986). Compaction and types of chemical diagenesis reduce porosity and increase formation density and thus influence the petrophysical and seismic response.

The sediment compactability varies with lithology (facies) as well as geo-history (compaction timing, burial velocity etc). As mudstones and softer sediments (including coals) are more strongly influenced by compaction compared to sandstones (i.e. higher compactability), in particular in early stages of sediment burial (e.g. Worden and Burley, 2003; Nadon, 1998), differential compaction takes place in heterogeneous rock units. One of the unanswered questions of diagenesis concerns the impact of differential compaction

on reservoir architecture and, hence, flow properties. The properties are also influenced by early cementation that may prevent compaction, whereas dissolution may enhance the compaction.

More detailed comparisons of compacted rocks with uncompact depositional environment scenarios require decompaction, i.e. reconstruction of original sediment thicknesses. This is in particular dealt with in regional and basin scale palaeobathymetry modeling (e.g. Kjennerud et al., 2001; Kominz and Pekar, 2001), using generalised decompaction models (Sclater and Christie, 1980). More detailed knowledge of influences of diagenesis and differential compaction may help improving the techniques of compaction in backstripping modeling enabling reservoir scale reconstruction.

The present study deals with sandstone correlation problems of heterogeneous reservoirs offshore Mid-Norway, and the practical work is in part based on collaboration with Statoil. Statoil provided sample material and data from the Heidrun Field (Koenig, 1986; Schmidt, 1992; Whitley, 1992) offshore Mid-Norway (Figs. 1.1 and 1.2). The main study of this thesis is within the Upper Triassic to Lower Jurassic Åre Formation (Fm.) (Dalland et al., 1988; Svela, 2001; Kjærefjord, 1999; Leary et al., 2007; Thrana et al., 2009) with distinct reservoir correlation problems related to vertical and lateral heterogeneous facies. The normal faulted Early-Middle Jurassic pre-rift play sequence (including the Åre Formation) is here draped by a Late Jurassic syn-rift sequence of variable thickness and a thick Cretaceous post-rift sequence topped by a passive margin sequence of Tertiary age (Koch and Heum, 1995) and 1000-1500m of Late Pliocene to Pleistocene glacially derived sediments (Ottesen, 2006).

1.1.1 Hydrocarbon account and description of Heidrun and the Haltenbanken region

The Haltenbanken region is an important hydrocarbon province on the Norwegian continental shelf with close to one fourth of the total amount of Norwegian petroleum resources. For the Heidrun Field the total amount of recoverable reserves per June 2008 is estimated

to be 186 million scm (1170 mill. bbl.) oil and 50 billion scm (1.9TCF) gas with an overall recovery factor of 40 %, where remaining reserves amount to ~64 mill. scm oil and ~31 billion scm gas. In the Åre Fm., however, the recovery factor is as low as 17% with a calculated oil hydrocarbon pore volume estimated to 122 mill scm (Kjærefjord, 1999). The Haltenbanken hydrocarbon province is situated offshore Mid-Norway between 64°N-65°N and 6°E-8°E in water depths from 200m to more than 300m. The basin is 600km long and 200km wide and several discoveries have been made in this region (Fig. 1.2). All hydrocarbon reservoirs are of Late Triassic and/or Jurassic age and located at burial depth between 1500m and 4000m. Source rocks are shales of Late Jurassic age with minor contribution from coals and shales of Late Triassic/Early Jurassic age. Middle Jurassic sandstones constitute the major part of the reservoirs in this region, but significant accumulations also occur in sandstones of Late Triassic and Early Jurassic age. The area is, in addition to being sedimentologically heterogeneous, structurally complex with large N-NE to S-SW trending faults truncating the region. The Heidrun Field is located in blocks 6507/7 and 6507/8, in water depths of approximately 350m. The field was discovered by Conoco in 1985 (Koenig, 1986) by the drilling of well 6507/7-2 (Hemmens et al., 1994), and production was initiated in 1995. The gross production of 2007 was close to 8 mill scm oil and gas. The main reservoirs are the Middle Jurassic shallow marine/deltaic sands of the Fangst Group, and the fluviodeltaic, Upper Triassic - Lower Jurassic Tilje and Åre Fms. The primary source for petroleum is the anoxic marine shales of the Spekk Fm. with the coaly beds of the Åre Fm. as a secondary source.

1.2 Objectives and approach

The main objective of the thesis is to get an improved geological understanding of the origin and architecture of selected heterogeneous reservoir cases, below seismic resolution, and to elucidate the geological parameters controlling compactability of identified facies associations. The effect of differential compaction on the correlatability of reservoir sands is examined in the context of the identified relation between facies and compactability vs.

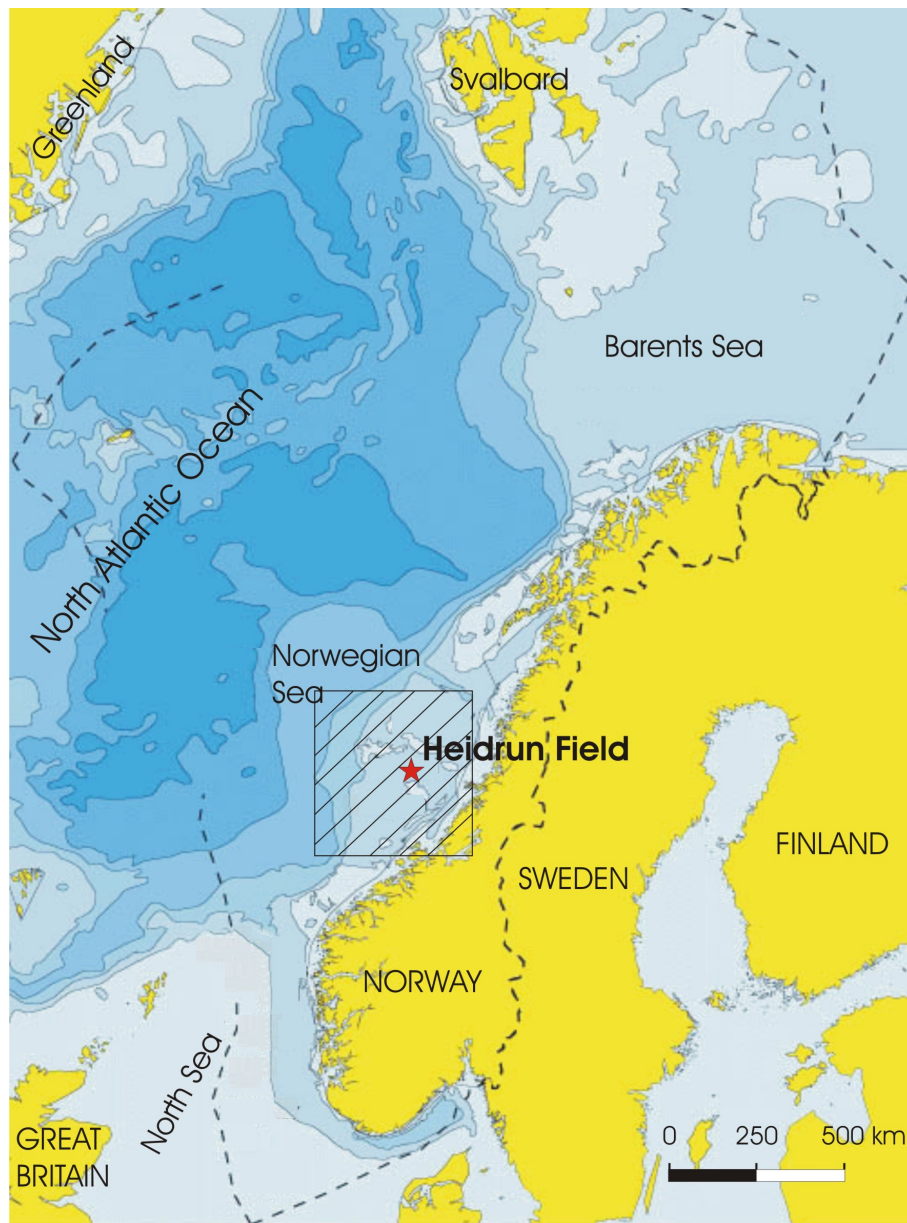


Figure 1.1: Location of the study area and the Heidrun Field on the Norwegian Continental Shelf.

burial depth. This is done by first elucidating facies associations from sedimentological interpretations of core and petrophysical wireline logs. A robust sequence stratigraphic model based on interpreted facies associations is presented and discussed in relation to

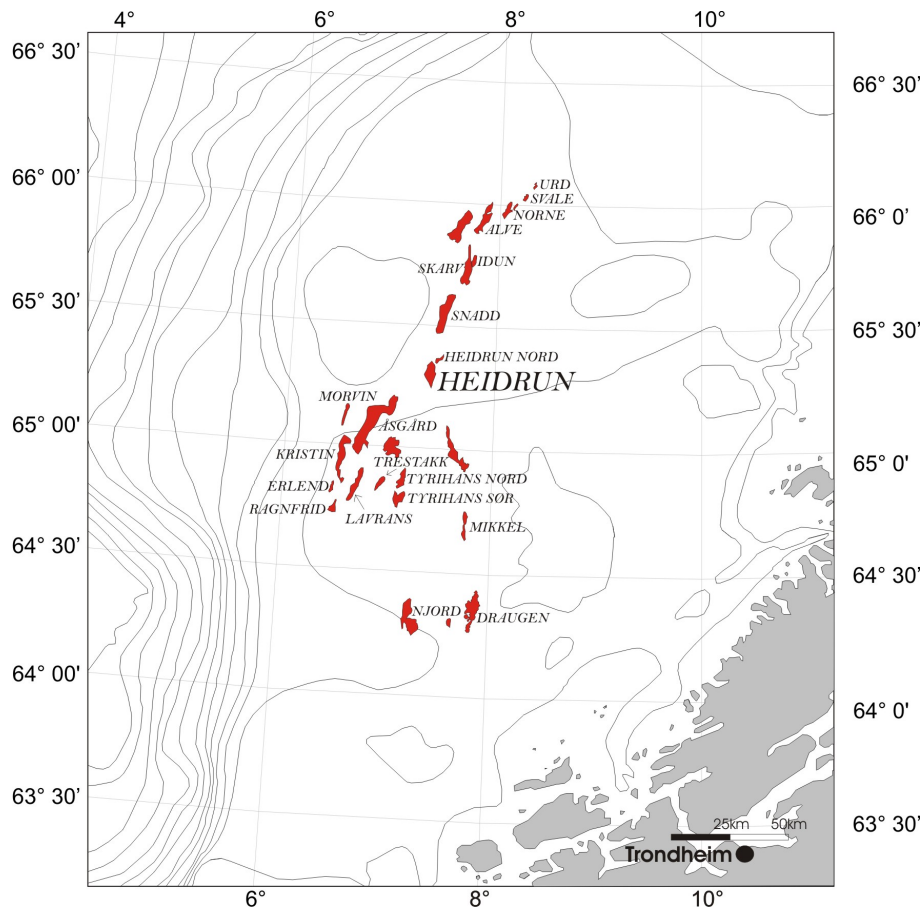


Figure 1.2: Hydrocarbon fields on the Halten Terrace including the Heidrun Field. The bathymetric contours are shown in 100m intervals. The location of the study area is illustrated by the shaded box in Fig. 1.1.

the effects of depositional controlling factors suggested for the Åre Fm. In addition, interpreted flooding surfaces from this study, assumed to represent palaeohorizontal surfaces, are utilized in algorithms for reservoir reconstruction. The facies controls on diagenesis and compaction are thereafter investigated on micro scale to find the role of diagenesis on the compactability of identified facies associations. These results are then applied for well correlation studies based on facies dependent decompaction algorithms, where porosity vs depth-relationships are used and applied for each facies association in a sequence strati-

graphic backstripping. An additional study on refined lithological classification through multivariate statistical methods has been investigated with the aim of identifying small scale heterogeneities. These studies display the possibilities of utilizing and combining calculated principal components of petrophysical parameters to extract more and hidden information from the dataset. The differentiation between facies associations is thereby enhanced, creating the possibility for a semi-automatic facies identification tool, saving time-consuming log interpretations.

Correlation exercises on decompacted sequences can enhance the correlatability of reservoir units, improving the reservoir architectural description and again lead to more optimized field development. This includes targeted infill drilling and improved recovery. A good correlation is essential for constructing a workable geomodel, and one hypothesis is that differential compaction may be a source of large errors in correlation exercises if not accounted for.

1.3 Research methods

The practical work in this thesis includes literature survey of selected relevant topics. These include regional geology and geological evolution of the Haltenbanken area with respect to sedimentology and structural geology, sedimentology of the interpreted depositional environments, diagenesis and its controlling factors including differential compaction and compactability. Theory on sequence stratigraphic concepts and sequence stratigraphic backstripping methodology is also studied, in addition to earlier work on multivariate statistical methods which have been applied in this thesis. Data acquisition was performed in collaboration with Statoil at Stjørdal and Rotvoll Research Center, and ResLab in Stavanger. Core logging was done at core stores in Stavanger and Stjørdal, including sedimentary facies interpretation from core observations, acquisition of rock samples for petrographic microscopy studies of thin sections, XRD and SEM investigation, and petrophysical wireline data interpretation of gamma ray (GR), density (RHOB) neutron porosity (NPHI), sonic (DT) and permeability (KLOGH). Landmark™ OpenWorks software

was used in wireline log investigations. Correlation and sequence stratigraphic analysis was based on interpreted facies association from core data, petrophysical logs signatures and conventional 2D seismic profiles. In addition, data from an internal Statoil reservoir characterization project has been included in some of the discussions (e.g. Leary et al., 2007; Thrana et al., 2008, 2009).

To achieve more realistic 3D experience in interpretation of the relevant reservoir architecture and heterogeneity, analogues of ancient depositional environments were studied. Observations from field work and excursions to onshore analogues were used to investigate facies association distribution and depositional architecture. Outcrops of fluvial to marginal marine deposits near Peniche, Portugal were visited as part of a Statoil expedition in collaboration with other universities spring 2005. In addition, the Ainsa region (2004) in the Spanish Pyrenees, the Yorkshire coast (2005, 2006 & 2007) in northern England, Wessex Basin in southern England (2006) and several localities on Svalbard (2005 & 2006) have been visited as part of student and Ph.D. field courses. Such analogue studies are important to fully understand the behavior of ancient and modern fluvial and deltaic systems.

Diagenesis and compaction have been evaluated using optical- and scanning electron (SEM) microscopy of thin sections, XRD and core data studies. A detailed core description was carried out to analyze the depositional environment in the Åre Fm., Heidrun Field. The description was done at a scale 1:50 and later reduced to 1:200 for comparison reasons with respect to petrophysical log scale. These core descriptions are used as a reference in the geological interpretation of petrophysical logs in 1:200 scale. Signal responses for different facies associations were mapped and used as correlation criteria. The reservoir correlation "tools" include interpreted sedimentary facies associations, biostratigraphy, sequence stratigraphy, petrophysical logs and seismic data. Further description of the different methods and data described above is presented in the Appendix.

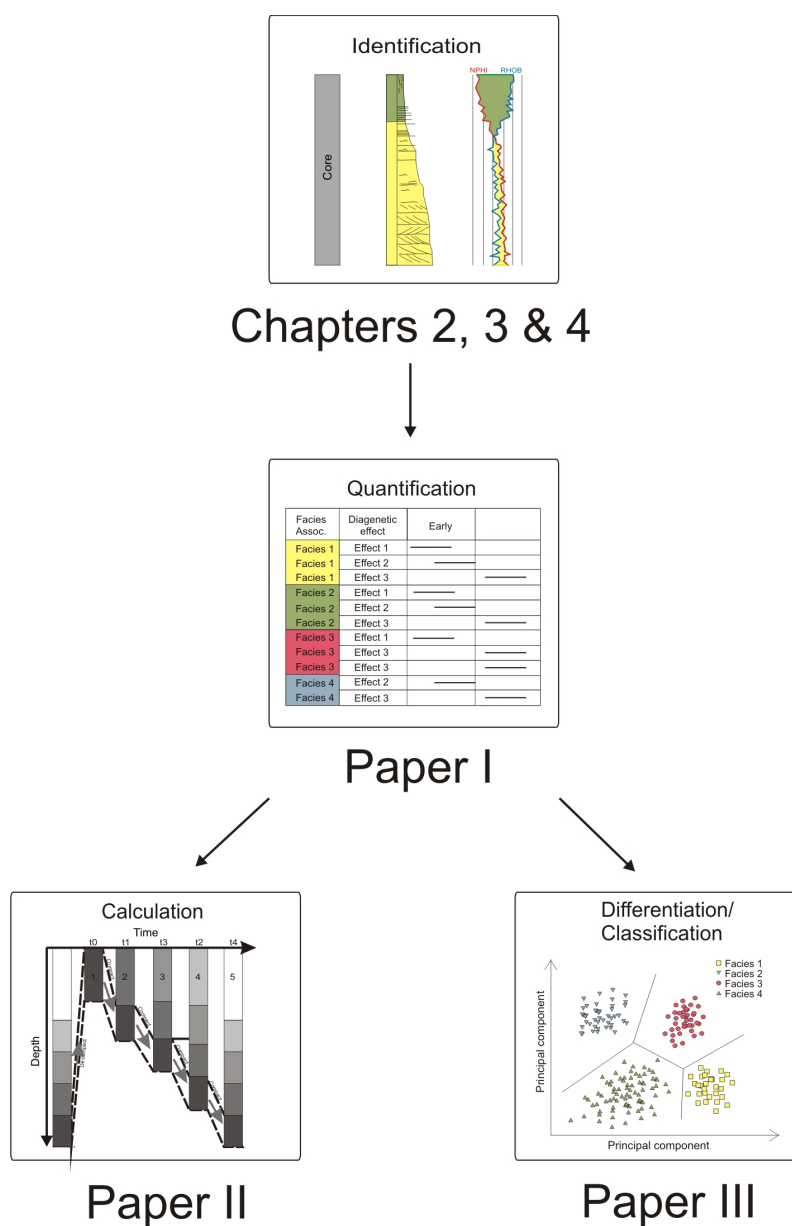


Figure 1.3: Sketch of thesis outline including four main parts: Chapter 2 to 4 including classification and interpretation of regional and local (reservoir) geology, reservoir units and sequence stratigraphy, Paper I dealing with quantification of compactability of identified facies associations, Paper II suggesting a workflow for improved reservoir characterization based on calculations of and correlations on decompacted reservoir sequences, and Paper III presenting a workflow for refined lithofacies differentiations.

1.4 Funding

This study was funded by the Department of Geology and Mineral Resources Engineering and by Statoil for the last 6 months of the study. In addition I have received funding to cover travel costs from Norge-Amerika Foreningen v/Alf og Bergljot Kolflats stipendfond, Lise og Arnfinn Hejes Fond, Hans og Helga Reusch Legat and Norges tekniske høgskoles fond.

1.5 Outline of the thesis

This thesis consists of three parts. The first part includes a general introduction to the project, the rationale and purpose for the thesis and a short introduction to the applied research methods. A short summary of the research papers enclosed in Part III is presented, in addition to overall concluding remarks and recommendations for further research. Part II includes three introductory chapters on regional geology, facies description and sequence stratigraphy within the Åre Fm., in the Heidrun Field. Results from these chapters are used in the scientific work presented in three research papers of Part III. The geological evolution of the studied region is presented in Chapter 2 and summarizes the structural and sedimentological evolution of the Haltenbanken area and the Heidrun Field. The chapter is based on a literature compilation of relevant articles related to the studied area (Haltenbanken region and the Heidrun Field) and studied interval (Åre Fm.). Chapter 3 presents and discusses facies association descriptions and interpretations of the Åre Fm. based on core descriptions and interpretations of data from fourteen studied wells. The results from Chapter 3 are used in the work presented in Chapter 4, discussing a sequence stratigraphic model for the Åre Fm, and in the research papers enclosed in Part III. Part III includes three papers. Paper I deals with the effects of diagenesis and compaction within facies associations identified within the Åre Fm. Paper II utilizes the results from Paper I in calculating decompacted sedimentary columns of the lower part of the Åre Fm (Åre 1 to 3.3). This interval contains abundant coals which are thought to have had a

significant effect on differential compaction. These studies combined (Paper I & II) were carried out for the purpose of contributing to the improvement of the present Åre Fm. Heidrun Field reservoir model, with respect to reservoir sand correlation, by taking into account the effect of differential compaction in such depositional architectures. Paper III identifies small scale heterogeneities on sub seismic scale using PCA analysis on petrophysical wireline log data. An appendix is enclosed describing in more detail data, material and methods used in this thesis. The outline of the thesis is sketched in Fig. 1.3.

1.6 Summary of main results

1.6.1 Chapters 2 to 4

The sedimentary rocks of the Åre Fm. comprise eight interpreted facies associations including single- (SFCH) and multi-storey (multi-lateral) channels (MFCH), crevasses (CCH), flood plain fines (FF) and sandy and muddy bay fills (SBF & MBF), tidally influenced channel sandstones (TCH) and transgressive shallow marine shoreface deposits (TSMS).

The sediments of the Åre Fm. in the Heidrun Field show evidence of deposition in a fluviodeltaic environment under rising eustatic sea level, where fluvial deposits dominate the lower part of the stratigraphy whereas transitional and open marine facies associations dominate the upper part.

Fourteen sequence stratigraphic surfaces are suggested within the Åre Fm. These include four local (field wide) and one regional sequence boundaries and nine flooding surfaces, of which three are regional events and one represents a transgressive surface.

The sequence stratigraphy is interpreted in relation to changing base level, which is associated with the decrease and increase in accommodation space. These changes are either controlled by regional allogenic, base level events, or local authigenic, factors. In the fluvial part of the succession, the changing accommodation space is related to changing stacking pattern of the fluvial sands. Stacking of single storey, meandering type, channel sand units is related to steadily rising regional base level. Vertical amalgamated, anastomosing type, channel sand units are often associated with thick, underlying coals

suggesting a relationship between compaction of peat and channel sandstone deposition indicating a local factor.

A lateral amalgamated coal unit situated in the middle part of the lower fluvial Åre Fm. resulted from several, and overlapping, peat swamp deposits interpreted as a regional correlatable flooding surface.

In the upper more marine influenced part of the Åre Fm. (above Åre 2) local to large scale delta lobe switching is suggested as the driving mechanism for the changing depositional environments. Local shifts are represented by bay fills displaying cyclic stacking pattern of mud SBFs and MBFs. Large scale lateral shifts are suggested as the cause for the Åre 4 coastal incursions.

In the upper part of Åre progradation of tidally influenced channel sandstones indicate a shift in source area from northwest to east followed by a flooding of the Åre Fm. and a general transition into the Tilje Fm. above. Amalgamated, multi-storey, multi-lateral, channel sands form field wide correlatable sandstone units in several stratigraphic levels (Åre 1, 2, 4 5 and 6), some of which are suggested as sequence boundaries created during base level fall.

1.6.2 Paper I - Facies controls on the distribution of diagenesis and compaction in fluviodeltaic deposits.

In Paper I the facies controls on the distribution of diagenesis are discussed for the purpose of elucidating and quantifying the compactability of the fluviodeltaic sediments of the Åre Fm. in the Heidrun Field. From these studies differences in the precipitation and timing of authigenic minerals were identified within the fluvial channel sands (FCH), floodplain fines (FF), sandy bay fill (SBF) and muddy bay fill (MBF).

The porosity data together with studies on plug porosities revealed relatively high porosity values in all the sandstone facies associations amounting to 29% ($\pm 6\%$), except where cementation had taken place.

A clear relationship between early (eogenetic) siderite cements and the presence of or-

organic matter and bands rich in mica is seen. Siderite was found to be especially widespread in organic rich MBF facies associations, amounting up to >10% of the rock. Due to the early precipitation timing of siderite cement, a reduced compactability of such cemented intervals is suggested.

Dissolution of mica probably acted as a local source of iron to form siderite. A trend of reduced iron concentration in precipitated carbonate cements with time is apparent, suggesting exhaustion of the Fe-source and/or a lowering of permeability in the rock during compaction.

Fluvial channel sands are relatively rich in kaolinite and show a decrease in detrital feldspars compared to the SBF sandstones. This has been interpreted in terms of meteoric flushing and subsequent leaching of feldspars in the sediments shortly after deposition and early during the consecutive burial.

A regionally correlatable calcite cemented bed is suggested to be associated with a deepening event which has been interpreted in the upper part of the succession (top Åre 3.3). This zone is therefore suggested as a potentially significant sequence stratigraphic marker, which may be utilized during sequence stratigraphic interpretations.

Overall compaction in the Åre Fm. is interpreted as predominantly mechanical. Feldspar dissolution in sandstones subjected to meteoric flushing may have acted as a local factor increasing the compactability of these sediments by creation of secondary porosity.

The burial depth is presently at maximum due to large amount of glacial derived sedimentation during the last few million years. This implies a relatively short time span at the present burial depth limiting the available time for chemical compaction processes to take place within the sediments.

The results from this study emphasize the importance of quantifying small scale diagenetic effects on the effect of differential compaction between facies associations.

1.6.3 Paper II - Reconstruction of Heterogeneous Reservoir Architecture based on Differential Decompaction in Sequential Re-burial modelling.

In this paper a methodology for sequence stratigraphic reconstruction on reservoir scale is proposed based on seven wells from the lower part of the Åre Fm. (Åre 1 to 3.3) in the central parts of the Heidrun Field. The lower part of the Åre Fm. contains abundant and thick peat deposits, which have had a significant impact on differential compaction within this interval. Based on correlation exercises performed on decompacted reservoir sections within the Åre Fm., new horizons are identified, suggesting new correlatable units within the Åre Fm. and a refinement of the present sequence stratigraphic framework.

Ten "lithofacies" classes are identified (FCH, FF, Coal, TCH, MBF, SBF, Undiff.sst, Undiff.mud, seawater and faults) and tied to uniquely calculated porosity-depth curves using average, measured and published porosity values for each class and relating compaction to an exponential decrease in porosity. Backstripping calculations are applied using porosity-depth relationships and interpreted flooding surfaces, suggested as palaeo-flat surfaces, as backstripping surfaces and six correlated, decompacted cross-sections are presented.

Several new intra reservoir zone correlation surfaces, including channel sandstones and coals, are identified within the Åre Fm. The refined sequence stratigraphic interpretation based on decompacted reservoir units provides additional intra-zone interpretations of facies correlations and contributes to understanding the effect of early differential compaction on sediment deposition.

The proposed methodology for reservoir reconstruction is especially advantageous to refine reservoir models in heterogeneous, highly compactable deposits subjected to differential compaction, such as fluviodeltaic reservoirs. Correlation difficulties often occur and, in addition, the majority of the size of the reservoir bodies may be below seismic resolution creating a dependency on well-to-well correlation exercises for interpreting the connectivity of reservoir sands.

1.6.4 Paper III - A comparison of unstructured and structured principal component analyses and their interpretation.

A workflow to perform separate analysis of lithofacies types by principal component analysis (PCA) of five petrophysical wireline logs; density (RHOB), neutron porosity (NPHI), gamma ray (GR), sonic (DT) and resistivity (RT), is created to quantify small scale reservoir heterogeneities related to second order lithological variability.

The analyzed wireline log interval supported by core analyses was manually classified into two types of rock classes; (1) lithofacies relating to rock type, which include sandstone (ss), shale (sh), coal (co) and cemented intervals (cc) and (2) lithofacies associations related to fluvial channel sands (FCH), floodplain fines (FF), sandy bay fill (SBF) and muddy bay fill (MBF).

The unstructured PCA approach, which is based on the complete well record, identified the major variability from all lithological units, whereas the structured PCA approach, calculated from separate well record subsets (rock type) highlighted the internal variations within these units, named PC_ss, PC_sh, PC_co and PC_cc for sandstone, shale, coal and cement, respectively, that enabled interpretation of populations within these subsets. The weights derived from structured PCA for specific lithological units (PC_ss, PC_sh, PC_co, PC_cc) enabled interpretation of intra-lithological variability for different depositional units. This permitted a more precise separation of the lithological units compared to initial wireline log data. This procedure thereby allowed observing and quantifying heterogeneities within the sample interval which are not visible in traditional wireline log data.

The weighting of PC_ss applied to the entire analyzed interval enabled an enhanced discrimination between FCH and SBF interpreted facies associations. Likewise the PC_sh weighting applied to the entire analyzed interval enabled enhanced discrimination between FF and MBF facies association.

This paper shows that a structured PCA procedure, based on specific lithological units, may enable enhanced discrimination between rock types by quantification of within-

lithology variations, indicating a potential for developing a semi-automatic lithofacies classification algorithm where threshold values may be applied on enhanced lithofacies discriminations.

Part II

The geology of the Haltenbanken region, the Heidrun Field and the Åre Formation

Chapter 2

Regional geological evolution

2.1 Introduction

In order to understand the small scale heterogeneities within the Åre Fm. in the Heidrun Field, it is necessary to understand the large scale processes, such as regional scale tectonic and sedimentological evolution, to be able to identify smaller scale processes, such as facies deposition, diagenesis etc. in a larger context. In this chapter the general geological evolution of the study area and the studied formations is presented based on a literature study supplemented by interpreted available geological (sedimentological, tectonic) data.

2.2 Tectonic evolution of Haltenbanken region

The structural configuration of the Haltenbanken region is dominated by the Møre and Vøring Basins to the west and the Trøndelag Platform to the east separated by an area containing a series of normal faults (Fig. 2.1). This area is referred to as the Halten Terrace with the narrower Dønna Terrace further north. To the south this transition zone passes into the Klakk Fault Complex, which also constitutes the western limit of the Terrace. The Vingleia and Bremstein Fault Complexes define the eastern limit, whereas the Revfallet Fault Complex defines the northern extension of the Dønna Terrace. The fault zones are associated with major uplifted domes; the Nordland Ridge along the Revfallet Fault

Complex and the Frøya and Sklinna Highs along the Klakk Fault Complex. The Heidrun Field is located on the southernmost extension of the predominantly SW-NE trending Nordland Ridge and formed as a south-dipping triangular shaped horst block (Harris, 1989).

The Halten Terrace is located at a north-trending dogleg bend in the overall northeast-trending Kristiansund-Bodø Fault Complex between the Vøring and Møre Basins to the west and the structurally higher Trøndelag Platform to the east (Hemmens et al., 1994; Schmidt, 1992). The terrace is dipping gently to the S-SW. The fault patterns of the Halten Terrace are characterized by interference of NE- and N-trending fault segments (Bukovics et al., 1984) This observation is supported by Bukovics et al. (1984) and related to three-dimensional coaxial strain (Schmidt, 1992) implying a ESE-WNW extension direction. An E-W cross-section is shown in Fig. 2.2, which displays the general structural configuration of the Haltenbanken area.

A similar NE- and N-trending fault pattern is observed in plane view of the top Åre reservoir structure in the Heidrun Field (Fig. 2.3) and the faults are easily seen on seismic sections (Fig. 2.4) The minor faults typically have throws of less than 50m with an average 20-30m, but a few in the north and northwestern part of the field have throws in the order of 100-150m. The faults create segments that are typically elongate in a north to south direction and are usually 500-1000m wide. This complex structural configuration influences the correlatability of reservoir sands and must be taken into consideration in backstripping exercises (Paper II). Interpretation of the structural evolution of the Haltenbanken region is beyond the scope of this thesis and the reader is referred to earlier work by Marsh et al. (2009); Richardson et al. (2005); Corfield and Sharp (2000); Doré (1991); Eldholm et al. (1987); Cohen and Dunn (1987); Bukovics and Ziegler (1985); Bøen et al. (1984); Gabrielsen et al. (1984); Bukovics et al. (1984). A general outline is however presented in order to emphasise the importance of tectonic activity on depositional control. The structural configuration of the Mid-Norwegian shelf is the result of a divergent continental margin development from the Carboniferous to the opening of the Norwegian Sea in the Early Tertiary. The main structural features were established

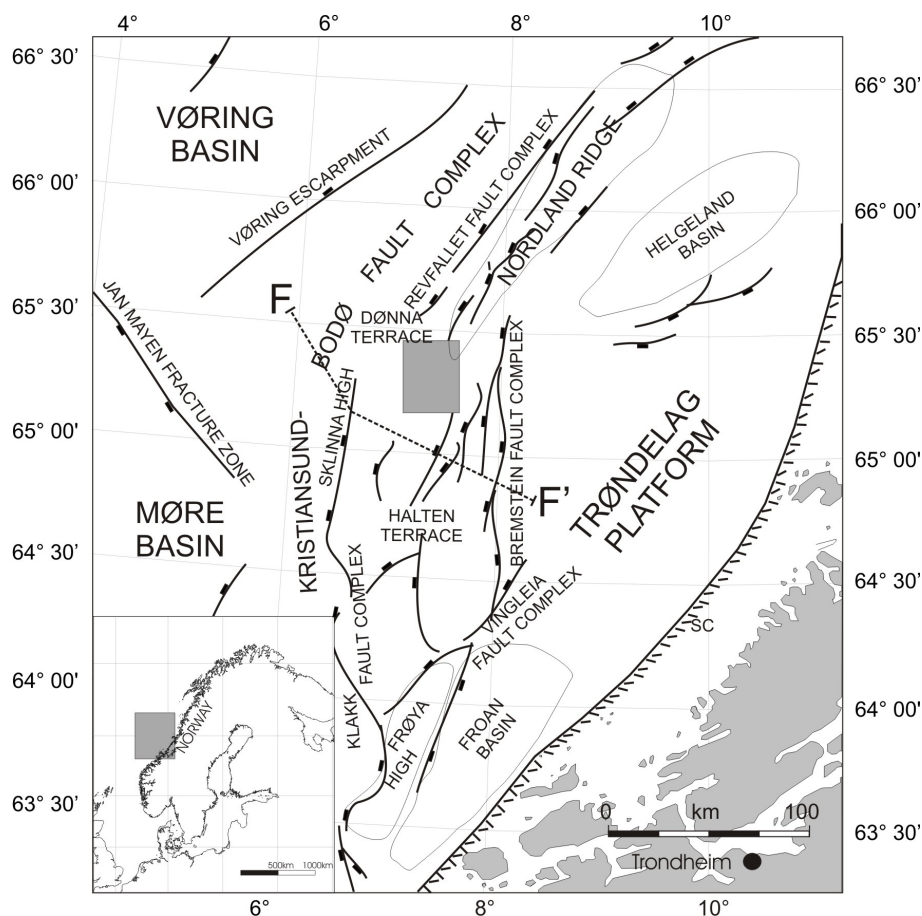


Figure 2.1: The structural elements of the Mid-Norwegian continental shelf (modified from Gabrielsen et al., 1984; Koch and Heum, 1995) and the location of the study area (shaded rectangle). The Kristiansund-Bodø Fault Complex is the name for the lineament forming the Klakk Fault Complex, Sklinna High and the Revfallet Fault Complex.

in the Late Jurassic and Early Cretaceous, essentially exploiting the Caledonian suture zone (Doré, 1991) and is referred to as the late Kimmerian phase discussed below. Marsh et al. (2009) argued that the Jurassic fault activity in the Halten Terrace area initiated as early as Early Jurassic (Hettangian-Pliensbachian) synchronous with the Åre Coal to Top Åre deposition. They observed seismic reflectors from Åre Coal to top Åre sequence diverge into synclines, suggesting that basement faults were active during this time. Rift initiation was characterized by distributed deformation along blind faults within the base-

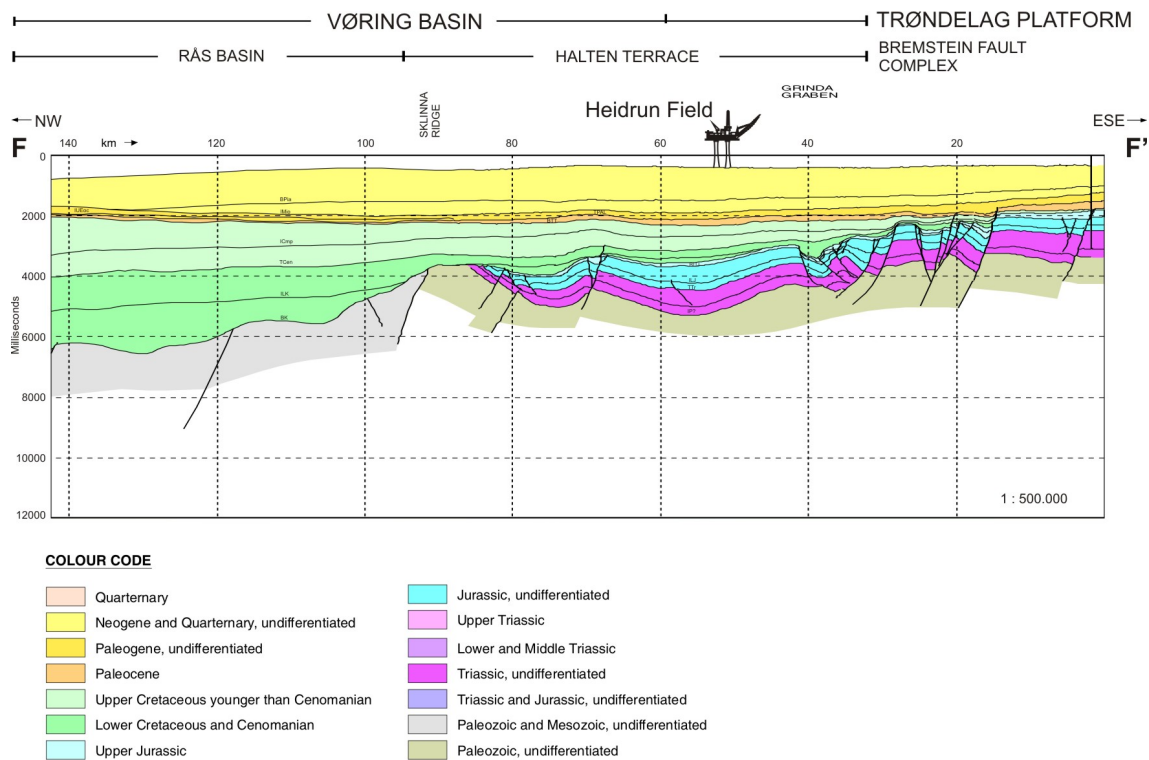


Figure 2.2: Cross-section of the Mid-Norwegian continental shelf. A distinct rotated fault block configuration is evident where antithetic faults have developed in the Triassic/Jurassic sequence in the east. For location, see Fig. 2.1. Cross-section taken from www.npd.no.

ment, and localized deformation along major faults within the cover above the Triassic salt (Marsh et al., 2009). According to Cohen and Dunn (1987) this episode started already in the Late Triassic with highest intensity during the Bathonian/Callovian (Middle Jurassic). Isochore maps of three seismically mapped Jurassic intervals in the Smørbukk area to the south illustrate a south to north evolution associated with progressive northwards evolution in fault activity illustrating the dynamics of vertical and lateral fault movements of the rift-basin in contrast to a "static" structural framework Corfield and Sharp (2000). During the rifting episode between Greenland and Norway, the Triassic salt is believed to have acted as a decollement zone for the more competent overlying Jurassic rocks, which eventually developed into the fault blocks seen on seismic sections today (Fig. 2.4). Nevertheless, ample evidence exists for two major extensional events at the Heidrun

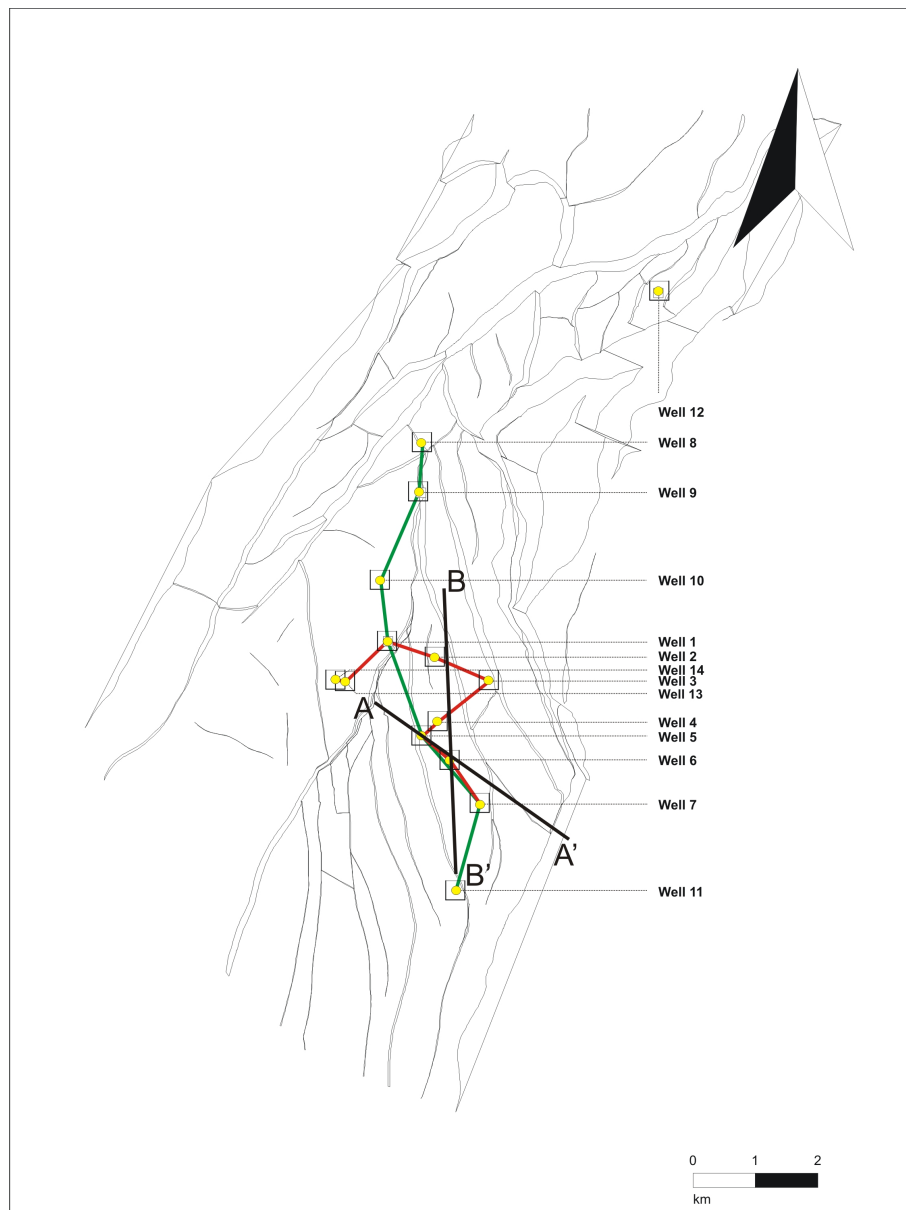


Figure 2.3: Top Åre reservoir structure of the Heidrun Field and location of wells, cross-sections and seismic sections. See Fig. 2.1 for location of the field on the Halten Terrace.

Field. The first of Mid-Permian age (Doré, 1991) and the second of Early/Late Jurassic to Early Cretaceous. The first extension event followed the NE trend already established in the Caledonian basement, created NE-striking tilted fault blocks. During this rifting

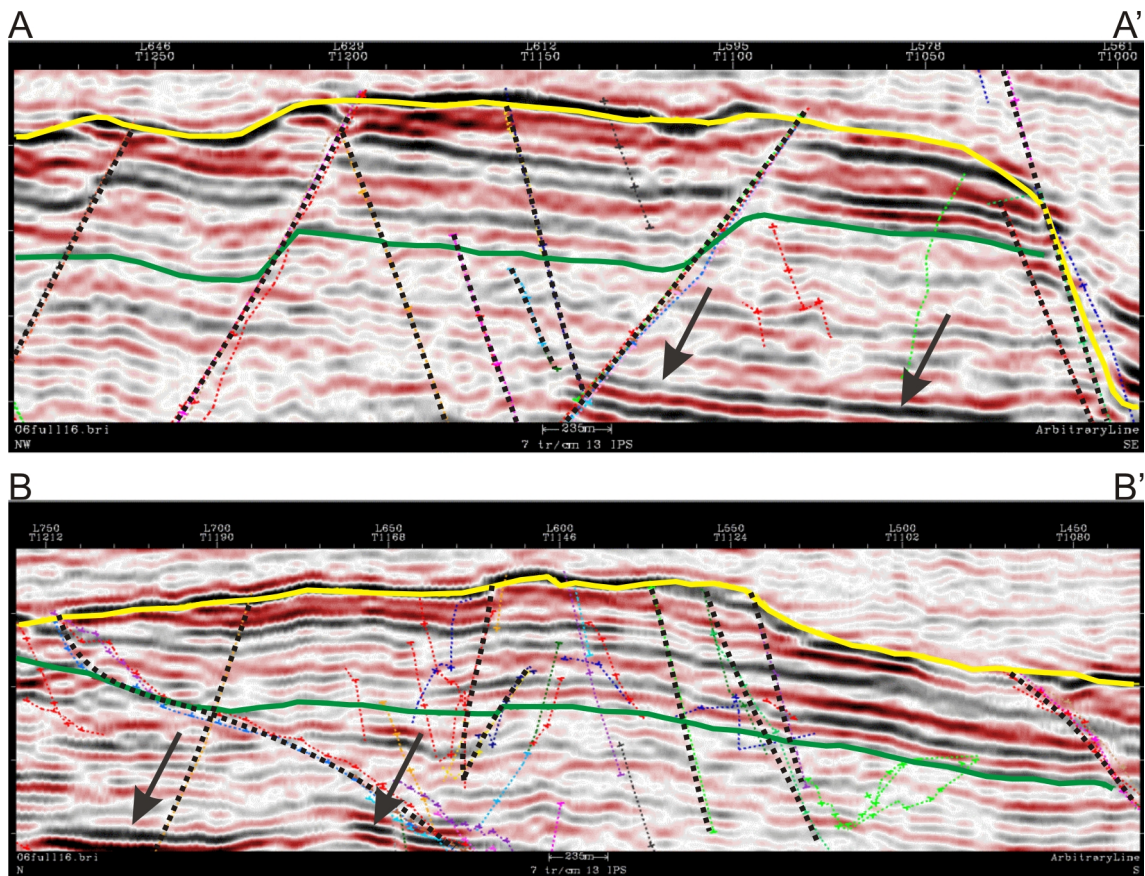


Figure 2.4: Seismic profiles showing cross sections of the Åre reservoir. A-A' is NW-SE, B-B' is N-S. Yellow line = BCU, Green line = top Åre 6.2. Dotted lines = faults. The Åre 1 coal marker is easily observed as a large seismic (black) reflector in the lower part of the sections (arrows). See Fig. 2.3 for location of cross-sections.

episode half grabens filled with "red-beds" developed in the Haltenbanken region along the Møre-Trøndelag Fault Zone. Late Triassic to Early Jurassic was a period of tectonic quiescence. No significant fault activity is recorded except for minor uplift and faulting on the Nordland Ridge and the Frøya High. During the Triassic the Heidrun area consisted of a broad sedimentary basin (Harris, 1989) in which Gabrielsen and Robinson (1984) documented a relatively constant thickness of an assumed Triassic sequence indicating that the area acted as one sedimentary basin. No evidence of connection between the Boreal

and Tethyan Realms is found (Doré, 1991).

The second major extensional event is usually referred to as the Kimmerian tectonic phase (Jurassic-Early Cretaceous) (e.g. Lundin and Doré, 1997; Whitley, 1992; Schmidt, 1992; Bukovics and Ziegler, 1985; Bukovics et al., 1984; Gabrielsen et al., 1984; Rawson and Riley, 1982; Øvrebø and Talleraas, 1977). During this Kimmerian episode tilted fault blocks and horsts developed, which contain most of the hydrocarbon reservoirs in the region. This configuration is easily observable in E-W cross-sections of the region (c.f. Fig. 2.2) and seen as NE- and N-trending fault sets in plan view in Figs. 2.1 and 2.3. The N-trending sets are often antithetic to the NE-trending fault sets (Whitley, 1992; Schmidt, 1992). The orientation suggests major E-SE - W-NW extension. During this phase the area was uplifted and eroded as evidenced by the Base Cretaceous Unconformity (BCU). The rhombic shape of the Halten Terrace probably formed as a pull-apart basin in a sinistral fault system (Brekke and Riis, 1987).

During the Cretaceous, basin infill and subsidence ensued and the Halten Terrace also subsided relative to the Trøndelag Platform. This was followed by the initiation of seafloor spreading and continental drift of Greenland from Norway in the Paleocene - Eocene (Whitley, 1992; Eldholm et al., 1984). Through the Tertiary, thick marine shales accumulated on both the Halten Terrace and the Trøndelag Platform due to subsidence in the developing Norwegian Sea.

Rapid subsidence occurred during the Late Pliocene to Pleistocene. This was due to incipient glaciations and deposition of 1-2km of glacially derived sediments in the Kai and Naust Fms. during the last 3 million years, prograding from the southeast across the Halten Terrace (Ottesen, 2006). This episode resulted in rapid burial and thermal heating of the underlying strata accompanied by accelerated hydrocarbon generation and of overpressure generation in Jurassic reservoir sandstones in the western part of the Halten Terrace. A sediment burial curve for Åre Fm. based on calculations from age and thicknesses of formations from well Well 5 in the Heidrun Field is shown in Fig. 2.5.

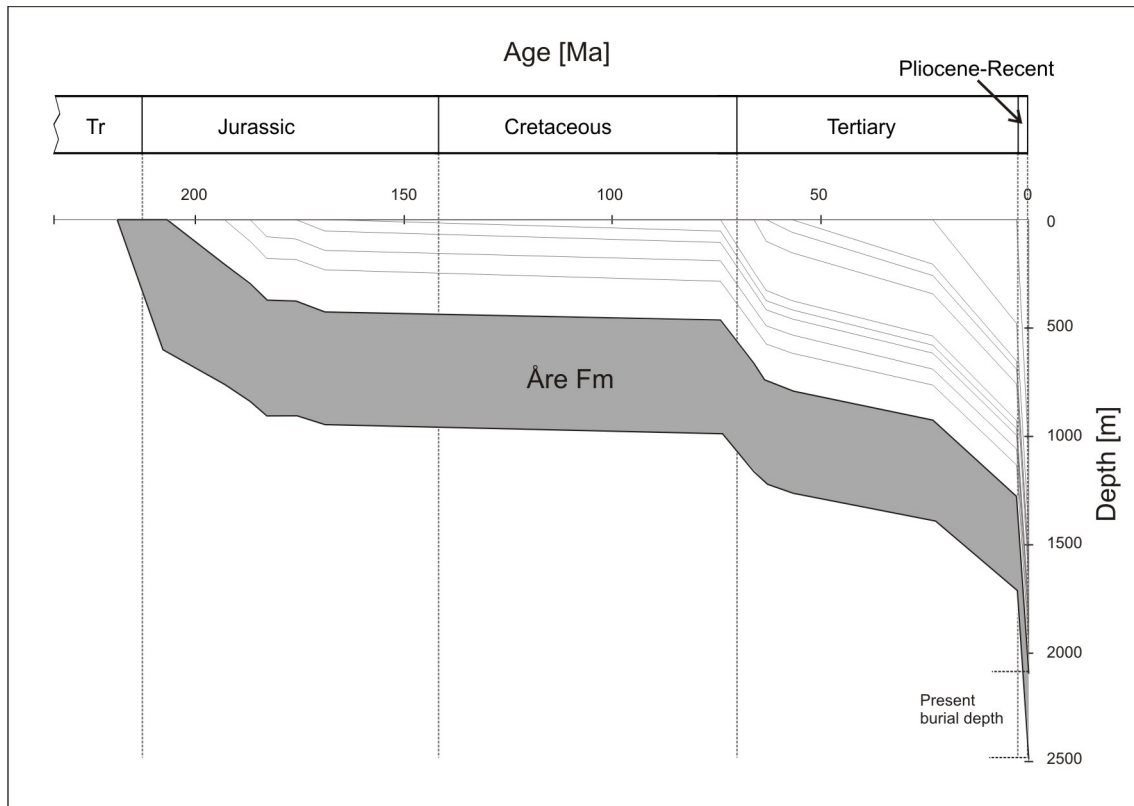


Figure 2.5: Burial curve calculated for Well 5 based on calculations from age and present formations thicknesses.

2.3 Sedimentological and paleogeographic evolution

The general lithostratigraphy on the Mid-Norwegian continental shelf follows the nomenclature of Dalland et al. (1988) and is presented in Fig. 2.6. The oldest sediments penetrated in the Haltenbanken region are a thick sequence of Middle to Late Triassic age which can be traced throughout the region with little thickness variation (Ehrenberg et al., 1992). Continental conditions associated with uplift and half graben development related to the proto-Atlantic rift, resulted in the deposition of red siltstones, shales and thin sandstones in a fluvial setting (Whitley, 1992). These sediments are referred to as the Triassic "red-beds", deposited in a mud-dominated, fluvial, arid (oxidizing) environment. The presence of halite sequences probably represented marine incursions from the Boreal

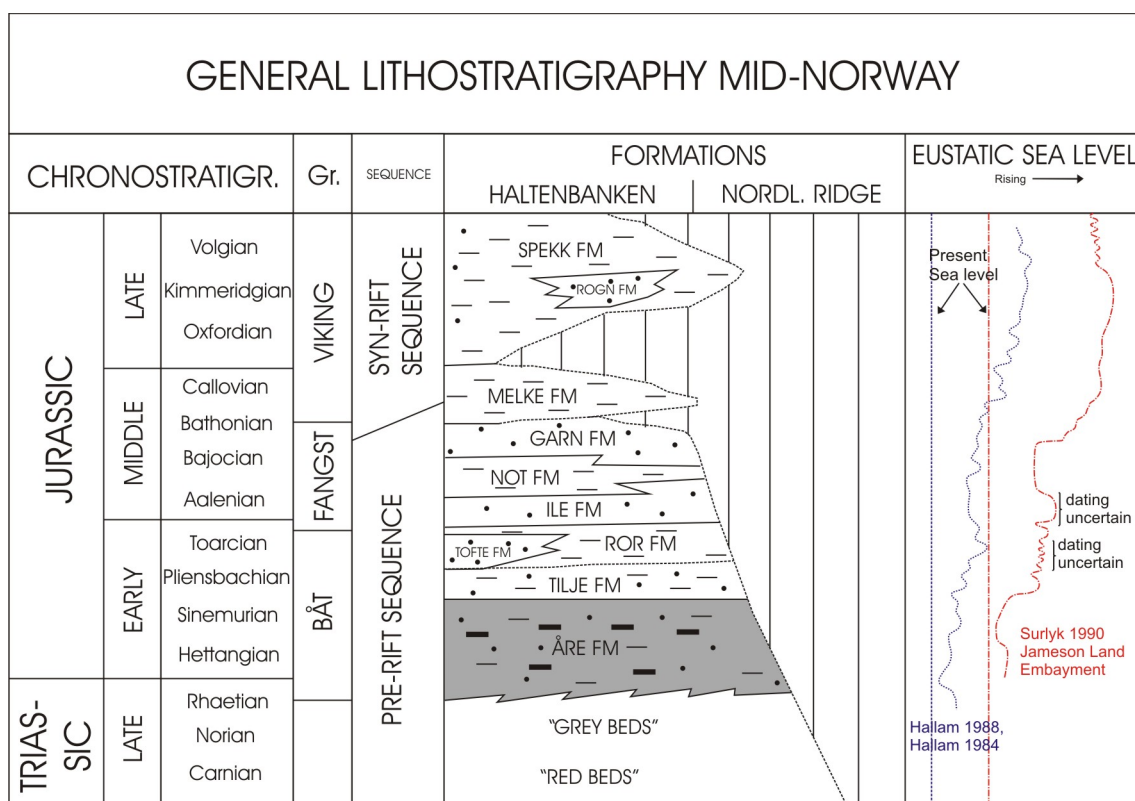


Figure 2.6: Stratigraphic compilation of the Mid-Norwegian continental shelf (modified from Dalland et al., 1988) and tectonic development from Schmidt (1992) and Bukovics et al. (1984). The eustatic sea level curve is based on Hallam (1984) and Surlyk (1990).

Sea (Whitley, 1992).

A change from arid to more humid climatic conditions and a gradual rise in sea-level in the Late Triassic (Rhaetian) to Early Jurassic brought paralic, swampy conditions to the Haltenbanken area, resulting in deposition of coals, sands, silts, and shales which comprise the Triassic "grey-beds" (Dalland et al., 1988). The Rhaetian transgression continued into the Triassic/Jurassic boundary depositing the Åre Fm. in the Heidrun Field and similarly the Kap Stewart Fm. in East Greenland (Surlyk et al., 1981). During this period the area was situated at approximately 43°N latitude (Fig. 2.8), suggesting a subtropical environment at that time. The Åre Fm. of Rhaetian to Early Pliensbachian age (Dalland et al., 1988; Svela, 2001; Gjelberg et al., 1987), present in both Haltenbanken

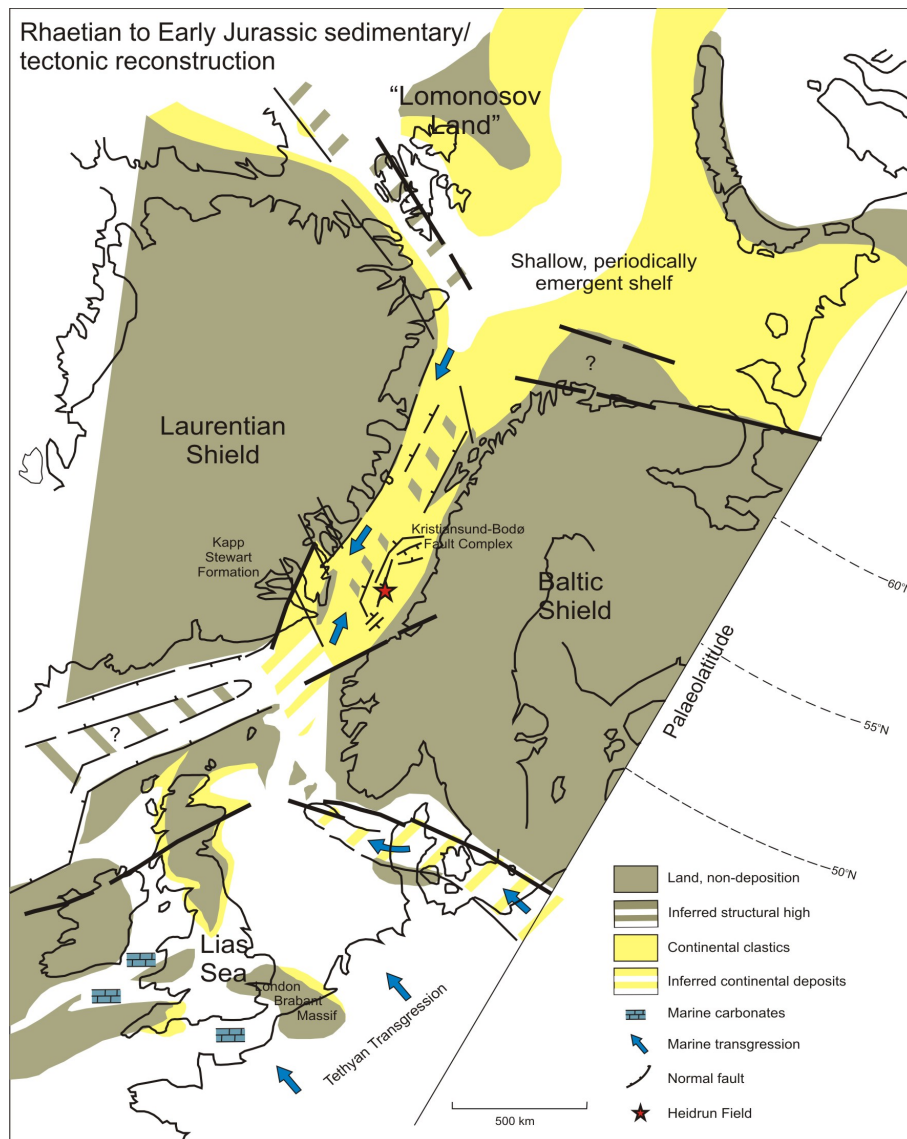


Figure 2.7: Schematic Rhaetian-Early Jurassic reconstruction showing the regional tectonic elements in the North Sea region and between Greenland and Norway (after Doré, 1992). The map clearly illustrates the level of tectonic activity during the Pangea break-up. Also indicated is the connection of the seaway between the Boreal and Tethys palaeoceans during this period. Notice the location of the Kap Stewart Fm. in East Greenland as discussed in the text.

and Trænabanken areas, consists of sediments deposited in a fluviodeltaic environment with swamps and channels, passing upwards into marginal marine facies, hence displaying

an overall transgressive trend. The formation is usually between 300 and 500m thick (the thickest development is in the northern Haltenbanken area). The coals are important gas-prone source rocks with possible oil generation potential (Hvoslef et al., 1988) and are present throughout the Haltenbanken and Trænabanken areas. The sediments of the Åre Fm. are time-equivalent to the East Greenland Kap Stewart Fm. (Surlyk et al., 1981; Surlyk, 1990) and the Statfjord Fm. in the North Sea (Ryseth and Ramm, 1996). Gjelberg et al. (1987) interpreted, based on lateral facies distribution, that the system drained mainly from an easterly source. This is supported by the more proximal facies development in the east, the presence of time-equivalent alluvial fan conglomerates east of the Halten region, and the onset of marine sedimentation in the west at the end of the delta plain depositional period. The formation is thickest in the western part (150-250m) and displays a dramatic thinning towards the east due to an eastward retreat of the Åre and Tilje deltaic system through time (Gjelberg et al., 1987). Hemmens et al. (1994) proposed both eastern, and western source areas, whereas Thrana et al. (2008) proposed, based on correlation of facies belts and interpreted depositional dip directions from image log data, a N-NW source area for the Åre Fm. This study supports the conclusion made by Thrana et al. (2008) as backstripping shows that correlatable sand units display increased tidal influence towards the southeast (ref PaperII) suggesting a palaeoshoreline in the E-SE.

The latest Triassic and beginning of the Jurassic was a period of general sea level rise which, by the end of the Early Jurassic, created a continuous seaway through the Atlantic rift system, linking the Boreal and Tethyan Realms (Fig. 2.7). Major transgressive pulses in the Rhaetian established paralic conditions along the flanks of the Atlantic rift domain, depositing the coaly Åre Fm. on the Mid-Norwegian side and the similar Kap Stewart Fm. in East Greenland (Doré, 1992). These transgressive events occurred together with a series of tectonic events referred to as the Kimmerian tectonic phase described earlier.

The Åre Fm. passes gradually upwards into the tidally dominated, shallow marine Tilje Fm. following a transgression in the Sinemurian-Pliensbachian (Doré, 1992). The Åre and Tilje Fms. constitute a transgressive delta plain/delta front scenario ending in the deposition of open marine shales and sands of the overlying Ror Fm. reflecting a

major transgression in the Toarcian. In general, the Åre, Tilje and Ror Fms. (Båt Gp. of Dalland et al. (1988)) comprise a large scale transgressive systems tract (Gjelberg et al., 1987; Kjærefjord, 1999). The Åre and Tilje Fms. were deposited in a narrow seaway after the final connection between the Tethys Sea in the south and the Boreal Sea in the north was established (Kjærefjord, 1999). Because of the narrow restriction between these two oceans, tidal currents were probably extreme at this time (Coleman and Wright, 1975). During Early and Middle Jurassic times the Trøndelag Platform and the Halten Terrace were both part of the same deltaic to shallow marine depositional environment. A middle

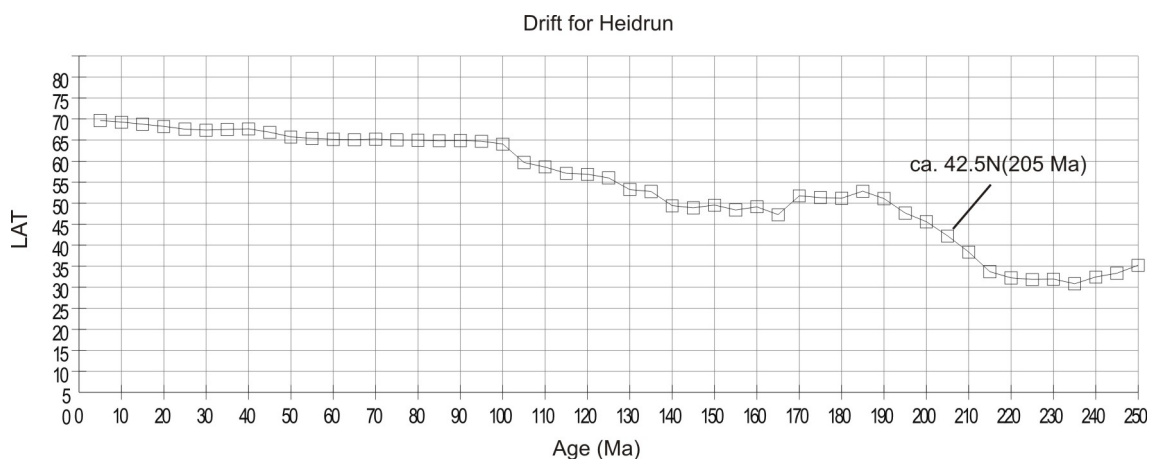


Figure 2.8: Drift of the Heidrun Field using the global polar drift curve of Torsvik et al. (2008) and corrected for earth obliquity (after Steinberger and Torsvik, 2008). The curve is calculated for 65°N and shown in 5 million year intervals from 250 mill years. Printed by kind permission from Trond Torsvik.

Jurassic regression originating from a regional up-doming, and a global sea level lowstand (Harris, 1989) followed the transgressive Ror Fm. resulting in clastic influx and deposition of the Fangst Group, including the Ile (50-100m), Not (10-50m) and Garn (10-100m) Fms. The Kimmerian tectonic phases caused partial or total erosion of the Fangst Group on the major highs and resulted in the formation of a widespread unconformity (BCU). As the reservoir structure of the Heidrun Field dips slightly towards the south-southwest (Koenig, 1986; Heum et al., 1986), the northern parts were more subject to erosion. This

is observed by the Cretaceous Springar Fm. directly overlying Åre and Tilje Fms. in northern wells (ex. Well 10). This event was succeeded by deposition of the Melke shales (Dalland et al., 1988), indicating fully marine conditions in the Haltenbanken area that persisted for the remainder of the Jurassic. The Late Jurassic transgression culminated with the deposition of the organic rich Spekk Fm. (5 to 8% TOC) in deeper water with anoxic bottom conditions during the Kimmeridgian - Ryazanian (Dalland et al., 1988). Mudstone dominated the sedimentation in the Cretaceous and marine shales of the Cromer Knoll and Shetland Groups were deposited (Dalland et al., 1988).

Sea floor spreading commenced in the Early Tertiary, and Haltenbanken subsequently developed as part of a passive margin (Doré and Gage, 1987). Post-Paleocene sedimentation was primarily of marine mudstone, accumulating on a passively subsiding ocean margin. A thick, 1500-2000m, sequence of alternating grey shale and poorly sorted sandstones was deposited in the Naust Fm. as a glacially derived prograding wedge (Ottesen, 2006). The Tertiary - Quaternary section is nearly 2000m thick in the Haltenbanken area.

Chapter 3

Sedimentological interpretation of the Åre Fm.

3.1 Introduction

To be able to correlate sandstone intervals between wells in a fluviodeltaic setting, a facies description is performed in selected wells and correlated to associated distinct petrophysical wireline log signatures which are used as identification tools in the correlation. This section documents the main facies associations recognized in the Åre Fm. This work is based on the detailed description of 407,5m core taken from four wells. A total of nine facies associations and examples of their sedimentological log record and wireline log signature have been recognized. Core intervals from wells 2, 4, 5 and 10 have been examined in detail for sedimentological interpretation. The core from well 5 has also been discussed and interpreted earlier by Svela (2001). A 1:50 sedimentological log was created by sedimentological logging for all selected core sections to identify sedimentary structures used for facies determination, and later reduced to 1:200 scale for petrophysical log comparisons. The sedimentological interpretations and interpreted facies associations form a basis for correlating sedimentary facies from wireline logs, including their petrophysical log signatures, to be able to correlate wells where core data were unavailable. Also, the

presented papers discuss different aspects of these facies associations (compactability, similarities and differences in mineralogy, chemistry, petrophysical data etc.) and first-hand knowledge was therefore desired. Where additional data from studies by Statoil and/or consultants have been used (e.g. Svela, 2001; Leary et al., 2007; Thrana et al., 2008), it has been cited accordingly. The results from this work are utilized in Chapters 3 & 4 and Papers I, II, III & IV, forming the framework for this thesis.

3.2 Previous work on the Åre Fm., Heidrun Field

The Åre Fm. overlies the Triassic "grey-beds" and comprises a succession of sandstones, mudstones and coals deposited in a coastal plain to lower delta plain environment with swamps and channels passing upwards into marginal marine facies (Whitley, 1992; Gjelberg et al., 1987; Pedersen et al., 1989; Kjærefjord, 1999; Svela, 2001). Detailed sedimentological and sequence stratigraphical studies in the last few years have revealed a new reservoir zonation scheme for the Åre Fm. (Leary et al., 2007; Thrana et al., 2008), which includes seven reservoir zones (i.e. Fig. 4.4) based on facies association descriptions; trace fossil assemblages and depositional environment interpretations. Results from these studies, with emphasis on the identified correlatable surfaces, are included in the sequence stratigraphy discussed in Chapter 4 and in the backstripping model presented in Paper II.

Gjelberg et al. (1987) presented a regional interpretation of the Åre Fm. (previously Hitra Fm.) and concluded that it had an overall transgressive trend. The formation base is defined directly underneath the lowermost coal bed identified on sonic logs (Dalland et al., 1988). Non-marine, coastal plain sediments in the Lower Åre Fm. are overlain by marginal marine to non-marine strata deposited in a lower delta plain environment. Marginal-marine, tidally-influenced and shallow marine shelf strata dominate the uppermost Åre. This upper unit has been interpreted by Kjærefjord (1999), as transgressive shallow marine shoreface deposits, or according to Martinius et al. (2001), laid down in a storm-dominated prodelta setting, deposited between storm wave base and fair-weather wave base, and with a gradual transition into the overlying Tilje Fm. The Top Åre- Base Tilje transition has

3.3. COMMENTS REGARDING CHRONOSTRATIGRAPHY AND ICHNOFACIES.37

been defined by the first full marine flooding as seen from biostratigraphy and clearly reflected by a GR-peak on wireline logs (Svela, 2001). The age of the Åre Fm. is Rhaetian to Pliensbachian based on palynostratigraphy (Dalland et al., 1988). However, the shallow marine shoreface facies association observed in core data in the uppermost Åre has been dated to Pliensbachian (C. Thrana pers.comm. 2009) and has recently been reinterpreted as part of the Tilje Fm. None of the wells presented in this study penetrate into Rhaetian sediments. Consequently, the Åre Fm. in this study is of Hettangian to Pliensbachian age.

3.3 Comments regarding chronostratigraphy and ichnofacies.

A lack of ammonite zones within the Åre Fm. has resulted in a poor calibration to an established chronostratigraphic system. Despite of this lack of chronostratigraphic potential the age of the Åre Fm. has been defined by palynostratigraphy on relatively reliable marine datums in the Tilje Fm. above, and terrestrial datum levels in the lower Åre 1.1. Based on palynostratigraphic studies performed by Statoil researchers, four age intervals are recognized within the Åre Fm. in the Heidrun Field. Within the dominant part of the Tilje Fm. horizons indicate a Pliensbachian age. Horizons in the lowermost part of Tilje Fm., however, are more unprecise, which result in an age range for the Åre/Tilje transition from Sinemurian to Pliensbachian. A distinct marine event has also been identified in the upper parts of the Åre Fm., Åre 6.2 to 7 with Acritarchs *Tasmanites* spp. And *Micrhystridium* spp. This event is similar to the marine Late Sinemurian in the North Sea indicating a Late Sinemurian age for the upper most part of the Åre Fm. Increased frequency of *Trachysporites* spp. from the upper part of Åre 2.1 and downwards indicates a Hettangian to Early Sinemurian age for the lower most part of the Åre Fm. A distinct *Limbosporites lundbladii/Ricciisporites tuberculatus* occurrence in the lower most part of Åre 1 zone has been taken as relatively solid evidence of an Upper Rhaetian age. None of the selected wells penetrate down to this level. Hence, the Åre Fm. in this study is of Hettangian to Pliensbachian age.

Based on a depositional modelling study of the Åre and base Tilje Fms. Heidrun Field performed by Statoil consultants in January 2005 a total of 21 *ichnotaxa* (trace fossils) were recorded. They combined these trace fossils into a set of recurring *ichnofabrics* (Ichnofabrics may be regarded as trace fossil building blocks of similar scale to lithofacies (Taylor et al., 2003)), named after the principal ichnotaxa present and a total of eight ichnofabrics associations were recognized (Table 3.1).

A key observation was the absence of the brackish-water indicator *Arenicolites carbonarius* in the fluvial dominated part of the Åre Fm., which was the main ichnological criterion used to separate lacustrine and bay-floor deposits, i.e. the lower, fluvial dominated succession from the upper marine influenced deposits. A number of workers have described *Arenicolites carbonarius*, often associated with *Planolites montanus* occurrences in variably salinity interdistributary bays (Eagar et al., 1985; Pollard, 1988; Moslow and Pemberton, 1988; Bromley, 1996), freshwater lakes (Bromley and Asgaard, 1979) and tidal sandflats (Ireland et al., 1978; Beynon et al., 1988). In the Åre Formation, *Skolithos* ichnofabrics are typical of bay-margin deposits subject to wave and current influence (in-house). *Taenidium* was observed in the lacustrine and floodplain sediments in the Åre; however, *Taenidium* is most common in marine depositional environments (Bromley, 1996).

3.4 Present study; identified facies associations

To obtain the best possible stratigraphic coverage of the Åre Fm., cored sections from wells 2, 4, 5 and 10 were selected for sedimentological interpretation. A sedimentological core description and correlation of the four cored wells interpreted in this study is attached at the end of this chapter. Stratigraphical overlap exists between the cored sections, enabling well to well correlation and nearly complete core coverage of the Åre reservoir zones (Fig. 3.1). These core interpretations form the basis for facies association descriptions and interpretation in this thesis. In general, the present study supports the work done by previous authors (e.g Svela, 2001; Gjelberg et al., 1987; Whitley, 1992), however with some differences related to the classification of fluvial channel type and their controlling

Table 3.1: Trace fossils and their depositional environmental habitat within the Åre Fm.

Ichnofabric	Depositional habitat
<i>Diplocraterion</i>	Transgressive shallow marine shoreface
<i>Planolites beverleyensis</i>	Transgressive shallow marine shoreface
	Tidal channel
	Sandy bay fill
<i>Skolithos</i>	Sandy bay fill
<i>Arenicolites carbonarius</i>	Tidally influenced distributary channel
	Muddy bay fill
	Sandy bay fill
<i>Planolites montanus</i>	Tidally influenced distributary channel
	Sandy bay fill
	Muddy bay fill
	Fluvial channel
	Lacustrine muds, Crevasse splay, Palaeosol
<i>Taenidium</i>	Fluvial channel
	Crevasse splay, Palaeosols, Lacustrine muds

factors (discussed below). This study is also including material and petrophysical logs from additional new wells (available due to consecutive drilling in the following years). The sediments of the Åre Fm. include conglomerates, sandstones ranging from very coarse (VC) to very fine (VF), mudstone and coal. The sediments are generally loosely consolidated; however, local calcite, ankerite and siderite cementation is encountered throughout the cored interval (Paper I). Description and interpretation of each facies association identified in the studied wells are carried out using examples from the sedimentological core log in combination with the petrophysical log responses (c.f. Figs. 3.2, 3.4, 3.5, 3.6, 3.7).

A total of eight facies associations are described and interpreted below, including stacked (multi-story) (MFCH) and meandering (single-story) channel (SFCH) sands, flood-plain fines (FF) (comprising three subfacies; flood plain (lacustrine) muds, peat swamps

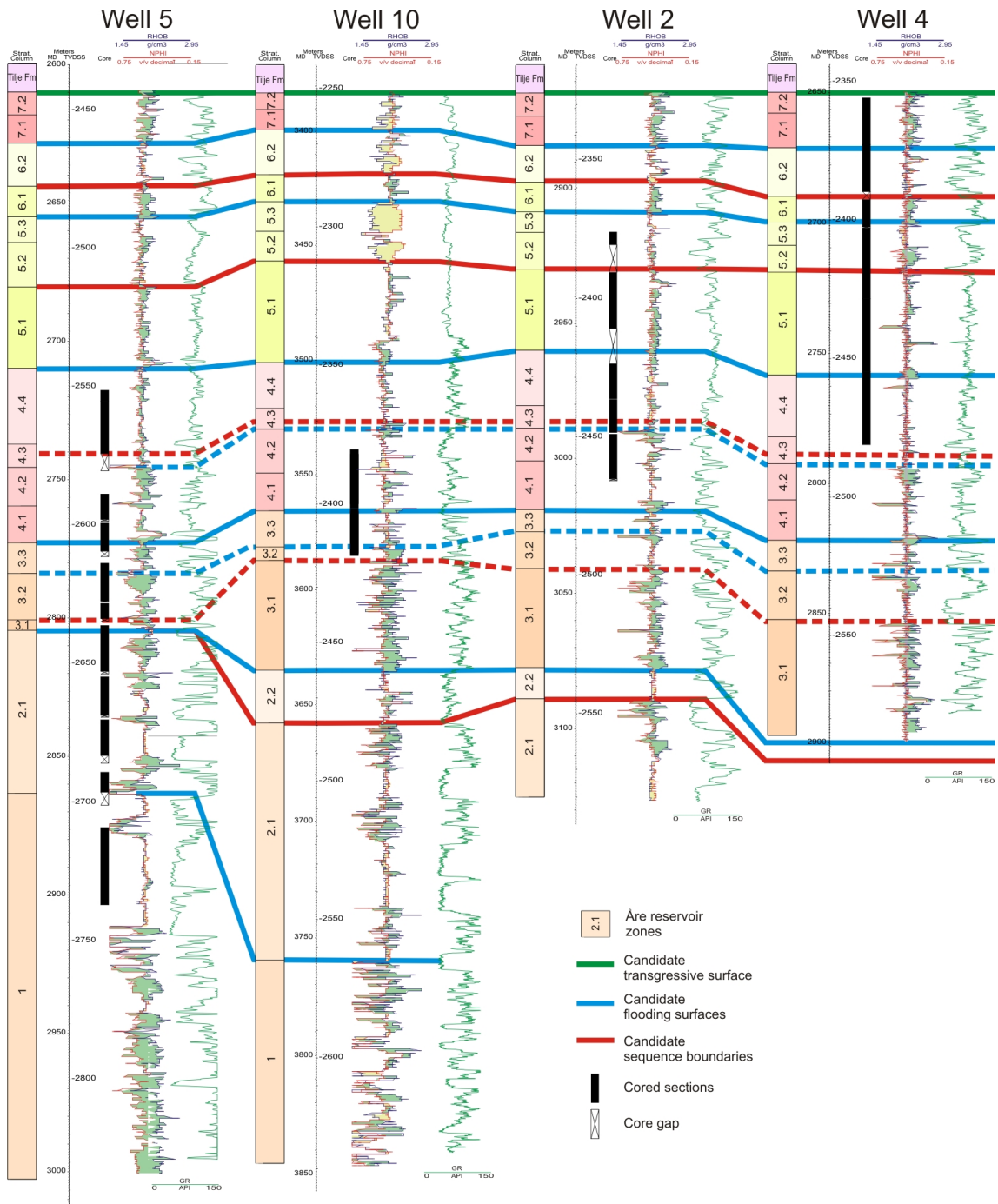


Figure 3.1: Overview of core coverage from wells, 2, 4, 5 and 10 used as sedimentological framework for well-to-well correlation. Sequence stratigraphic surfaces modified from Thrana et al. (2009)

and palaeosols), crevasse channels, -splays and -complexes (CCH), tidally influenced distributary channels (TCH) and lower delta plain interdistributary bay fills. Both sand prone (SBF) and mud prone (MBF) interdistributary bay fills occur. MFCH, SFCH, CCH, LEV and FF dominate the lower part of the Åre stratigraphy, gradually replaced by bay fill deposits and tidally influenced sediments upwards. Transgressive shallow marine shoreface deposits (TSMS) are interpreted in the uppermost part of the Åre Fm. indicating the gradual transition into the overlying Tilje Fm.

3.4.1 Stacked, multi-storey channel facies association (MFCH)

Up to 34m thick, medium to very coarse-grained sand successions comprising several amalgamated units, occur regularly in wells penetrating the lowermost part of the Åre Fm. The individual sand units, ranging from ~7 to 10m, display a blocky to slightly fining-up trend both in core and on wireline logs (Fig. 3.2 and Sedimentological logs attached). An erosional, gravelly base lag, often containing coal clasts, is observed in some units (Fig. 3.11(a)). Sedimentary structures are dominated by tabular cross stratification and occasional plane parallel stratification (Fig. 3.11(b)). Carbonaceous debris is also found on the foresets of some beds as thin, black, draping lamina (Fig. 3.11(c)). Set boundaries are normally erosional within co-sets. The upper boundary to the overlying coal is abrupt (Fig. 3.11(d)). No indications of marine influence are found. Two types of MFCHs are observed in the Åre Fm. Well-to-well correlatable MFCHs and single well MFCHs. They do, however, appear similar in core and on wireline log data. In the lower part of the fluvial interval, stacked sandstone units occur regularly above thick peat deposits. No clear well-to-well correlation of these successions is observed except for one particular unit described in Chapter 4. Further up in the Åre interval, a specific stacked sandstone interval (up to 34m thick in well 12) occurs at approximately the same stratigraphic level in several wells (Åre 2.2 zone) although in varying thickness (see Fig. 4.10 in Chapter 4.3).

The sedimentary structures observed and the overall relatively constant grain size, suggests that these deposits were laid down by a more or less constant unidirectional

current with shorter periods of changing energy level. The observed stacking of slightly fining-up units bounded by erosional surfaces, also indicates at least an element of vertical accretion. In the lower, single-well events, these sandstone units are interbedded in fluvial dominated strata (floodplain deposits), further emphasizing a fluvial origin for these sands, where the occurrences of coal clasts at erosional boundaries may indicate erosion of nearby vegetated floodplain or peat swamp deposits.

Successions displaying these features are often found in stacked (multi-story) channel complexes deposited during vertical accretion, such as sediments deposited by braided rivers on a braidplain, in an incised valley, or by anastomosing rivers on a stable, vegetated (often intensely) floodplain. The problem, however, is to elucidate whether these deposits represent either braided channel, incised valley fills as proposed by Svela (2001), channel sands deposited on a braidplain, or vertical accreted channel sands similar to anastomosing type rivers as interpreted by Gjelberg et al. (1987). A candidate incised valley, braided river deposit is observed in the studied wells, represented by the Åre 2.2 channel sandstone, reaching a thickness of 34m. Whether this unit was deposited as an incised valley fill or on a braid plain is uncertain; however, the thickness of up to 34 m suggests at least a factor of incision. In addition, a lag of rip-up clasts of peat is regularly observed at the base of the channel suggesting heavy erosion of floodplain deposits and possibly incision. Other MFCHs identified in the Åre Fm. are interpreted as anastomosing and exemplified by the stacked channel sand corresponding to the lowermost part of the cored section in well 5. As seen in cores and on wireline logs this sand interval is bounded above and below by thick *in situ* coals (Fig. 3.3).

In petrophysical log signature, the blocky appearance of the MFCH is easily recognized where the internal, fining-up units can be seen as small increases in GR, RHOB and NPHI. The sharp base and top, due to a sharp change in petrophysical parameters (coal) is striking. This is especially the case for anastomosing river deposits, where coals appear below, and above, the channel unit.

Permeability measurements display values in the Darcy range, indicating very good reservoir potential if the sands are lateral extensive with sufficient connectivity. As these

deposits are composed of relatively pure sand, their compactability is relatively low and limited to mechanical compaction processes (reorientation, rearrangement, crushing) and a 20% volume reduction has been measured (Hammer et al., 2009).

The different types of MFCHs are discussed further in Section 3.5 and in Chapter 4.

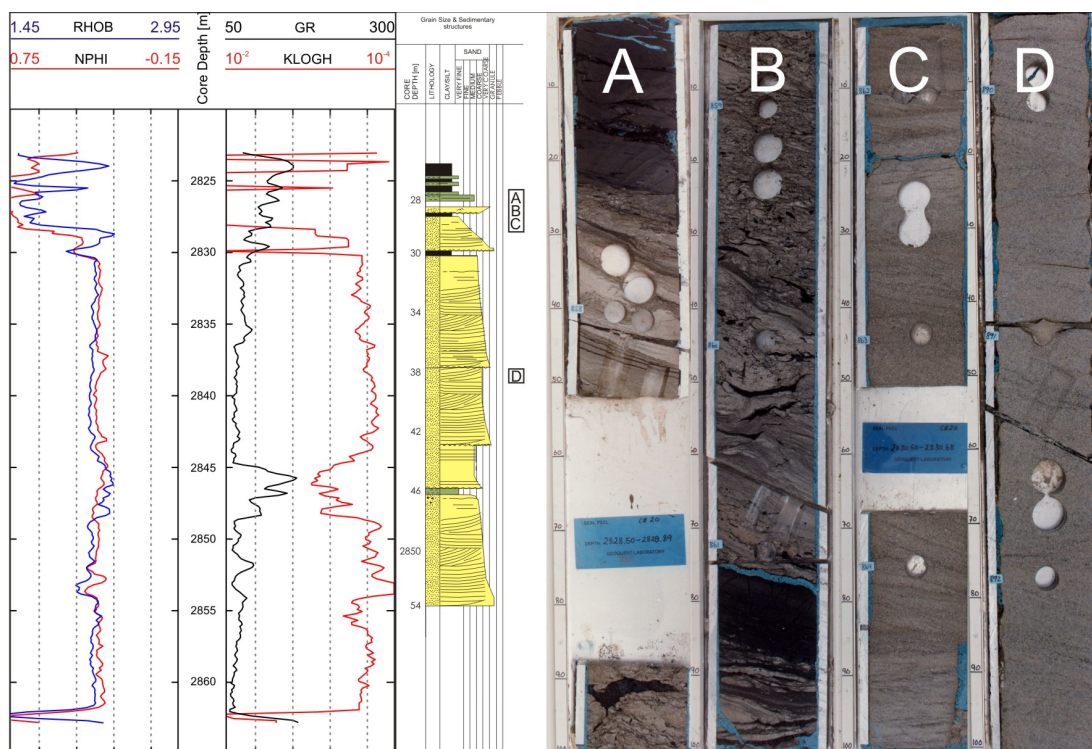


Figure 3.2: Wireline log signatures and core examples of multi-storey channel (MFCH) facies association illustrating the blocky nature of these deposits. The main body of the channel deposit comprises "clean" channel sand displaying excellent reservoir properties (high NPHI and KLOGH). Notice the abrupt change at the upper (seen on core A-C) and lower boundary of the unit on the wireline log data illustrating the abrupt change in sedimentation and depositional style. This change is possibly autogenic and resulting from peat compaction and avulsion.

3.4.2 Single storey channel facies association (SFCH)

This facies association comprises single, ~8 to 12m thick units with a distinct fining-up trend, ranging from very coarse sand at the base to fine sand and silt at the top. The

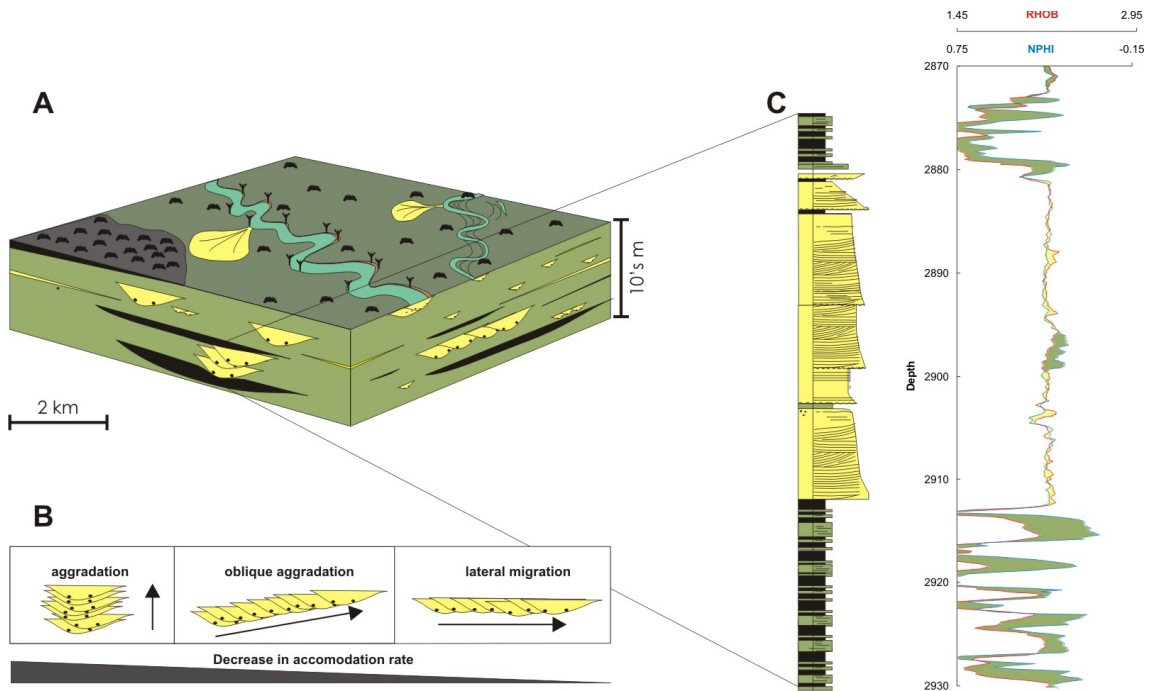


Figure 3.3: Stacked channel sands occurring interbedded in coaly FF (peat swamp) deposits. Interpreted and extrapolated sedimentological log from well 5. Modified from Rajchl and Uličný (2005).

lower boundary is erosional with occasionally distributed coal clasts. The lower part of the units display tabular- and trough cross stratification, grading into current ripples and plane parallel lamination towards the top, and shows increasing heterogeneity upwards. The units are regularly capped by heavily rooted silty successions, sometimes several meters thick, with coal often terminating these units (Fig. 3.12(a), 3.12(b), 3.12(c) and 3.12(d)). No marine water indicators are observed. Three reoccurring units are observed in well 5, and similar units are also observed in core sections from well 10 penetrating the same stratigraphic interval. The SFCHs mainly populate Åre 1, 2.1 and 3.1 although they have been identified up to the Åre 4.4 level (Leary et al., 2007).

The erosional lower base and the overall fining-upwards trend, from coarse sand to silt and the upwards increasing heterogeneity indicate a lowering of the energy level. In-

terpreted sedimentary structures also indicate reduced unidirectional current upwards through the successions. Also observed, in intervals of the same stratigraphic level, is the occurrence of this facies association with those of fine-grained, non marine, sediments interpreted as floodplain (lacustrine) muds, palaeosols and peat swamp coals (see below) suggesting a fluvial origin for the SFCH facies association. Combined, these observations suggest that the SFCH was deposited by meandering channels, i.e. point bar successions, on a vegetated floodplain. Coal clasts found at erosion boundaries suggest that the river cut into vegetated floodplain during avulsion. High sinuosity (meandering) channels formed a broad meander belt on the fluvial dominated Åre palaeoplain comprising a complex distribution of active and abandoned channels. Distal areas were probably dominated by flood plain deposits and occasional peat swamps, interbedded with overbank deposits (crevasses) in closer vicinity to the channels. The heavily rooted upper part of the pointbar represents paleosols and may sometimes be capped by *in situ* coals representing peat swamp deposits. The pointbars comprising parts of the lower Åre Fm. have a distinct petrophysical signature (Fig. 3.4). Intervals of decreasing GR and increasing NPHI and RHOB constitute easily recognizable features on wireline log data. Based on this characteristic petrophysical signal trend, three SFCHs can be identified in well 5, which is confirmed by sedimentological interpretation of core data. This interpretation is supported by Svela (2001) who interpreted the single storey channel deposits as lateral channel accretion, developing pointbar successions.

3.4.3 Floodplain fines facies association (FF)

Successions of predominantly fine-grained sediments (very fine sand, silt and coal) comprise up to 6m thick intervals in the well 5 core and even thicker units are observed on wireline log data from un-cored sections from the lower most part of the Åre Fm. The FF facies association comprises three subfacies: Relatively pure coal (subfacies 1) intervals occur regularly within the Åre succession (Fig. 3.13(a)), where one stratigraphic level in particular displaying a concentration of coal layers is referred to as Åre Coal marker. These coals

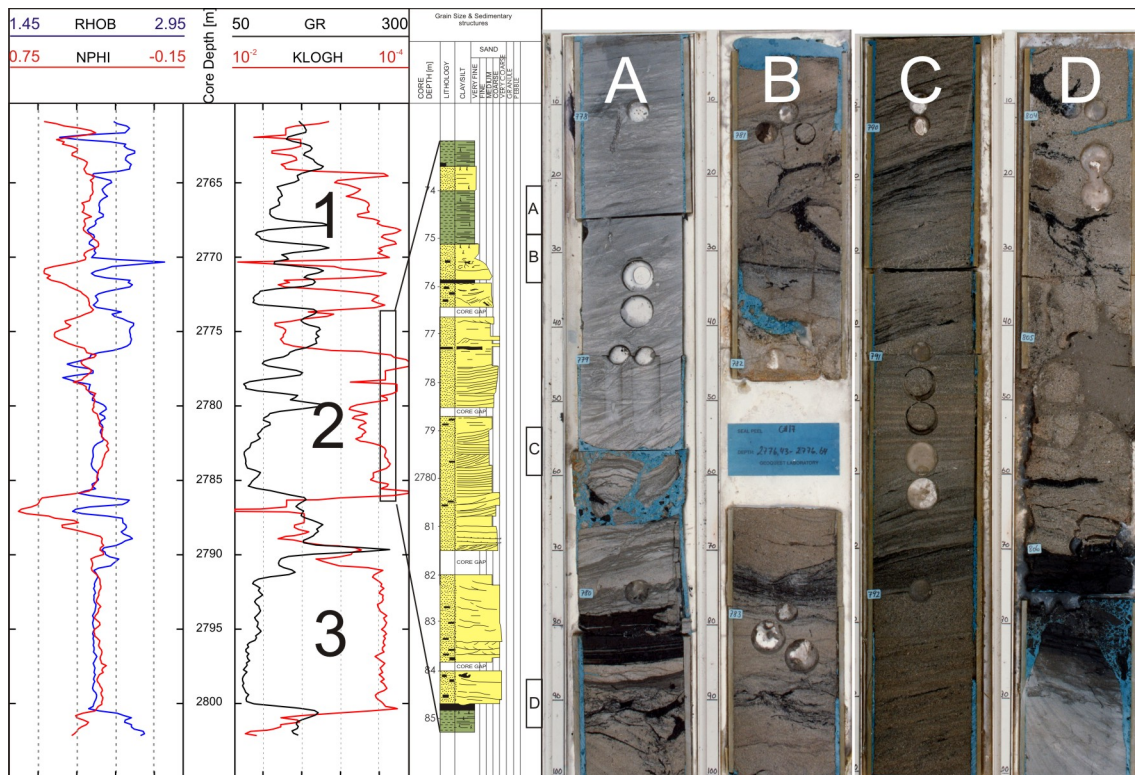


Figure 3.4: Wireline log signatures and core examples of single-storey channel (SFCH) facies association. The fining-up trend is clearly seen on both sedimentological (core-sections A-D) and wireline log data. Three channel units can be observed in the presented interval (1-3). Notice the basal erosion surface directly above a thin coal in core-section. A coal interval has been observed in several channel deposits in the Åre Fm. illustrating the erosion resistance of such peat layers.

are regularly underlain by pedogenic reworked intervals (subfacies 2) displaying rootlets as cm thick and dm long structures (Fig. 3.12(c)). Some intervals, confined to the lower part of the Åre Fm., exhibit significant pedogenic reworking and appear "bleached" in places (Fig. 3.13(b)). These intervals are largely confined to dm- to m scale thicknesses, occasionally up to several m thick siltstones, and very fine sandstones. Very fine-grained sand laminae with sharp lower boundaries appear in some places, with plane parallel lamination and current ripples (Fig. 3.13(c)), although primary sedimentary structures have mainly been replaced by pedogenic alteration. The third subfacies is dominated by plane parallel

laminated siltstones and claystones. Occasional rooting is present, although the majority of primary sedimentary structures have been preserved (Fig. 3.13(d)). No marine water indicators have been found in these deposits. The mudstones often appear as dark to black organic rich mudstones with a TOC content of about 20% to nearer 50% in the true coals (Leith, T.L., pers.comm. 2009).

The fine-grained material constituting this facies association and the sedimentary structures observed therein indicate a low flow regime with occasional pulses of increased flow energy levels. These pulses are represented by the very fine to fine-grained, plane parallel to current rippled sand. The intensely rooted horizons capped by coal suggest that the coals and the underlying pedogenic reworked zone are formed *in situ*. This is also supported by the presence of a bleached zone directly below some coals suggesting acidic waters influence. Destruction of organic matter resulted in bleaching of the sandstone below by dissolution of labile components. The coals are interpreted as peat swamps developed during a high and rising base level, and the rooted intervals constitute palaeosols, and may be regarded as *in situ* seat-earths (Jackson and Bates, 1997). The thin, fine-grained sand fringers, occasionally current rippled, are suggested to represent crevasse splays deposited during floods, whereas the plane parallel laminated siltstones and claystones are interpreted as lacustrine muds deposited in shallow ponds and lakes.

According to Statoil data the rare occurrence of *Planolites montanus* and *Taenidium* ichnofabrics reflects the preservation of an "aquatic" signature prior to, or as an interruption to, pedogenesis.

On wireline logs FF differs from other fine-grained deposits by high RHOB ($\sim 2.53 \frac{g}{cm^3}$) and NPHI (45 LPU) values (Fig. 3.5). FF also appears less heterolithic as compared to MBF (discussed below) and comprise thicker (up to >10m thick) intervals. Coals are easily recognized on petrophysical log intervals of very low RHOB and very high NPHI. As discussed in Chapter 4 and Paper II, the compactability of FF deposits, especially the timing and magnitude of compaction of coals, is critical when concerning decompaction studies and fluvial reservoir reconstruction, since coals compact significantly more than mudstones, and mudstones more than sandstones.

The relatively regular occurrence of peat swamps and palaeosols indicates a relatively wet climate and swampy conditions (poorly drained). Regarding correlation a distinction should be made between coals deposited in peat swamps on floodplains, which may be of limited correlatable value, as compared to peat swamps developed during the abandonment phase of bay fill cycles, which may be several km wide and act as local correlation surfaces (Chapter 4).

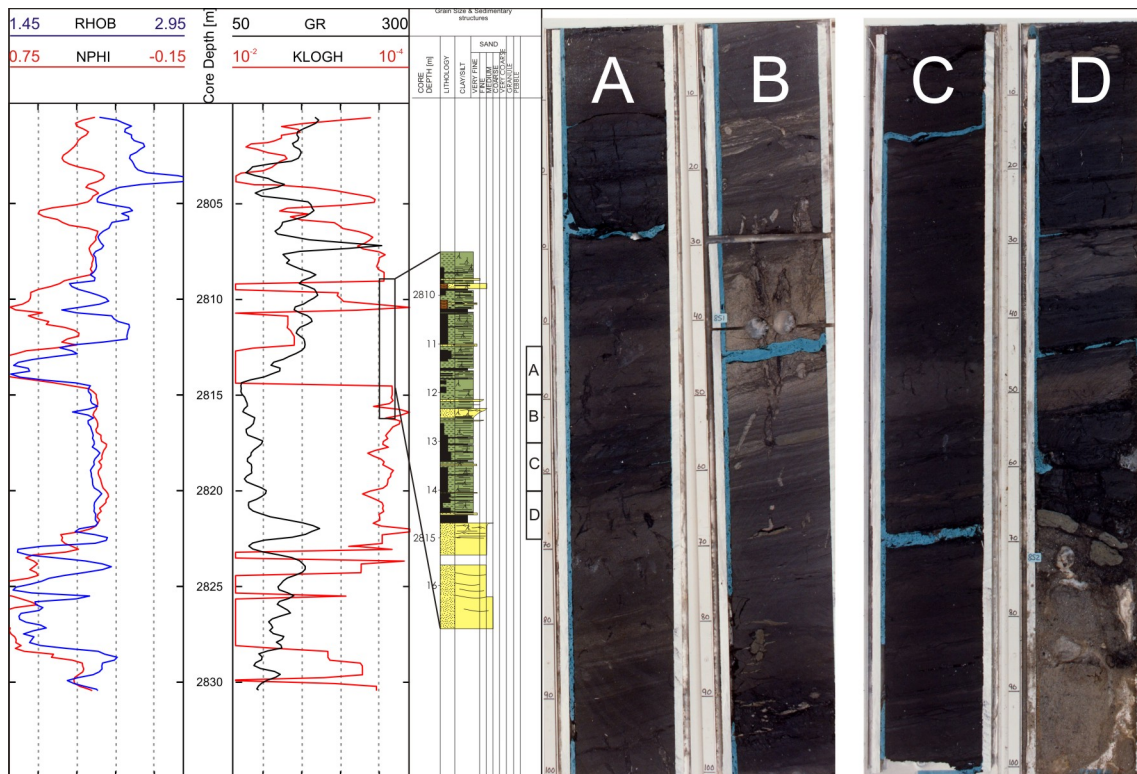


Figure 3.5: Wireline log signatures and core examples of floodplain fines (FF) and crevasse (CCH) facies associations. The deposit is organic rich seen as dark grey to black color on the core photographs indicating relatively wet floodplain conditions. The thin coarsening sand at 2812.5m is interpreted as a levee deposit. A crevasse splay deposit is seen at approximately 2810m. Wireline log signatures showing very low RHOB and equally high NPHI values indicate the presence of coal interbedded in high RHOB and low NPHI intervals displaying higher GR values. These comprise intervals of lacustrine mudstones/claystones and paleosols.

3.4.4 Crevasse facies association (CCH)

This facies association comprises up to 2m thick units of siltstones and sandstones with grain sizes ranging from very fine to medium. The units display a relatively sharp, often erosive or loaded base, followed by a fining up trend often with an abrupt upper boundary (Figs. 3.14(a) & 3.14(b)). Sedimentary structures such as plane parallel lamination and current ripples are dominant, as are climbing ripples (Figs. 3.14(c) & Fig. 3.14(d)). Rooting occurs regularly, in some places it is intense. CCH appears closely associated with floodplain deposits (paleosols, lacustrine muds and peat swamp deposits) or occasionally as discrete beds within bay-fill deposits (Fig. 3.5). Complexes comprising up to 6m thick units with internal erosional boundaries also occur regularly.

The presence of climbing ripples indicates high rates of net deposition as in decreasing flows, such as river floods (Allen, 1971). The regular occurrence of CCH sandstones interbedded in floodplain deposits indicates a close relation between them and suggests that CCHs are crevasse sands deposited as a result of channel-breaching during peak floods. If the levee breaks at approximately the same place on several succeeding flooding episodes, complexes of stacked crevasse sands may develop, as observed in the Åre Fm (e.g. at 2815-2817m in well 5). During normal conditions vegetation starts to develop, which may result in the development of paleosols if enough time is available and conditions are favorable.

As CCH deposits predominantly comprise sandstone with increasing abundance of silt and organic matter (roots) towards the top, compactability is probably similar to that of SFCH. A clear distinction between CCHs and SFCHs on wireline logs, except possibly thickness to some extent, is difficult and therefore treated alike when it comes to decompaction studies in Paper II. On petrophysical logs crevasse deposits are seen as intervals thinner than 8m of higher NPHI and lower PHOB values in sections dominated by FF signature. A few meters thick coarsening up unit from very fine to medium-grained sand probably represents a levee deposits composed of a stack of subsequently coarser CCH deposits in well 5 at 2812-2813m. Sedimentary structures are plane parallel lamination

changing gradually upwards into current ripples and intense rooting. Intense vegetation is common due to the steady influx of fresh nutrients and clastic material from the river.

3.4.5 Bay fill facies association (SBF/MBF)

This facies association comprises on average 3-5m thick coarsening units (up to 10m thick intervals has been observed in well 2), often composed as a silty lower part (MBF) and a sandier upper part (SBF), usually of very fine sand grade (Fig. 3.15(a) & (Fig. 3.5)). Dark, organic rich mudstones are common in the lower, more fine-grained interval (Fig. 3.15(b)). A more light colored and siltier unit follows, which in part displays plane parallel lamination and occasional wave ripples (Fig. 3.15(c)), whilst the upper, sandier part is dominated by current ripples, wave ripples and hummocky cross-stratification (Fig. 3.15(d)). Internal erosion-surfaces are common. Rooting in the upper part is commonly associated with coals occasionally capping the units. Trace fossils *Arenicolites carbonarius*, *Planolites montanus* (Statoil) and *Skolithos* (Kjærefjord, 1999) are also found in these units. Small, vertical, up to a few centimeter deep, wrinkled threads of sand in mudstone are located throughout the more fine-grained parts of this facies association (Fig. 3.16(a)). These threads are common features in MBFs and SBFs while no such threads have been observed in FF deposits.

These observations suggest that the coarsening units were deposited in a semi-protected bay environment where shifting salinity occurred regularly (synaeresis). A fluvial dominated environment generates deltas with bird-foot morphology (similar to the Mississippi delta) and inter-distributary bays. The filling of most inter-distributary bays is dominated by fluvial processes, and they may be both sand filled and/or mud filled. The organic rich silt at the base indicates periods with very low sedimentation rate and anoxic conditions, preserving organic debris. This is interpreted as an early phase of filling after the drowning of older bay fills during a relative base level rise. The siltier/sandier sediments are deposited during elevated energy levels (floods), and the sands are the result of crevassing, equivalent to the crevasse splay. These sands are then later reworked by waves forming

wave ripples and hummocky cross-stratification. If time and source material were available, these events would have filled the entire bay and eventually lead to intense vegetation and peat formation, which is regularly observed in the Åre Fm. The cm-sized, sand filled threads are interpreted to be synaeresis cracks. Such cracks develop sub-aqueous as a result of shrinkage of rapidly floccated clay or clay that has undergone shrinkage of swelling-clay mineral lattices owing to increase in salinity of surrounding waters (dehydration) (Burst, 1965). This can occur either by deposition in saline waters, where salinity increases due to evaporation, or when the sediments, usually clay/silt, are deposited in fresh water and later flushed by marine incursions (sediments are sub-aqueous at all time). The latter is suggested for the synaeresis observed in the Åre Fm. at Heidrun. The cracks are later filled with sand, buried and compacted to form the zig-zag shaped geometry seen in core sections.

The fine-grained hummocky cross stratified sandstones are interpreted as storm-reworked bay fill deposits. Kjærefjord (1999) interpreted these deposits as wave influenced bay fill and that during periods of delta lobe switch, the distributary-mouth bar sands of the old delta lobe were subjected to wave reworking. Delta lobe switching is an autogenic process that results in the deposition of parasequences originating from avulsion, which causes the abandonment of previously active delta lobes (Emery and Myers, 1996). An abandoned lobe subsides and is transgressed, generating a local flooding surface, represented by coals capping the bay fill successions. These coals may be locally correlatable surfaces as compared to the peat swamp coals deposited on the floodplain. The process is repeated, generating a stacking of bay fill deposits as observed in the upper part of the Åre Fm (i.e. Åre 5). Due to the presence of roots and coals in these units, the water depth must have been relatively limited. According to Kjærefjord (1999) such bay fills are usually 2 to 8m thick and 2 to 7km wide.

Upwards through the Åre stratigraphy *Arenicolites carbonarius* first starts appearing in the bay fill deposits (in-house data, Leary, S., pers.comm. 2005). This trace fossil is often described from brackish environments (interdistributary bays) (Eagar et al., 1985; Pollard, 1988; Moslow and Pemberton, 1988; Bromley, 1996) and the observation was used

as an indicator for a marine flooding surface (Top Åre 3.3). On wireline logs these bay fill cycles are easily seen as stacks of coarsening intervals on GR. Individual bay fill cycles as well as stacks of progressively coarser or finer bay fill units can be recognized. These stacking patterns can be used in sequence stratigraphic interpretations as discussed further in Ch. 4. As SBFs display a slightly lower volume reduction (17%) during compaction compared to FCHs (20%), they are separately modelled in the decompaction study in Paper II. Regarding MBFs, however, although relatively muddy, these are modelled significantly differently compared to FF mudstones. As revealed from diagenetic investigations (Hammer et al., 2009), a 10% bulk volume of pre-compactional formed siderite cement occurs regularly within MBFs which resulted in a 10% greater porosity preservation (Inter Granular Volume) during burial compared to FF mudstones.

3.4.6 Tidally influenced distributary channel facies association (TCH)

Fining upward units, up to 10 m thick, displaying a lower sandy part and an upper heterolithic interval occur in the upper part of the Åre Fm (Åre 3 and upwards). These deposits may sometimes comprise a stacked complex of individual channels which are suggested correlatable between wells (Chapter 4). The lower, sandy part displays an erosional base and usually comprises fining upwards, fine to medium-grained sandstone displaying tabular and trough cross stratification (Fig. 3.7). Carbonaceous drapes are common together with coal and mud intra-clasts (Fig. 3.16(c) & 3.16(d)). Upper coarse grained concentrations occur at bed bases enhancing foreset definitions. The units fine upwards into more heterolithic intervals of alternating lenticular and flaser bedded deposits comprising fine to very fine sandstones and mudstones (Figs. 3.17(a), 3.17(b), 3.17(c), 3.17(d) & 3.18(a)). Mud drapes, often paired, are common. The unit is regularly capped by an interval of carbonaceous siltstone, displaying rootlets and sometimes *in situ* coals (Fig. 3.18(b)).

Sedimentary structures, such as double mud drapes and colonizations by distinctive brackish water ichnotaxa *Arenicolites carbonarius*, (Statoil - in house), indicate variable

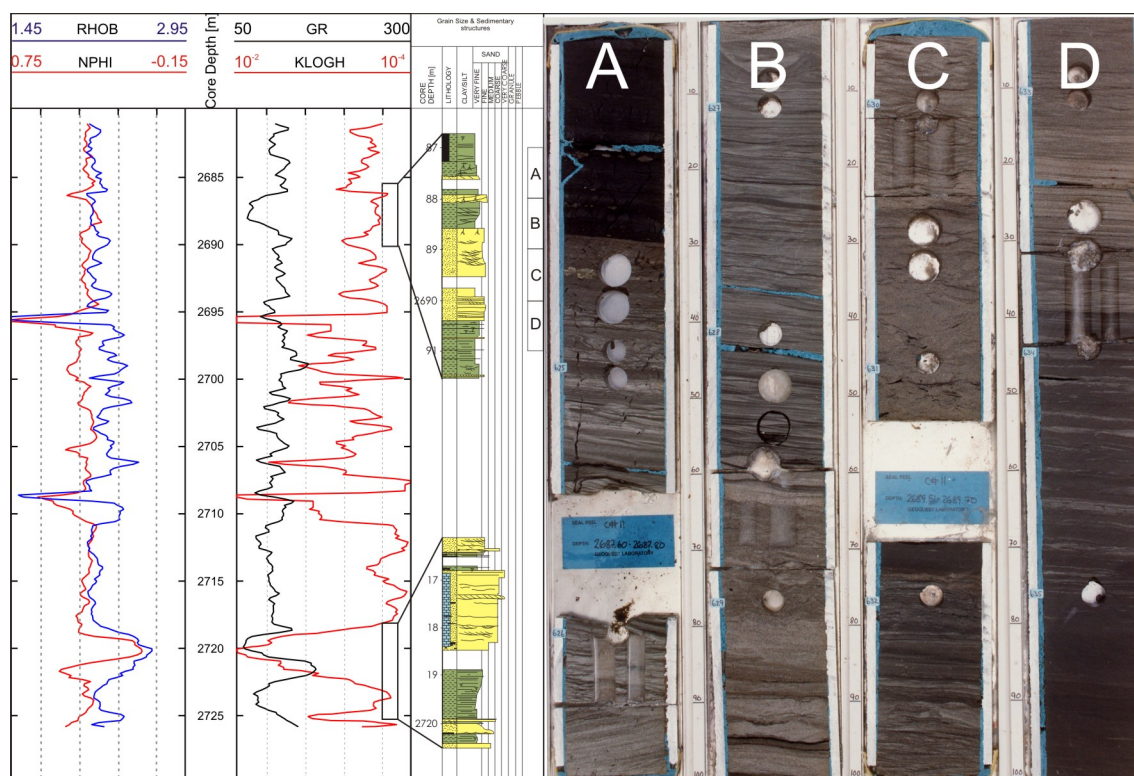


Figure 3.6: Wireline log signatures and core examples of sandy (SBF) and muddy (MBF) bay fill facies association. Core photographs show a clear coarsening trend from core-section D (MBF) to A (SBF) capped by coal. A clear trend of increasing GR and KLOGH values are observed from the base to the top of individual bay fill units as observed on the uppermost bay fill cycle. A slight decrease in RHOB and similar decrease in NPHI is also observed. For the lowermost bay fill cycle a cemented zone is masking the petrophysical signal profile.

influence of tidal energy during deposition of these units. The lower sandstone interval, comprising cross stratified sandstone, shows possible tidal influence in the form of carbonaceous and silty drapes on foresets. The overlying heterolithic interval, comprising flaser to lenticular bedding with common mud drapes, sometimes double, and locally rooted, is strongly suggestive of tidally influenced accretionary channel-margin deposits. Furthermore, the presence of *Planolites montanus* and, in the overlying heteroliths, *Arenicolites carbonarius*, indicates brackish water influences within the channel. A typical example of a discrete, single storey TCH fill is observed in core interpretation of well 4 at 2715.40-

2708.00m. Tabular and trough cross-stratified, fine to medium-grained sandstones defined by carbonaceous and micaceous drapes, fine upwards to thinly bedded, rippled, silty fine to coarse-grained sandstones, and is capped by a carbonaceous siltstone interval with rootlets and *in situ* coals. The presence of underlying and overlying MBF deposits, with the same ichnotaxa, suggests that the distributary channel developed proximal to the margins of an embayment, possibly feeding a bay fill cycle down-dip. Separating TCH from SFCH on wireline logs is difficult. The two-part structure of the TCHs may be evident in some places, such as the drop in permeability (KLOGH) observed at 2740m in well 5 in Fig. 3.7. The stacked TCH complexes occurring in Åre 3.2, 4.2, 5.2 and 6.2 are suggested to represent significant base level events (Chapter 4).

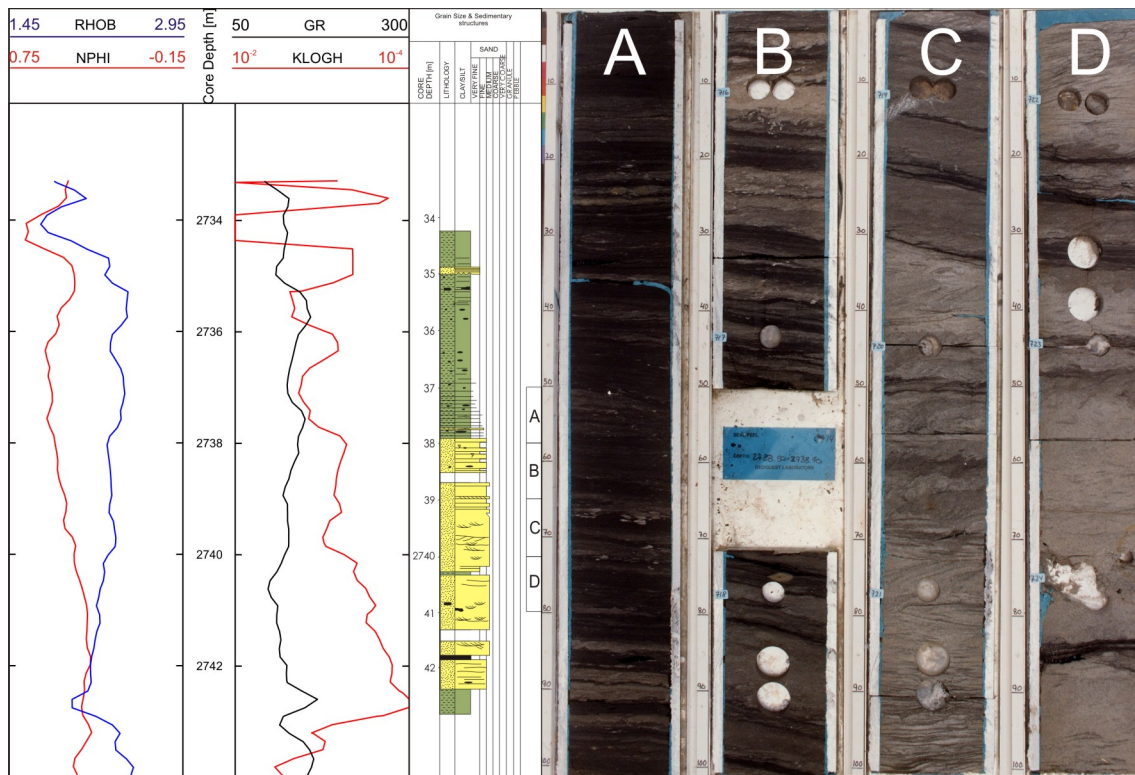


Figure 3.7: Wireline log signatures and core examples of tidally influenced channel (TCH) facies association. A significant drop in KLOGH response is observed at the transition from the lowermost "clean" sandstone interval to the overlying more heterolithic channel fill at ca 2740m. A slight increase in GR is also observed at this transition.

3.4.7 Transgressive shallow marine shoreface facies association (TSMS)

The uppermost part of the Åre Fm. comprises heterolithic deposits of alternating cm scale mudstones with cm scale, lenticular to wavy, very fine to medium-grained sandstones (Figs. 3.18(c) & 3.18(d)). The sandstones often display ripple cross lamination. Some units are more sand-dominated, occasionally comprising swaley and hummocky cross-stratification, alternating with more fine-grained wave rippled cross laminated sandstone. A vertical U-shaped spreiten burrow identified as *Diplocraterion parallelum* Torell, 1870 (c.f. Fürsich, 1974a) (e.g. Fig. 3.18(d)) is present just above the base Tilje transgressive surface (c.f. Chapter 4). *Diplocraterion* is classified as a domichnial permanent dwelling structure (Bromley, 1996) produced by suspension feeders or benthic predators (Fürsich, 1975). They are characteristic of high-energy, intertidal shallow water environments (e.g. Fürsich, 1974a), and has recently been described by Bromley and Uchman (2003) from the Jurassic of Bornholm and interpreted as the result of a local transgression.

These sediments are suggested deposited in an environment characterized by mixed wave and tidal influence (similar to base of the Tilje Formation) and interpreted as heterolithic, transgressive subtidal heteroliths, or, as suggested by Leary et al. (2007); Kjærefjord (1999), comprising transgressive shallow marine shoreface deposits (TSMS).

The similarities in the sediments of the Top Åre and base Tilje Fms. demonstrate the transitional character of the Åre - Tilje boundary. TSMSs are recognized on wireline logs as the transition from the sandy deposits of Åre 6.2 below, into more silty TSMS deposits displaying a higher NPHI - RHOB separation (Fig. 3.8). The top Åre 6.2 boundary is identified in cores as a very coarse-grained lag, 1-2cm thick (Fig. 3.16(b)).

3.5 Discussion on MFCH and their driving mechanisms

The facies associations interpreted for the Åre Fm. indicate a fluvial to lower delta plain depositional environment where their vertical stacking suggests a deepening event throughout the Åre epoch as described in Chapters 2 and in earlier work by others. Some differences in the interpretation of depositional controlling factors and terminology are however pro-

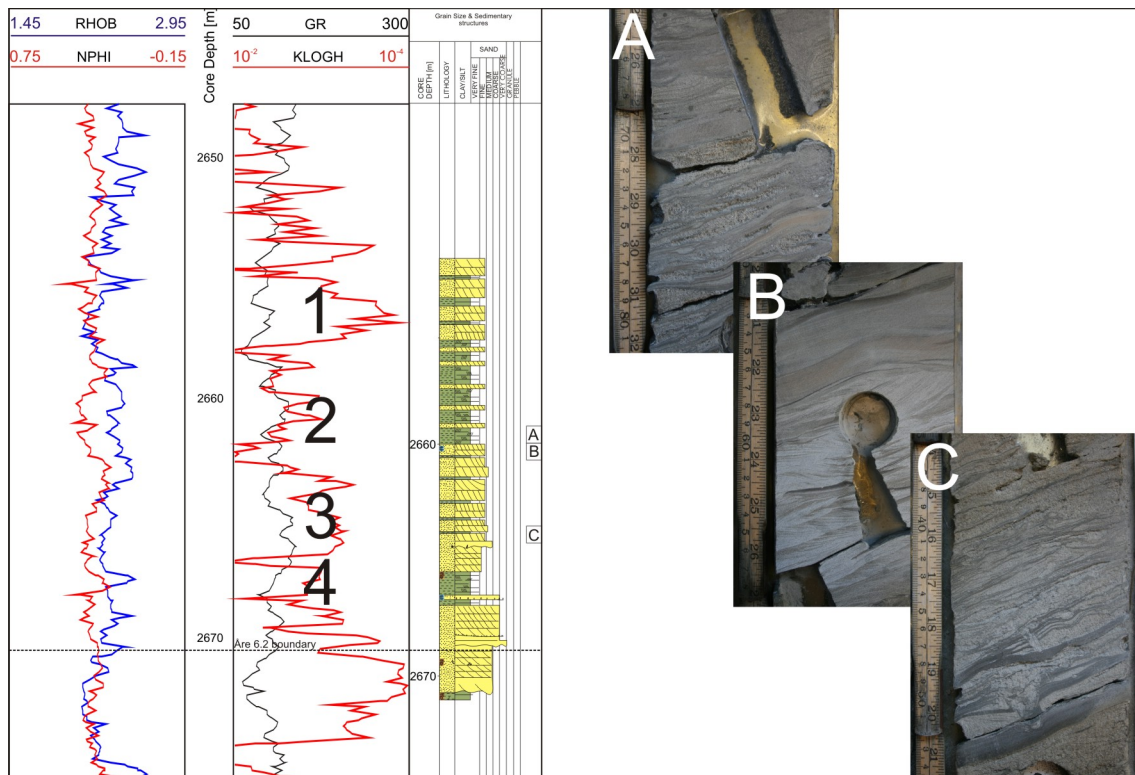


Figure 3.8: Wireline log signatures and core examples of transgressive shallow marine shoreface (TSMS) facies association. TSMSs are recognised on wireline logs as the transition from the sandy deposits of Åre 6.2 below into more silty TSMS deposits displaying a higher NPHI - RHOB separation. The alternating intervals of mud dominated (2 & 4) and sand dominated (1 & 3) intervals can be seen as high KLOGH intervals in sand prone TSMS whereas mud prone TSMS display low KLOGH intervals and slightly higher RHOB-NPHI separation. No clear fining or coarsening trends are observed.

posed, and are related to the occurrence of the vertically aggraded channel sands described above.

River channel patterns are controlled by three factors; discharge, sediment supply and gradient (Bridge, 1985), in addition to sediment compaction. These factors are again controlled by sea level change, climate and tectonic activity (discussed further in Section 4.1.1). Based on sedimentological interpretation of core data and petrophysical wire line log signatures, three different types of fluvial styles are recognized within the Åre Fm.;

braided, meandering and compactional-driven anastomosing. Of these three, two types of stacked channel deposits (MCFHs) occur in the Åre Fm. They look quite similar in both core and on wireline logs, however their nature and origin relates to somewhat different controlling factors.

The up to 34m thick, lateral correlatable sand unit corresponding to the Åre 2.2 reservoir zone (See Section 4) could have been deposited by braided rivers as an incised valley fill following a base level fall and subsequent rise. Braided rivers usually form where the system is dominated by coarser grain sizes where the lack of cohesive bank deposits leads to rapid channel course shifts as in an incised valley. Whether or not the unit is exclusively controlled by base level fall or merely the result of a decrease in base level rise, decreasing accommodation space creation, resulting in deposition of a sand sheet braid plain, is uncertain as both scenarios would result in the deposition of a laterally persistent sand unit with an erosive base. However, due to the vertical dimension in some wells (up to 34m), and the fact that the unit thins towards the southeast, suggests at least a factor of incision. In addition, preserved floodplain facies have been identified, interbedded in this sand unit which may constitute remnant valley terraces. According to Emery and Myers (1996) terraces are common in incised valleys. Another factor that would strengthen the interpretation of an incised valley fill for this unit is the presence of a well developed paleosol on the interfluves due to prolonged exposure during the period of incision. This paleosol will be the continuation onto the interfluves of the sequence boundary at the base of the valley such as suggested for the fluvial Dunvegan Fm., NE British Columbia, Canada (e.g. McCarthy et al., 1999; McCarthy and Plint, 1998). However, no clear differentiation between "normal" paleosols and paleosols associated with a sequence boundary of this type can be made from the studied data. Regarding the vertically aggraded channel sands in the lowermost part of the Åre Fm. (Åre 1 & 2.1), the occurrence of these channel sands directly above thick peat (now coal) units suggests that they are, at least in part, anastomosing channel deposits. Calculating the fraction of decompacted sand vs. decompacted coal, as discussed in Paper II, reveals a possible correlation between channel sands and peat deposits (Fig. 3.9). This further suggests that the compaction of peat may have acted as

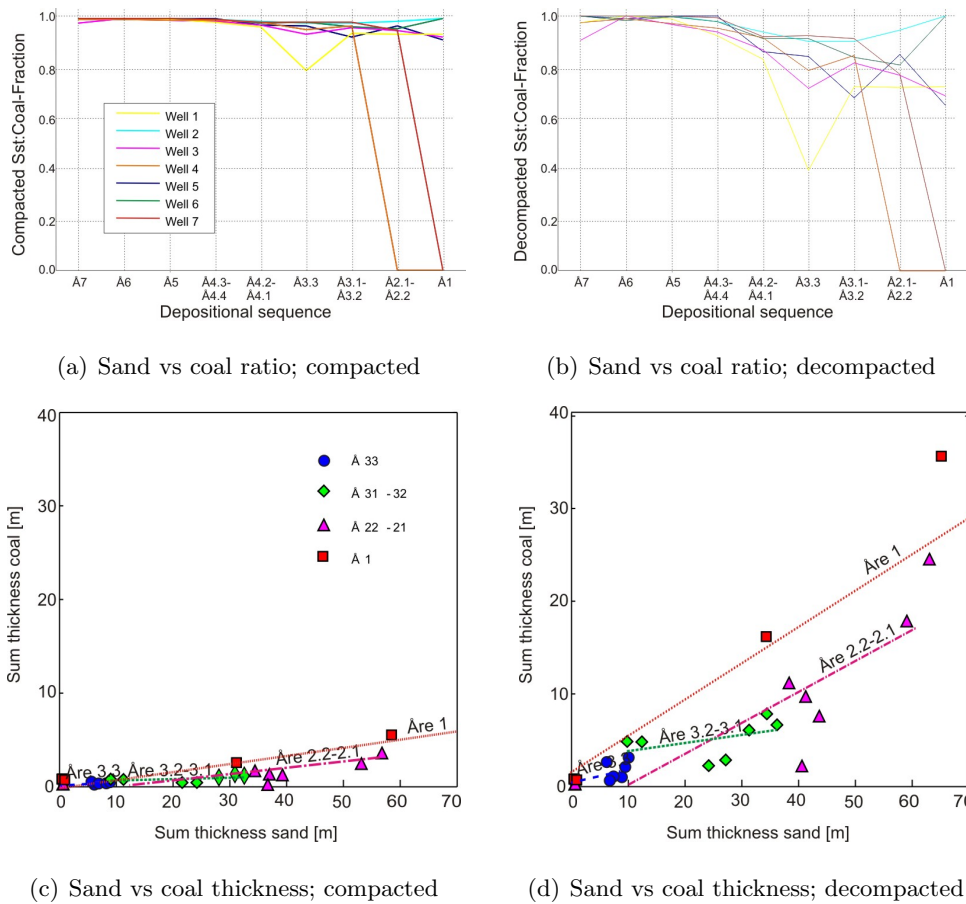


Figure 3.9: Plots displaying a trend of correlation between thickness of sand vs thickness of coal suggesting a peat-to-coal compaction controlling factor on the presence of sand units (c.f. Rajchl and Uličný, 2005). (a) and (b) are plots of compacted and decompact sand-to-coal ratios indicating the importance of early compaction of peat in the fluvial part of the Åre Fm. (c) and (d) display the correlation between thickness of sand vs thickness of coal displayed for four reservoir zones in seven wells.

a channel catchment ("channel catching"). Accommodation space may have been created due to peat compaction (c.f. Rajchl and Uličný, 2005) as it would be expected that the weight of the sand laid down by the river would compact the underlying peat, increasing accommodation space further, consequently resulting in more sand being deposited, hence

vertical accretion. These observations strongly suggest that anastomosing rivers deposited these units. Anastomosing rivers form interconnected networks of low-gradient, relatively deep and narrow channels of variable sinuosity, characterized by stable, vegetated banks composed of fine-grained silt or clay (Smith and Smith, 1980; Rust, 1981; Smith, 1983; Smith and Smith, 1980). Lateral channel migration is limited by the highly vegetated, relatively cohesive (fine-grained silt or clay) bank sediments, and occurs through avulsion i.e. by flooding events resulting in breaching and crevassing of the river banks leading to the subsequent formation of a new channel course. The depositional environment for the Åre Fm. is interpreted to be very similar to this description, although such rivers may form in a variety of climates: warm arid (Gibling et al., 1998; Rust, 1981), warm humid (Wang et al., 2005), savanna-humid tropical (Smith, 1986), temperate-humid (Gradzinski et al., 2003) and temperate-cold (Smith and Smith, 1980). A comprehensive review of anastomosing rivers has been published by Makaske (2001) who also defined these based on channel pattern and floodplain geomorphology: "An anastomosing river is composed of two or more interconnected channels that enclose floodbasins". Anastomosing rivers may form in two ways (Fig. 3.10). Either the substratum is highly compactable (i.e. peat) and the sediments aggrade due to peat compaction (e.g. Rajchl and Uličný, 2005) in a process which is here termed channel catching, or by vegetation producing an erosive-resistant peat layer or cohesive bank sediments stimulating aggradation of bedload material on the channel bottom, contributing to avulsion by blocking the channels (Gradzinski et al., 2003). Vertical accretion of the peat layer that covers the intra-channel areas controls the rise of the depositional system. The interpretation of these units as anastomosing channel sands is in accordance with the interpretation of Gjelberg et al. (1987), although they did not comment on the peat-to-coal compaction as a factor influencing the vertical accretion. They did however interpret all the channels in the Åre Fm. as anastomosing. This is not the case as some deposits are clearly meandering in origin as discussed above. Svela (2001), on the other hand, interpreted all vertical aggraded channel sands that seemed to be correlatable between wells as incised valley fill laid down by low sinuosity braided channels, and he related these deposits to a relative fall in sea level (i.e. LST deposits

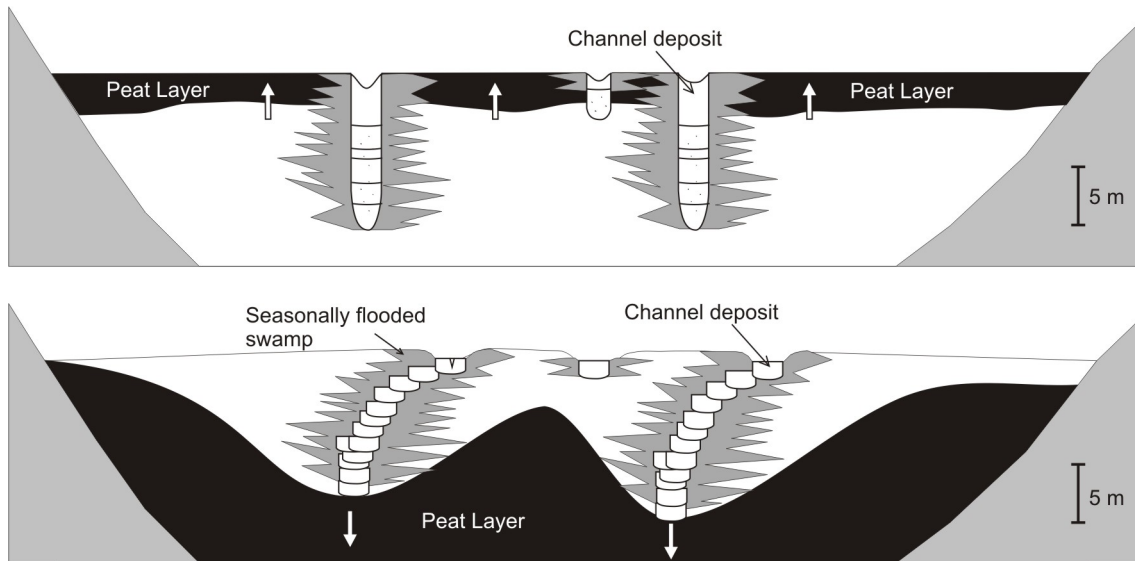


Figure 3.10: Upper: Anastomosing river deposits formed by avulsion in an erosion-resistant bank sediment environment (after Gradzinski et al., 2003). Lower: Anastomosing river formed by aggradation due to peat-compaction. Note the shift from vertical, to oblique to lateral channel migration due to decreasing accommodation rate reflecting declining compactability of the peat layer (after Rajchl and Uličný, 2005)

(Van Wagoner et al., 1990)). Svela (2001) based his interpretation on the observation of the abrupt change from the underlying fine-grained floodplain deposits, and the fact that these sands could be correlated between wells. Erosion resistivity of the underlying peat caused the channel to migrate laterally, as opposed to vertically, extending the lateral dimensions of these channel fill (Svela, 2001). A component of lateral migration due to erosion-resistant peat may have occurred, however peat compaction must have been at least a factor with regards to accommodation space creation. Similar features with vertical aggraded channel fills overlying relatively thick units (several meters) of highly compactable peat deposits are observed in several wells in this part of the stratigraphy on Heidrun suggesting a control of peat compaction on the vertical stacking of channel sands. The observation of accommodation space creation due to compaction of peat also illustrates the importance of defining depositional patterns in fluvial deposits by base level

terminology as accommodation space may be independent of sea level fluctuations (See discussions in Ethridge et al., 1998; Shanley and McCabe, 1994). The Exxon terminology (Van Wagoner et al., 1990) relates to sea level changes and may therefore be insufficient for application in fluvial deposits, especially when lacking a clear connection to the marine realm.

In Chapter 4 the interpreted facies associations are discussed in relation to base level changes and a sequence stratigraphic interpretation of the Åre Fm. is presented based on regional wireline log correlation, applying the interpreted log response of each facies association in addition to core data where available.

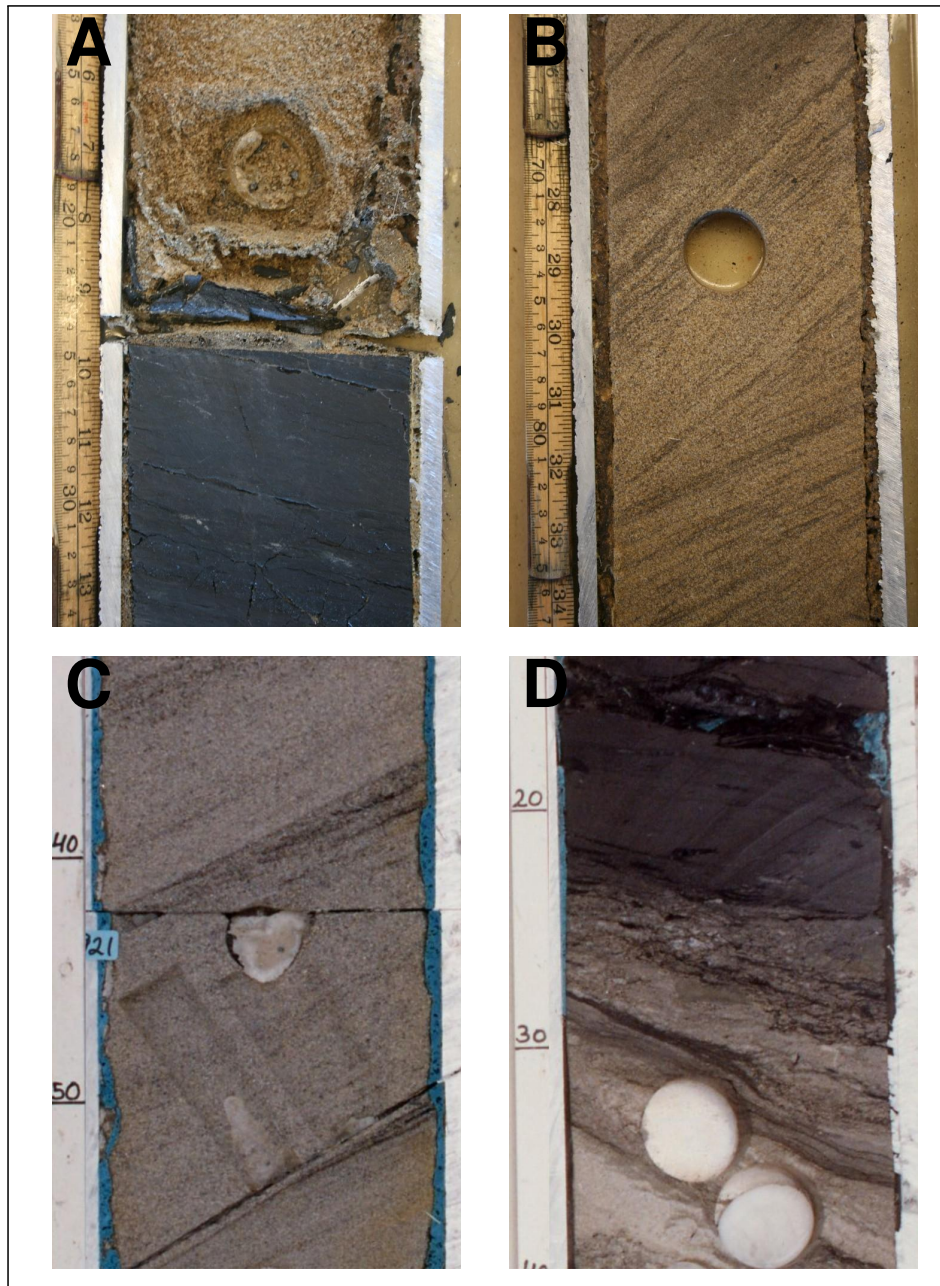


Figure 3.11: (A) Gravelly base lag containing coal clasts in FCH in well 10 at 3545,80m. (B) Cross stratified medium sand grade FCH in well 10 at 3581,70m (C) Carbonaceous drapes on x-bed foresets in well 5 (Photo: NPD). (D) Abrupt upper boundary of an MFCH (Photo: NPD).

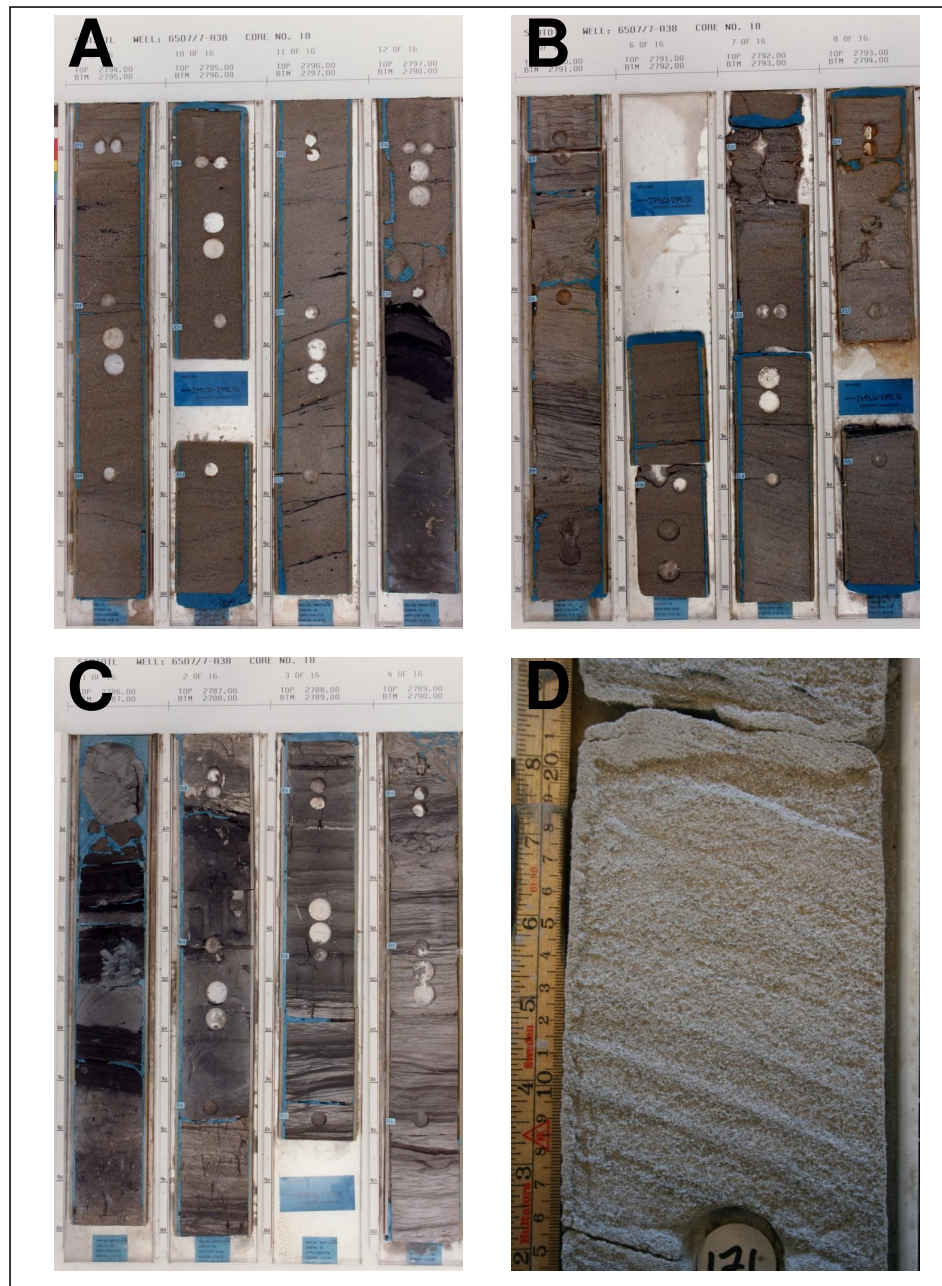


Figure 3.12: A, B & C comprises a 12 m thick fining up succession of a SFCH deposit in well 5 at 2786-2798m(Photo:NPD). (A) Cross-stratified, coarse to medium grained sandstone constituting the lower part of the SFCH. The erosional base of the channel is easily seen to the right of the photo. (B) Fining up succession of cross-stratified sandstone changing into current ripples towards the top, constituting the middle part of the SFCH. (C) Fine to very fine current rippled sandstone passing into mudstone displaying roots and capped by in situ coals comprising the upper most part of the SFCH. (D) Cross-stratified sandstone of a FCH from well 2 at 3005,90m.

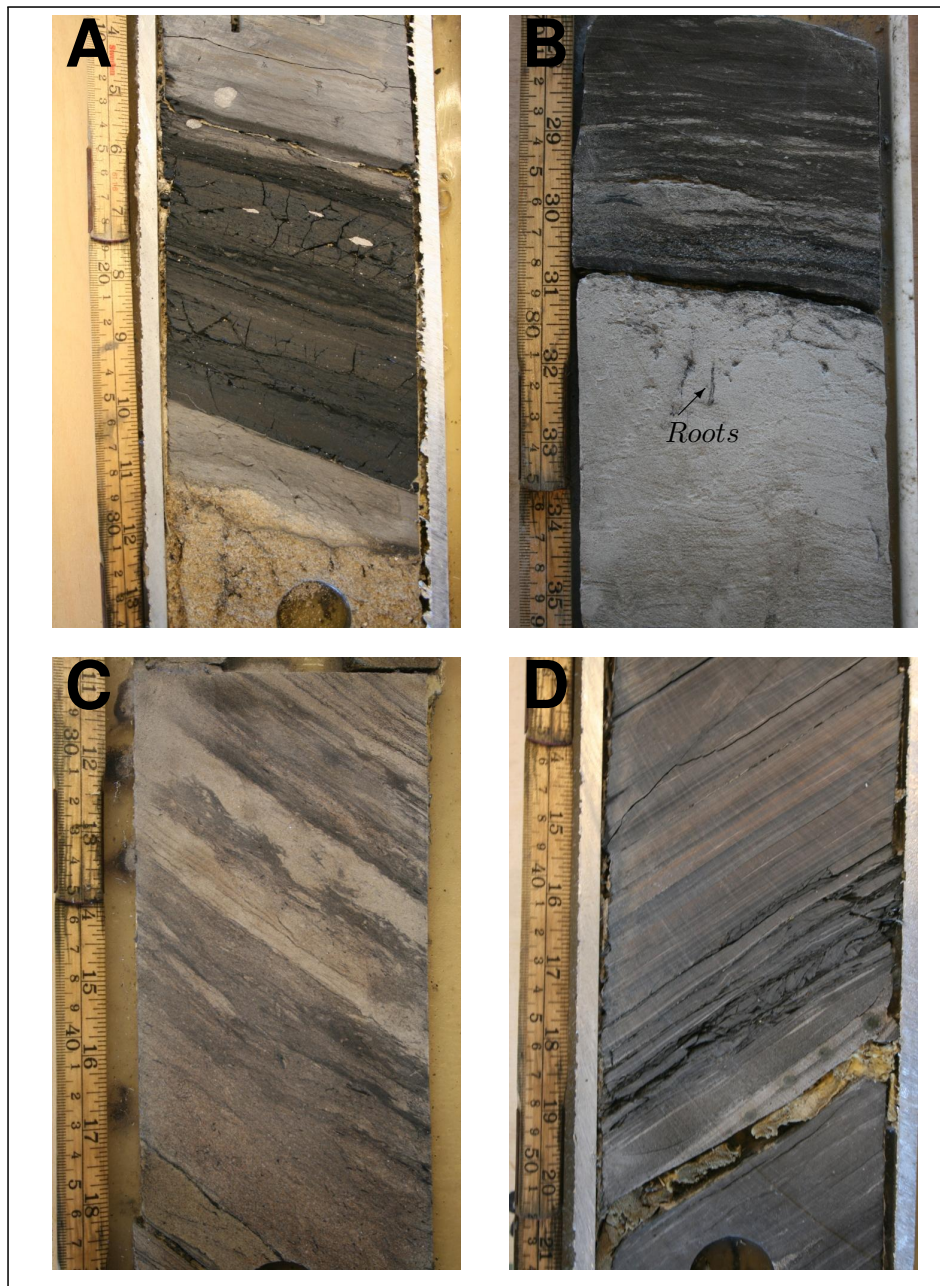


Figure 3.13: (A) In situ coal deposited as a flood plain peat swamp in well 10 at 3575,80m (B) Rooted seat earth underlying a carbonaceous interval from well 2 at 2977,80m. (C) cm scale intervals of very fine to fine sand grade. The sands display abrupt upper and lower boundaries where the lower boundary often appear erosional. Photo from well 10 at 3578,20m. (D) Plane parallel laminated lacustrine mudstone from well 10 at 3566,40m

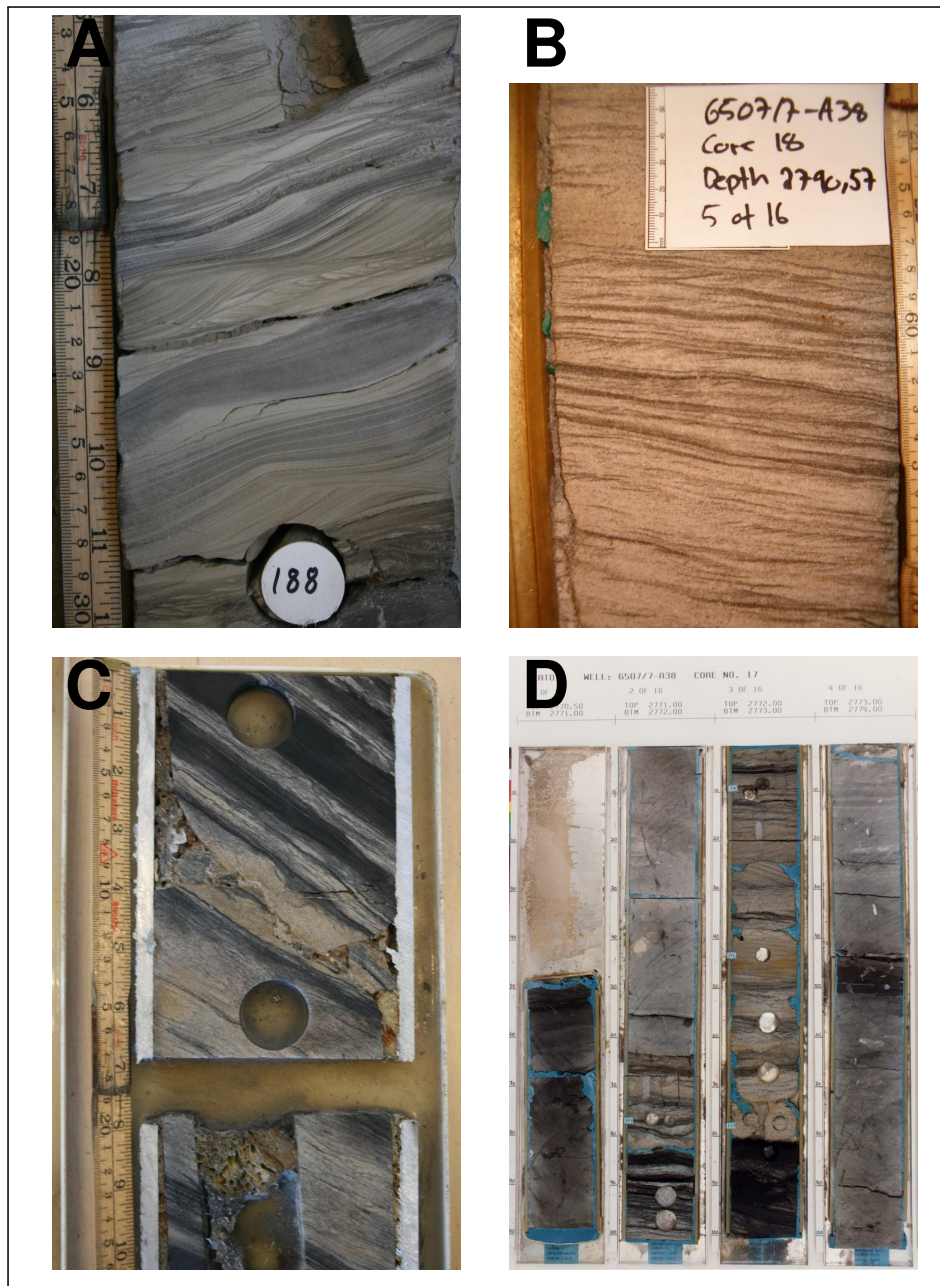


Figure 3.14: (A) Climbing ripples in a CCH interval interbedded in a SBF deposit from well 4 at 2717,10m. (B) Climbing ripples in a CCH interval interbedded in FF deposit (not seen on photo) from well 5 at 2790,57m. (C) cm scale intervals of very fine to fine sand grade composing CCH (crevasse splay) deposits. Photo from well 10 at 3546,90m. (D) Crevasse channel complex as seen in well 5 at 2772-2774m. Notice the relatively sharp lower and upper boundary of the m-scale sand unit.

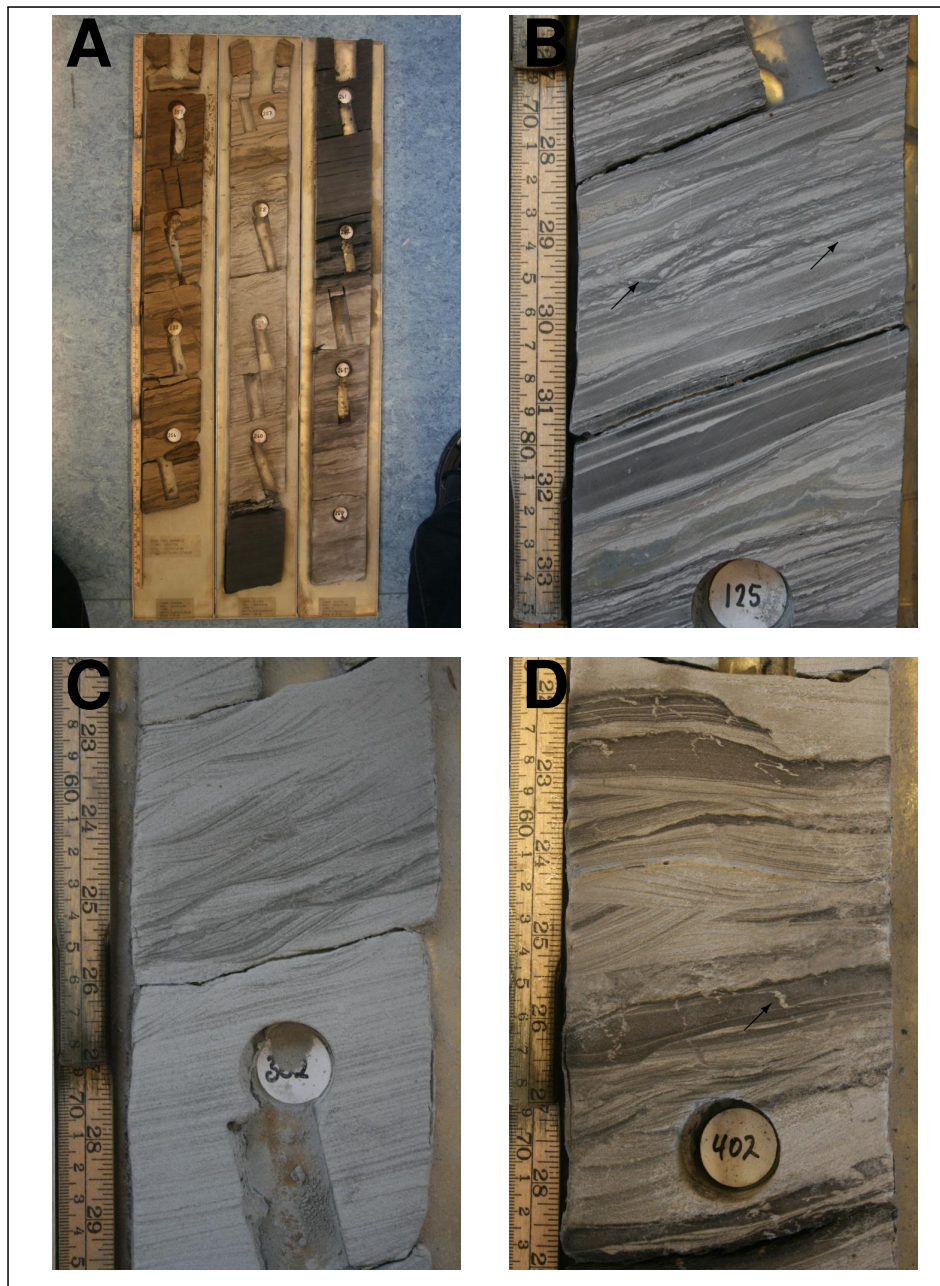


Figure 3.15: (A) 3m section displaying the coarsening nature of a bay fill cycle in well 4 at 2735,00-2738,00m. A dark grey, plane parallel laminated muddy interval is succeeded by a lighter interval comprising ripple x-laminated sand of very fine grade and fine grained, wave and hummocky cross-stratified sandstone at the top. (B) Typical Åre MBF deposit with *Arenicolites carbonarius* (arrows) traces from well 4 at 2696,80m. (C) Very fine grained SBF sandstone displaying wave ripples from well 4 at 2746,60m. (D) Rippled and hummocky cross-stratified, very fine to fine grade SBF sandstone with occasional muddy intervals displaying synaeresis (arrow) from well 4 at 2777,60m.

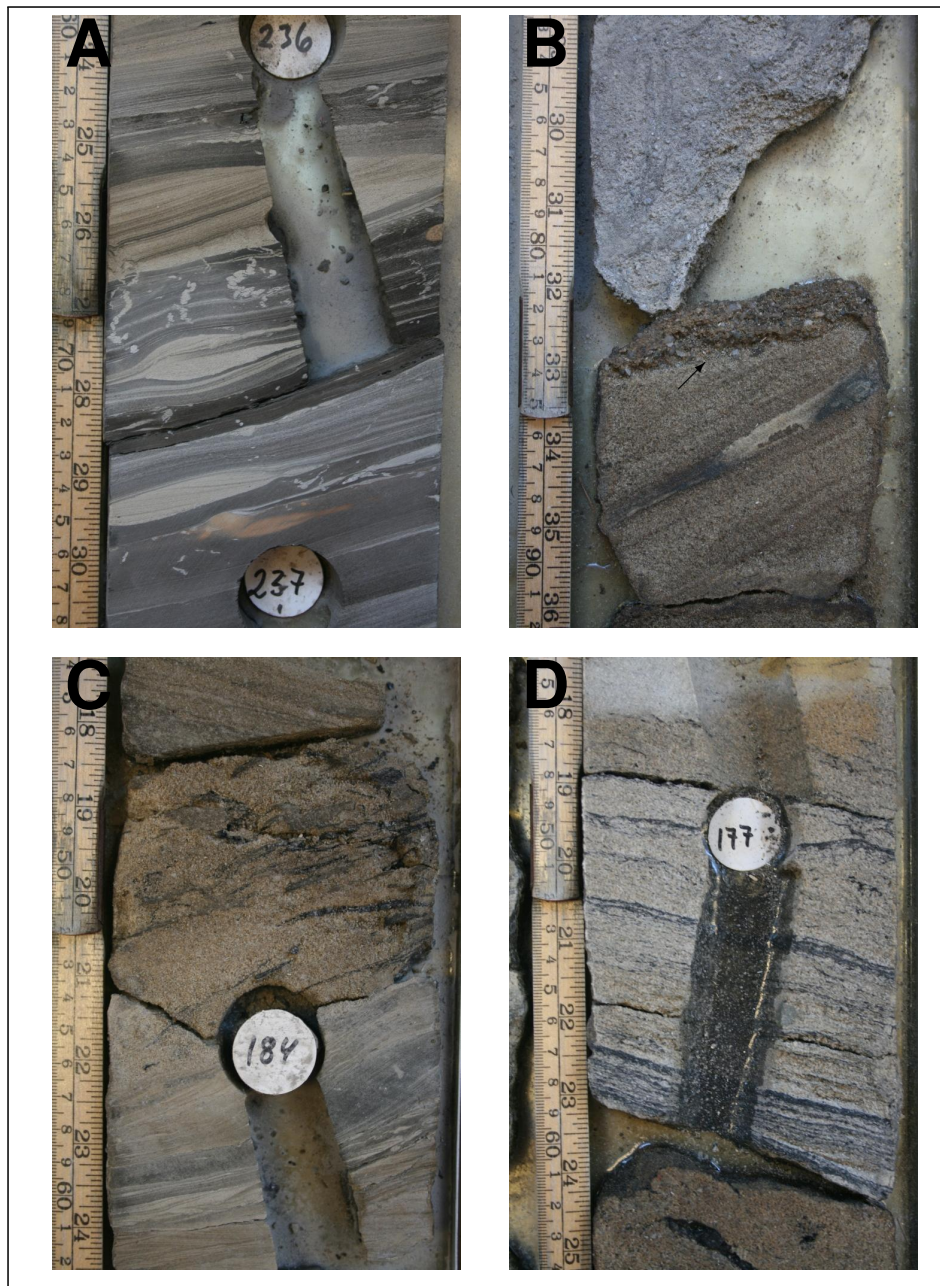


Figure 3.16: (A) SBF/MBF displaying synaeresis. Notice the wrinkled shape due to mudstone compaction. (B) The top Åre 6.2 boundary (1-2 cm thick gravelly lag) marking the transition into transgressive shallow marine shoreface deposits above (arrow). (C) Basal erosion surface of a TCH in well 4 at 2716,5m. (D) Carbonaceous drapes enhancing ripple x-lamination in TCH in well 4 at 2714,50m.

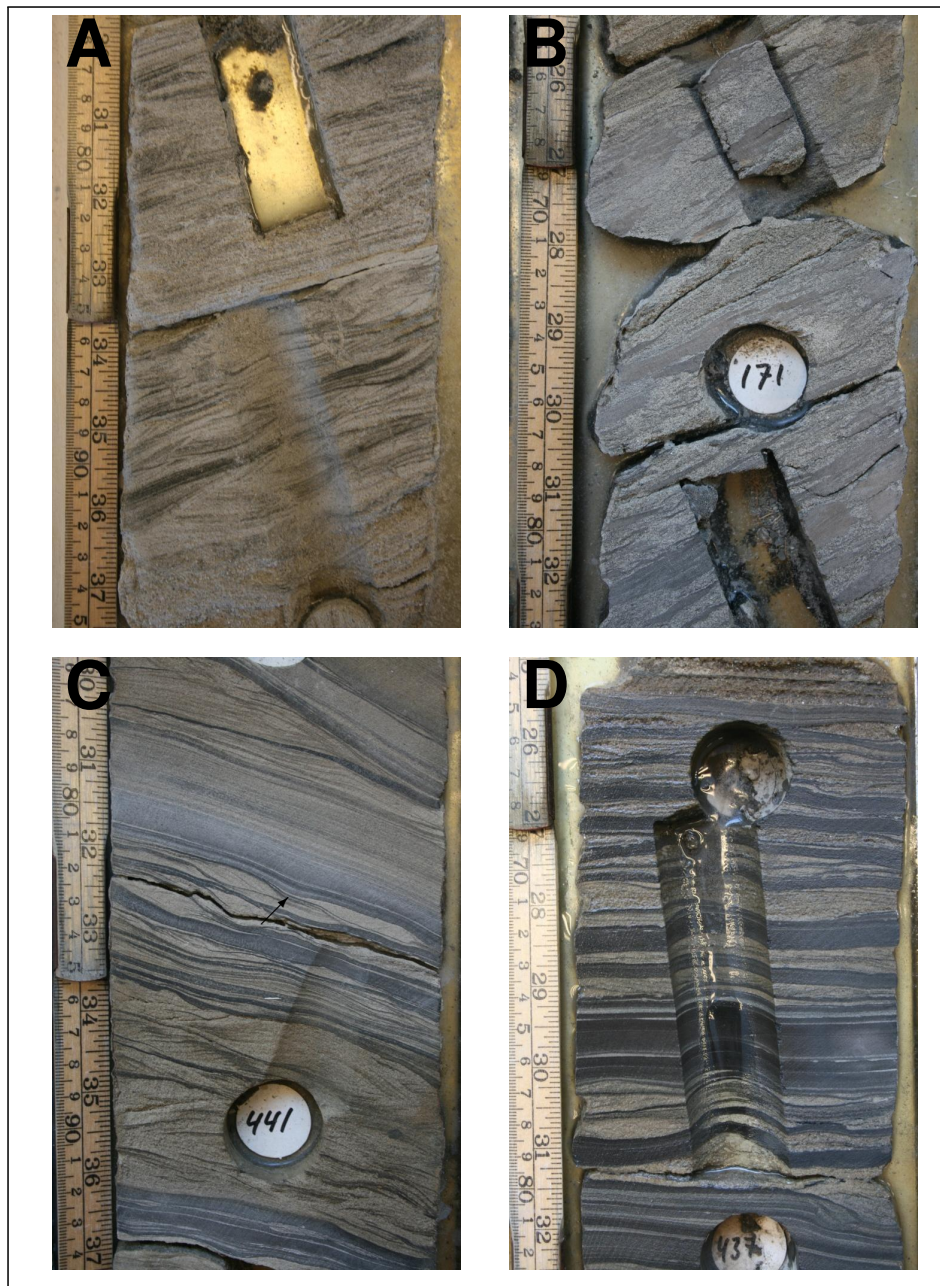


Figure 3.17: (A) Ripple x-lamination enhanced by carbonaceous drapes in a TCH in well 4 at 2771,80m. (B) Heterolithic interval in the upper part of a TCH in well 4 at 2712,7m. (C) Sandstone dominated heterolithic interval of alternating fine sandstone and siltstone also displaying double mud drapes in well 4 at 2686,90m (arrow). (D) Mudstone dominated heterolithic interval as observed in the upper part of a TCH from well 4 at 2685,70m.

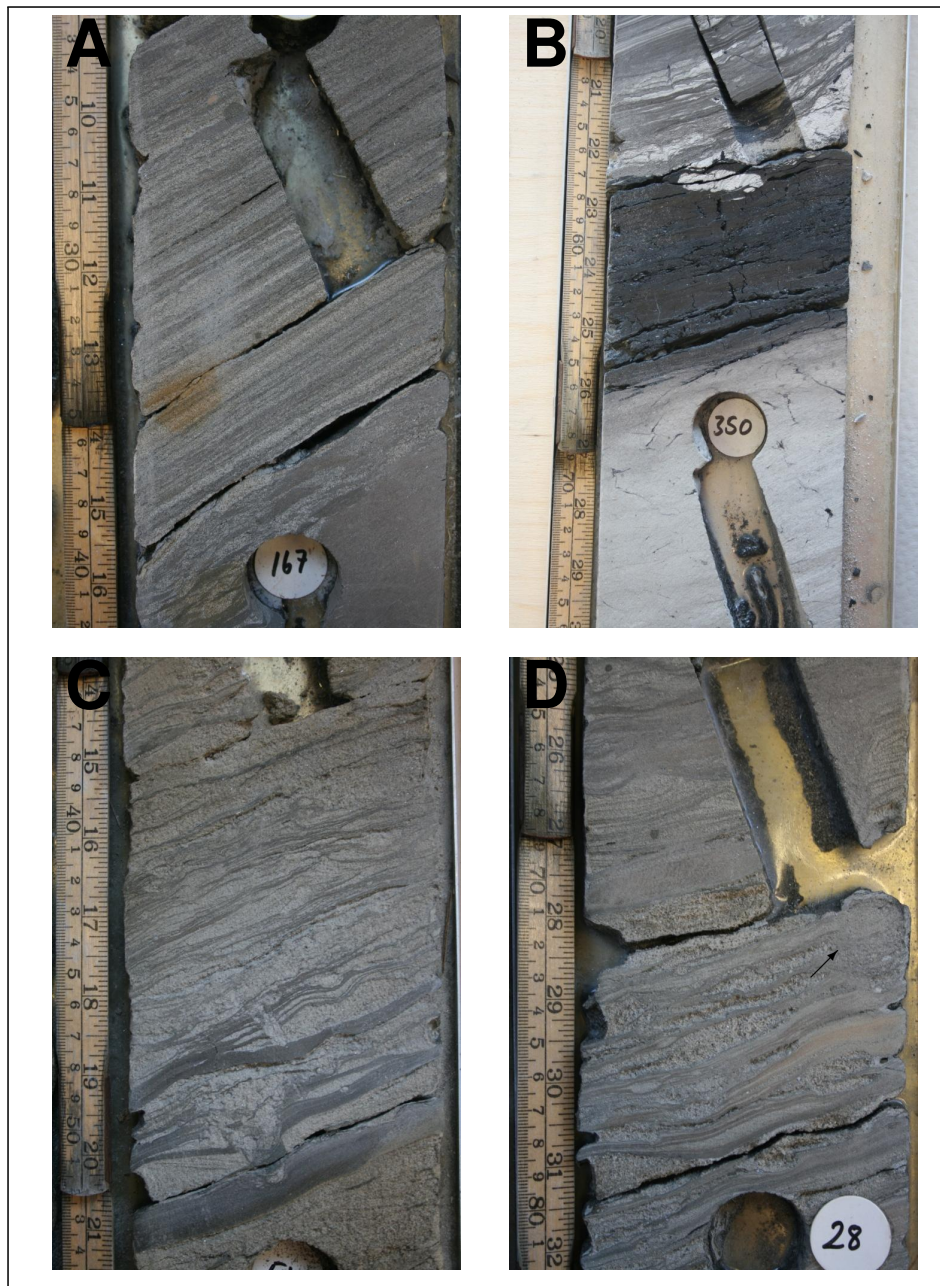
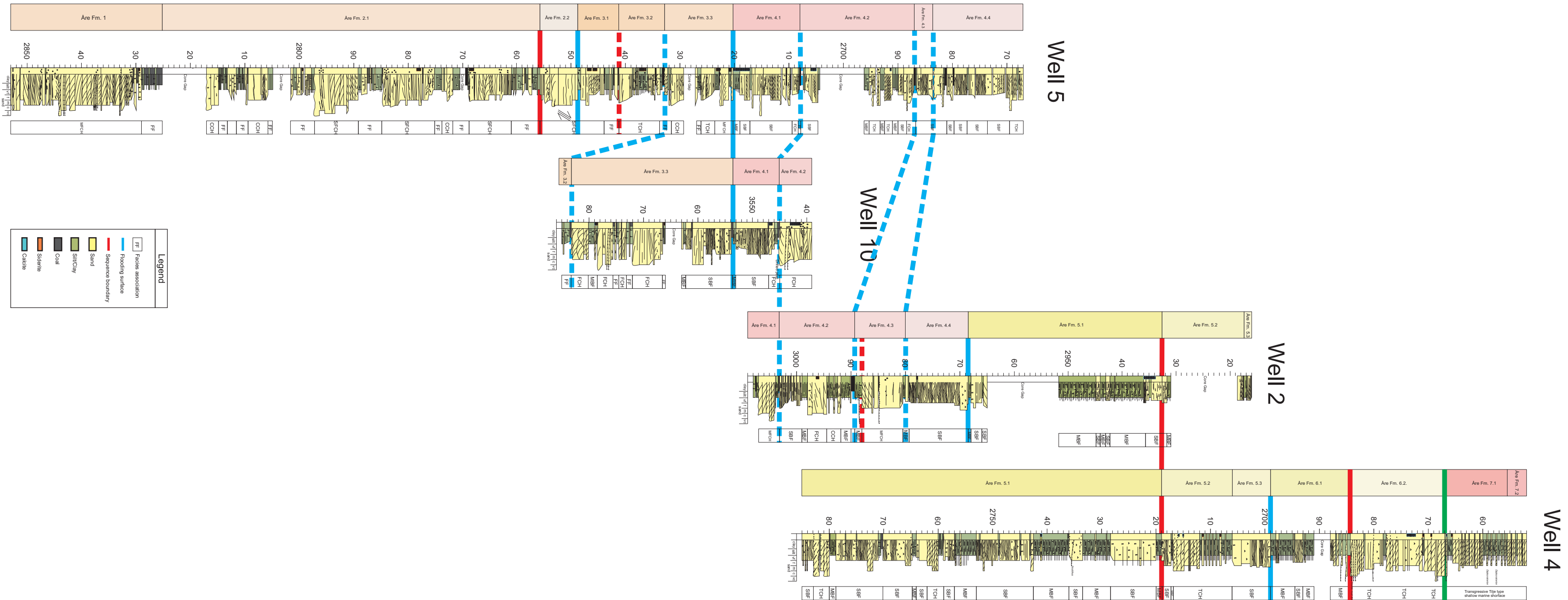


Figure 3.18: (A) Mudstone dominated heterolithic section of the upper part of a TCH in well 4 at 2711,30m. (B) Rooting and *in situ* coal capping a TCH in well 4 at 2759,60m. (C) Sandstone dominated heterolithic TSMS interval of alternating fine sandstone and siltstone in well 4 at 2664,4m. (D) Mudstone dominated heterolithic TSMS deposit comprising *Diplocraterion* trace in alternating medium grained sandstone and siltstone in well 4 at 2658,7m.

Fig. 3.19 Sedimentological core description



Chapter 4

Stratigraphy in fluvial deposits

In the following sections a sequence stratigraphic analysis of the Åre Fm. is discussed. The presented sequence stratigraphic model of the Åre Fm. at Heidrun is in part based on the work of Leary et al. (2007) and updated by Thrana et al. (2009) (c.f. Fig. 4.4) utilizing their published reservoir zonation nomenclature. In addition to these studies, facies association interpretation of selected core intervals and their petrophysical signature is used to analyze and interpret a sequence stratigraphic model for the studied well data (c.f. Chapter 3). As a basis a detailed study of the depositional environment, including facies association interpretation of both wireline log and core data is utilized, enabling identification, interpretation and definition of correlatable sequence stratigraphic surfaces in the data set (core and wireline log data). In addition, correlation of decompacted sedimentary columns has contributed to the interpretation of intra zone reservoir units (i.e. Paper I and II). In earlier work on describing the sequence stratigraphy of the Åre Fm. (c.f. Svela, 2001) the interpretation was based on Exxon terminology relating base level changes to changes in relative sea level. As the Åre Fm. is interpreted as partly fluvial and therefore partly independent of changing sea level, this study instead relates the observed changes in depositional style to changes in base level and the creation and destruction of accommodation space (AS) (Jervey, 1988).

4.1 Base level changes and their controlling factors

Alluvial architecture is defined as the geometry, proportion and spatial arrangement of channel-belt deposits within floodplain deposits (Allen, 1978) where sequences and their stratigraphic components are interpreted to form in response to the interaction between the rates of eustasy, subsidence, and sediment supply (Van Wagoner et al., 1988). The stratigraphic response to increase or decrease in the amount of accommodation is a key issue in sequence stratigraphic models (Posamentier et al., 1988; Posamentier and Vail, 1988; Van Wagoner et al., 1988). The application of sequence stratigraphy in alluvial (fluvial) deposits has, however, been proven difficult as the role of relative sea level fluctuations in controlling the fluvial stratigraphic record is less clear (Shanley and McCabe, 1994; Ethridge et al., 1998), as fluvial systems respond to both allogenic and autogenic controls (Schumm, 1968; Karszenberg and Bridge, 2008; Stouthamer and Berendsen, 2007). Allogenic factors originate outside the alluvial plain, and include climate, extrabasinal tectonic activity and sea level change, whereas autogenic factors originate within the alluvial plain, and result from the floodplain processes and their interaction, such as meandering and delta lobe switching due to avulsion, and/or compactional subsidence. Fluvial/alluvial systems may therefore in many cases be independent of sea level fluctuations. The problem of applying sequence stratigraphic models to fluvial deposits relates to rapid lateral facies shifts and a lack of internal features in thick alluvial successions which allow them to be sub-divided into time stratigraphic sequences. When identified, these sequences may be divided either by sequence boundaries (abrupt decrease in the ratio between accommodation (ΔVa) and sediment supply (ΔVs) or by expansion surfaces or zones such as flooding surfaces (abrupt or gradual increase of A/S-ratio respectively) (Martinsen et al., 1999; Posamentier et al., 1992).

Some authors have classified observed changes in sediment architecture based on interpreted relations to changes in stratigraphic base level (Olsen et al., 1995; Willis, 1997; Currie, 1997; Martinsen et al., 1999). Base level is here defined using the definition of Sloss (1962) as a surface "above which a particle cannot come to rest and below which

deposition and burial is possible". Martinsen et al. (1999) suggested dividing the sequence stratigraphic architecture in the fluvial to estuarine Ericson Sandstone, SW Wyoming, into low- or high-accommodation systems tracts based on the alluvial architecture and the ratio between accommodation and sediment supply (A/S-ratio)(Eq. 4.1) where the accommodation is controlled by changes in base level.

$$\frac{\frac{\Delta V_a}{\Delta t}}{\frac{\Delta V_s}{\Delta t}} \longrightarrow \frac{\Delta V_a}{\Delta V_s} \quad (4.1)$$

To be able to relate Åre deposition to base level changes an analysis of the depositional controlling factors was necessary.

4.1.1 Controlling factors; allogenic vs. autogenic

As mentioned above, avulsion greatly influences the alluvial architecture. Therefore, when interpreting the sequence stratigraphy of a fluvial deposit, the effect of allogenic and autogenic processes on floodplain dynamics (e.g. aggradation, degradation, evolution of the channel network by bifurcation and avulsion) must be explored. Koss et al. (1994) present an experimental study of the effect of base level change on fluvial, coastal plain and shelf systems. Stouthamer and Berendsen (2007) attributed long-term (>1000 yr) cycles to changes in allogenic parameters, whilst autogenic factors were attributed to short-term cycles (~500 yr) in the Rhine-Meuse delta. Gordon and Bridge (1987) related decrease in sinuosity and increase in grain size, slope, and braiding index with distance from the palaeoshoreline. These are examples of why understanding these controlling factors is important and that they need to be explored in order to construct a sequence stratigraphic model of a fluvial deposit.

4.1.2 Allogenic factors

As mentioned earlier, allogenic controlling factors include climate, extrabasinal tectonic activity and sea level change.

Palaeoclimate

A wide of variety of interpretations of the effect of climate change on ancient fluvial successions exists, and a selection is presented in Ethridge et al. (1998, Table 4). In general four factors affect climate: latitude, altitude, winds and distance from the sea. Temperatures decrease and temperature range increases with increasing latitude. Also, temperatures decrease with altitude. If winds are warm they will raise temperatures, if cold they will lower temperatures. Land heats and cools faster than the sea, consequently coastal areas have a lower temperature range than areas inland. Thompson et al. (1985) reported a palaeolatitude of approximately 30°N indicating a subtropical climate. Doré (1992) on the other hand suggested a palaeolatitude of approximately 50°N (equal to present day Paris) for the Halten Terrace during the Early Jurassic when the Åre Fm was deposited (Fig. 2.7), indicating a temperate, humid climate. However, the progression to more humid facies in the studied interval (from red beds to coal rich grey beds/Åre Fm.) would reflect the drift of this area into the temperate humid belt (30°-55°N) during the Triassic, as suggested for the Kap Stewart Fm., East Greenland (McElwain et al., 1999). This interpretation is also supported by the model of Torsvik et al. (2008) and Steinberger and Torsvik (2008) which suggests a palaeolatitude of 43°N (c.f. Fig. 2.8). The climate at this latitude today is in the polar front zone - the battleground of polar and tropical air masses. Seasonal changes between summer and winter are very large. Daily temperatures also change often. Abundant precipitation falls throughout the year. Hallam (1994) indicated that the Jurassic climate was warm with rather equable global conditions where strong seasonal differences in temperature and rainfall may have existed.

Winds and continentality however are more difficult to predict, but a transition to a more marine influenced depositional environment towards the end of the Åre deposition has been reported, with the development of the Tethyan - Boreal seaway. A "large bay" opening towards the Boreal ocean to the north would introduce cold air and cold waters to the area, an opening towards the south would introduce the opposite scenario, with warm winds and warm waters. The studied interval is interpreted as coastal plain, lower delta

plain deposits laid down in relative vicinity to the sea, however, still within the Pangea super-continent, in a relatively flat landscape. Therefore no significant palaeoclimate change is interpreted for the Heidrun area during the deposition of the Åre Fm. although minor changes may have occurred.

Eustasy

In general, of the various possible causes of eustatic changes, only two are of any significance: melting and freezing of polar ice caps, and changes in the volume of the ocean basins (glacio- and tectonoeustasy) (Donovan and Jones, 1979; Hallam, 1992). Besides the establishment of the Antarctic ice cap about Mid-Miocene (Shackleton and Kennett, 1975), no evidence of polar ice caps exists since Mid-Permian (Frakes, 1979) or at least, if there was, these were confined to relatively limited periods of time (Hallam, 1992). Consequently, any eustatic sea level change occurring within this time span must have been tectonoeustatic in origin.

Shortly before the end of the Triassic, a notable transgression event occurred in northern Europe, bringing to an end the long persisting non-marine regime (Hallam, 1992). This transgression was followed by a sharp regressive event at the Triassic-Jurassic boundary (Hallam, 1981; Mørk and Smelror, 2001). This event may possibly have resulted in the sequence boundary recognized in the Åre 2.2 seen as the laterally persistent channel sand discussed in Section 3.5. On the other hand, biostratigraphic studies indicate this boundary at base Åre Fm. (Thrana, C. pers. comm. 2010). Local tectonic activity at the Nordland Ridge may also, however, have contributed to a lowering of the base level (See Chapter 2). Thereafter, a long term eustatic sea level rise is seen, from the lowest value at the start of the Jurassic, to a Kimmeridgian/Early Tithonian highstand (Hallam, 1988; Surlyk, 1990), as a result of the break-up of Pangea. Both the Nordland Ridge uplift and the Pangea break-up are suggested as possible allogenic factors for local and global tectonic activity respectively, controlling the local base level change observed in the Åre Fm.

Tectonism

As mentioned, the eustatic sea level changes during Åre deposition were controlled by large scale tectonic activity with a possible local factor. During the Rhaetian-Sinemurian, the study area consisted of a broad sedimentary basin. In conjunction with continued rifting activity, and cyclically rising sea levels (Embry, 1997), the Boreal and Tethys Seas linked up during the Rhaetian-Hettangian (Ziegler, 1982). A continuously subsiding North-west European Basin and eustatic rising sea level is inferred in response to continued crustal extension. Minor uplift and faulting on the Nordland Ridge may however, have affected the Heidrun Field, resulting in base level fall and the formation of the Åre 2.2 channel sand deposit (See Section 3.4.1). Fluviodeltaic conditions prevailed until the end-Hettangian to Early Sinemurian. It has been proposed that the Åre Fm. in the Heidrun area was sourced from the northwest (Thrana et al., 2008) (possibly the Sklinna High and/or the Nordland Ridge). This fits well with the assumption that uplift of the Nordland Ridge controlled the sediment influx into the Heidrun Field area. A palaeogeographic map of the North Atlantic margin is presented in Figure 2.7.

4.1.3 Autogenic factors

Autogenic processes include meandering, delta lobe switching and sediment compaction. These are intra basinal controlling factors and may be independent of allogenic processes.

Meandering

The Åre 1, 2 and 3 zones display clear single storey channel features interpreted as meandering, pointbar deposits resulting from avulsion. Avulsion may be abrupt or gradual and is primarily a feature of aggrading floodplains, although it is not restricted to any particular pattern or size (Slingerland and Smith, 2004). According to Slingerland and Smith (2004), any given configuration of bifurcated channels is stable as long as the sediment moving through the upstream trunk channel is partitioned between the two bifurcated downstream channels in exact proportion to their sediment-carrying capacities, where the

Table 4.1: Table showing the effects of autogenic and allogenic factors in the Åre Fm.

	Effect	Evidence in the Åre Fm.
Allogenic factors		
	Eustatic rise	Overall deepening trend throughout the Åre Fm. observed as a transition in depositional environment (from fluvial in the lower part of the succession, to delta plain in the upper part)
	Eustatic fall/still-stand?	Shallowing observed as (incision?) change in fluvial style from meandering to braided. Possibly linked to the rapid eustatic sea level fall at the Rhaetian-Hettangian border (Hallam, 1992)?
	Tectonic activity	Regional subsidence related to crustal extension. Sea level fall related to uplift of the Nordland Ridge?
	Climate	No change observed
Autogenic factors		
	Meandering	Single storey channels. Stacking pattern. Crevassing frequent (seasonal?)
	Lobe switching	Stacked bay fill deposits
	Compactional subsidence	Thick peat (now coal) deposits observed immediately below vertical aggraded channel fills.

ability of channels to change their capacities is determined by stream power and cohesion of banks. In the Åre Fm. the change in river style reflects these changing criteria for avulsion. The avulsion frequency is reportedly high when aggradation rate is low (Stouthamer and Berendsen, 2000), and the probability of avulsion increases during subsidence and decreases during uplift and incision (Stouthamer and Berendsen, 2007) during the first stages of aggradation. Consequently, the lateral and vertical amalgamated channel sand discussed in Section 3.5 is either a product of decreased avulsion frequency as the channel course is confined by the valley, or increased avulsion as a result of lowered aggradation rate. As stated by Stouthamer and Berendsen (2000), extensive peat formation leads to low cross-valley gradients and thus reduced opportunities for avulsion resulting in confined river channels, i.e. anastomosing type.

Substrate (coal) compaction

The development of thick peat deposits generates a large potential for accumulation space creation through early differential compaction. During channel avulsion, the new river course may be selected partly based on the compactability of the substratum, as proposed by Rajchl and Uličný (2005) for an avulsive fluvial system controlled by peat compaction in the Most Basin, Czech Republic. Compaction, and subsequent channel aggradation, is highest during the initial stages of channel deposition onto the peat swamp deposits. As the compactability of the peat decreases during compaction, channel aggradation changes from vertical to oblique and finally switches to a new course through avulsion (c.f. Fig. 3.3). This development results in relatively blocky sand deposits (as seen on sedimentological- and wireline logs from the Åre Fm.) and with a sharp boundary towards the underlying peat and the overlying floodplain developed after channel abandonment. This strongly resembles the observations from the Åre Fm. discussed in Section 3.5. In addition to the compaction effect, peat deposits are relatively resistant to lateral channel erosion and stabilize the river channels, preventing lateral accretion (Stouthamer and Berendsen, 2000).

Delta lobe switching

The stacked, coarsening bay fill deposits observed in the Åre Fm. represent parasequences resulting from the autogenic process of delta lobe switching (Emery and Myers, 1996) due to river channel avulsion. A hint of allogenic influence may, however, be evident from the stacking pattern of several bay fill sequences, such as a stack of subsequently more mud prone bay fills could suggest a possible sea level rise. Abandoned delta lobes subside due to relative base level (sea level) rise, e.g. due to sediment compaction. When a channel switches back, a new delta lobe develops on top of the older, abandoned lobe. If this process continues over time, a stack of coarsening units (delta lobes) will be deposited, which resembles that observed in the upper part of the Åre Fm, e.g. Åre 4.4 and 5.1. As a delta evolves, the main depocenter of the river forming the delta may shift laterally. Consequently, an area previously located in the vicinity of the river mouth, which is dominated by comparably coarser material than distal areas, will move away from the main depocenter. The overlying deposits will thereafter be of finer-grained material, hence comprise more mud prone bay fills.

4.1.4 Summary

The deposition of the Åre Fm. in the Heidrun Field area is interpreted to have been controlled by global tectonic activity with minor(?) effects from local uplift controlling both eustatic and local base level changes. In addition, autogenic processes, such as meandering, delta lobe switching and peat compaction have shaped the depositional architecture into the Åre Fm. as it appears today. Allogenic and autogenic controls on the Åre sequence and their associated variations in alluvial plain slope, grain size and channel pattern are summarized in Table 4.1.

4.2 Compaction controls on autocyclicality

In clastic systems, autocyclic processes (cyclic autogenic processes) are well known. For example, in Pennsylvanian mixed clastic and carbonate cycles, autocyclic influences were

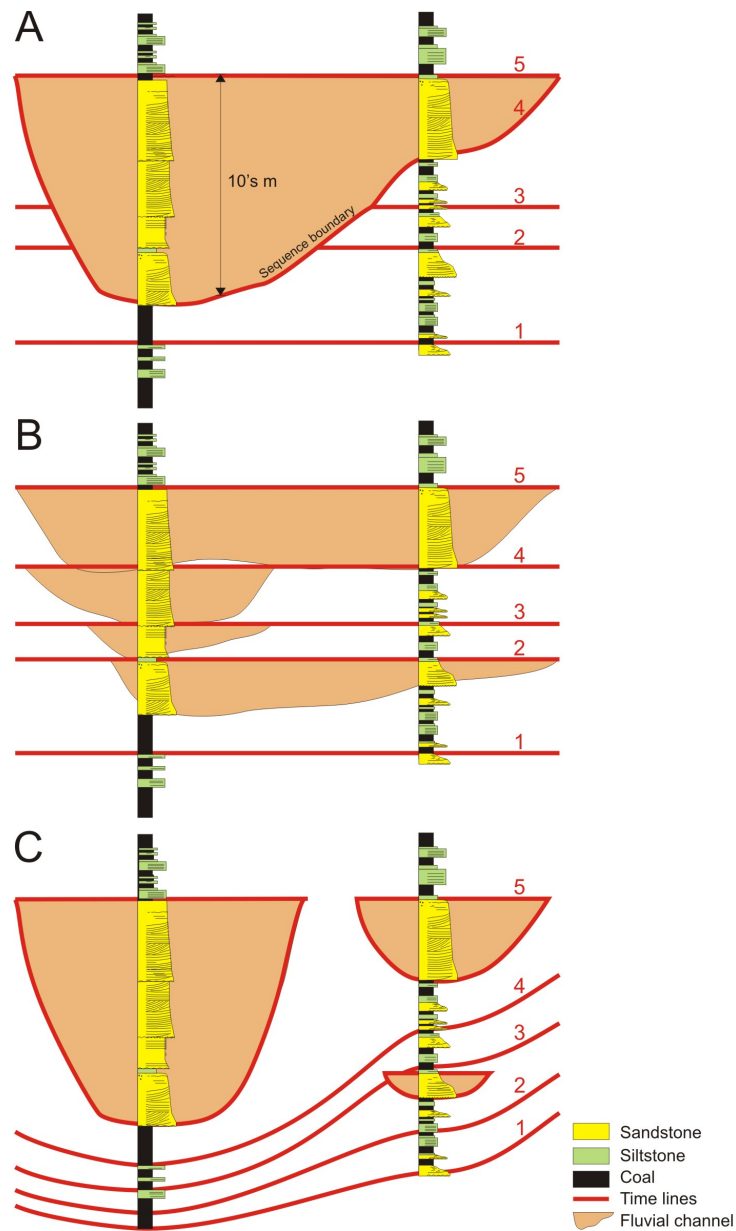


Figure 4.1: Sketch illustrating three opposing interpretations of a fluvial reservoir. (A) The deposits are interpreted as an incised valley fill deposited as a result of a fall and subsequent rise in base level. Time-lines 1-3 are truncated by the sequence boundary (4). (B) Channel sands deposited in a scenario with a vertical accreting floodplain with horizontal time-lines. (C) Interpretation of these sediments as vertical accreted, anastomosing channel sandstone where the accommodation space was created by compaction of the underlying peat. Note the bending of the time-lines as a result of peat compaction and the different sandstone volumes keeping in mind the well spacing is in the order of 100s of meters to km scale.

suggested by Van der Heide (1950) who speculated that compaction of peat layers in clastic portions of cyclothems (repetitive stratigraphic succession of marine and non-marine strata that are indicative of cyclic depositional regimes) in the Netherlands could have induced sudden marine transgressions contributing to cyclic deposition. More recently, autocyclic models of delta lobe switching have been applied to Upper Pennsylvanian mixed clastic-carbonate cyclothems (Galloway and Brown, 1973; Elliott, 1976). The sediments of the Åre Fm., in particular the upper, marginal marine interval, suggest elements of this model comprising stacked bay fill deposits. In addition to the cyclic stacking of bay fills, cyclicity is also seen in sets of bay fill stacks as alternating SBF and MBF-dominated successions. In the fluvial part of the stratigraphy, although not necessarily cyclic, elements of autogenic processes are also suggested.

The relationship of anastomosing channel sandstone and thick peat deposits regularly occurring beneath vertically accreted sandstones suggests that compaction of peat created accommodation space necessary for the vertical accretion of the sand. The process of compaction, which lowers the sediment surface relative to the tidal frame, has the effect of creating significant accommodation space, in particular in peat deposits, that is additional to that provided by any relative sea level rise (Long et al., 2006). In the example detailed in this study, this accommodation space was partly created and rapidly filled by fluvial channel sands. This process resulted in thick, probably relatively narrow sandstones which are difficult to correlate between wells. Such deposits are a challenge in a scenario with few wells where they could easily be mistaken as a correlatable, vertical amalgamated, multi-lateral channel sand complex, similar to the Åre 2.2 sandstones. This misinterpretation would cause large overestimates of the reservoir volume, and perhaps lead to improper and costly drainage solutions. Compaction driven vertical accretion would also appear rather similar to normal floodplain accretion in an anastomosing depositional environment, however lateral correlation of sand bodies would be different, as seen on time-lines drawn for these two scenarios (Fig. 4.1). Compaction of peat providing increase in accommodation space required to drive channel activity has also been suggested by Baeteman et al. (2002) and Baeteman (2005), for late Holocene tidal channels in the Belgian coastal wetlands,

by Long et al. (2006), for Holocene coastal wetlands in the eastern English Channel, UK, and by Rajchl and Uličný (2005) for the Neogene Most Basin, Czech Republic.

Peat accumulation depends on a high groundwater table, which, in coastal lowlands, is related to a high sea level and its transgressive tendency (Streif, 1990). Higher rates of a sea level rise are more likely to drown the coastal lowlands and overcome the peat accumulation. "The best development of coal is at the turnarounds between progradational and retrogradational parasequence sets or landward of aggradational sets, where the shorelines were stabilized for a long time" (McCabe and Shanley, 1992). In this study, the first is likely to be assumed for the bay fill deposits, where the turnaround is seen as coals capping the coarsening bay fills. Each turnaround is represented by the abandonment of one delta lobe and the creation of a new one elsewhere, i.e. delta lobe switching, where the bay fill cycle starts with a transgression of the sea. When the delta lobe is abandoned, the depositional environment abruptly changes from "shallow" to "deep" due to abrupt decrease in sediment input and continuous compaction acting on the deposited sediments. This is seen as an abrupt change in the sediments, from sandstone (or possibly coal) to organic rich mudstones, i.e. a change from SBF to MBF deposits. Whereas the change from SBF to MBF is abrupt, the change from MBF to SBF is usually transitional, reflecting the gradual filling of the bay.

4.3 Sequence stratigraphic analysis of the Åre Fm.

The following section discuss a sequence stratigraphic model for the Åre Fm. The model is discussed in relation to local and regional base level changes and their controlling factors, based on data from the studied wells. Facies associations, based on core data interpretations, are used as the basic correlation units, they are mapped within specific stratigraphic intervals, and they constitute the building blocks for reservoir reconstruction modelling (Paper II). Vertical facies changes and lateral facies continuity observed in the investigated data set is discussed for identified regional and field wide sequence stratigraphic surfaces. From this analysis four sequence stratigraphic surfaces related to regional changes in base

level and eleven field wide base level events (increase/decrease in accommodation space) have been identified in this study (Fig. 4.4). The reservoir zonation nomenclature from Leary et al. (2007) and Thrana et al. (2009) has been adapted, dividing the Åre Fm. into seven reservoir zones. Their zonation scheme was based on the results from the reservoir characterization project mentioned in Chapter 1 briefly summarized in two posters (Leary et al., 2007; Thrana et al., 2008) and one oral presentation (Thrana et al., 2009). The following sequence stratigraphic discussion utilizes their reservoir zonation nomenclature, on the studied wells and core data. Surfaces additional to the Thrana et al. (2009) model are also discussed and proposed as local (field wide) base level events, some of which are defined and discussed in Paper II.

Twelve cross-section panels created for selected reservoir zones (Cross-sections 1 to 12 attached at the end of this chapter (See Fig. 2.3 for location)) are presented and a sequence stratigraphic interpretation of the Åre Fm. is presented in north-south and east-west oriented cross-sections (Figs. 4.9 and 4.10).

4.3.1 Åre 1

The lowermost part of the fluvial dominated Åre Fm. has been cored in well 5 (i.e. sedimentological core descriptions attached in Chapter 3 appendix) and penetrated and logged by petrophysical wireline logs in wells 1, 3, 5, 8 & 10. The interval (Åre 1) is dominated by a thick (>100m) succession of single and multi storey, fluvial channel sandstones, crevasses and floodplain sediments (Cross-sections 1 and 2). Coals are abundant in this succession and the succession is transitional to the underlying continental "grey-beds" of Triassic age (van Veen et al., 1992). Vertical aggraded channel fills, probably anastomosing in nature, are common in this interval and are observed as more than 30m thick successions, regularly occurring above thick peat (now coal) successions (Fig. 3.3). These underlying coals either created accommodation space during compaction or acted as erosion resistant channel bank vegetation enabling vertical rather than lateral aggradation. One multi storey channel sandstone does, however, seem correlatable in wells 1, 3 and 5 (c.f. Cross-section

1), occurring directly beneath the extensive coal zone capping the Åre 1 interval, but thins out towards the north and south.

The presence of abundant and thick coal units in the Åre 1 zone suggest a relatively high and rising base level during deposition. Comparing Åre 1 with the overlying Åre 2.1 also reveals a tendency of thicker successions of FF in Åre 1 thicker MFCHs, suggesting that the floodplain was more stable (more vegetated?) compared to Åre 2.1. These factors suggest that base level rise was more rapid in Åre 1 than in Åre 2.1.

The Åre 1 zone is capped by a regional extensive coal zone 10-15 meters thick TVD. The nature of this coal zone varies laterally, occurring as a few meters thick, relatively pure coals in some wells, heterogeneous units of sand and organic rich mud reaching thicknesses of more than 20 m in other wells (Fig. 4.2). This suggests that this was not one regionally extensive swamp, but rather a series of overlapping swamps and ponds developed during elevation of relative base level (expansion zone) in the study area, hence a flooding. According to Emery and Myers (1996), it may in many cases be difficult to recognize a single discrete surface, and instead a "flooding zone" is recognized. Within the Åre coal marker, several discrete candidate flooding surfaces may occur. This coal unit, which appears in all wells penetrating this part of the stratigraphy, is visible on seismic sections crossing the Heidrun Field (i.e. Fig. 2.4) and is identified regionally (e.g. Smørbukk and Njord Fields), indicating that this coal zone originated from a regional flooding event. The unit marks a gradual increase of the A/S-ratio upwards in the Åre 1 zone and is interpreted as a stratigraphically significant flooding surface in the Heidrun Field. On wireline log data the zone is easily recognized as intervals of abundant high neutron (NPHI) and low density (RHOB) units at approximately the same stratigraphic level.

4.3.2 Åre 2

The coaly sequence is followed by the up to 130m thick Åre 2.1 unit comprising coastal plain sediments including multi storey and single storey channels, point bar deposits,

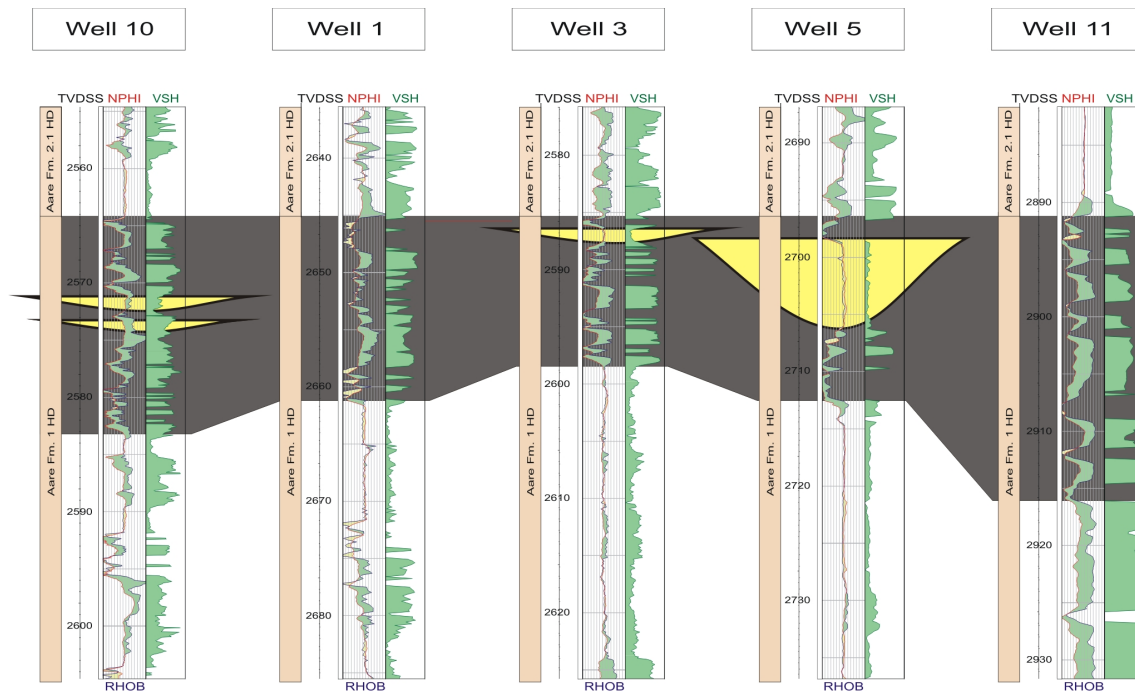


Figure 4.2: Correlation panel illustrating the nature and variability of the top Åre 1 coal marker. As seen from the well data, this coal marker corresponds to a coal rich interval, where in some wells it appears more mud prone, whereas in others the coal corresponds to more true coal deposits separated by sandy intervals.

crevasses, floodplain muds and coals as interpreted from sedimentological interpretation of core from well 5. This interpretation reveals four distinct fining-up sandstone bodies interpreted as meandering channel deposits separated by 3-5 m thick successions comprising floodplain muds, coals and crevasse deposits. As seen on the petrophysical logs from wells penetrating this interval (all wells except well 4), MFCHs also occur, however, they appear thinner compared to MFCHs in the underlying Åre 1 interval. The coals are also thinner in 2.1 compared to the coals observed in Åre 1, which may explain why the MFCHs are thinner in the 2.1 interval; less coal to create accommodation space and/or less stable channel banks. The proportion of MFCHs compared to that found in the underlying Åre 1, however, seems unchanged (compare Figs. 4.3 & 4.9). These changes in depositional style may be due to a reduction in base level rise, reducing the amount of peat formation and

subsequently the potential for accommodation space creation due to peat compaction. A shift in dominant autogenic processes from predominantly compactional to predominantly avulsion driven (meandering) is proposed. Towards the top of Åre 2.1 MFCHs start ap-

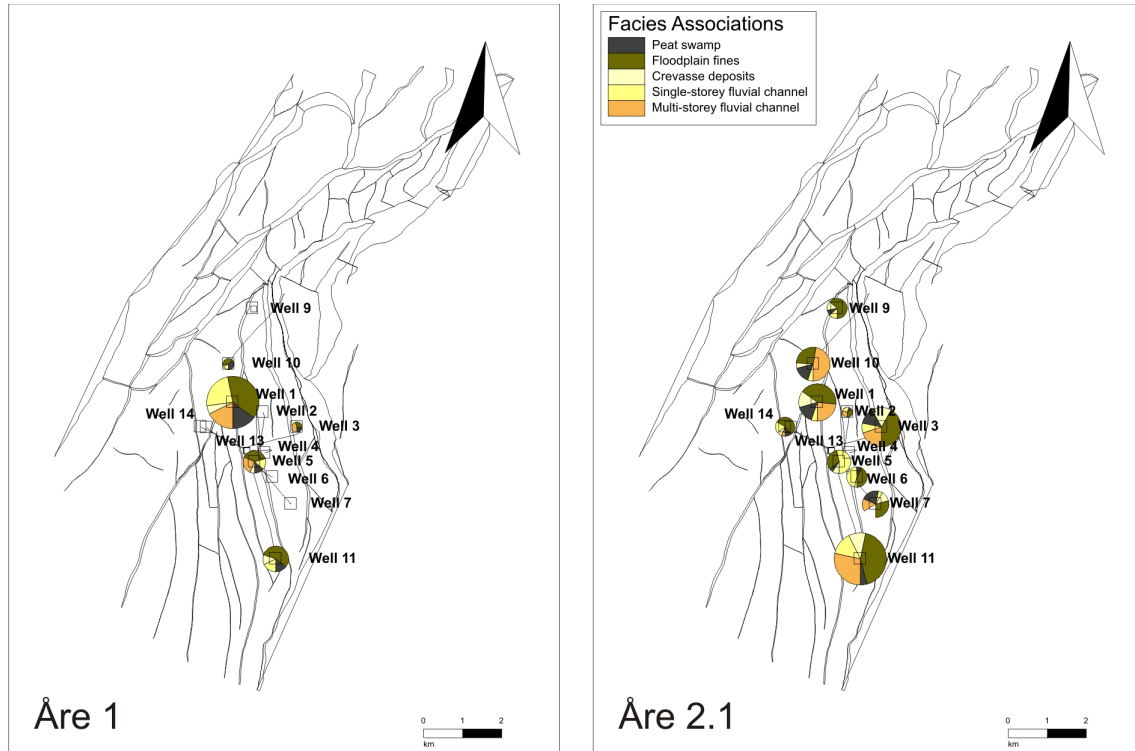


Figure 4.3: Two bubble maps displaying the facies distribution of MFCH, SFCH, CCH, FF and coals in Åre 1 (left) and Åre 2.1 (right). The facies distribution between the two zones seems rather similar, however, interpretation of wireline log data from these zones indicates that MFCHs appear thicker in Åre 1 compared to Åre 2.1. Bubble proportions reflect reservoir zone thicknesses.

pearing in several wells (e.g well 1 & 10) where one channel feature has been correlated between wells occurring beneath a zone rich in peat deposits (i.e Cross-sections 3 and 4). The coal zone is in a way similar, although thinner, compared to the coal zone occurring in Åre 1. However, the zone has not been correlated successfully across the cross-sections, suggesting that this zone represents a very local, authigenic controlled base level rise and therefore not added in the sequence stratigraphic interpretation.

This increase in MFCHs culminates in the laterally correlatable MFCH defining the

Åre 2.2 reservoir zone (i.e. Figs. 4.10, 4.9). Svella (2001) interpreted Åre 2.2 (his Åre 1B 1) to represent a LST, suggesting a lowering, and subsequent rise in sea level, and filling of the valley with braided river deposits. Internal Statoil studies have suggested that the top Åre 2.1 channels represent late highstand, whereas the Åre 2.2 represents lowstand deposits. This interpretation is supported if the base level decrease is interpreted as a result of regional sea level fluctuations (tectonics?). As mentioned in chapter 2, uplift of the Nordland Ridge may have influenced the Heidrun area at this time. Based on this interpretation a regionally extensive sequence boundary may be suggested along the base of the Åre 2.2 channel feature, representing erosion of up to 34m (thickness of the thickest sand interval of this unit) of the underlying coastal plain sediments. A local sequence boundary is, however, suggested as the regional extensiveness (outside the Heidrun area) of this surface is yet to be proven. The transition towards more abundant MFCHs upwards through the Åre 2.1 suggests a lowering of base level rise upwards and finally fall as represented by the sequence boundary. The river channel style changed from meandering to braided as a result of increased slope and sediment supply, related to a change from autogenic dominated to allogenic dominated controlling factors.

A possible interpretation is that subsequent rise in base level filled the Åre 2.2 incised valley with braided river deposits now seen as the thick amalgamated Åre 2.2 channel sandstone. This sand unit may therefore be interpreted as laid down during the latest stages of base level fall and the first stages of base level rise. Experimental studies by van Heijst and Postma (e.g. 2001) show aggrading fluvial valleys during successive fall in sea level until one of the shelf canyons was connected with the fluvial valley. One could argue, however, that the upper parts of Åre 2.1 and Åre 2.2 are both deposited during the late highstand and that no fall in base level occurred. On the other hand, the thickness of 34 m, as compared to the average FCH thickness of 8-12m and the lack of thick peat deposits in this interval, suggests at least a factor of incision due to base level fall. The Åre 2.2 to 3.1 transition is seen as a change from multi-storey to single-storey channel development, i.e. a change from dominating allogenic to autogenic processes. Equally important, the first evidence of marginal marine influence (bay fill development) is observed in the Åre

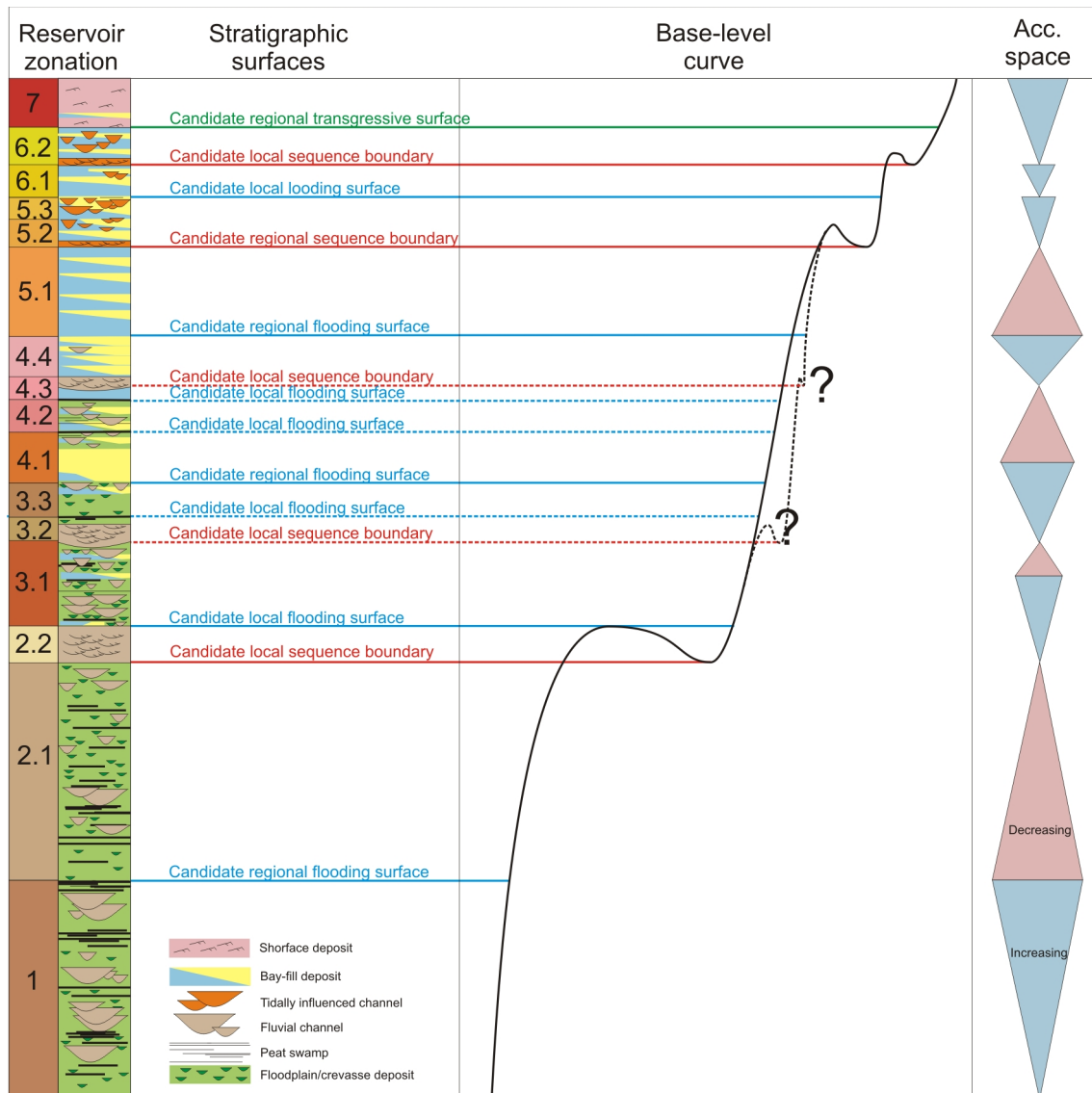


Figure 4.4: Base level curve for the Åre Fm. in the Heidrun Field identified from the studied well data suggests an overall increase halted by shorter periods of base level drop. Associated changes in accommodation space are presented as upwards or downwards pointing triangles, where upwards pointing triangles indicate decreasing accommodation space and vice versa. The overall increasing base level is also seen on the regional base level curve presented in Fig. 2.6. The sequence stratigraphic interpretation is based on interpreted surfaces (dotted lines) and surfaces adapted from Thrana et al. (2009) (whole lines). Local surfaces define field wide correlation surfaces, whereas regional surfaces extend beyond the Heidrun Field.

3.1. The change is the result of a sudden increase in accommodation space (increase in A/S-ratio), as a result of a complete filling of the valley by braided channel deposits, and continued base level rise. When filled with sediments, the restriction of the valley was suspended, instantly increasing the accommodation space significantly, and the river style changed from braided back to meandering due to changed landscape morphology (from valley to plain). When a valley has been filled to the level of the old coastal plain, the next increment of relative base level rise will flood the interfluves, generating a large volume of accommodation space. During such flooding a sharp, erosive surface, which is the product of ravinement, may result in a transgressive lag (Emery and Myers, 1996). Such an erosion lag has not, however, been observed in the data set, indicating that the flooding of the interfluves was not energetic enough to cause erosion, i.e. the base level rise was too slow to produce one. Another factor that would indicate the presence of an incised valley is extensive, dry paleosol development along the continuation of the sequence boundary onto the interfluves (c.f. McCarthy et al., 1999; McCarthy and Plint, 1998). During incision, the interfluves are exposed sub-aerially and subjected to erosion and prolonged pedogenesis. Although the Åre Fm. contains abundant paleosol development, no candidates are found to represent a sequence boundary of this kind, although there might be one.

The top of the Åre 2 reservoir zone is a field wide distinctive flooding surface/zone which marks an abrupt change in architecture, from multi-storey, multi-lateral channels to single storey channels in a mudstone-dominated delta plain setting. This is an expansion surface/zone according to the classification of Martinsen et al. (1999) marking the change from a compressed to an expanded architecture, i.e. a flooding surface.

On wireline log data the top Åre 2.2 flooding surface is interpreted at the top of the blocky feature seen on gamma and combined neutron density logs. Mapping of this sandstone unit on seismic data would have been of great help; unfortunately the density contrast between this sandstone and the mudstones above and below is not sufficient to produce a detectable seismic reflection. A channel deposit in the Åre 1 interval has, however, been mapped on seismic sections (Brekken, M. 2010, pers. comm.) due to the large contrast between the channel sandstone and the coals confining it (i.e. anastomosing

channel).

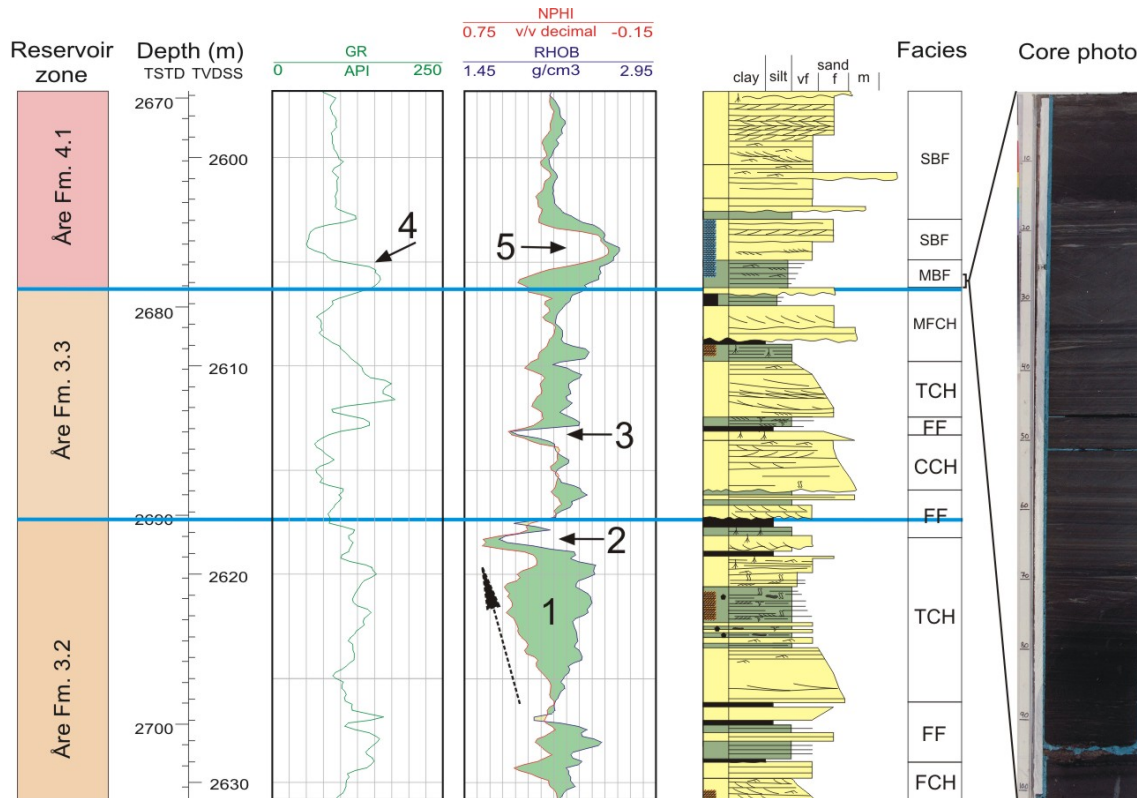


Figure 4.5: Wireline log signature and core image of the Åre 3.2 channel feature (1) and top Åre 3.3 flooding surface. The funnel shaped NPHI/RHOB log signature corresponding to the Åre 3.2 channel is interpreted as a TCH from core in well 5 terminated by a correlatable coal unit (2). A second coal (3) a few meters above is often observed in the well data and may represent a local flooding event. The flooding surface representing top Åre 3.3 has a very distinct wireline log signature (4) and is regularly associated with a calcite cemented interval (5). The intricately laminated mudstone representing the flooding surface is striking in core sections (photo).

4.3.3 Åre 3

Overlying the Åre 2.2 is an approximately 40m thick interval comprising a highly variable assemblage of facies associations, including coastal plain deposits, bay fills and fluvial channels, mainly tidally influenced, as observed from the core in wells 5 and 10. Although

fluvial deposits dominate the succession, a tendency of more marine influenced deposits occur upwards through the Åre 3 zone. The lower part (3.1) comprises predominantly floodplain deposits and single storey channels, some with possible tidal influence, and a few cases of MFCHs also occur (well 1). A slight upwards trend of increased marine influenced deposits is also observed in cross-sections 5 and 6 indicating a base level increase.

A distinctive fining up profile ("funnel shaped" on neutron - density logs) capped with coal is observed in nearly all the wells (out-faulted in well 1) and identified in both core and on wireline logs (Fig 4.5). This feature is interpreted as a laterally persistent, tidally influenced channel deposit, as seen from core data, probably representing delta distributaries. The funnel shaped channel feature on separated neutron - density logs, is observed across the Heidrun Field, suggesting field wide base level decrease during the deposition, i.e. a candidate local sequence boundary. A sea level drop resulting in the presence of an incised valley seems unlikely due to the relatively limited thickness (up to 10 m thick in well 2) of the sandstones, in addition to the lack of any indicator that would suggest incision (see Åre 2.2 discussion). Increased, avulsion processes constantly removing interfluvial sediments does, however, seem more likely as the depositional mechanism for this channel sandstone.

The channel sandstone is followed by a several meter (up to more than 10 m in well 4) succession dominated by floodplain fines and crevasse deposits. In some wells, such as in wells 3 and 7, MBFs dominate this termination phase. The presence of MBFs directly overlying fluvial sandstones suggests that the depositional environment was close to the sea. In areas where the main channel sandstone is thin (only a few m) this channel termination phase seems to comprise more abundant $\sim m$ scale sandstone units (crevasse channel) deposits. This could indicate that the palaeo channel developed preferred courses, represented by the thicker channel sandstone units such as in well 4, and that the sand rich termination phase deposits represent an area close to these main channels and subjected to steady influx of crevasse sands during floods.

The 3.2 channel deposition terminated as a result of continued base level rise, probably as the result of local delta lobe switching or as regional sea level rise in the area, resulting

in flooding of the channel complex. This deepening event resulted in a high and rising water table, reduced sediment influx and the development of a field wide peat swamp deposit, represented by the correlatable coal unit capping the Åre 3.2 channel succession. This coal is therefore interpreted as a local flooding surface.

The Åre 3.2 coal unit is followed by a succession dominated by crevasse and floodplain deposits followed by a second coal unit. This is suggested to represent small shifts in deltaic deposition where the crevasse and floodplain deposits represents a period of clastic delta lobe deposition, whereas the coal represent a second abandonment due to lateral shifts in delta lobe deposition. The inter-coal sediment package probably represents delta lobe margin deposits, where crevasse and floodplain deposits are thought to dominate.

SBFs and MBFs increase in appearances upwards in the 3.3 zone (i.e. wells 10, 5, 7, 11, 6), suggesting base level rise throughout this interval. However, at the top of Åre 3.3 one channel sandstone appears to be correlatable in cross-section 5, probably autogenic in origin due to the limited thickness ($\sim 3\text{m}$) and lateral extent. The overall base level rise culminates with the first regional correlatable bay fill succession interpreted by Leary et al. (2007) at the top of Åre 3.3. Where this bay fill is penetrated by wells it always shows the same character and has a very distinct wireline log response (c.f. Fig 4.5). This signature is identified in nearly all of the wells which penetrate this part of the stratigraphy. The bay fill unit consists of an intricately laminated mudstone which varies in thickness from 3-5m. Above this unit, mudstones become slightly more sandy and trace fossil assemblages of *Arenicolites carbonarius* and *Skolithos* start to appear. The unit is sharply overlain by a relatively thick succession of SBF sandstones (10-20m) displaying wave dominated structures and hummocky cross stratification. This probably represents the first main phase of brackish interdistributary bay development. This unit, due to its lateral extent, is one of the best correlative beds in the Åre Fm., and because of the above described facies development it could probably represent a relative base level rise (here sea level rise) - hence a flooding surface (S. Leary pers. comm. 2006). This transition from a fluvial to a marine dominated environment is a regional event observed also in neighboring fields on the Halten Terrace (Smørbukk), and the surface may therefore represent a regional flooding

event. A relatively persistent carbonate (calcite) cemented interval occurring above this flooding surface is interpreted to be associated with this deepening event (See Paper I) and consequently suggested to be correlatable between wells. Carbonate cemented zones associated with flooding events are also suggested elsewhere (Kantorowicz et al., 1987; Taylor et al., 1995).

4.3.4 Åre 4

Sandy bay fill deposits, often capped by coal, dominate the 15-20m succession above the 3.3 flooding surface and are observed as 2-6m thick SBF sandstones in the studied cored wells 2, 5 & 10 from this interval. Autogenic processes dominated as cyclic delta lobe deposition (SBF/MBF).

After the regional base level rise and flooding of the Heidrun area, culminating in the top Åre 3.3 surface, continental deposition gradually returned to the area as a wedge of fluvial deposition dominated by two laterally correlatable MFCHs. These are relatively thin FCH sandstones of ~1-2m thickness (up to 6m thick in well 10) capped by paleosols and coal. The channel termination infill phase represented by the paleosol and coal units are correlatable between wells in the central parts of Heidrun Field defining the top Åre 4.1 and 4.2, respectively and defined as local flooding surfaces (Cross-sections 7 and 8). In core sections these channels have been identified as up to 10m thick fluvial sandstones of relatively constant grain-size. The constant grain-size may suggest that the channels were relatively straight, resembling delta distributary channel deposits (Bridge, 2003). In the correlation panels these channel sands thicken towards the NW reaching a maximum TVD thickness of ~10m for the 4.2 channel sandstone in well 1 and ~20m for the 4.3 channel sandstone in well 14. Thicknesses can vary significantly over short distances, as exemplified in well 13 only 190m SE of well 14 where the 4.3 channel sandstone is missing completely. The sandstones thin towards the S-SE and N suggesting a palaeoflow in a southeast direction. A progradation of fluvial sediments into the area from the northwest, either as the result of renewed tectonic uplift of the Nordland Ridge, or more

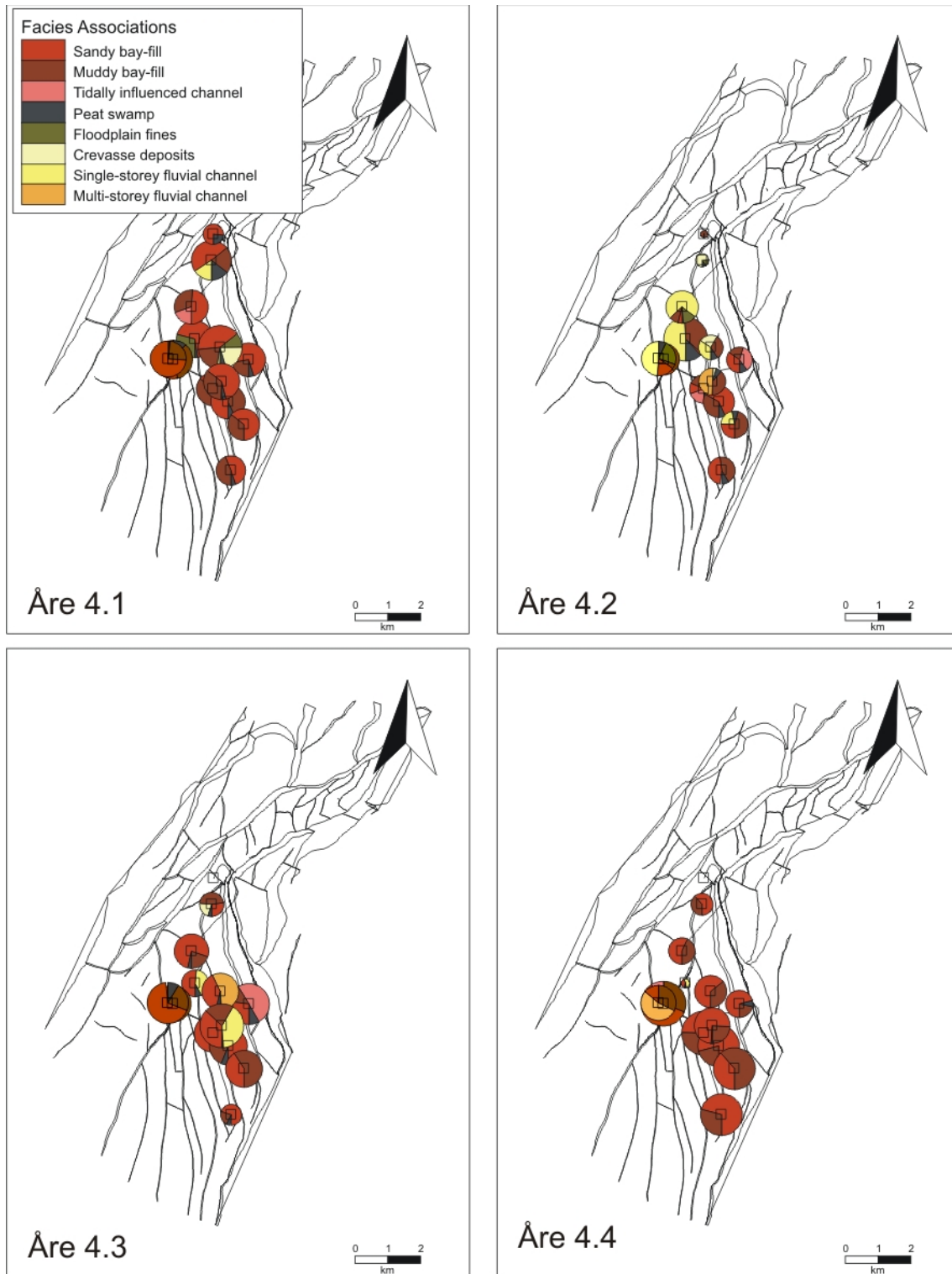


Figure 4.6: Bubble maps constructed from 11 wells of the Åre reservoir zones 4.1 to 4.4 illustrating a shift in dominant facies associations with time. Zones 4.1 and 4.4 are dominated by SBF/MBF deposits, whereas 4.3 and especially 4.2 have a more abundant fluvial composition.

likely, as the result of large-scale autocyclic deltaic processes occurred. However, the Heidrun Field represents only a fraction of a much larger tributary system and the main depocenter of the system may shift laterally. These two channel sandstones therefore probably originated by large-scale deltaic autogenic shifts in the fluvial sedimentation focus, representing periods of sediment focus into the Heidrun area. This level therefore constitutes important field wide correlation surfaces and the base of the Åre 4.3 channel sandstone is therefore defined as a candidate local sequence boundary (unconformity). A period of floodplain and interdistributary bay deposition, including abundant peat swamp development, separates these two pulses, either as a result of reduced sediment influx, sediment starvation or rising water table due to sediment compaction.

Coal intervals, correlatable at least in the central parts of the study area, are identified at top Åre 4.1 and top Åre 4.2 as terminations of FCH/CCH deposition. Although coals associated with fluvial deposition are considered as less correlatable in the Åre Fm., they seem to appear in several wells at the same stratigraphic interval (i.e cross-section 7). In fact, the top 4.2 coal is suggested as a confident field wide correlation surface and a well known pressure barrier in the Heidrun Field (Camilla, T. pers. comm. 2010). These fluvial sediments probably represent the last increment of deposition completely filling the bay with sediments, halting marine reworking. In this sense these coals are more related to the interdistributary bay area and therefore have larger lateral continuity compared to fluvial peat swamp deposits.

Above the top Åre 4.3 sand, wireline log signatures indicate a transition from a relatively heterogeneous coastal plain interval below, to more homogeneous coarsening sequences interpreted as stacked SBFs above, represented by a $\sim 10m$ thick SBF sandstone in the core from well 4. An abrupt change in deposition occurred above the second channel sandstone where SBF and MBF sedimentation returned to the study area (Fig. 4.6).

4.3.5 Åre 5.1

The sediment flux into the study area became subsequently muddier after Åre 4.4, depositing predominantly MBFs, as represented by the >20m thick MBF dominated interval seen in the core from wells 2 and 4 and on wireline log data from several other wells. The thickness of this muddy interval, generally ~20m and up to more than 35m in well 4, indicates that this change is related to more than just main delta depocenter adjustments, suggesting a possible regional deepening event controlled by relative sea-level rise. In addition, no channels are identified within the 5.1 interval. The transition from sand prone to mud prone deposition is therefore interpreted as an expansion surface and, hence, a flooding surface and is clearly observed on wireline log data (cross-sections 9 and 10). On GR and NPHI-RHOB logs, 2-3 upwards fining intervals representing stacks of heterogeneous bay fills are recognized within the Åre 5.1 zone. On the core from wells 2 and 4 these stacks are interpreted as ~10-15m thick successions comprising bay fill deposits with increasing fractions of MBFs upwards in each stack. The deposits are suggested to represent delta lobe deposits subjected to both authigenic and allogenic controlling factors where two orders of cyclic base level change can be recognized in addition to general sea level rise. The first order is represented by the 2-3 coarsening stacks of bay fills observed, related to large-scale autogenic deltaic processes and suggested as parasequence sets. The second order of cyclicity is related to delta lobe switching represented by the individual bay fill deposits and these are interpreted as individual parasequences within the first order parasequence sets. In addition, sedimentation in the southeast became increasingly muddier upwards, observed as an overall increase in GR in wells 4, 5, 6 and 7, indicating regional deepening during the deposition of the Åre 5.1.

4.3.6 Åre 5.2 - 6

As seen from the sedimentological log from well 4, the mud prone bay fills of the Åre Fm. 5.1 zone is down-cut by a 10m thick tidally influenced distributary channel complex sandstone. The tidally influenced distributary channel complex appears as a 5 m thick

sandstone unit capped by 7 m thick heterolithic succession strongly suggestive of tidal influence. This sharp boundary separating mud prone bay fills below from tidal channel deposits above is also recognized on petrophysical logs in the studied wells suggesting that this is a significant sequence stratigraphic event related to base level fall. Similar development of tidal channels cutting into bay fill deposits is observed on data from neighboring fields (e.g. Smørbukk), suggesting that this boundary represents a regional base level fall and is therefore interpreted as a sequence boundary (Cross-sections 11 and 12).

The TCH channel sandstone is followed by a 5-20 m thick succession comprising SBF and MBF deposits with occasional tidally influenced single storey channel sandstones. The abundance of channels decreases upwards in the Åre 5.2 and 5.3, up to a level where an abrupt change from SBF to MBF dominated deposition occur. This abrupt change in N/G suggests increased accommodation space due to base level rise and is suggested as a flooding surface. In fact, according to palynostratigraphic data (Statoil - in house) mentioned in Leary et al. (2007), a major transgressive event took place at the 5.3 to 6.1 boundary with a well expressed reworking of Triassic palynomorphs.

The interval overlying this flooding surface comprises ~15m thick succession dominated by MBF sediments, including thin intervals (dm-up to 1 m) of SBF sandstones. On cross-sections 11 and 12 increasing abundance of SBF sediments is observed towards the uppermost part of Åre 6.1, indicating a shallowing in the area. This shallowing culminated in a second incision of tidally influenced distributary channel sandstones correlatable across the Heidrun Field. In the core from well 4 this channel complex is represented by a 17 m thick amalgamated section of three channel sandstone bodies. On average the Åre 6.2 channel complex is twice the thickness of the 5.2 channel sandstone. Either the base level drop prior to deposition was larger compared to Åre 5.2, or the system focus was closer to the feeder channel or possibly represents the feeder channel delivering sediments into the Åre basin. Nevertheless, a significant change in depositional style and sediment composition occurred. In Åre 6.1-6.2 tidally influenced channel deposits dominate the middle and eastern most part of the field as compared to bay fills in the west, north and south.

This may be explained by a shift of source area towards the east, which would represent a significant change in coastal morphology at the time of deposition. The first abundant occurrences of true marine dinoflagellate cysts, marine acritarchs and prasinophycean algae is represented in the Åre 6.2 (Statoil - in house). No clear trend revealing palaeocurrent direction can be made from the cross-sections alone, however, a slight increase in thickness towards the southeast may be recognized (Fig. 4.7). Provenance studies of heavy mineral assemblages in sandstones from the Early Jurassic succession in the Heidrun Field (Morton et al., 2009) support a source area from the Norwegian mainland to the east for the tidally influenced part of the Åre Fm. The channel sandstone is followed by a heterogeneous 2-10m thick interval very similar to the 5.2 interval, comprising SBF and MBF deposits and occasional single storey TCH sandstone indicating continued base level rise during deposition of the remainder of Åre 6.2.

4.3.7 Åre 7

A significant change in sedimentation style is observed in the core from well 4 above the Åre 6.2 bay fills, marked by a ~10 cm thick gravelly lag. The sediments overlying this lag are strongly heterolithic packages of flaser to lenticular laminated sand and siltstones and have been interpreted as transgressive shallow marine shoreface deposits by Leary et al. (2007) and Kjærefjord (1999). The sandstone laminae are in places composed of grains up to very coarse grade. Two depositional slightly different intervals are recognized, although both are interpreted as TSMS deposits; both sand prone TSMS and mud prone TSMS. In well 4 two pulses of coarsening upwards (mud prone TSMS followed by sand prone TSMS) intervals occur, possibly representing prograding pulses of shoreface deposits in a transgressive, back stepping system.

The top Åre 6.2 gravelly lag is interpreted as a transgressive surface according to Thrana et al. (2009) suggesting that this is a marine flooding surface separating the underlying lowstand systems tract (Åre 5-6) from the overlying transgressive systems tract (Tilje Fm.).

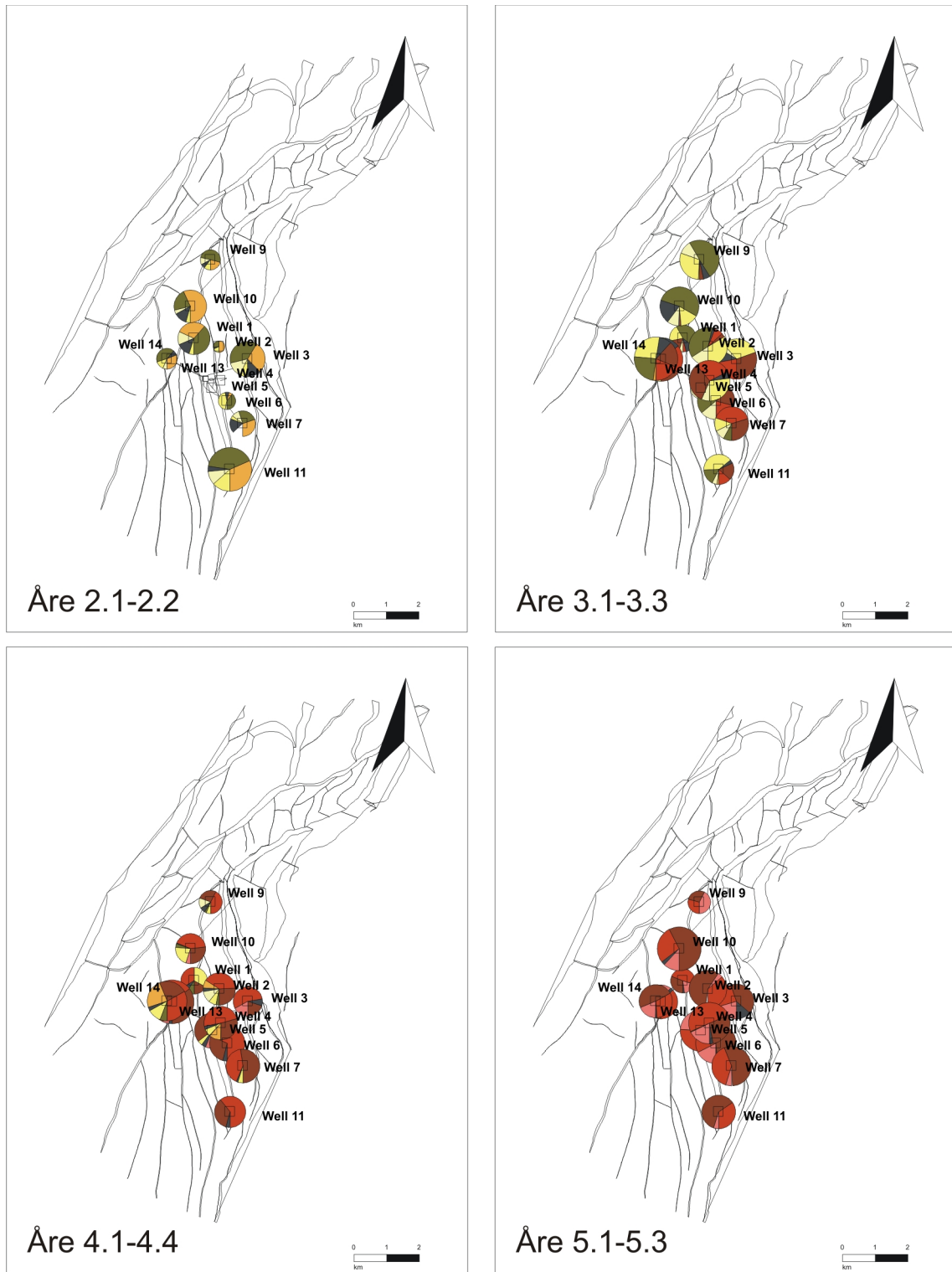


Figure 4.7: Bubble maps (cont.)

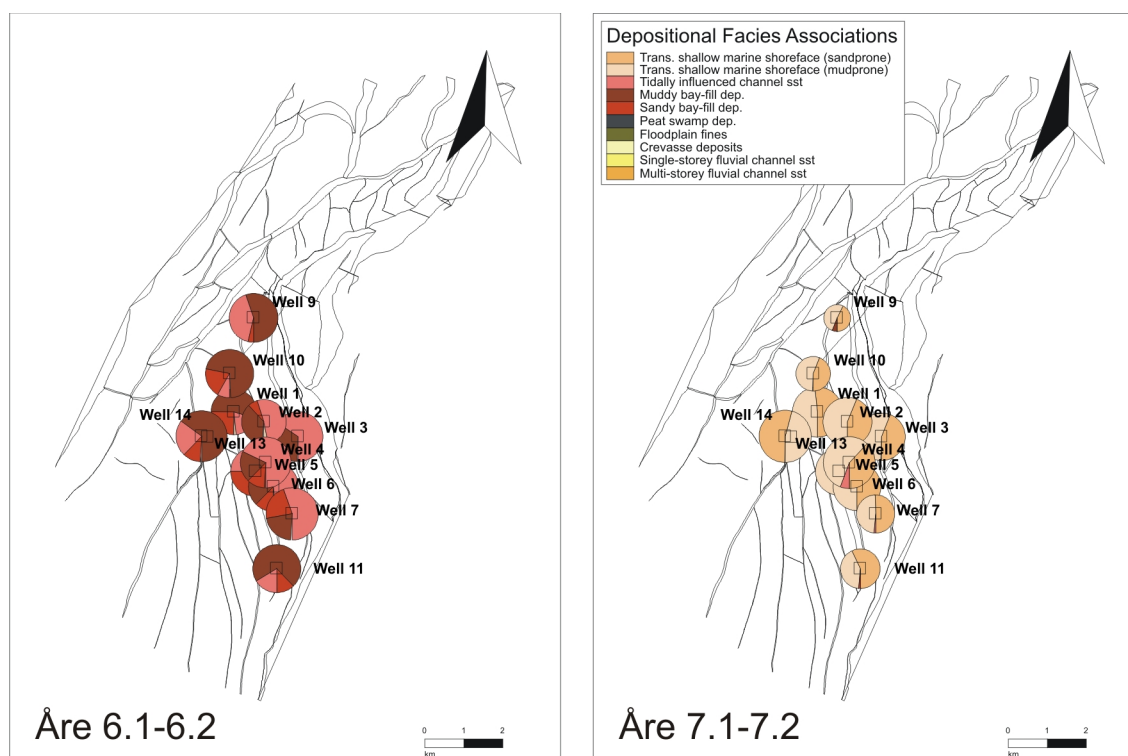


Figure 4.7: Bubble maps showing proportional facies distribution within selected Åre intervals. From the facies proportion distribution a NW-SE proximal to distal trend of facies associations is revealed in the lower parts of Åre (up to Åre 4.4) as more abundant proximal facies associations dominate in the NW parts of the field compared to more distal in the SE (e.g. Åre 3.1-3.3, Åre 4.1-4.4). A possible shift in source area is observed at the deposition of Åre 6.1-6.2 where tidally influenced channel deposits dominate the middle and eastern most parts of the field compared to bay fills in the west, north and south. This shift in source area during the Åre deposition is supported by Morton et al. (2009).

4.4 Summary

Five candidate sequence boundaries (including one regional event) and nine candidate flooding surfaces (four regional and including the transgressive surface at top Åre 6.2) are identified in the dataset, enabling a relatively detailed sequence stratigraphic division within the fluvial-deltaic Åre sediment package of the Heidrun Field.

Throughout the Åre Fm. the signature of base level rise is striking. A clear transgressive trend is evident throughout the interval where the typical fluvial processes dominating the lower part of the stratigraphy are gradually replaced by tidal and marine processes towards the top (Fig. 4.8). The depositional environment was probably similar to the environment interpreted for the Ivishak Fm., Prudhoe Bay (Tye et al., 1999), at least up to Åre 5.1, omitting the tidally influenced incursions from the east. Although the Ivishak Fm. is progradational compared to the transgressive trend of the Åre Fm., Heidrun Field, type and stacking of facies associations appear very similar. Inter-channel floodplains dominated by shallow lakes and ponds, occasionally filled with crevasse splays during floods. Towards the basin, the fluvial channels bifurcated, forming tidally influenced, delta distributary channel systems, feeding delta lobes dominated by SBF deposits. Adjacent to these lobes, low energy, muddy interdistributary bay fills (MBF) deposition dominated, where some areas may even have become completely enclosed forming lagoons and marsh environments.

By mapping out the facies distribution within specific Åre reservoir intervals the evolution of the depositional environment during the deposition of the Åre Fm., becomes apparent (Figs. 4.7 and 4.7). The transgressive trend is seen as a change from fluvial dominated to marine influenced deposits upwards. The coastal incursions during deposition of the Åre 4 is also visible. A trend of progradation/retrogradation towards the east/southeast for the lower part of the Åre Formation is seen from the generally more distal facies association distribution in the E-SE, whereas a shift to an easterly source area can be interpreted for the uppermost part of Åre (Åre 6).

Multi storey channel sands (Åre 2.2, 3.2, 5.2 and 6.2) are correlatable between wells several kilometers apart, some of which resulted from local or regional base level events, and therefore are important sequence stratigraphic markers. Single storey channel sandstones have also been correlated within specific zones, as exemplified by the Top Åre 3.3 channel sandstone. Coals constitute important sequence stratigraphic surfaces within the Åre Fm., where one coal interval is related to a regional base level increase (top Åre 1). However, a distinction should be made regarding coals developed on the fluvial plain and

those developed in interdistributary bays. Peat swamps developing on the fluvial plain are thought not to represent laterally extensive features. Except from the coal marker defined at top Åre 1 and 2.1, no clear candidate for inter-well correlation exists for the fluvial part of the succession (up to Åre 2.2), despite significant thicknesses (several meters). Coals developed in interdistributary bay (3.2, intra 3.3, 4.1, 4.2) areas, on the other hand, are suggested to have potential as correlatable horizons, at least of distances of a few kilometers, which is sufficient for inter-well correlation of the Åre Fm. in the Heidrun Field. Although bay fill dimensions are large enough for inter-well correlation (top Åre 3.3), their stacking pattern, revealing similar trends of increased or decreased occurrences of MBF/SBF, may in addition reveal strong evidence for local and regional base level fluctuations.

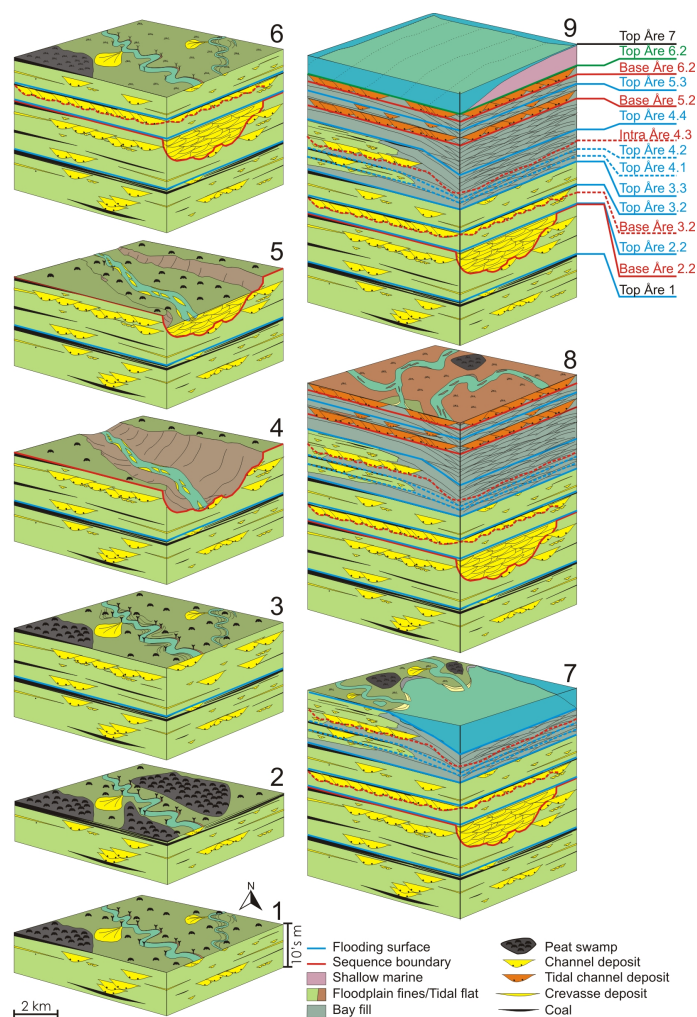


Figure 4.8: Conceptual sketch of stacked palaeogeography interpreted for the Åre Fm. illustrating the shift in sedimentation related to shifts in base level. Base level rise is indicated for Stage 1 comprising floodplain deposits (FF, LEV, CCH) and meandering channel fills (SFCH), and culminating with the deposition of a lateral amalgamated peat unit (Stage 2). Stage 3 displays a rising base level similar to Stage 1. Stage 4 represents a base level fall (still stand?) and subsequent erosion (incision?). This incision filled with braided river deposits during a rise in base level during Stage 5. Stage 6 represents deposition after the complete filling of the valley and increasing base level rise. This rise is related to a sea level rise which continues for the remainder of the Åre Fm. Stage 7 represents the bay fill development and clear marine influence. Stage 8 represents the two dominant tidal channel incursions resulting from base level lowering. Stage 9 is the final transgression of the Åre Fm. marking the gradual transition to the overlying Tilje Fm. Base level changes are schematically presented in Fig. 4.4.

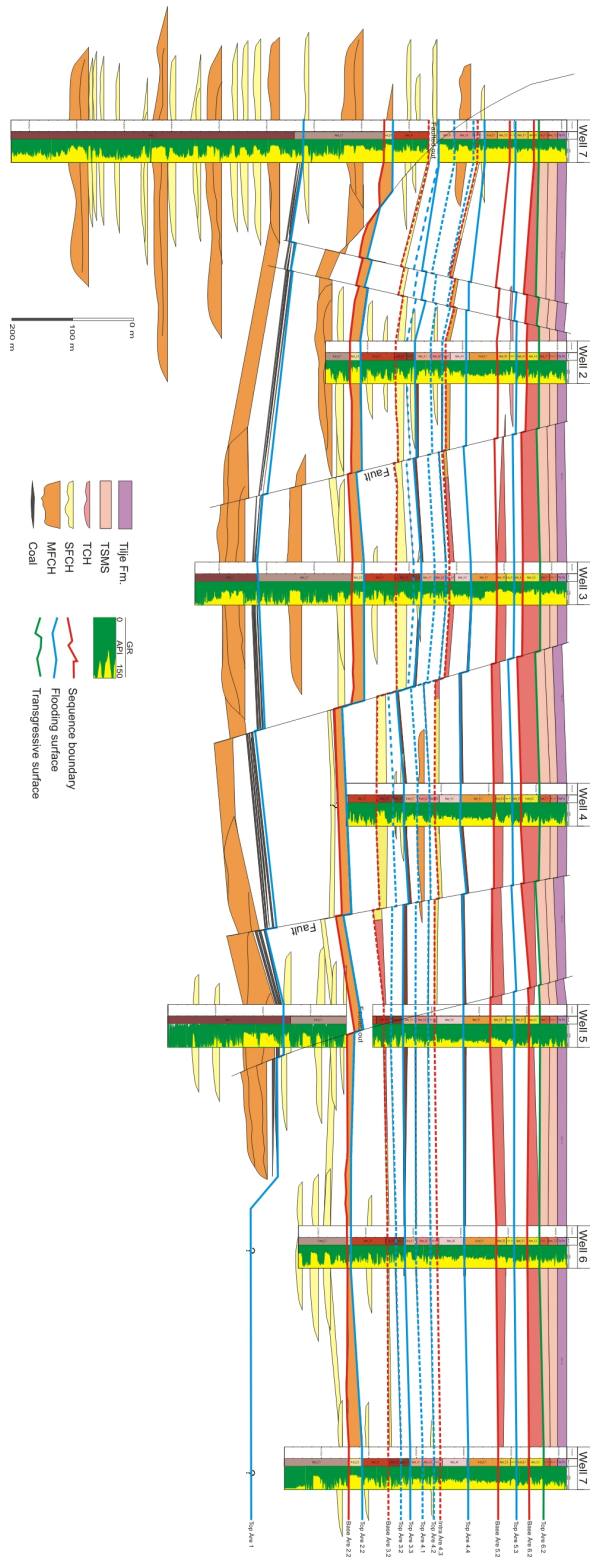


Figure 4.9: N-S correlation panel for the central parts of the Heidrun Field displaying changing depositional patterns related to base level changes. The difference in proportions of SFCHs and MFCHs in Åre 1 and 2.1 is easily seen in the lower half of the cross-section. The laterally persistent channel deposits in Åre 2.2, Åre 4.2, Åre 4.3, Åre 5.2 and 6.2 reflect times of base level lows and appear correlatable between wells. In addition, nine flooding surfaces are recognized as sequence stratigraphic surfaces. Four are related to Hooding coals (Top Åre 1, 3.2, 4.1, 4.2), one related to the filling of an incised valley (Top Åre 2.2), one related to a regional trend of correlatable bay fill development (Top Åre 3.3), and two related to a dominant change in N/G (Top Åre 4.4 and 5.3). In addition a transgressive surface marks the transition from a LST to a TST at top Top Åre 6.2 defining the ninth Hooding surface. See Fig. 2.3 for location of the cross-section.

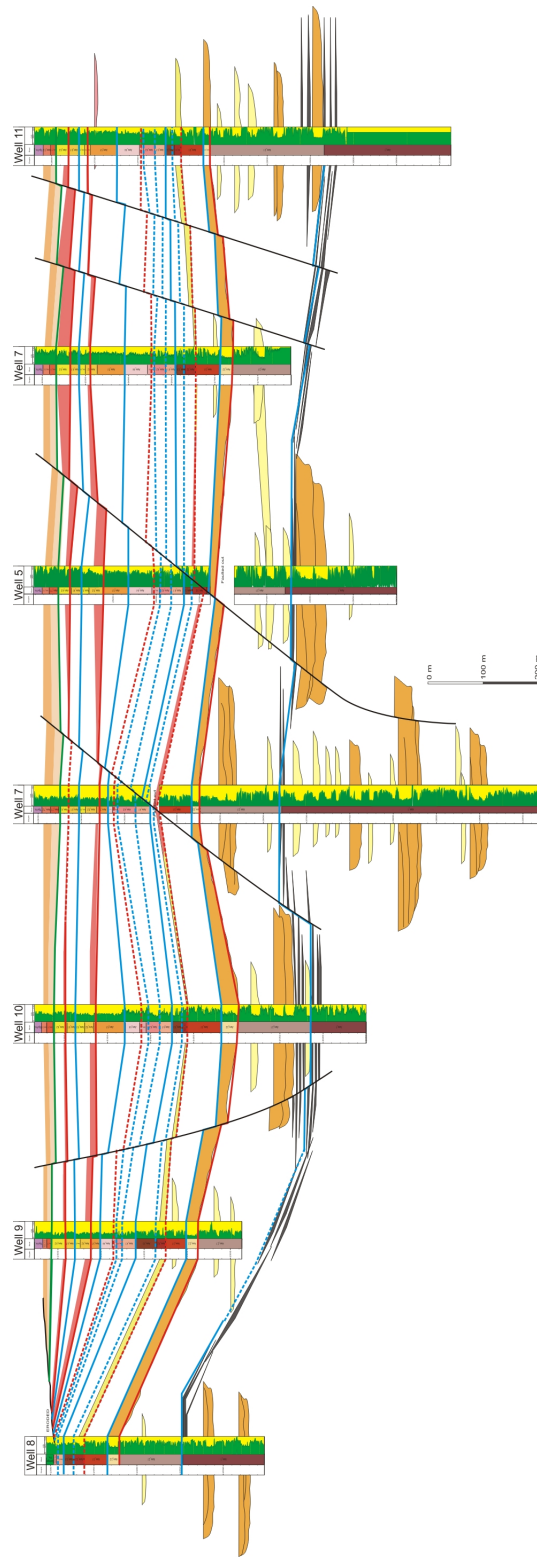


Figure 4.10: E-W correlation panel for the central parts of the Heidrum Field displaying changing depositional patterns related to base level changes. See Fig. 4.9 for discussion and Fig. 2.3 for location of the cross-section.
















Facies associations		Sequence stratigraphic surfaces	Wireline log data						
 Transgressive shallow marine shoreface (mud prone)	 Single storey fluvial channel (SFCH)	 Transgressive surface	<table border="1"> <tr><td colspan="3">VSH</td></tr> <tr><td>0</td><td>v/v decimal</td><td>1</td></tr> </table>	VSH			0	v/v decimal	1
VSH									
0	v/v decimal	1							
 Transgressive shallow marine shoreface (sand prone)	 Multi storey fluvial channel (MFCH)	 Regional sequence boundary	<table border="1"> <tr><td colspan="3">NPHI</td></tr> <tr><td>0.45</td><td>v/v decimal</td><td>-0.15</td></tr> </table>	NPHI			0.45	v/v decimal	-0.15
NPHI									
0.45	v/v decimal	-0.15							
 Muddy bay fill (MBF)	 Tidally influenced distributary channel (TCH)	 Regional flooding surface	<table border="1"> <tr><td colspan="3">RHOB</td></tr> <tr><td>1.95</td><td>g/cm3</td><td>2.95</td></tr> </table>	RHOB			1.95	g/cm3	2.95
RHOB									
1.95	g/cm3	2.95							
 Sandy bay fill (SBF)	 Peat deposit (Coal)	 Local sequence boundary							
 Floodplain fines (FF)		 Local flooding surface							
 Carbonate cemented									

Figure 4.11: Legend for cross-sections 1 to 12.

Fig. 4.12 Cross-section 1

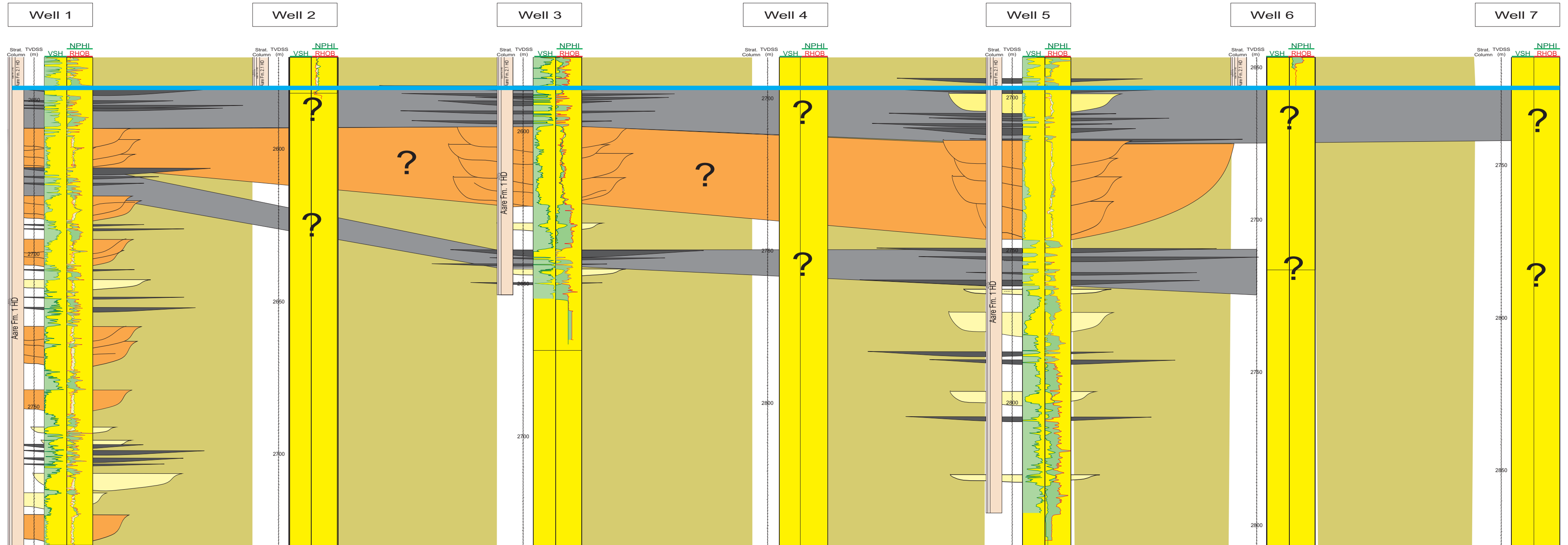


Fig. 4.13 Cross-section 2

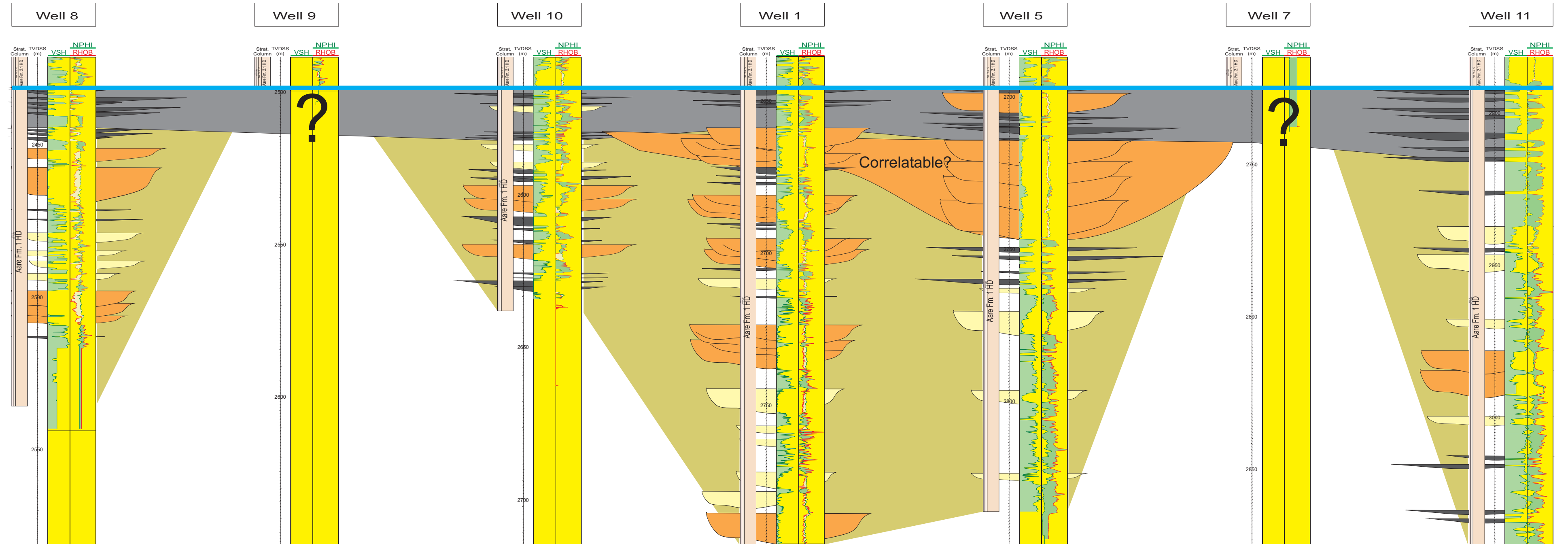


Fig. 4.14 Cross-section 3

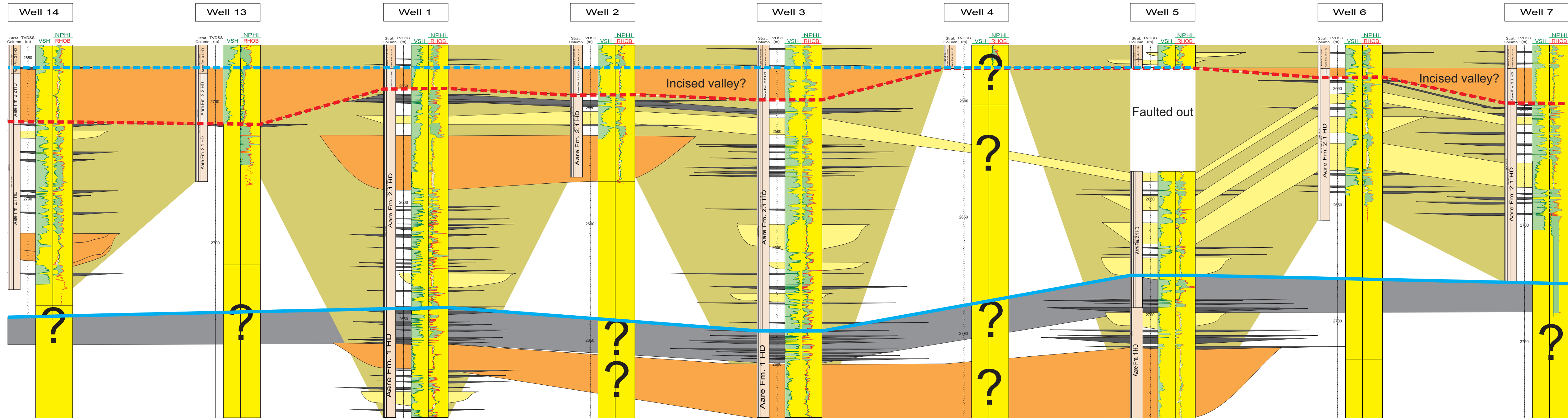


Fig. 4.15 Cross-section 4

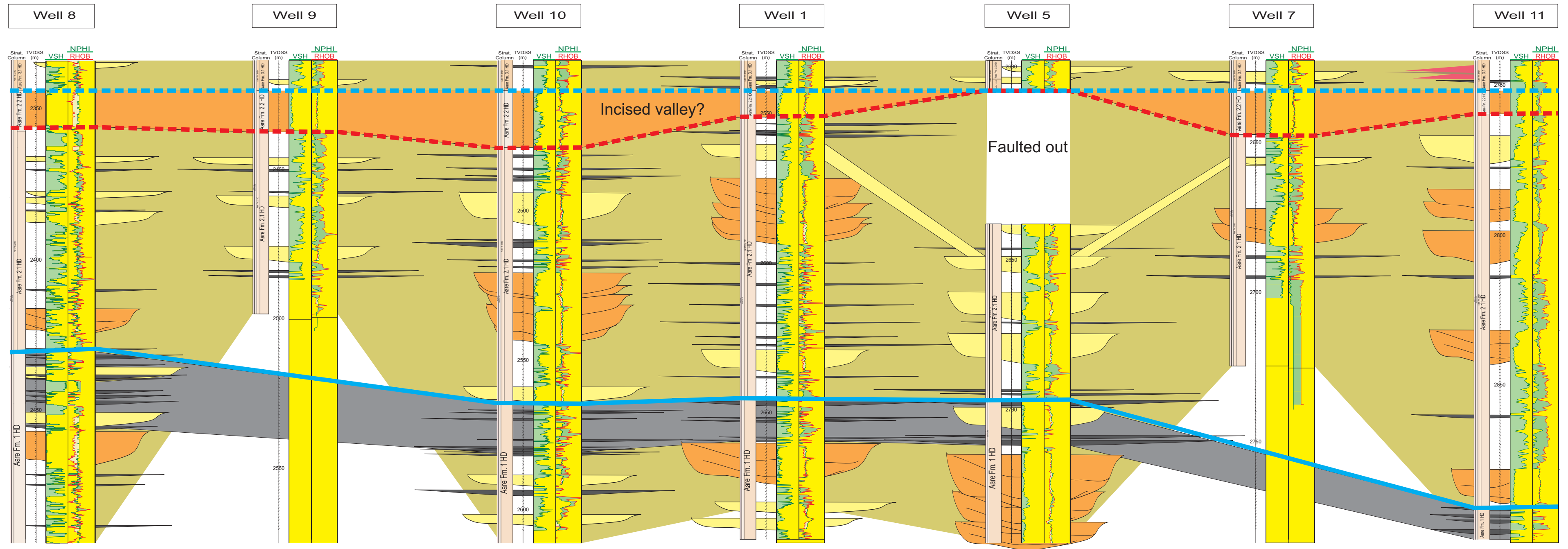


Fig. 4.16 Cross-section 5

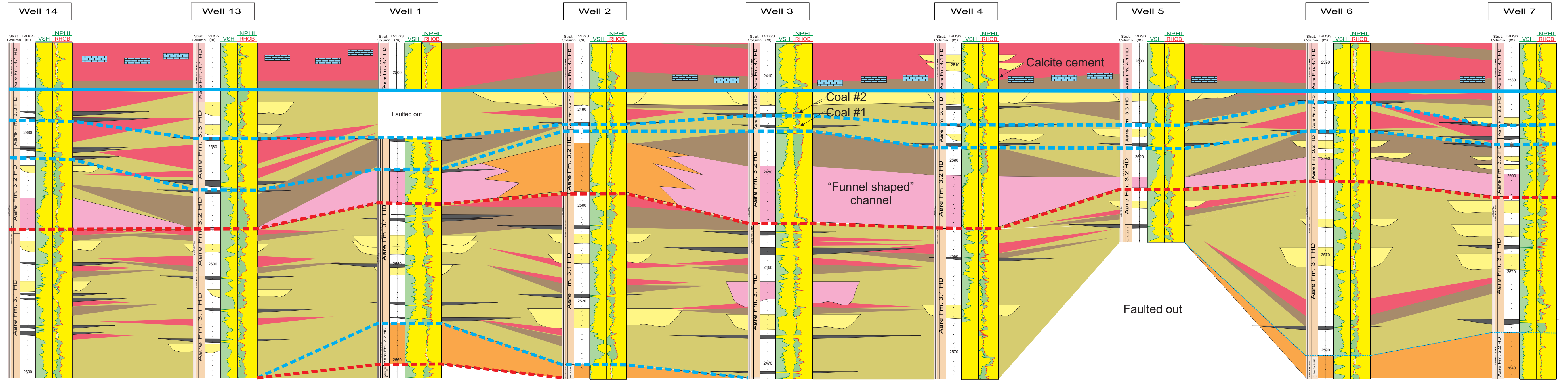


Fig. 4.17 Cross-section 6

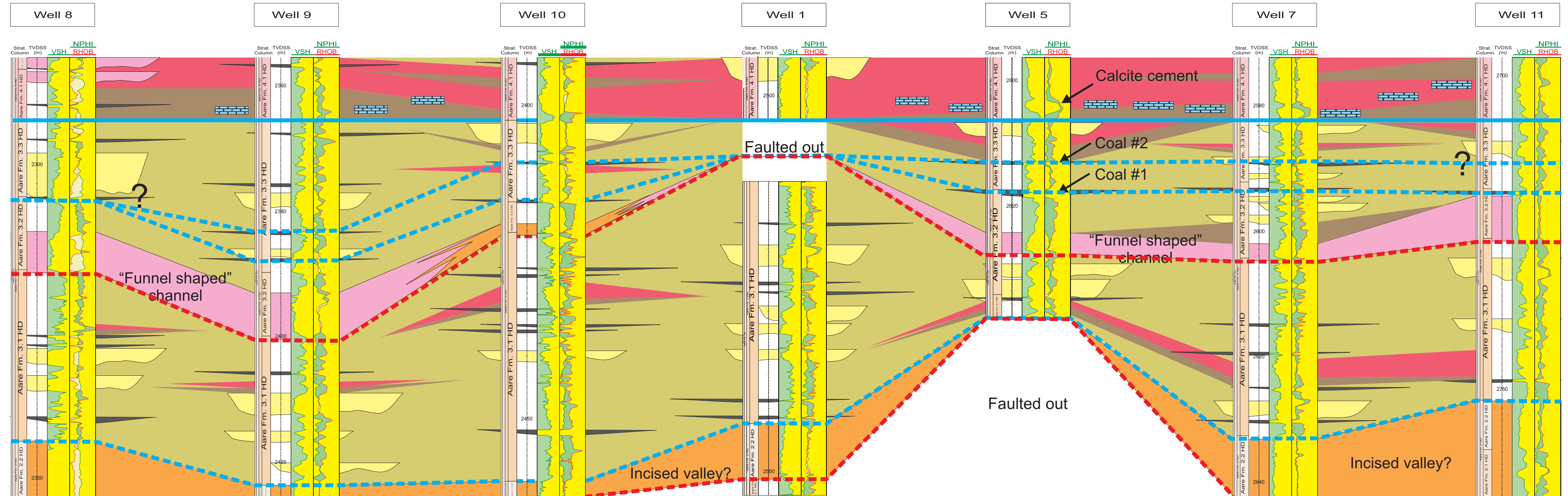


Fig. 4.18 Cross-section 7

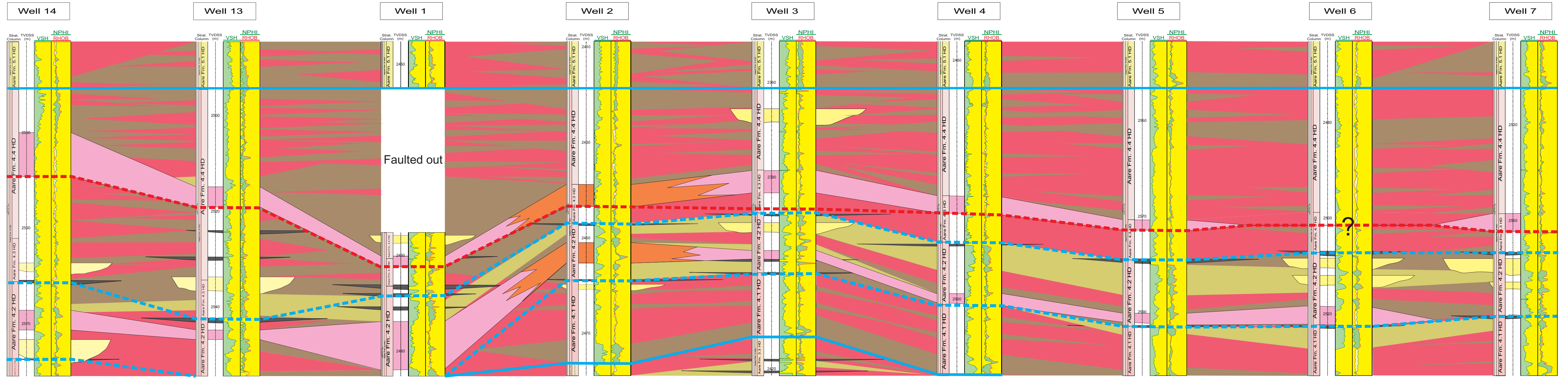


Fig. 4.19 Cross-section 8

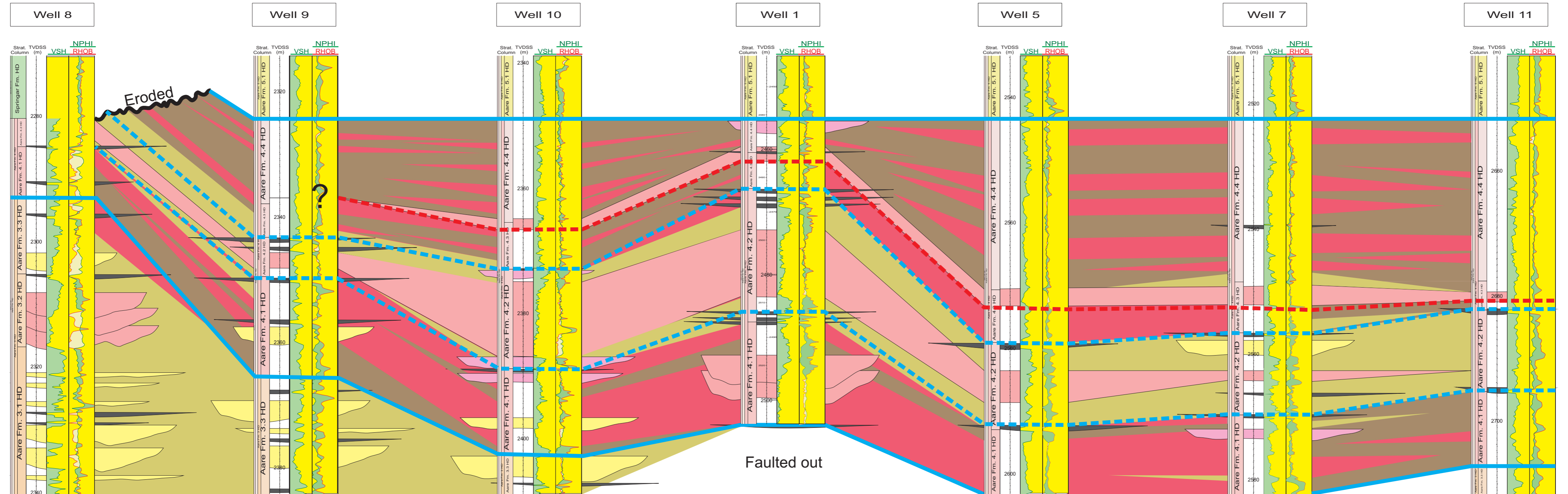


Fig. 4.20 Cross-section 9

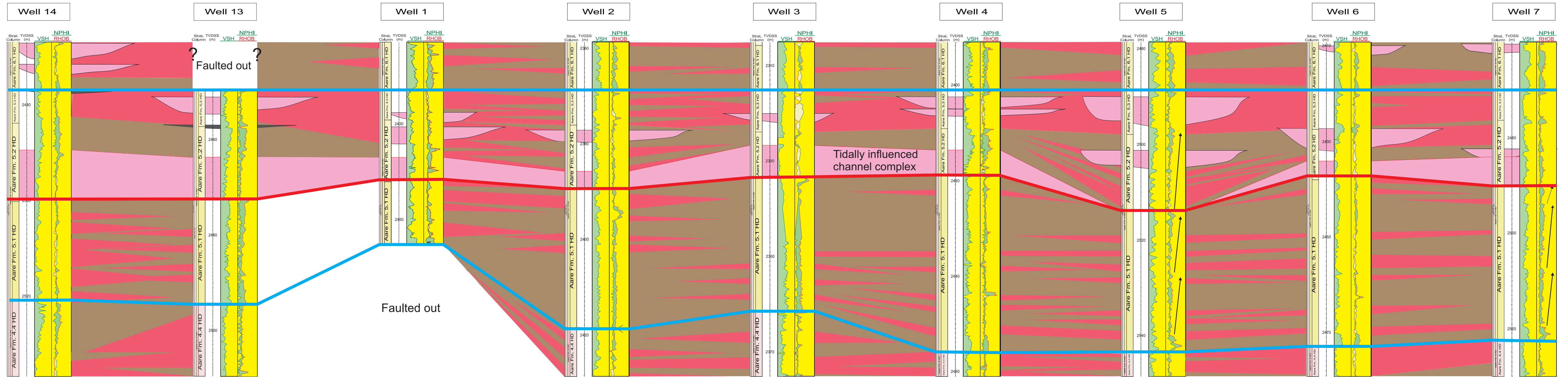


Fig. 4.21 Cross-section 10

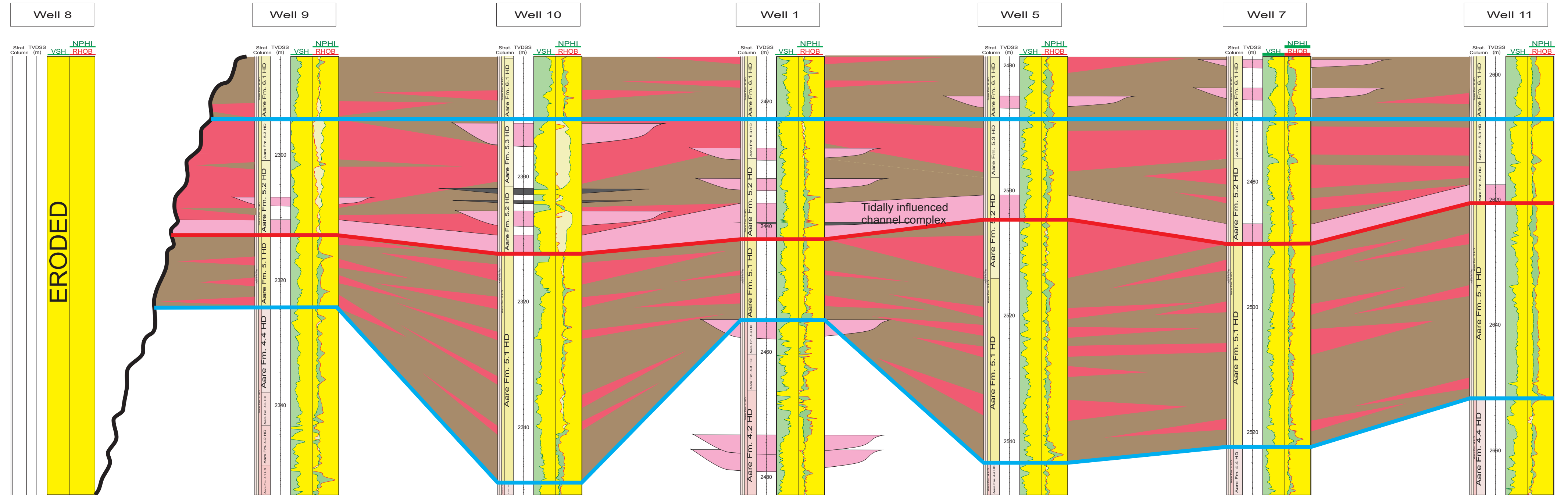


Fig. 4.22 Cross-section 11

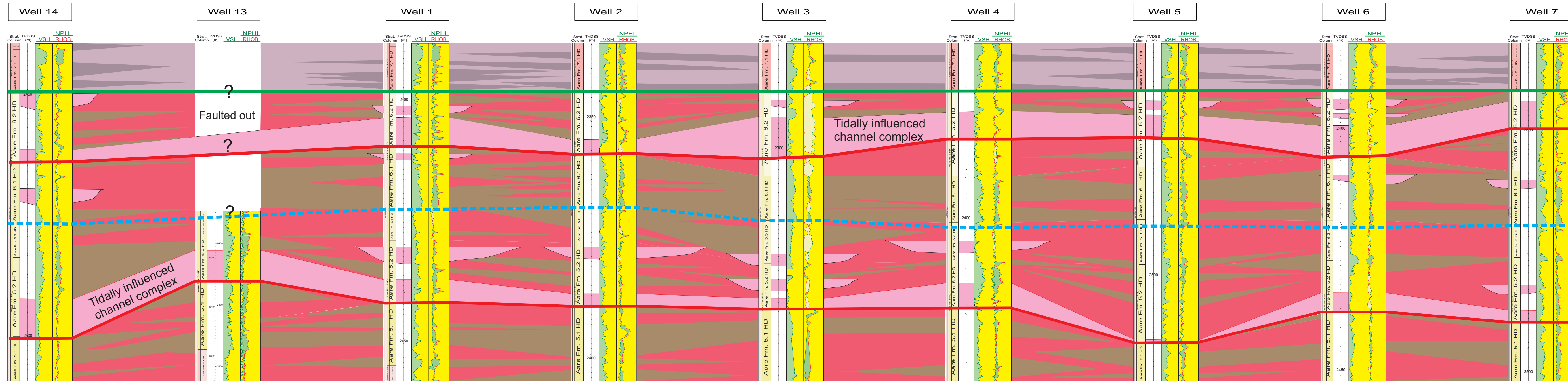
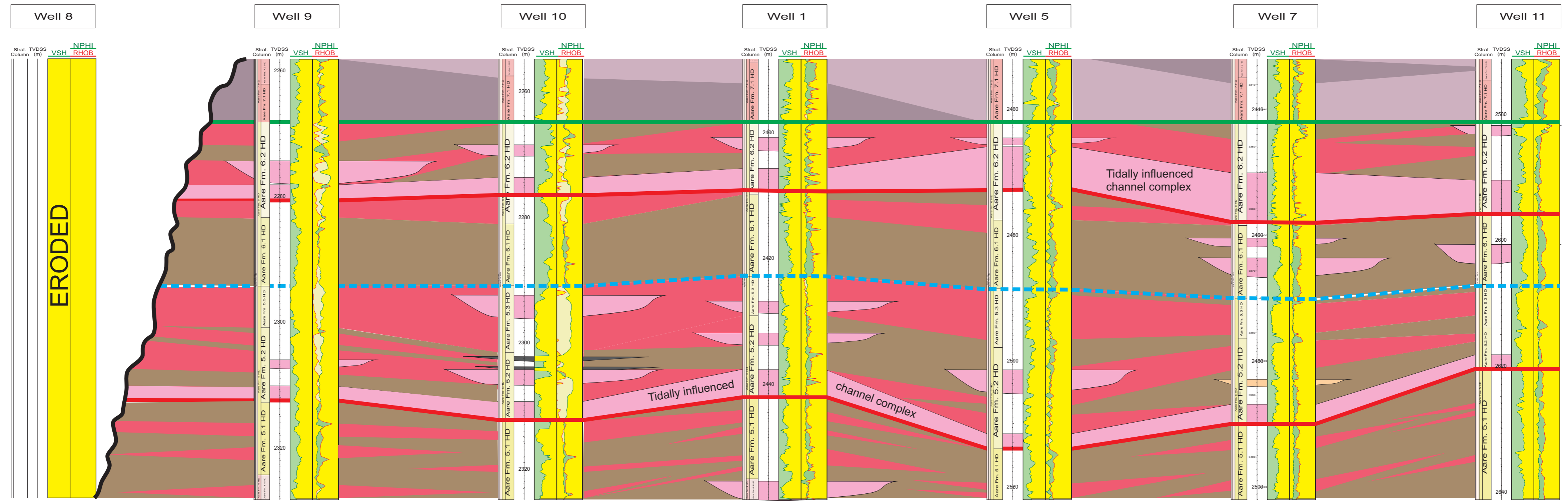


Fig. 4.23 Cross-section 12



References

- Allen, J., 1971. A theoretical and experimental study of climbing-ripple cross-lamination, with a field application to the uppsala esker. *Geografiska Annaler* 53A, 157–187.
- Allen, J., 1978. Studies in fluvial sedimentation: an exploratory quantitative model for architecture of avulsion-controlled alluvial suites. *The American Association of Petroleum Geologists Bulletin* 21, 129–147.
- Aplin, A., Warren, E., Grant, S., Robinson, A., 1993. Mechanisms of quartz cementation in North Sea reservoir sandstones: constraints from fluid compositions. In: Horbury, A., A.G., R. (Eds.), *Diagenesis and Basin Development*. Vol. 36 of *Studies in Geology*. pp. 5–22, American Association of Petroleum Geologists.
- Baeteman, C., 2005. How subsoil morphology and erodibility influence the origin and pattern of late holocene tidal channels: case studies from the Belgian coastal lowlands. *Quaternary Science Review Letters* 24 (18-19), 2146–2162.
- Baeteman, C., Scott, D., van Strydonck, M., 2002. Changes in coastal zone processes at a high sea-level stand: a late holocene example from Belgium. *Journal of Quaternary Science* 17, 547–559.
- Beynon, B., Pemberton, S., Bell, D., Logan, C., 1988. Environmental implications of ichnofossils from the Lower Cretaceous Grand Rapids Formation, Cold Lake Oil Sands Deposit. In: James, D., Leckie, D. (Eds.), *Sequences, Stratigraphy, Sedimentology*:

- Surface and Subsurface. Vol. 15 of Canadian Society of Petroleum Geologists Memoir. pp. 275–290.
- Bjørlykke, K., 1998. Clay mineral diagenesis in sedimentary basins - a key to prediction of rock properties. Examples from the North Sea. *Clay Minerals* 33, 15–34.
- Bjørlykke, K., Aagaard, P., Dypvik, H., Hastings, D., Harper, A., 1986. Diagenesis and reservoir properties of Jurassic sandstones from the Haltenbanken area, offshore Mid-Norway. In: Spencer, A. (Ed.), *Habitat of Hydrocarbons on the Norwegian Continental Shelf*. Norwegian Petroleum Society, Graham and Trotman, pp. 275–286.
- Bjørlykke, K., Høeg, K., 1997. Effects of burial diagenesis on stresses, compaction and fluid flow in sedimentary basins. *Marine and Petroleum Geology* 14 (3), 267–276.
- Bøen, F., Eggen, S., Vollseth, J., 1984. Structures and basins of the margin from 62 to 69°N and their development. In: Spencer, A., Holter, E., Johnsen, S., Mørk, A., Nysæther, E., Songstad, P., Spinnanger, Å. (Eds.), *Petroleum Geology of the North European Margin*. Norwegian Petroleum Society, Graham and Trotman, London.
- Brekke, H., Riis, F., 1987. Tectonics and basin evolution of the Norwegian shelf between 62°N and 72°N. *Norsk Geologisk Tidsskrift* 67, 295–322.
- Bridge, J., 1985. Palaeochannel patterns inferred from alluvial deposits: a critical evaluation. *Journal of Sedimentary Petrology* 55 (4), 579–589.
- Bridge, J., 2003. *Rivers and floodplains. Forms, processes and sedimentary record*. Oxford, Wiley-Blackwell Publishing.
- Bromley, R., Uchman, A., 2003. Trace fossils from the Lower and Middle Jurassic marginal marine deposits of the Sorthat Formation, Bornholm, Denmark. *Bulletin of the Geological Society of Denmark* 52, 185–208.
- Bromley, R. G., 1996. *Trace Fossils: Biology and Taphonomy and Applications*, 2nd Edition.

- tion. Special Topics in Palaeontology. London, Glasgow, Weinheim, New York, Tokyo, Melbourne, Madras: Chapman & Hall.
- Bromley, R. G., Asgaard, U., 1979. Triassic freshwater ichnocoenoses from Carlsberg Fjord, East Greenland. *Palaeogeography, Palaeoclimatology, Palaeoecology* 28, 39–80.
- Bukovics, C., Shaw, N., Cartier, E., Ziegler, P., 1984. Structure and development of the Mid-Norway continental margin. In: Spencer, A., Holter, E., Johnsen, S., Mørk, A., Nysæther, E., Songstad, P., Spinnanger, Å. (Eds.), *Petroleum Geology of the North European Margin*. Norwegian Petroleum Society, Graham and Trotman, London, pp. 407–423.
- Bukovics, C., Ziegler, P., 1985. Tectonic development of the Mid-Norway continental margin. *Marine and Petroleum Geology* 2, 1–22.
- Burst, J., 1965. Subaqueously formed shrinkage cracks in clay. *Journal of Sedimentary Petrology* 35, 348–353.
- Chillingar, G., 1964. Relationship between porosity, permeability, and grain size distribution. In: Van Straten, L. (Ed.), *Deltaic and shallow marine deposits*. Vol. 1 of *Developments in Sedimentology*. Elsevier, Amsterdam, pp. 71–75.
- Cohen, M., Dunn, M., 1987. The hydrocarbon habitat of the Haltenbank-Trænbank area offshore Mid-Norway. In: Brooks, J., Glennie, K. (Eds.), *Petroleum Geology of North West Europe*. Graham and Trotman, pp. 1091–1104.
- Coleman, J., Wright, L., 1975. Modern river deltas: variability of processes and sand bodies. In: Broussard, M. (Ed.), *Deltas, Models for Exploration*. Houston Geological Society, Houston, TX, pp. 99–149.
- Corfield, S., Sharp, I., 2000. Structural style and stratigraphic architecture of fault propagation folding in extensional settings: a seismic example from the Smørbukk area, Halten Terrace, Mid-Norway. *Basin Research* 12, 329–341.

- Currie, B. S., 1997. Sequence stratigraphy of nonmarine Jurassic-Cretaceous rocks, central Cordilleran foreland-basin system. *Geological Society of America Bulletin* 109 (9), 1206–1222.
- Dalland, A., Augedahl, H., Bomstad, K., Ofstad, K., 1988. The post-Triassic succession of the Mid-Norwegian Shelf. In: Dalland, A., Worsley, D., Ofstad, K. (Eds.), *A lithostratigraphic scheme for the Mesozoic and Cenozoic succession offshore mid - and northern Norway*. Vol. 4 of *Norwegian Petroleum Directorate Bulletin*. pp. 5–42.
- Donovan, D., Jones, E., 1979. Causes of world-wide changes in sea level. *Journal of the Geological Society* 136 (2), 187–192.
- Doré, A., 1991. The structural foundation and evolution of Mesozoic seaways between Europe and the Arctic Sea. *Palaeogeography, Palaeoclimatology, Palaeoecology* 87, 441–492.
- Doré, A., 1992. Synoptic palaeogeography of the northeast Atlantic Seaway: Late Permian to Cretaceous. In: Parnell, J. (Ed.), *Basins on the Atlantic Seaboard: Petroleum Geology, Sedimentology and Basin Evolution*. Vol. 62 of *Geological Society Special Publication*. pp. 421–446.
- Doré, A., Gage, M., 1987. Crestal alignments and sedimentary domains in the evolution of the North Sea, northeast Atlantic margin and the Barents Shelf. In: Brooks, J., Glennie, K. (Eds.), *Petroleum Geology of NW Europe*. Graham and Trotman, London, UK, pp. 1131–1148.
- Eagar, R., Baines, J., Collinson, J., Hardy, P., Okolo, S., Pollard, J., 1985. Trace fossil assemblages and their occurrence in Silesian (Mid-Carboniferous) deltaic sediments of the Central Pennine Basin, England. In: Curran, H. (Ed.), *Biogenic structures: their use in interpreting depositional environments*. Vol. 35. *Society of Economic Paleontologists & Mineralogists Special Publication*, Graham and Trotman, London, UK, pp. 99–149.

- Ehrenberg, S., Gjerstad, H., Hadler-Jacobsen, F., 1992. Smørbukk Field: a gas condensate fault trap in the Haltenbanken province, offshore Mid-Norway. In: Halbouty, M. (Ed.), *Giant Oil Fields of the Decade 1978-1988*. Vol. 54 of American Association of Petroleum Geologists Memoir. pp. 323–348.
- Eldholm, O., Sundvor, E., Myhre, A., Faleide, J., 1984. Cenozoic evolution of the continental margin off Norway and western Svalbard. In: Spencer, A., Holter, E., Johnsen, S., Mørk, A., Nysæther, E., Songstad, P., Spinnanger, Å. (Eds.), *Petroleum Geology of the North European Margin*. Norwegian Petroleum Society, pp. 3–18.
- Eldholm, O., Thiede, J., Taylor, E., 1987. Evolution of the Norwegian Continental Margin: background and objectives. *Proceedings of the ODP International Reports* 104, 5–25.
- Elliott, T., 1976. Upper Carboniferous sedimentary cycles produced by river-dominated, elongate deltas. *Journal of the Geological Society* 132 (2), 199–208.
- Embry, A., 1997. Global sequence boundaries of the Triassic and their identification in the Western Canada Sedimentary Basin. *Bulletin of Canadian Petroleum Geologists* 45, 415–433.
- Emery, D., Myers, K. J., 1996. *Sequence stratigraphy*. Blackwell Science Ltd.
- Ethridge, F. G., Wood, L. J., Schumm, S., 1998. Cyclic variables controlling fluvial sequence development: problems and perspectives. In: Shanley, K. W., McCabe, Peter, J. (Eds.), *Relative role of eustacy, climate, and tectonism in continental rocks*. No. 59 in *Society of Economic Palaeontologists and Mineralogists Special Publication*. SEPM, pp. 17–29.
- Fisher, Q., Casey, M., Clennel, M., Knipe, R., 1999. Mechanical compaction of deeply buried sandstones of the North Sea. *Marine and Petroleum Geology* 16, 605–618.
- Frakes, L. A., 1979. *Climates Throughout Geologic Time*. Elsevier Science & Technology.

- Fürsich, F., 1974a. Trace fossils as environmental indicators in the Corallian of England and Normandy. *Lethaia* 8, 151–172.
- Fürsich, F., 1975. On diplocraterion Torell 1870 and the significance of morphological features in vertical, spreiten-bearing, U-shaped trace fossils. *Journal of Paleontology* 48, 952–954.
- Gabrielsen, R., Færseth, R., Hamar, G., Rønnevik, H., 1984. Nomenclature of the main structural features on the Norwegian Continental Shelf north of the 62nd parallel. In: Spencer, A., Holter, E., Johnsen, S., Mørk, A., Nysæther, E., Songstad, P., Spinnanger, Å. (Eds.), *Petroleum Geology of the North European Margin*. Norwegian Petroleum Society, pp. 41–60.
- Gabrielsen, R. H., Robinson, C., 1984. Tectonic inhomogeneities of the Kristiansund–Bodø fault Complex, offshore Mid-Norway. In: Spencer, A., Holter, E., Johnsen, S., Mørk, A., Nysæther, E., Songstad, P., Spinnanger, Å. (Eds.), *Petroleum Geology of the North European Margin*. Norwegian Petroleum Society, pp. 397–406.
- Galloway, W. E., Brown, L. F., 1973. Depositional systems and shelf-slope relations on cratonic basin margin, Uppermost Pennsylvanian of North-Central Texas. *American Association of Petroleum Geologists Bulletin* 57 (7), 1185–1218.
- Gibbs, R., Mathews, M., Link, D., 1971. The relationship between sphere size and settling velocity. *Journal of Sedimentary Petrology* 41, 7–18.
- Gibling, M. R., Nanson, G. C., Maroulis, J. C., 1998. Anastomosing river sedimentation in the Channel Country of central Australia. *Sedimentology* 45 (3), 595–619.
- Gjelberg, J., Dreyer, T., Høie, A., Tjelland, T., Lilleng, T., 1987. Late Jurassic to Mid-Jurassic sandbody development on the Barents and Mid-Norwegian shelf. In: Brooks, J., Glennie, K. (Eds.), *Petroleum Geology of Northwest Europe*. Graham and Trotman, London, pp. 1105–1129.

- Gordon, E., Bridge, J., 1987. Evolution of Catskill (Upper Devonian) river systems; intra- and extrabasinal controls. *Journal of Sedimentary Research* 57 (2), 234–249.
- Gradzinski, R., Baryla, J., Doktor, M., Gmur, D., Gradzinski, M., Kedzior, A., Paszkowski, M., Soja, R., Zielinski, T., Zurek, S., 2003. Vegetation-controlled modern anastomosing system of the upper Narew River (NE Poland) and its sediments. *Sedimentary Geology* 157 (3), 253–276.
- Hallam, A., 1981. The end-Triassic bivalve mass extinction event. *Palaeogeography Palaeoclimatology Palaeoecology* 35, 1–44.
- Hallam, A., 1984. Pre-Quaternary sea-level changes. *Annual Review of Earth and Planetary Sciences* 12, 205–243.
- Hallam, A., 1988. A reevaluation of Jurassic eustasy in the light of new data and the revised Exxon curve. In: Wilgus, C., Hastings, B., Ross, C., Posamentier, H., Van Wagoner, J., Kendall, C. (Eds.), *Sea-level changes - an integrated approach*. No. 42 in *Society of Economic Palaeontologists and Mineralogists Special Publication*. SEPM, pp. 261–273.
- Hallam, A., 1992. *Phanerozoic sea-level*. Columbia University Press, New York.
- Hallam, A., 1994. Jurassic climates as inferred from the sedimentary and fossil record. In: Allen, J. R. L., Hoskins, B. J., Sellwood, B. W., Spicer, R. A. (Eds.), *Palaeoclimates and their modelling: with special reference to the Mesozoic Era*. Vol. 12. Chapman & Hall, London, pp. 79–88.
- Hammer, E., Mørk, M., Næss, A., 2010. Facies control on the distribution of diagenesis and compaction in fluvial-deltaic deposits. *Marine and Petroleum Geology* 27, 1737–1751.
- Harris, N., 1989. Reservoir geology of Fangst Group (Middle Jurassic), Heidrun Field, offshore Mid-Norway. *The American Association of Petroleum Geologists Bulletin* 73 (11), 1415–1435.

- Hemmens, P., Hole, A., Reid, B., Leach, P., Landrum, W., 1994. The Heidrun Field. In: Aasen, J., Berg, E., Buller, A., Hjelmeland, O., Holt, R., Kleppe, J., Torsæter, O. (Eds.), North Sea Oil and Gas Reservoirs III. Kluwer Academic Publishers, Dordrecht, pp. 1–23.
- Heum, O., Dalland, A., Meisingset, K., 1986. Habitat of hydrocarbons at Haltenbanken (PVT-modelling as a predictive tool in hydrocarbon exploration). In: Spencer, A., Holter, E., Campbell, C., Hanslien, S., Nelson, P., Nysæther, E., Ormaasen, E. (Eds.), Habitat of Hydrocarbons on the Norwegian Continental Shelf. Norwegian Petroleum Society, pp. 259–274.
- Hvoslef, S., Larter, S., Leythaeuser, D., 1988. Aspects of generation and migration of hydrocarbons from coal-bearing strata of the Hitra Formation, Haltenbanken area, offshore Norway. *Organic Geochemistry* 13 (1-3), 525–536.
- Ireland, R., Pollard, J., Steel, R., Thompson, D., 1978. Intertidal sediments and trace fossils from the Waterstones (Scythian-Anisian?) at Daresbury, Cheshire. *Proceedings of the Yorkshire Geological Society* 41, 399–436.
- Jackson, J. A., Bates, R. L., 1997. Glossary of geology, 4th ed. American Geological Institute, Alexandria.
- Jervey, M. T., 1988. Quantitative geological modeling of siliciclastic rock sequences and their seismic expression. In: Wilgus, C., Hastings, B., Ross, C., Posamentier, H., Van Wagoner, J., Kendall, C. (Eds.), Sea-level changes: an integrated approach. Vol. 42 of Society of Economic Paleontologists and Mineralogists, Special Publication. pp. 47–70.
- Kantorowicz, J., Bryant, I., Dawans, J., 1987. Controls on geometry and distribution of carbonate cements in jurassic sandstones: Bridport Sands, southern England and the Viking Group, Troll Field, Norway. In: Marshall, J. (Ed.), Diagenesis of Sedimentary Sequences. Vol. 36 of Geological Society, London, Special Publications. pp. 103–118.

- Karssenberg, D., Bridge, J. S., 2008. A three-dimensional numerical model of sediment transport, erosion and deposition within a network of channel belts, floodplain and hill slope: extrinsic and intrinsic controls on floodplain dynamics and alluvial architecture. *Sedimentology* 55, 1717–1745.
- Kjærefjord, J., 1999. Bayfill successions in the Lower Jurassic Åre Formation, offshore Norway: sedimentology and heterogeneity based on subsurface data from the Heidrun Field and analog data from the Upper Cretaceous Neslen Formation, eastern Book Cliffs, Utha. In: Hentz, T. (Ed.), 19th Annual Research Conference. Advanced reservoir characterization for the Twenty-First Century. Gulf Coast Section and Society Economic Paleontologists and Mineralogists Foundation, Special Publication. pp. 149–157.
- Kjennerud, T., Faleide, J., Gabrielsen, R., Gillmore, G., Kyrkjebø, R., Lippard, S., Løseth, H., 2001. Structural restoration of Cretaceous - Cenozoic (post-rift) palaeobathymetry in the northern North Sea. In: Martinsen, O., Dreyer, T. (Eds.), *Sedimentary Environments Offshore Norway - Paleozoic to Recent*. Vol. 10 of Norwegian Petroleum Society Special Publication. pp. 347–364.
- Koch, J., Heum, O., 1995. Exploration trends of the Halten Terrace. In: Hanslien, S. (Ed.), *Petroleum Exploration in Norway*. Vol. 4 of Norwegian Petroleum Society Special publication. pp. 235–251.
- Koenig, R., 1986. Oil discovery in 6507; an initial look at the Heidrun Field. In: Spencer, A., Holter, E., Campbell, C., Hanslien, S., Nelson, P., Nysæther, E., Ormaasen, E. (Eds.), *Habitat of Hydrocarbons on the Norwegian Continental Shelf*. Norwegian Petroleum Society, pp. 307–311.
- Kominz, M. A., Pekar, S. F., 2001. Oligocene eustacy from two-dimensional sequence stratigraphic backstripping. *Geological Society of America Bulletin* 113 (3), 291–304.
- Koss, J. E., Ethridge, F. G., Schumm, S., 1994. An experimental study of the effects of

- base-level change on fluvial, coastal plain and shelf systems. *Journal of Sedimentary Research* 64 (2b), 90–98.
- Leary, S., Næss, A., Thrana, C., Brekken, M., Cullum, A., Gowland, S., Selnes, H., 2007. The Åre Formation, Heidrun Field, Norwegian Sea. In: 25th International Association of Sedimentologists, Meeting of Sedimentologists, Patras, Greece. Poster.
- Long, A., Waller, M., Stupples, P., 2006. Driving mechanisms of coastal change: Peat compaction and the destruction of late Holocene coastal wetlands. *Marine Geology* 225, 63–84.
- Lundin, E., Doré, A., 1997. A tectonic model for the Norwegian passive margin with implications for the NE Atlantic: Early Cretaceous to break-up. *Journal of the Geological Society* 154, 545–550.
- Makaske, B., 2001. Anastomosing rivers: a review of their classification, origin and sedimentary products. *Earth-Science Reviews* 53 (3-4), 149–196.
- Marsh, N., Imber, J., Holdsworth, R., Brockbank, P., Ringrose, P., 2009. The structural evolution of the Halten Terrace, offshore Mid-Norway: extensional fault growth and strain localisation in a multi-layer brittle-ductile system. *Basin Research* 46 (2), 1–20.
- Martinius, A., Kaas, I., Næss, A., Helgesen, G., Kjærefjord, J., Leith, D., 2001. Sedimentology of the heterolithic and tide-dominated Tilje Formation (Early Jurassic, Halten Terrace, offshore Mid-Norway). In: Martinsen, O., Dreyer, T. (Eds.), *Sedimentary Environments Offshore Norway - Paleozoic to Recent*. Vol. 10 of Norwegian Petroleum Society Special Publication. Elsevier Science B.V., Amsterdam, pp. 103–144.
- Martinsen, O. J., Ryseth, A., Helland-Hansen, W., Fleshe, H., Torkildsen, G., Sahire, I., 1999. Stratigraphic base level and fluvial architecture: Ericson Sandstone (Campanian), Rock Springs Uplift, SW Wyoming, USA. *Sedimentology* 46 (2), 235–263.
- McCabe, P. J., Shanley, K. W., 1992. Organic control on shoreface stacking patterns: Bogged down in the mire. *Geology* 20 (8), 741–744.

- McCarthy, P., Faccini, U., Plint, A., 1999. Evolution of an ancient coastal plain: palaeosols, interfluves and alluvial architecture in a sequence stratigraphic framework, Cenomanian Dunvegan Formation, NE British Columbia, Canada. *Sedimentology* 46, 861–891.
- McCarthy, P., Plint, A., 1998. Recognition of interfluve sequence boundaries: integrating paleopedology and sequence stratigraphy. *Geology* 26 (5), 387–390.
- McElwain, J., Beerling, D., Woodward, F., 1999. Fossil plants and global warming at the Triassic-Jurassic boundary. *Science* 285, 1386–1390.
- Mørk, A., Smelror, M., 2001. Correlation and non-correlation of high order Circum-Arctic Mesozoic sequences. *Polarforschung* 69, 65–72.
- Morton, A., Hallsworth, C., Strogon, D., Whitman, A., Fanning, M., 2009. Evolution of provenance in the NE Atlantic rift: The Early-Middle Jurassic succession in the Heidrun Field, Halten Terrace, offshore Mid-Norway. *Marine and petroleum geology* 26, 1100–1117.
- Moslow, T., Pemberton, S., 1988. An integrated approach to the sedimentological analysis of some lower cretaceous shoreface and delta front sandstone sequences. In: James, D., Leckie, D. (Eds.), *Sequences, Stratigraphy, Sedimentology: Surface and Subsurface*. Vol. 15 of Canadian Society of Petroleum Geologists Memoir. pp. 373–386.
- Nadon, G. C., 1998. Magnitude and timing of peat-to-coal compaction. *Geology* 26 (8), 727–730.
- Olsen, T., Steel, R., Høgseth, K., Skar, T., Røe, S.-L., 1995. Sequential architecture in a fluvial succession; sequence stratigraphy in the Upper Cretaceous Mesaverde Group, Prince Canyon, Utah. *Journal of Sedimentary Research* 65 (2b), 265–280.
- Ottesen, D., 2006. Ice-sheet dynamics and glacial development of the Norwegian continental margin during the last 3 million years. Dr.philos, Department of Earth Science, University of Bergen, Norway.

- Øvrebø, O., Talleraas, E., 1977. The structural geology of the Troms Area (Barents Sea). *GeoJournal* 1, 47–54.
- Pedersen, T., Harms, J., Harris, N., Mitchell, R., Tooby, K., 1989. The role of correlation in generating the Heidrun Field geologic model. In: Collinson, J. (Ed.), *Correlation in Hydrocarbon Exploration*. Norwegian Petroleum Society, Springer, pp. 327–338.
- Pollard, J., 1988. Trace fossils in coal-bearing sequences. *Journal of the Geological Society* 145, 339–350.
- Posamentier, H., Allen, G., James, D., Tesson, M., 1992. Forced regressions in a sequence stratigraphic framework; concepts, examples, and exploration significance. *The American Association of Petroleum Geologists Bulletin* 76 (11), 1687–1709.
- Posamentier, H., Jervey, M., Vail, P., 1988. Eustatic controls on clastic deposition, i. conceptual framework. In: Wilgus, C., Hastings, B., Ross, C., Posamentier, H., Van Wagoner, J., Kendall, C. (Eds.), *Sea-Level changes: an integrated approach*. Vol. 42 of *Society of Economic Palaeontologists and Mineralogists Special Publication*. Society of Economic Paleontologists, Mineralogists, pp. 109–124.
- Posamentier, H., Vail, P., 1988. Eustatic controls on clastic deposition, II. Sequence and systems tract models. In: Wilgus, C., Hastings, B., Ross, C., Posamentier, H., Van Wagoner, J., Kendall, C. (Eds.), *Sea-Level Changes: An Integrated Approach*. Vol. 42 of *Society of Economic Palaeontologists and Mineralogists Special Publication*. Society of Economic Paleontologists, Mineralogists, pp. 125–154.
- Rajchl, M., Uličný, D., 2005. Depositional record of an avulsive fluvial system controlled by peat compaction (Neogene, Most Basin, Czech Republic). *Sedimentology* 52, 601–625.
- Rawson, P., Riley, L., 1982. Latest Jurassic-Early Cretaceous events and the Late Cimmerian Unconformity in the North Sea. *The American Association of Petroleum Geologists Bulletin* 66, 2628–2648.

- Richardson, N., Underhill, J., Lewis, G., 2005. The role of evaporite mobility in modifying subsidence patterns during normal fault growth and linkage, Halten Terrace, Mid-Norway. *Basin Research* 17, 203–223.
- Rust, B. R., 1981. Sedimentation in an arid-zone anastomosing fluvial system: Cooper's Creek, Central Australia. *Journal of Sedimentary Research* 51, 745–755.
- Ryseth, A., Ramm, M., 1996. Alluvial architecture and differential subsidence in the Statfjord Formation, North Sea; prediction of reservoir potential. *Petroleum Geoscience* 2 (3), 271–287.
- Schmidt, W., 1992. Structure of the Mid-Norway Heidrun Field and its regional implications. In: Larsen, R., Brekke, H., Larsen, B., Talleraas, E. (Eds.), *Structural and Tectonic Modelling and its Application to Petroleum Geology*. Vol. 1 of Norwegian Petroleum Society Special Publication. pp. 381–395.
- Schumm, S. A., 1968. Speculations concerning paleohydraulic controls on terrestrial sedimentation. *Geological Society of America Bulletin* 79, 1573–1588.
- Slater, J., Christie, P., 1980. Continental stretching: an explanation of the post Mid-Cretaceous subsidence of the Central North Sea basin. *Journal of Geophysical Research* 85, 3711–3739.
- Shackleton, N., Kennett, J., 1975. Paleotemperature history of the Cenozoic and the initiation of Antarctic glaciation: oxygen and carbon isotope analyses in DSDP, sites 277, 279, and 281. *Initial Reports of the Deep Sea Drilling Project* 29, 743–755.
- Shanley, K. W., McCabe, P. J., 1994. Perspectives on the sequence stratigraphy of continental strata. *The American Association of Petroleum Geologists Bulletin* 78 (4), 544–568.
- Slingerland, R., Smith, N. D., 2004. River avulsions and their deposits. *Annual Review of Earth and Planetary Sciences* 32, 257–285.

- Sloss, L., 1962. Stratigraphic models in exploration. *Journal of Sedimentary Research* 32 (3), 415–422.
- Smith, D. G., 1983. Anastomosed fluvial deposits: modern examples from western Canada. In: Collinson, J. D., Lewin, J. (Eds.), *Modern and Ancient Fluvial Systems*. Vol. 6 of International Association of Sedimentologists Special Publication. pp. 155–168.
- Smith, D. G., 1986. Anastomosing river deposits, sedimentation rates and basin subsidence, Magdalena River, northwestern Colombia, South America. *Sedimentary Geology* 46, 177–196.
- Smith, D. G., Smith, N. D., 1980. Sedimentation in anastomosed river systems: examples from alluvial valley near Banff, Alberta. *Journal of Sedimentary Research* 50 (1), 157–164.
- Steinberger, B., Torsvik, T. H., 2008. Absolute plate motions and true polar wander in the absence of hotspot tracks. *Nature* 452, 620–624.
- Stouthamer, E., Berendsen, H. J. A., 2000. Factors controlling the Holocene avulsion history of the Rhine-Meuse delta (The Netherlands). *Journal of Sedimentary Research* 5, 1051–1064.
- Stouthamer, E., Berendsen, H. J. A., 2007. Avulsion: the relative roles of autogenic and allogenic processes. *Sedimentary Geology* 198, 309–325.
- Streif, H., 1990. Quaternary sea-level changes in the North Sea, an analysis of amplitudes and velocities. In: Brosche, P., Sündermann, P. (Eds.), *Earth's Rotation from Eons to Days*. Springer, Berlin, pp. 201–214.
- Surlyk, F., 1990. Stratigraphy, tectonics and palaeogeography of the Jurassic sediments of the areas north of Kong Oscars Fjord, East Greenland. *Palaeogeography, Palaeoclimatology, Palaeoecology* 78, 71–85.

- Surlyk, F., Clemmensen, L., Larsen, H., 1981. Post-Paleozoic evolution of the East Greenland continental margin. In: Kerr, J., Fergusson, A.J., E. (Eds.), *Geology of the North Atlantic borderlands*. Vol. 7 of Canadian Society of Petroleum Geologists Memoir. pp. 611–645.
- Svela, K., 2001. Sedimentary facies in the fluvial-dominated Åre Formation as seen in the Åre 1 Member in the Heidrun Field. In: Martinsen, O., Dreyer, T. (Eds.), *Sedimentary Environments Offshore Norway - Paleozoic to Recent*. Vol. 10 of Norwegian Petroleum Society Special Publication. Elsevier Science B.V., Amsterdam, pp. 87–102.
- Taylor, A., Goldring, R., Gowland, S., 2003. Analysis and application of ichnofabrics. *Earth-Science Reviews* 60, 227–259.
- Taylor, K., Gawthorpe, R., Van Wagoner, J., 1995. Stratigraphic control on laterally persistent cementation, Book Cliffs, Utah. *Journal of the Geological Society* 152 (2), 225–228.
- Thompson, S., Cooper, B., Morley, R., Barnard, P., 1985. Oil-generating coals. In: B.M., T. (Ed.), *Petroleum geochemistry in exploration of the Norwegian shelf*. Norwegian Petroleum Society. Graham and Trotman, London, pp. 59–73.
- Thrana, C., Brekken, M., Næss, A., Leary, S., Gowland, S., 2008. Revised reservoir characterization of the Åre Fm., Heidrun Field, Halten Terrace, Abstract, the 33rd IGC, Oslo, Norway. In: 33rd International Geological Congress, Oslo, Norway. Lillestrøm, poster.
- Thrana, C., Brekken, M., Næss, A., Leary, S., Gowland, S., 2009. Milking the goat: revised reservoir characterization of the Åre Formation, Heidrun Field, offshore Mid-Norway. In: *Search and Discovery Article # 20069* (2009). Adapted from oral presentation at AAPG International Conference and Exhibition, Cape Town, South Africa, October 26-29, 2008.

- Torsvik, T. H., Müller, R. D., Voo, R. V. d., Steinberger, B., Gaina, C., 2008. Global plate motion frames: towards a unified model. *Reviews of Geophysics* 46, 1–44.
- Tye, R., Bhattacharya, J. P., Lorsong, J. A., Sindelar, S. T., Knock, D. G., Puls, D. D., Levinson, R. A., 1999. Geology and stratigraphy of fluvio-deltaic deposits in the ivishak formation: Applications for development of prudhoe bay field, alaska. *AAPG Bulletin* 83 (10), 1588–1623.
- Van der Heide, S., 1950. Compaction as a possible factor in Upper Carboniferous rhythmic sedimentation. In: Report of the 18th International Geologic Congress. Vol. 4. pp. 38–45.
- van Heijst, M., Postma, G., 2001. Fluvial response to sea-level changes: a quantitative analogue, experimental approach. *Basin Research* 13, 269–292.
- van Veen, P., Skjold, L., Kristensen, S., Rasmussen, A., J., G., Stølan, T., 1992. Triassic sequence stratigraphy in the Barents Sea. In: Vorren, T., Bergsager, E., Dahl-Stammes, Ø., Holter, E. Johansen, B., Lie, E., Lund, T. (Eds.), *Arctic Geology and Petroleum Potential*. Vol. 2 of Norwegian Petroleum Society (NPF) Special Publication. Elsevier, Amsterdam, pp. 515–538.
- Van Wagoner, J. C., Mitchum, R. M., Campion, K. M., Rahmanian, V. D., 1990. Siliciclastic Sequence Stratigraphy in Well Logs, Cores, and Outcrops: Concepts for High-Resolution Correlation of Time and Facies. Vol. 7 of American Association of Petroleum Geologists, *Methods in Exploration* series. The American Association of Petroleum Geologists.
- Van Wagoner, L., Posamentier, H., Mitchum, R., Vail, P., Sarg, J., Loutit, T., Hardenbol, J., 1988. An overview of the fundamentals of sequence stratigraphy and key definitions. In: Wilgus, C., Hastings, B., Ross, C., Posamentier, H., Van Wagoner, J., Kendall, C. (Eds.), *Sea-Level Changes: An Integrated Approach*. Vol. 42 of Society of Economic Palaeontologists and Mineralogists Special Publication. Society of Economic Paleontologists, Mineralogists, pp. 39–45.

- Wang, S., Chen, Z., Smith, D. G., 2005. Anastomosing river system along the subsiding middle Yangtze River basin, southern China. *Catena* 60, 147–163.
- Whitley, P., 1992. The geology of Heidrun. A giant oil and gas field on the Mid-Norwegian Shelf. In: Halbouty, M. (Ed.), *Giant Oil Fields of the Decade 1978-1988*. Vol. 54 of *The American Association of Petroleum Geologists Memoirs*. American Association of Petroleum Geologists, pp. 383–406.
- Willis, B. J., 1997. Architecture of fluvial-dominated valley-fill deposits in the Cretaceous Fall River Formation. *Sedimentology* 44 (4), 735–757.
- Worden, R., Burley, S., 2003. Sandstone diagenesis: the evolution of sand to stone. In: Burley, S., Worden, R. (Eds.), *Sandstone Diagenesis. Recent and Ancient*. Reprint Series 4 of the International Association of Sedimentologists. Blackwell Publishing, pp. 3–44.
- Ziegler, P., 1982. Triassic rifts and facies patterns in western and central Europe. *Geologische Rundschau* 71 (8), 747–772.

Part III

Papers

Paper I

Facies controls on the distribution of diagenesis and compaction in fluvial-deltaic deposits

Authors: Erik Hammer, Mai Britt E. Mørk and Arve Næss

Published: Marine and Petroleum Geology 27 (2010), pages 1737-1751



Facies controls on the distribution of diagenesis and compaction in fluvial-deltaic deposits

Erik Hammer^{a,*}, Mai Britt E. Mørk^a, Arve Næss^b

^a Department of Geology and Mineral Resources Engineering, Norwegian University of Science and Technology, N-7491 Trondheim, Norway

^b Statoil, E&P Norway, Strandveien 4, N-7501 Stjørdal, Norway

ARTICLE INFO

Article history:

Received 16 January 2009

Received in revised form

1 November 2009

Accepted 11 November 2009

Available online 18 November 2009

Keywords:

Diagenesis

Compaction

Fluviodeltaic

Siderite

Kaolinite

Micro analysis

ABSTRACT

The Upper Triassic – Lower Jurassic Åre Formation comprising the deeper reservoir in the Heidrun Field offshore mid-Norway consists of fluvial channel sandstones (FCH), floodplain fines (FF), and sandy and muddy bay-fill sediments (SBF, MBF) deposited in an overall transgressive fluvial to lower delta plain regime. The formation has been investigated to examine possible sedimentary facies controls on the distribution of cementation and compaction based on petrography and SEM/micro probe analyses of core samples related to facies associations and key stratigraphic surfaces. The most significant authigenic minerals are kaolinite, calcite and siderite. Kaolinite and secondary porosity from dissolution of feldspar and biotite are in particular abundant in the fluvial sandstones. The carbonate minerals show complex compositional and micro-structural variation of pure siderite (Sid I), Mg-siderite (Sid II), Fe-dolomite, ankerite and calcite, displaying decreasing Fe from early to late diagenetic carbonate cements. An early diagenetic origin for siderite and kaolinite is inferred from micro-structural relations, whereas pore filling calcite and ankerite formed during later diagenesis. The Fe-dolomite probably related to mixing-zone dolomitization from increasing marine influences, and a regional correlatable calcite cemented layer has been related to a flooding event. Porosity values in non-cemented sandstone samples are generally high in both FCH and SBF facies associations averaging 27%. Differential compaction between sandstone and mudstone has a ratio of up to 1:2 and with lower values for MBF. We emphasize the role of eogenetic siderite cementation in reducing compactability in the fine-grained, coal-bearing sediments most prominent in MBF facies. This has implications for modeling of differential compaction between sandstone and mudstones deposited in fluvial-deltaic environments.

© 2009 Elsevier Ltd. All rights reserved.

1. Introduction

The Heidrun Field is located on the Halten Terrace, approximately 240 km northwest of Trondheim (Fig. 1) in water depths of approximately 350 m, and was discovered by Conoco in 1985 (Koenig, 1986). The Halten Terrace (Haltenbanken area) is the most important hydrocarbon province offshore mid-Norway (Koch and Heum, 1995; Spencer et al., 1993), where shallow marine and deltaic sands of the Middle Jurassic Fangst Group and the fluvial-deltaic, Upper Triassic – Lower Jurassic Åre and Tilje Formations of the Båt Group (Dalland et al., 1988) constitute the principal reservoirs of the region. Studies of the Mesozoic sediments at Haltenbanken suggested that kaolinitization is the main diagenetic process at shallow depths and quartz cementation in deep reservoirs (Bjørlykke et al., 1989, 1986; Walderhaug, 1996; Walderhaug

et al., 2001), and the studies focused mainly on the role of chlorite and illite coatings in preventing quartz cementation in deep sandstone reservoirs (Ehrenberg, 1990, 1993; Storvoll et al., 2002). The reservoirs in the Heidrun Field are located at relatively shallow burial depths (2.5 km or less) and where quartz cementation has less or no impact on porosity. The target in this study is the Åre Formation of Rhaetian – Hettangian age comprising heterogeneous sediments deposited in a fluvial plain to lower delta plain environment with swamps and fluvial channel deposits passing upwards into marginal marine facies (Dalland et al., 1988; Kjærefjord, 1999; Koch and Heum, 1995; Olsen et al., 1999; Svela, 2001; Whitley, 1992). Due to the heterogeneous nature of the sediments there are large difficulties in correlating the sandstone beds/reservoir flow units. In this study we examine diagenesis and reservoir quality in the Åre Formation on the basis of four wells (6507/7-A-38, 6507/7-A-27, 6507/8-D-4 BHT3, 6507/7-A-46) in the Heidrun Field by petrographic and mineral-chemical analysis in combination with core study and wireline log interpretation. We report common carbonate cementation and varied carbonate

* Corresponding author. Tel.: +47 41501284; fax: +47 73590898.

E-mail address: erih@statoil.com (E. Hammer).

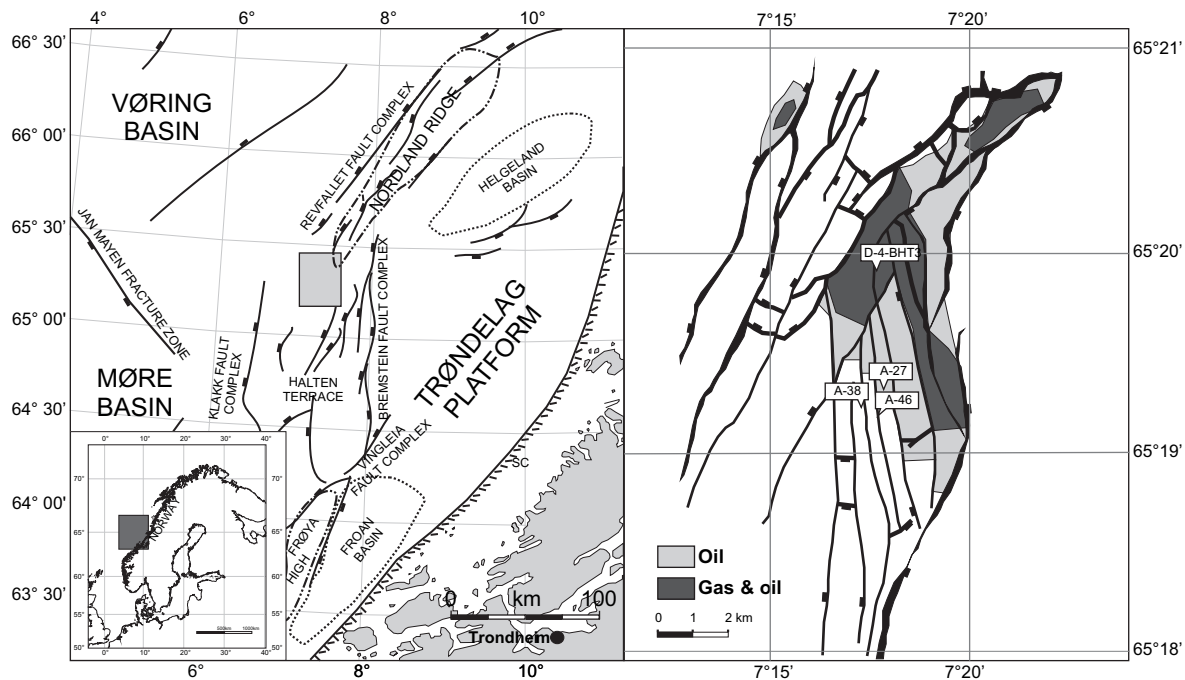


Fig. 1. Left: The structural elements of the mid-Norwegian continental shelf (modified from Gabrielsen et al. (1984); Koch and Heum (1995)) and the location of the study area. Right: Top Åre reservoir structure, fluid distribution (after Svela (2001)) and the location of studied wells.

mineralogy, which are discussed in relation to sedimentary facies. The aim of the study is to examine possible effects of diagenesis on reservoir quality, and sedimentary facies controls on distribution of cementation and compaction. Basin models account for compaction by relating porosity with depth and permeability with porosity often assuming one-dimensional compaction. This is the case for horizontally layered sedimentary basins of large lateral extent, and in the absence differential compaction (Nygård et al., 2004). Understanding the distribution of diagenesis and its possible impact on differential compaction can, when applied to reservoir reconstruction models, such as backstripping exercises, help correlation of reservoir units and contribute to more optimal drainage solutions. Introducing the effect of eogenetic facies dependent cementation, we suggest that a compaction model for the Åre Formation should be based on facies associations rather than lithology, taking into account the distribution and effect of the early cements.

2. Regional geology

The Haltenbanken area is structurally complex with large N–NE to S–SW trending faults truncating the region. The structural development of the Mid-Norwegian shelf (Blystad et al., 1995; Brekke et al., 2001; Bukovics et al., 1984; Bukovics and Ziegler, 1985; Dooley et al., 2003; Doré, 1991; Gjelberg et al., 1987; Swiecicki et al., 1998), and of the Heidrun Field (Schmidt, 1992) is the result of a divergent continental margin development from the Carboniferous to the opening of the Norwegian Sea in the Early Tertiary. The Early Jurassic basin can be typified as a late stage pre-rift basin (Nøttvedt et al., 1995) in which subsidence was caused mainly by sediment compaction, with local syn-sedimentary faulting (Martinius et al., 2001). The main structural features of the region were established in the Late Jurassic – Cretaceous, a period of widespread extension referred to as the Kimmerian tectonic phase (Bukovics et al., 1984; Schmidt, 1992; Whitley, 1992). During

the Cretaceous, basin infill and subsidence ensued, as reflected by onlap of marine calcareous shales against the Kimmerian structures (Whitley, 1992). This was followed by the initiation of seafloor spreading and separation of Greenland from Norway in the Paleocene – Eocene developing a passive margin (Doré and Gage, 1987).

The oldest Mesozoic sediments at Haltenbanken are represented by Triassic “red beds” and “grey beds”, deposited in continental environments under eustatic lowstand conditions. The Triassic “grey beds” and the overlying Åre Formation mark a change to paralic environments (Dalland et al., 1988; Gjelberg et al., 1987) initiated by the onset of a regional sea level rise. During this period a climatic change from arid to humid is evidenced by strongly kaolinitic sediment compositions and kaolinite-weathered basement rocks (Clemmensen et al., 1998; Hallam, 1984; Hurst and Kunkle, 1985; Mørk et al., 2003; Pearson, 1990). The transgression continued through the Early Jurassic culminating in the deposition of open marine shales of the Ror Formation in the Toarcian (Fig. 2). The burial history in the Haltenbanken area is related to the tectonic development during the Kimmerian phase in the Middle/Late Jurassic – Cretaceous and the initiation of seafloor spreading in Paleocene – Eocene, but with most rapid burial related to the deposition of ~1500 m glaciation-derived detritus from mid-Pliocene time. Fig. 3 is a constructed burial curve for well 6507/7-A-38 illustrating the phases of sedimentation/burial. At present the Åre Formation in the Heidrun Field is interpreted to be at maximum burial depth between 2200 and 3000 m.

3. Methods

Sedimentological core description has been done based on detailed logging of well 6507/7-A-38 covering 187 m of the Åre Formation, and used as reference for calibration for petrophysical wireline log interpretation of lithology and sedimentary facies associations. Diagenesis has been interpreted from core study and petrographic thin section analysis of well 6507/7-A-38 (water

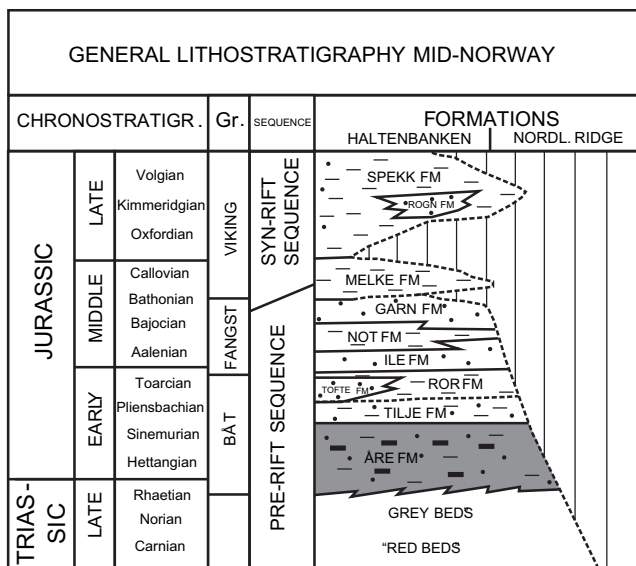


Fig. 2. Stratigraphic compilation of the mid-Norwegian continental shelf (modified from Dalland et al. (1988)).

zone) and wells 6507/8-D-4 BHT3 (oil zone), 6507/7-A-27 (water and oil zone), 6507/7-A-46 (water and oil zone), covering all the identified facies associations. Petrographic compositions are based on modal analysis counting 300 points per thin section. SEM electron backscatter image analysis in combination with quantitative micro probe analyses and X-ray scans have been done to identify cement compositions using a JOEL JXA-8500F Electron Probe Micro Analyzer (EPMA) and mineral standards. In addition, fine-grained sediment samples have been examined by X-ray diffraction (Phillips PW XRD) analyses of both crushed bulk rock samples and separated clay-sized particle fraction (<2 µm) for identification of the clay minerals. Porosity and permeability values from plug analysis are compiled for each facies association. Compaction was studied in thin-sections by modal analysis and by porosity variations vs depth based on plug and wireline log data.

3.1. Sedimentological framework

The studied wells from the Åre Formation have been correlated on the basis of conventional wireline logs and core description (Fig. 4). The studied lithology represents a 187 m thick interval in the selected reference well 6507/7-A-38. This interval can roughly be divided into coarse sandy beds in the lower part, three units fining up from coarse sand to clay and coal in the middle part, and in the upper part heterogeneous bay-fill sediments that include thin coarsening sands. This is interpreted as recording a change from fluvial dominated deposits in the lower part to deposition under increasing marine influence on a lower delta plain environment in the upper part, hence a transgression (e.g. Leary et al., 2007; Svela, 2001). A regional channel sand body complex (incised valley?) inferred in the middle of the succession is missing in the reference well due to normal faulting with a calculated throw of approximately 45 m, probably related to the Kimmerian tectonic phase (Schmidt, 1992). This channel complex is correlatable between neighboring wells reaching a maximal thickness of 22 m in the studied wells. Three flooding surfaces have been interpreted in the studied intervals; one as a “coal zone” in the lower part of the unit marking an increase in base level; the second as the top of the regional channel sand body complex, and the third as the base of the first regional correlatable bay-fill sequence (Leary et al., 2007).

A fourth possible flooding surface can be inferred at the top of a distinct channel feature in the upper part of the succession just below this regional flooding surface. A sequence boundary is interpreted at the base of the regional channel sand body complex created during a regional relative fall or stillstand in sea level. This sea level change, suggested as a sea level fall by Svela (2001) who interpreted the channel sand complex as an incised valley fill, may correspond to minor uplift and faulting on the Nordland Ridge and the Frøya High during this period (Ehrenberg et al., 1992) as uplift associated with the Nordland Ridge appears to have affected the Heidrun Field (Schmidt, 1992).

Based on lateral facies distribution (Gjelberg et al., 1987) interpreted that the system drained mainly from an easterly source into the study area. However, Hemmens et al. (1994) proposed both an east and westerly source and Thrana et al. (2008) proposed, based on correlation of facies belts and interpreted depositional dip directions from image log data a north-northwesterly source for the Åre Formation.

3.2. Core description

The following facies associations have been distinguished: 1) stacked and single story fluvial channels (FCH), 2) crevasse deposits (CCH), 3) levee (LEV), 4) floodplain fines (FF), and 5) sandy/muddy bay-fill facies (SBF/MBF). These facies associations have been identified in all the wells on basis of core sections and petrophysical log data and are briefly described below: Stacked channels (MFCH) up to 34 m thick comprise mainly blocky, large scale cross-stratified sands, probably deposited by braided rivers (Leary et al., 2007). The individual channel units (8–10 m thick) consist of medium to very coarse-grained sandstone which is poorly sorted and with angular to sub-angular grains. The lower part of the core in well 6507/7-A-38 has been interpreted as a local incision by Svela (2001). Single-story channels (SFCH) are 8–10 m thick, erosional based, fining-up units ranging from very coarse sand to fine sand and silt, sometimes capped by a rooted horizon and coal. The succession of sedimentary structures of basal tabular cross-stratified sand overlain by current rippled and plane parallel-laminated sand and silt at the top is interpreted as point bar deposits sometimes capped by a well developed paleosol (up to 3 m) and coal (Svela, 2001). Crevasse deposits (CCH) comprise up to 6 m thick units with very fine to medium-grained sand, displaying fining up trends and with sharp, sometimes erosive bases. This facies association includes both

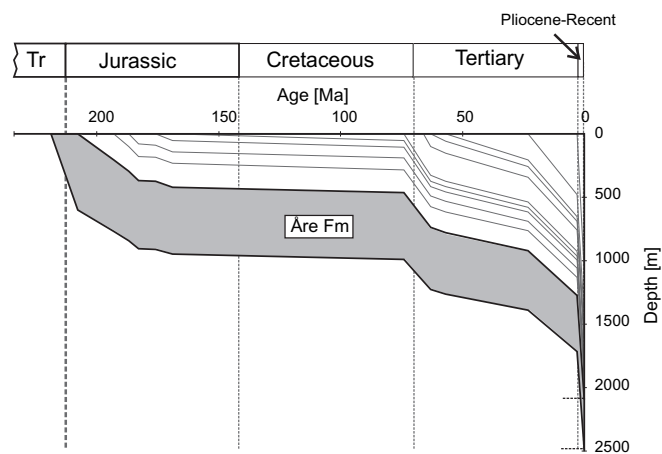


Fig. 3. Constructed burial curve for well 6507/7-A-38 displaying phases of burial: moderate burial from Triassic to Mid-Jurassic, slow burial during Jurassic and Cretaceous, moderate burial from the earliest Cretaceous to Late Pliocene and rapid burial from Late Pliocene to Recent.

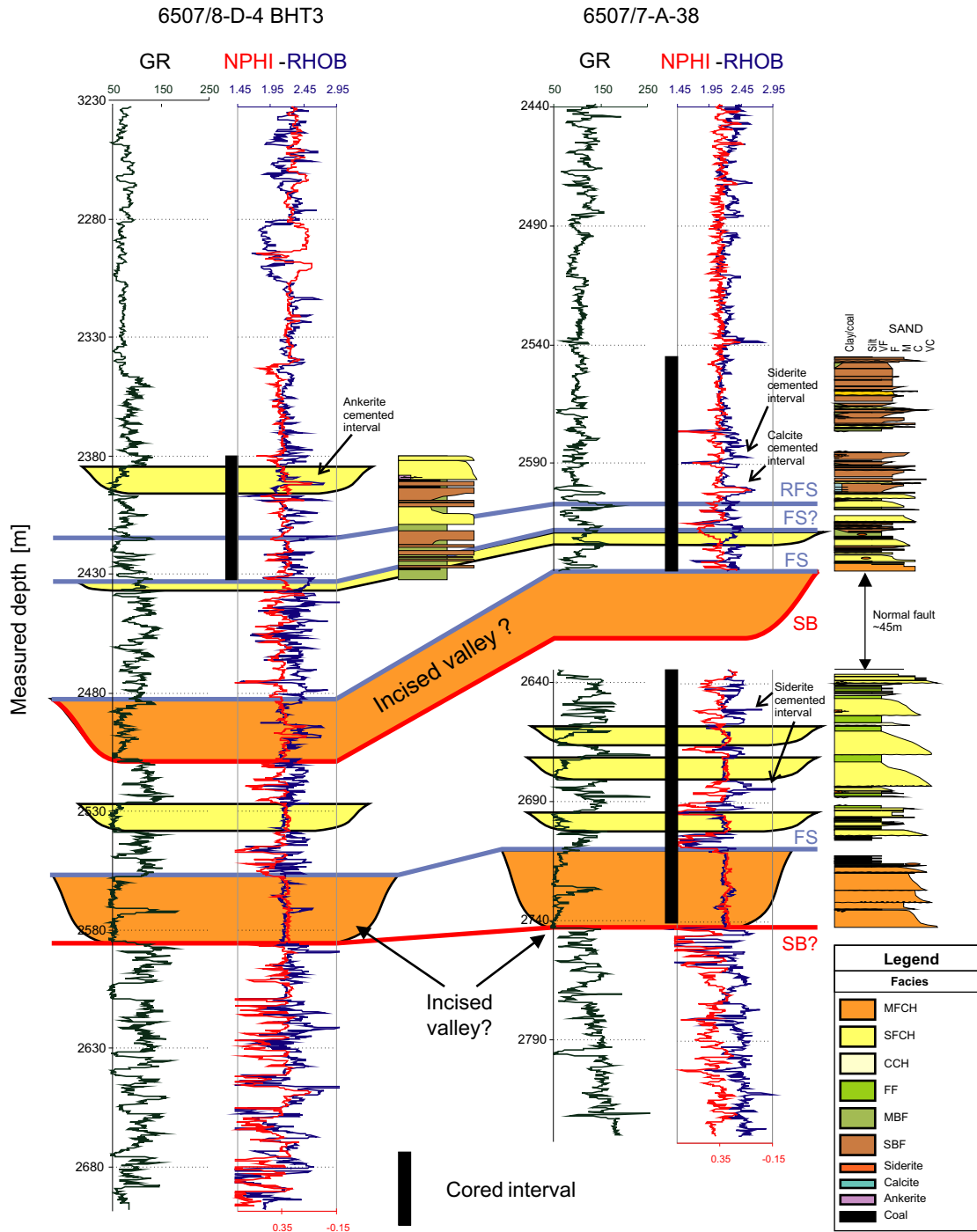


Fig. 4. Correlation and main surfaces in well 6507/7-A-38 and 6507/8-D-4 BHT3 interpreted on basis of sedimentary facies distribution from core sections and wireline log data. SB = Sequence boundaries, FS = Local flooding surfaces, RFS = Regional flooding surface. Studied cemented intervals are shown. Note the overall transgressive trend of the Are Formation in 6507/7-A-38 where fluvial deposits dominate the lower part of the stratigraphy and marginal marine deposits dominate the upper part. A lower significant channel feature (local incision?) is evident in both wells, followed by a point bar dominated succession. A regional fluvial sandstone complex (incised valley?) is interpreted in the middle part of the Are Formation consisting mainly of braided river deposits. The fluvial sandstones are succeeded by coarsening bay-fill sediments deposited in a marine influenced, lower delta plain environment. See Fig. 1 for location of wells.

crevasse channel, crevasse splay and crevasse complex deposits. Climbing ripples and root structures are common. Levees (LEV) comprise up to a few meters thick coarsening upward units from very fine to medium-grained sand. Sedimentary structures are plane parallel lamination changing gradually upwards into current ripples towards the top of the unit where intense rooting and coals are common. The intervals of floodplain fines (FF) are up to 6 m

thick and dominated by very fine sand, silt, clay and coal. Root structures are common below the coals and constitute paleosols locally up to several meters thick. Small crevasses of very fine-grained sand are common within this facies association, sometimes displaying current and climbing ripples. Sandy/muddy bay-fill (SBF/MBF) sediments are defined on the basis of sand prone (SBF) or mud prone (MBF) units comprising 1–5 m thick coarsening

intervals with a silty lower part and a sandier upper part. The units usually have organic rich clay/siltstone at the base, a silty middle part often displaying plane parallel lamination, and an upper sandy part which displays current ripples and occasionally wave ripples and micro-hummocks. Rooting in the sandy upper part is common and the unit is often capped by in situ coals indicating that the bay-fills occupied the entire accommodation space. Small, wrinkled, sand-filled cracks interpreted as syneresis cracks (c.f. *Burst, 1965*) are also found in these units, indicating a mixed freshwater-marine/brackish environment.

For practical purposes, and as it is sometimes difficult to differentiate between some of these facies associations (e.g. sediments from crevasse splays, crevasse channels and levees in petrophysical logs) analytical data in this study are compared referring to three main categories: fluvial channel fill (FCH) combining the stacked and single-story channels (FCH = MFCH, SFCH), floodplain fines (FF) and bay-fill sediments (SBF/MBF).

3.3. Detrital sandstone compositions

The sandstones of the Åre Formation are arkosic to sub-arkosic (classification of *Pettijohn et al. (1972)* and showing slightly more quartz rich compositions in the fluvial sandstones and more feldspathic in the bay-fill sandstones, mainly reflecting the grain sizes (Fig. 5). The sandstones are well sorted, very fine-grained and fine-grained in the bay-fill succession and with sub-angular to sub-rounded grains. Sandstones in the fluvial succession show well-moderate sorting in very fine, fine and medium-grained sandstones and moderate and poor sorting in coarser-grained sandstones at the base of channel fills, and with angular to sub-angular grain shapes. The main detrital minerals are quartz (mainly monocrystalline vs poly), K-feldspar (microcline), plagioclase and mica. As determined from X-ray diffraction (XRD) analyses K-feldspar is more abundant than plagioclase. Feldspar shows variable degrees of dissolution associated with kaolinitization and formation of secondary porosity. Muscovite is the most common mica present; however, the biotite content has been reduced by diagenetic alteration (see below). Rock fragments comprise chert, mica-schist and gneiss, and accessory heavy minerals identified in the

petrographic thin-sections are garnet, opaques (ilmenite), rutile, zircon, tourmaline, Cr-spinel, monazite and apatite, consistent with a provenance from metamorphic schists and gneisses and granitic rocks. The mica content varies between 1 and 5%, except in discrete laminae (mm) found in both fine-grained fluvial channel and bay-fill facies, where the concentration is higher (up to 12%).

4. Diagenesis

Diagenetic processes have modified the detrital grains and pore-space by mechanical compaction, grain alterations, dissolution and cementation. The modal porosity values are, however, relatively high with average values of 27%, and locally up to 39% in sandy facies. The porosity includes secondary porosity, in average 4% and 7% for FCH and SBF respectively and locally up to 10%. The main authigenic minerals are carbonate minerals (siderite, calcite, ankerite, Fe-dolomite), kaolinite, and more sporadic K-feldspar and pyrite, which are discussed in turn below. Carbonate cement occurs in massively cemented beds, occasionally up to 2 m thick intervals, but more commonly in cemented lamina and small scale patches, enhancing small scale heterogeneities within the sediments. Quartz cement is sparse or absent (< ~2–3%), and was in one case found to be reworked. According to *Bjørlykke et al. (1989)* sandstones containing little or no amorphous silica or highly unstable silicate minerals do not develop early quartz cement, as is the case for Jurassic reservoir rocks from the North Sea and Haltenbanken (*Bjørlykke and Brendsdal, 1986*). The diagenetic minerals and in particular the carbonate minerals show complex textural and chemical relations which are described in detail below. These descriptions will also form a basis for interpreting relations between compaction and cementation to be discussed later in this paper.

4.1. Siderite

Siderite is the most widely distributed authigenic carbonate mineral in the Åre Formation occurring both in sandstones and mudstones, and is in particular common in the finer-grained sediments and in layers rich in organic matter and mica. The siderite is commonly accompanied by other authigenic carbonate minerals such as calcite, ankerite or Fe-dolomite in addition to kaolinite. Extensively siderite cemented layers up to 20 cm thick are present in some FF and SBF intervals. In general, two types of siderite cement have been identified in the sediments on the basis of their composition; Sid I of relatively pure composition ($>Fe_{90}$) and more magnesium rich Sid II ($\sim Fe_{60-80}$). Sid I always predating Sid II based on textural relations for carbonate cements. The different cement appearances have been identified by optical microscopy and SEM backscattered electron images (BEI) in combination with electron micro probe analyses and are described for the different sedimentary facies. The presence of siderite in the mudstones has also been verified by XRD analysis from all facies associations. Siderite cementation in fluvial channel facies associations is most common in the upper, siltier parts of fining-up successions in point bar deposits occurring both as massively cemented intervals (up to 10–15 cm) and as cemented lamina (mm) of mica and organic matter. Sid I appears as fine particles of corroded grains (1–5 μm) or aggregates, or as irregular or elongate up to 10 μm long inclusions in Mg-rich siderite (Sid II) (Fig. 6a–c). Coarser Sid I in well 6507/7-A-38 forms irregular grains/aggregates resembling *Microcodium* fabrics (*Mamet and Stemmerik, 2000; Tugarova et al., 2008*) which would suggest a freshwater environment. Authigenic siderite occurs as pore filling cement in both FCH and SBF sands and in 2–3 mm thick organic rich laminae in the upper part of channel fills as rhomb-shaped, chemically zoned siderite, typically with Fe-rich

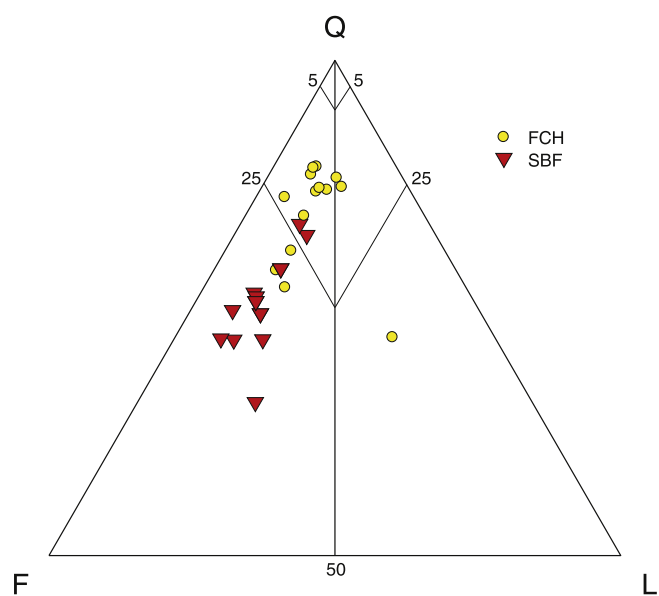


Fig. 5. Sandstone compositions compared for fluvial and sandy bay-fill deposits (classification after *Pettijohn et al., 1972*) (Q=Quartz, F=Feldspar, L=Lithic fragments).

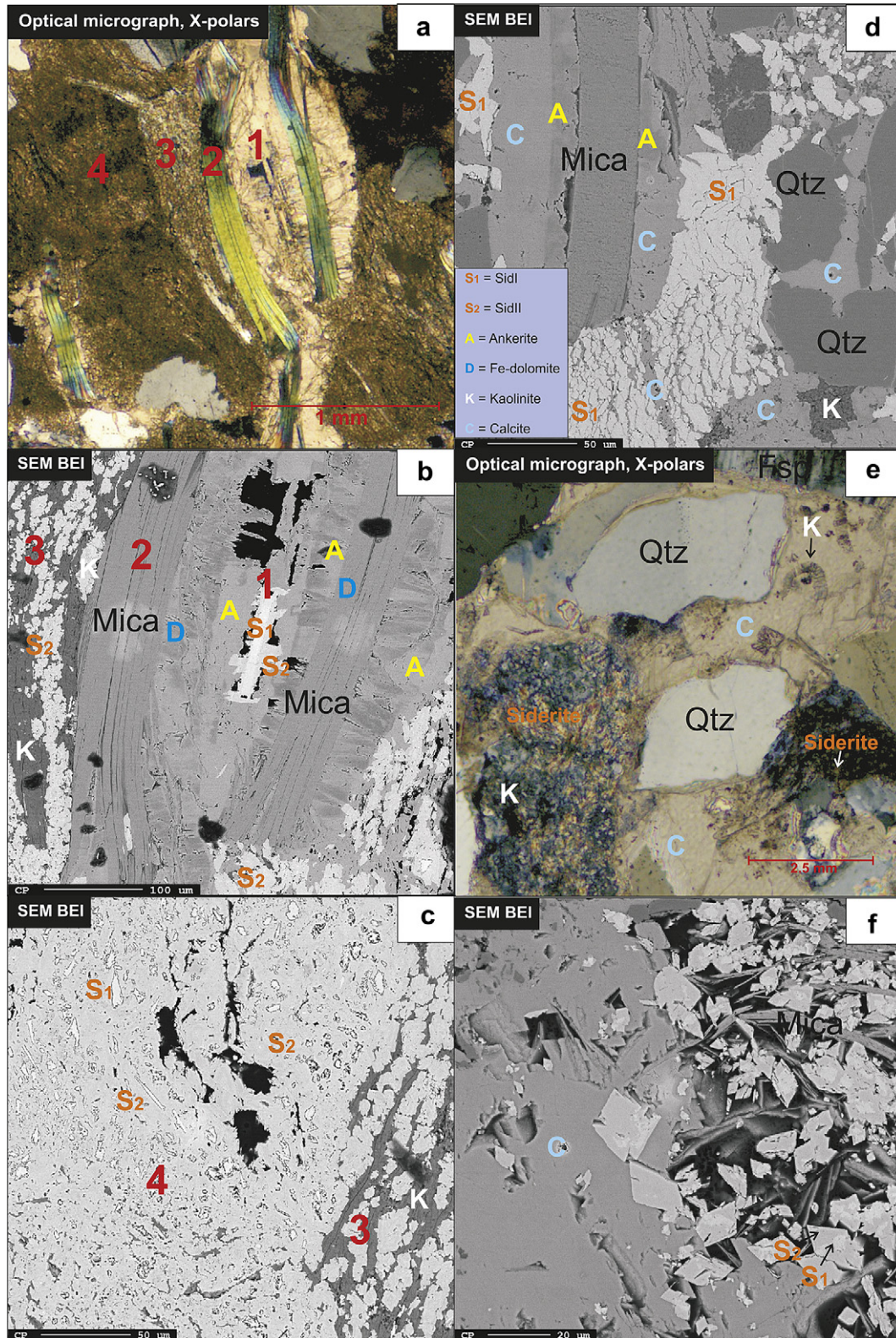


Fig. 6. Texture of carbonate cements. (a) Optical micrograph, X-polars displaying “massively” siderite cemented FCH sandstone from 6507/8-D-4 BHT3. Numbers (1,2,3,4) indicate locations discussed on image b & c. (b) SEM BEI image of location 1–3. 1–2 Fe-dolomite/ankerite rims on mica with ankerite replacing Fe-dolomite. (3) Mg-Sid II intergrown with kaolinite forms pseudomorphs after feldspar and biotite. (c) SEM BEI image of location 3–4. (4) Two generations of siderite where Sid I (S1) appear as irregular, corroded? inclusions in Mg-Sid II (S2). (d) SEM BEI image of a massively siderite cemented zone in FF displaying Sid I type siderite pseudomorphs in addition to calcite-replaced ankerite adjacent to mica. Calcite also fills fissures in the siderite pseudomorph and appears as pore filling cement. (e) Optical micrograph (ppl) of massively calcite cemented SBF related to a regional flooding surface. Note the inclusions of siderite and vermicular kaolinite and the high IGV of cement. (f) SEM BEI image of zoned, rhombic siderite crystals enclosed by calcite in an SBF.

core (Sid I) and Mg-rich rim (Sid II). This type often occurs within pseudomorphs after biotite (Fig. 6f). Intergrowths of Sid II and kaolinite also occur in pseudomorphs after feldspar (Fig. 6a–c). Occasionally, siderite rhombs show unusual zoning patterns in BE-images (6507/8-D-4 BHT3 (FCH) and well 6507/-A-38 (SBF)) as the Fe-rich (central) parts of the crystals commonly are lath-shaped or show irregular shape. This suggests possible controls of precursor minerals or organic debris on the carbonate growth. Pseudomorphic replacements are in particular common in the micaceous layers where Mg-rich siderite forms pseudomorphs after various detrital grains such as feldspar, biotite, and possibly clay clasts and organic debris. Depending on the precursor mineral the pseudomorphs consist of massive siderite or more complex intergrowths of siderite with kaolinite and other carbonate minerals. Siderite cementation in floodplain fines is extensive in zones up to ~10 cm thick within the floodplain mudstones, in pseudomorphs after biotite and feldspar and associated with veins or threads of authigenic kaolinite and calcite (Fig. 6d). The replacive siderite is pure Sid I, i.e. different from replacive Sid II described above. Only weak zoning is seen in BE-images of rhombs showing Fe_{99} in central areas and Fe_{91-98} in rims. Relatively pure siderite also occurs in patches of starred crystals (~10 μm) scattered in the finer-grained silty and clayey sediments, however they constitute less than 1% of the rock. Siderite cementation in bay-fill facies associations is common in VF-sand to silt intervals of SBF sediments in lamina rich in muscovite, altered biotite and organic matter, similar to that observed in FCH. Zoned Sid I and Sid II rhombs as in FCH also occur in this facies association. The zoned rhombs have grown in pseudomorphs after mica (biotite). The siderite rhombs are enclosed by calcite in a massively calcite cemented interval (Fig. 6e and f) which has been related to a flooding event. Also observed in this facies association are carbonate-filled pores in preserved cell-structures of coalified plants (Fig. 7a–c). These carbonates show decreasing Fe content from the cell wall to the pore center from Sid I → Sid II → ankerite indicating decreasing Fe availability during the cement growth. Alternating kaolinite and siderite cemented zones (mm scale) in finely laminated siltstone in MBF are also seen by optical microscopy (Fig. 7d–f). The siderite occurs as starred crystals and is concentrated in zones rich in organic debris where coaly fragments acted as substrate for the siderite precipitations. Siderite constitutes 10% in average of the MBF samples.

4.2. Ankerite and Fe-dolomite

Ankerite and Fe-dolomite are less common than siderite and calcite in the studied wells. However, an extensively ankerite cemented interval occurs in medium-grained channel sandstone (6507/8-D-4 BHT3) in a bay-fill dominated interval in the upper part of the Åre Formation. Minute inclusions of siderite in the pore filling ankerite, both corroded relatively pure Sid I and zoned, rhomb-shaped, slightly coarser Sid II, indicate that ankerite post-dates two generations of siderite. Ankerite accounts for >30–40% of the mode of the cemented interval located above a coaly and micaceous local flooding lag. The high proportion of pore filling ankerite (up to 47%) in thin section scale suggests that it is in part grain-replacive. Occurrence of bent muscovite flakes incorporated in the cement suggests that cementation was, in part, postdating mechanical compaction. Presence of ankerite cement in dissolution-enhanced fractures in feldspar support that ankerite formed relatively late in the paragenetic sequence. Ankerite also occurs in intergrowths with Fe-dolomite adjacent to muscovite grains (Fig. 6a and b), partly replacing and thus postdating the Fe-dolomite. Similar textural features, but where ankerite is partly replaced by late calcite, are observed in fine-grained sediments in the other wells in SBF and FF where the calcite/ankerite intergrowths seem to

replace Sid I and to replace biotite (Fig. 6d). More study is however needed to propose an explanation for these observations. Finally, ankerite is observed in the central part of carbonate-filled pore-space, as described above.

4.3. Calcite

Pore filling calcite appears in massively cemented intervals, up to 2 m thick, where it constitutes approximately 40% of the total rock volume with 4% average remaining porosity (from plug data) and slightly higher, ~7%, from thin-sections, and average permeability of 0.12 mD. Several such intervals are identified in well 6507/7-A-27 appearing in MBF, SBF and FCH. In core data from well 6507/7-A-38 only one calcite cemented zone occurs in VF-F sandstone in an SBF deposit. Other massively cemented intervals can be identified from petrophysical data, but whether the cement is ankerite or calcite is difficult to determine only from the log data. The high proportion of cement reflects that the calcite is in part replacive, it fills fractures in quartz and feldspar grains, occurs as veins (μm) in Sid I pseudomorphs, replaces ankerite in carbonate rims on mica, encloses mechanically deformed mica grains, partly dissolved mica, and authigenic kaolinite and siderite crystals, all suggesting a relatively late timing of the calcite cement.

Carbonate cement compositions in terms of Mg-Fe-Ca are plotted in Fig. 8 for the identified facies associations.

4.4. Kaolinite

Authigenic kaolinite is identified as the only pore filling clay mineral in the sandstones, in some places exceeding 10% of the total rock volume. Modal data of the different facies associations show that the SBF deposits have a higher concentration of K-feldspar (average 21%) compared to the FCH (average 11%) sandstones (Fig. 9), which are more strongly kaolinitized (5% vs 3% volume of kaolinite in average for FCH and SBF respectively). Kaolinite appears as pore filling blocky booklets, “massive” coarser grains, replacive pseudomorphs after feldspar and/or mica, wedges at mica edges and vermicular kaolinite. Kaolinite booklets are locally associated with dissolution and replacement of K-feldspar. “Massive” kaolinite was probably formed by deformation due to mechanical compaction of kaolinitized K-feldspar or mica grains.

4.5. Pyrite

Pyrite is rare in thin-sections, but shows a patchy distribution throughout the cores. Early diagenetic framboidal pyrite is identified in some samples and pyrite nodules occur sporadically in the cores as isolated, rounded to elongated nodules approximately a few cm in diameter. Pyrite nodules have been identified in all the facies associations of the Åre Formation. A nodule studied in the core from well 6507/7-A-38 shows grain-replacive texture such as rims and remnants of other grains (mica, feldspar). Feldspar grains in the pyrite also give evidence of extensive replacement, which is also shown by the high proportion of pyrite in the sample (56%). An early diagenetic origin for some pyrite nodules is evidenced in the core sections by the deformation of the sedimentary lamina around the nodule in both FF and MBF.

4.6. Feldspar overgrowths

Thin, authigenic K-feldspar overgrowths on microcline grains are preserved very locally and are observed in medium-grained channel sandstone in the SBF sequence (6507/8-D-4 BHT3). The K-feldspar overgrowths are enclosed by and postdated by ankerite

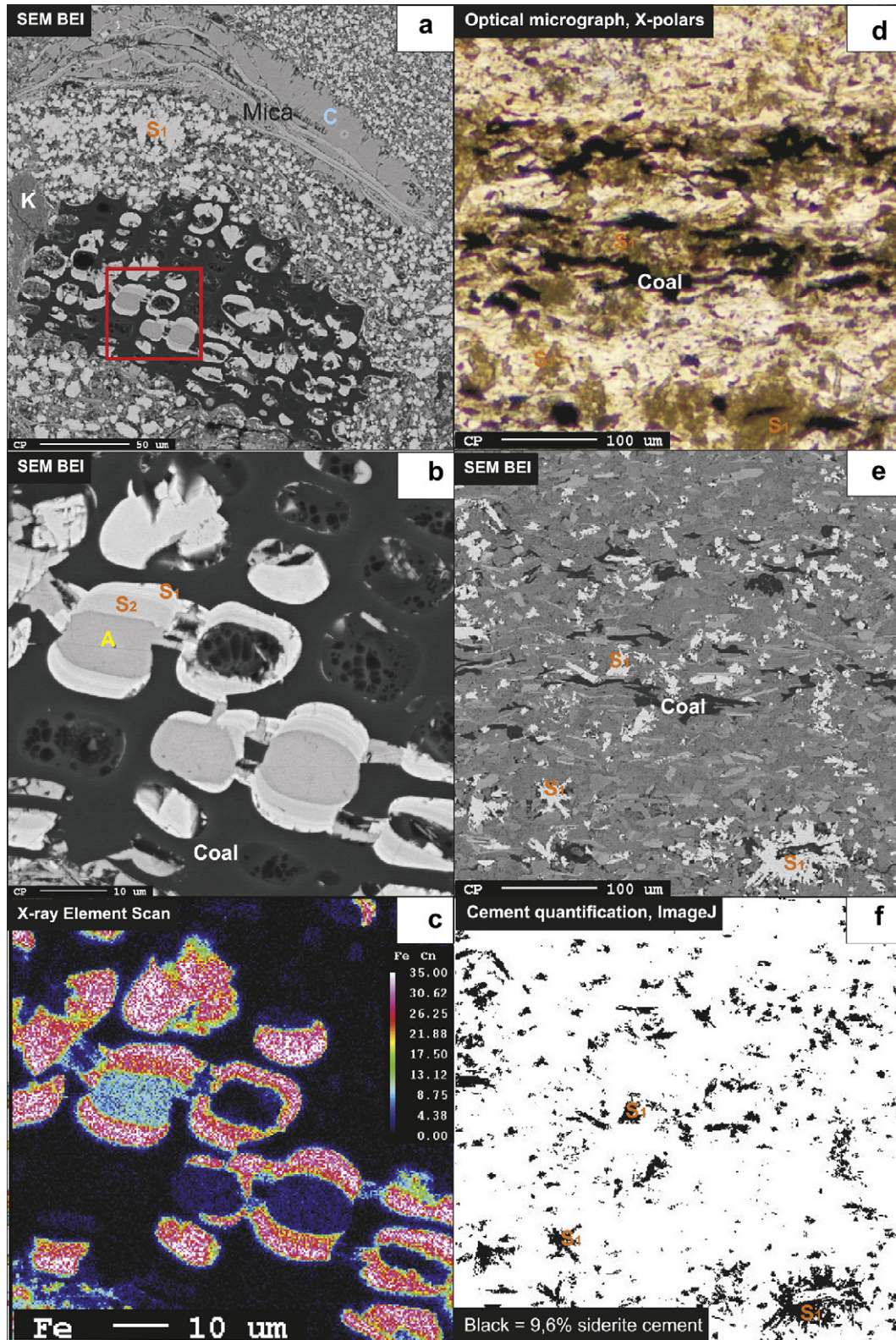


Fig. 7. Texture of carbonate cements. (a) SEM BEI image of carbonate cemented SBF showing Sid I dominating in the finest grained areas and calcite appears as rims on mica grains. (b) is a close-up of carbonate-filled pore-space in coalified plant cell-structure. The cements (Sid I, Sid II and ankerite) reflect decreasing Fe availability. (c) is an X-ray, element scan of the same area illustrating the decreasing Fe concentration in the cement. (d) Optical micrograph of an MBF indicating organic matter controlled growth of starred siderite crystals in finely laminated siltstone. (e) SEM BEI image of the same area. Siderite appears regularly with the presence of coal. (f) Quantification of siderite cement gives ~9.6% cement in the sample. (d), (e) and (f) are from the same sample area.

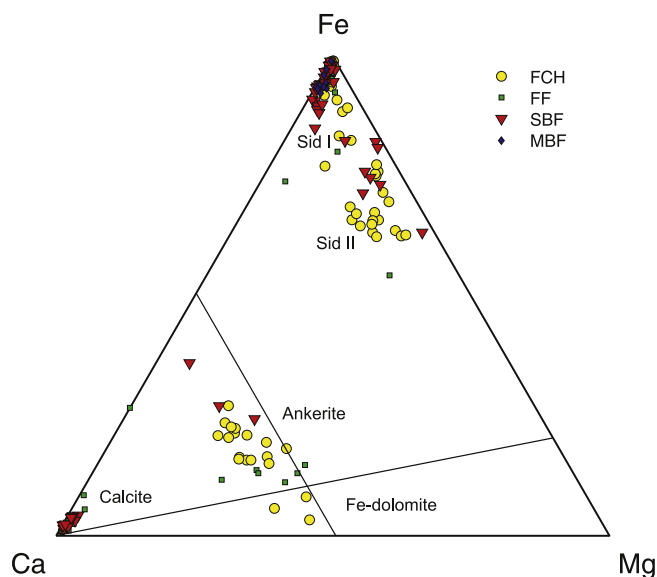


Fig. 8. Carbonate cement compositions in terms of Mg-Fe-Ca, element proportions for FCH, FF, SBF and MBF.

cement in the cemented zone. Traces of albite have been identified in SEM micro probe analysis from FCH.

5. Paragenetic sequence and cement origin

A paragenetic sequence for the authigenic minerals in the Åre Formation is summarized in Table 1. Kaolinite and Sid I are interpreted as the earliest minerals to form during eogenesis, although kaolinite also precipitated during the Sid II phase (see discussion below). The authigenic siderite (Sid I & II), kaolinite and framboidal pyrite are all interpreted as eogenetic, reflecting the initial sedimentary environment.

5.1. Kaolinite origin

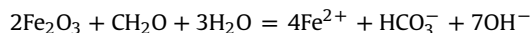
Based on the textural variations, kaolinite is interpreted as having formed both by replacement through leaching of feldspar and mica and by eogenetic precipitation in the pore fluid. Precipitation of kaolinite requires low pH, low ionic strength waters (Bjørlykke et al., 1989, 1986; Worden and Burley, 2003) inferring meteoric fluid flux through the sediments. The fluvial and deltaic environments of the Åre Formation, in combination with humid and warm climate, were favorable for kaolinite formation. In combination with the negative correlation between kaolinite and feldspar this further supports subsurface weathering and meteoric eogenetic alteration of K-feldspar as a source for kaolinite in the Åre Formation (Fig. 9). A flushing of the sediments transporting released silica and K^+ out of the system must have been active to ensure that the pore water composition remained within the kaolinite stability field. The K-feldspar growth suggests periods of local K-enrichment and possibly conditions of more alkaline pore fluids, perhaps related to episodic marine incursions or evaporation. The modal analyses compared for different facies show an increase in K-feldspar and mica with decreasing grain size and from fluvial to marginal marine bay-fill facies associations (c.f. Fig. 9). This is comparable with an increase in the gamma log signature from ~50 to ~80 API going from fluvial to marginal marine deposits, reflecting the increasing amount of potassium. The lower gamma value in fluvial sandstones is related to the more intense

feldspar leaching in these facies associations compared to the bay-fill deposits and a transport of K^+ out of the system.

5.2. Origin of carbonate cements

5.2.1. Siderite

Eogenetic siderite formation is favored in suboxic or reducing environments at low sulphide concentrations, typical in stagnant environments. In the studied FCH, FF and SBF/MBF the association of siderite as replacement of iron-bearing minerals such as biotite, and in clay and organic rich zones in the sediments, suggest local mineralogical controls and local sources of iron for the siderite formation (Mørk, 2008). Some siderite shapes also indicate sideritization of organic particles, and siderite is interpreted to have replaced organic matter in the fine-grained FF and MBF deposits. Notably, biotite is extensively altered in all the siderite-rich samples and replaced by kaolinite and siderite. The importance of detrital clay as carriers of iron oxide/hydroxide particles produced during weathering has been documented elsewhere (e.g. Bensing et al., 2005; Carroll, 1958). Thus, the combination of abundant minerals which can act as Fe-sources and high content of organic debris in the coaly beds seems to have been favorable for siderite formation. The source of carbonate ions could have been mainly from organic matter degradation reactions (Curtis et al., 1977) which are likely in the studied depositional environment, possibly with minor contributions from dissolution of carbonate debris. In iron-rich systems a pH-increase necessary for precipitation of carbonate cement can result from organic matter degradation reactions that also involve iron-reduction (Curtis, 1987; Curtis et al., 1977; Matsumoto and Iijima, 1981; Morad et al., 1998), e.g.:



This kind of reaction is likely to have occurred in the earliest stages of siderite formation when ferric iron was more available, explaining the relatively more Fe-rich Sid I compositions. In the studied samples from the Åre Formation intergrowths of siderite with kaolinite are common, suggesting a genetic relation between the two minerals. The observation of kaolinite as pseudomorphs after detrital feldspar (and mica) suggest that

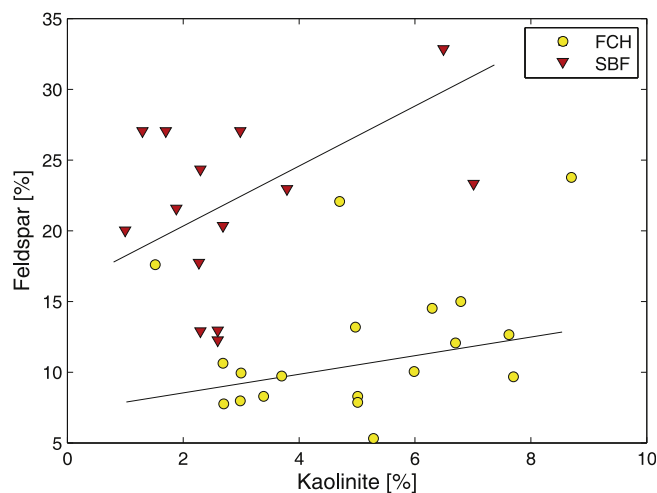


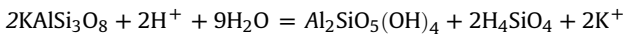
Fig. 9. Modal values for kaolinite vs feldspar for FCH and SBF indicating a relationship between fluvial depositional environment and kaolinite precipitation due to feldspar dissolution.

Table 1
Calculated and measured values for the identified lithoclass facies used.

Facies	Diagenetic event	Early	Late
All facies	Compactional bending of mica Kaolinite	—? ?—?	—
FCH	Sid I irregular, inclusions Sid I rhomb (core) Mg-Sid II rhomb & pseudomorphs Fe-dolomite, rims Feldspar overgrowths Ankerite	— — — ?—?	— — — —
FF	Sid I starred, core Mg-Sid II radiating crystal, rim Pyrite Ankerite Calcite, rims	— — — —	— — — —
SBF/MBF	Sid I rhomb/starred (core) Mg-Sid II rhomb/starred (rim) Calcite, "massive" Sid I → Mg-Sid II → Ankerite ^a	— — — —?	— — — —?

^acoal pore fill

other H⁺ consuming reactions could also have taken place (c.f. Bjørlykke, 1983, 1984), e.g.:



The change in mineral chemistry from Sid I to Sid II and the chemical zoning of the Sid I → Sid II rhombs suggest a change to more Mg²⁺ and Ca²⁺-rich compositions of the pore fluid during siderite growth. This change was observed in siderite from all the different facies, but less in the fine-grained sediments where siderite is iron-richer (e.g. in FF and MBF). Assuming the first reaction was important in initial stages of siderite formation, ferric oxides/hydroxides or possibly oxidized parts of biotite acted as initial iron sources for Sid I. Mechanisms that could lead to increasing Mg/Fe-ratio in the pore fluid, assuming a semi-closed system, involve Fe-depletion from precipitation of Fe-rich minerals such as Sid I and pyrite, kaolinitization of biotite with release of both Fe and Mg, and evaporation and mixing with more Mg-rich fluids, e.g. marine waters. Similar trends of increasing magnesium in later phases of cement growth have been observed in many studies of diagenetic siderites elsewhere (e.g. Curtis and Coleman, 1986; Matsumoto and Iijima, 1981; Rossi et al., 2001). This has been explained by an increase in Mg/Fe-ratio in solution as a result of siderite precipitation in a closed system (Curtis and Coleman, 1986) or to mixing of pore waters at depth making Mg available from connate water (Matsumoto and Iijima, 1981). In a fluvial system, as in the case of the Åre Formation, isolated sand units are common and fluid flow through the system may easily become restricted. The localization of siderite by replacement of biotite and the greater abundance of siderite in the laminated facies rich in altered mica and organic debris therefore suggest that these grains were important sources for both Fe and Mg. However, as the Åre Formation is interpreted as overall transgressive and sea water was introduced into the system possibly in several episodes, the mineral-chemical trend is also comparable with influences from mixing with marine waters. Sid I crystals dominate in low permeable, finer-grained MBF and FF sediments and Mg-rich Sid II in more permeable SBFs. This could also reflect permeability and facies controls on the degree of mixing.

5.2.2. Fe-dolomite

The formation of Fe-dolomite in channel sand within a bay-fill succession (well 6507/8-D-4 BHT3) could be related to marine influences as described above, as the channel is localized above a marine flooding surface. The Fe-dolomite was later partly

replaced by ankerite. Ferroan dolomite is common as early diagenetic carbonate in organic-rich marine sediments (mixing-zone) if sulphate is depleted (Curtis and Coleman, 1986; Morad et al., 1998). In organic-rich marine sediments pyrite formation can be related to decomposition of organic matter by bacterial sulphate reduction (Curtis et al., 1977; Morad et al., 1998), resulting in depletion of iron and increase in the Mg/Fe-ratio of the pore fluid. Authigenic pyrite in the Åre Formation is interpreted to have formed early, as evidenced by sparse occurrence of framboidal pyrite and scattered nodules which predate compaction structures, which can be taken as support of the marine influences.

5.2.3. Ankerite

Ankerite is interpreted to postdate Fe-dolomite in carbonate rims adjacent to mica in the laminated channel facies in the bay-fill sequence in well 6507/8-D-4 BHT3. Pore filling and replacive ankerite is interpreted as late cements as they are enclosing mechanically bent mica grains and crystals of eogenetic siderite and kaolinite. A relatively late origin is also supported by the occurrence as fracture fill in detrital quartz and feldspar grains. This is comparable with observations elsewhere that ankerite cement in sandstones tends to be late in the paragenetic sequence, formed at elevated temperatures (e.g. 80–125 °C, c.f. Dutton and Diggs, 1990). In the fine-grained facies associations in well 6507/7-A-38, ankerite was, however, noted to be postdated by, and in some domains, partly replaced by later calcite cement.

5.2.4. Calcite

Massively calcite cemented zones occur throughout the Åre Formation as sparry pore filling cement in up to 2 m thick intervals. One of the zones, in particular, occurs at approximately the same stratigraphic level in several wells in the sandy upper part of a bay-fill sequence. We relate this zone to a regional flooding event observed through large parts of the Heidrun Field (Leary et al., 2007). Leary et al. (2007) also described presence of carbonaceous foraminifera shells in this part of the stratigraphy of the Åre Formation, suggesting that marine organisms could be a possible source for the carbonate cement in this facies association. Genetic relations of cementation to flooding surfaces have also been documented elsewhere (Kantorowicz et al., 1987; Taylor et al., 1995). Such an event could be associated with prolonged residence time within the zone of bacterial sulphate reduction, due to the water deepening. Fossil fragments found in this part of the Åre Formation could also imply a marine source for carbonate. From

textural relations in the optical and SEM BEI micrographs calcite is, however, interpreted as the authigenic mineral that formed latest in the paragenetic sequence, postdating eogenetic cements, compaction and fracturing of detrital grains. A possible explanation is that marine carbonate components were dissolved by e.g. meteoric water influence or groundwater incursions (relative sea level fall?) and reprecipitated later during burial diagenesis. Another explanation is that the calcite cement precipitated at burial depth sufficient for compactional bending of mica but still within the zone influenced by marine pore water due to the regional transgression. Possible influences on calcite cementation in connection with telogenetic processes, e.g. related to the Cretaceous unconformity should also be considered in future studies.

6. Differential compaction of sandstone, shale and coal

Sandstones compact mechanically due to induced net stress ($\sigma_{\text{net}} = \sigma_{\text{geostatic}} - \sigma_{\text{pore}}$) reducing the bulk volume by rearrangement, fracturing and pseudo-plastic deformation of grains. Ramm (1992) showed that primary sorting and clay content are critical factors concerning porosity reduction in sandstones during mechanical compaction. Detrital grain composition is also a factor in mechanical compaction as sediments composed of quartz grains are more resistant to mechanical compaction than arkosic and lithic sandstones (e.g. Bjørlykke et al., 1989; Worden and Burley, 2003).

Clays and clay rich sediments undergo continuous compaction with notable porosity reduction by particle rotation normal to vertical load during burial (Djeran-Miagre et al., 1998), even during the first meters (Rieke and Chilingarian, 1974), resulting in an anisotropic permeability with larger values in the horizontal direction than in the vertical direction. Mondol et al. (2007) found that experimental mechanical compaction of hydrostatic pressured, brine-saturated pure kaolinite at 20 MPa, corresponding to about 2 km burial, compacted to about 20% porosity from initial porosity of 71%. However, these, experimental data are only valid for mechanical compaction, whereas natural samples will be affected also by chemical diagenetic processes. Sediments that have undergone chemical diagenesis become more difficult to compact mechanically, and mechanical compaction becomes less important.

Peat-to-coal compaction ratios have been compiled in the work of Ryer and Lange (1980) and show values ranging from 4:1 to 30:1 with a median ratio of 7:1. Nadon (1998) argued for ratios ranging as low as 1.2:1 to 2.2:1 based on dinosaur tracks and sand body geometry. However, because of the large variation, an order of magnitude estimate of 10:1 is commonly used and it is observed that a large part of the compression take place in the first few meters of burial.

6.1. Porosity and permeability distribution

6.1.1. Sandstone dominated facies associations (FCH and SBF)

Conventional core analyses (plug data) from sandstone intervals from three wells yield porosity values of 7–37%, with an average porosity of 27% for both FCH and SBF, and permeability values from less than 1 mD to the Darcy range. Average porosity values from modal analyses are presented in Table 2 for different facies associations and exemplified in Fig. 10. Secondary porosity average 4% and 7% in FCH and SBF respectively. Porosity values plotted against logarithm of permeability from plug data for FCH and SBF (Fig. 11) displays a higher average value of permeability in FCH (3000 mD) compared to SBF (500 mD). This may reflect the higher proportion of secondary porosity in SBF compared to FCH. As authigenic kaolinite is more abundant in FCH compared to SBF no significant effect of kaolinite precipitation on permeability is expected. The porosity includes both primary intergranular porosity and

Table 2

Average values for total, primary, and secondary porosity for identified facies associations. Values in percent.

Facies association	ϕ_{initial}	ϕ_{primary}	$\phi_{\text{secondary}}$	ϕ_{total}	μ [mD]
FCH	40	23	4	27	3000
FF ^a	60	18	0	18	n/a
SBF	40	20	7	27	500
MBF ^b	60	28	0	18 ^c	n/a

^a Data from literature.

^b Data from literature.

^c 10% early siderite cement.

secondary, dissolution porosity from dissolution mainly of feldspars and minor from mica. Due to the relatively high porosity the sand appears loose in some core samples. Porosity originating from the dissolution of K-feldspar constitutes locally up to 10% of the total rock volume, with fluvial sandstones more affected by dissolution than the marginal marine facies. The presence of secondary porosity illustrates the importance of dissolution effects regarding reservoir properties. Thin laminae rich in biotite, muscovite and organic matter have been more strongly cemented by siderite and they display lower porosity values compared to the overall trend and may act as local vertical permeability barriers. Massively

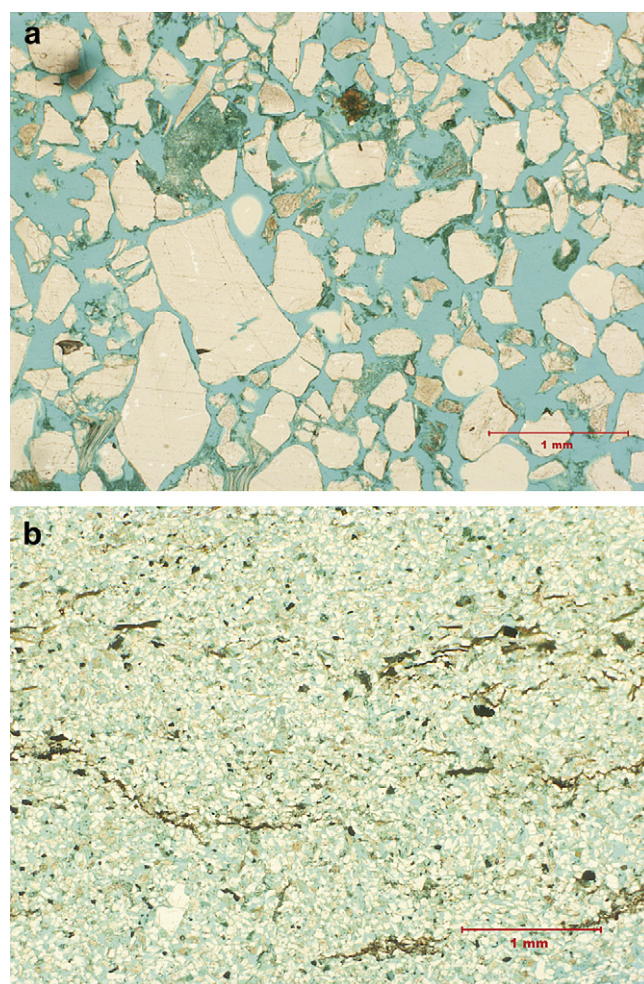


Fig. 10. Photomicrograph of two sandstone samples displaying the porosity and porosity distribution. Blue color indicate porosity. (a) Sandstone sample of an FCH from 2624.80 m TVD depth (2791.30 m core depth) from well 6507/7-A-38. (b) Sandstone sample of an SBF from 2507.13 m TVD depth (2673.63 m core depth) from well 6507/7-A-38. (For interpretation of the references to colour in this figure legend, the reader is referred to the web version of this article.)

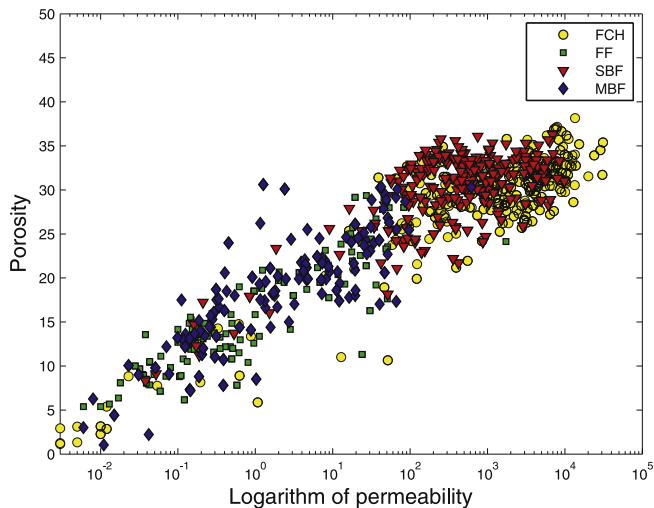


Fig. 11. Plot of porosity vs logarithm of permeability for identified facies associations (FCH, FF, SBF and MBF) determined from plug measurements. Permeability values for SBF facies appear lower (500 mD average) compared to FCH (3000 mD average), porosity values on the other hand are relatively similar (average 27%). FF and MBF are uniformly distributed between 0.1 and 100 mD and 5–25% porosity. Samples with permeability values <0.01 mD represents cemented intervals.

cemented zones display the lowest porosities, (1–5% (core plug)). Although the modal proportions of carbonate cement vary both laterally and vertically, it is locally significant in reducing porosity and permeability and may be important vertical permeability barriers where they are laterally extensive (c.f. Kantorowicz et al., 1987). Intergranular volume (IGV), i.e. the sum of porosity and pore filling cement is commonly used for discussion of compaction. In the present case the extensive calcite and ankerite cemented samples include a high proportion of replacive carbonate leading to 10–15% higher IGV compared to uncemented samples of the same facies association. However, as quantification of replacive vs non-replacive cements is not always possible, IGV volumes are not used as indicators of compaction in this study.

6.1.2. Fine-grained facies associations (MBF and FF)

Concerning mudstones, a wide range of initial porosities are found in published porosity–depth trends (c.f. Fig. 9 in Mondol et al., 2007), with an average of $\sim 60\%$. Some of these present initial porosities lower than 60%, which are explained by presence of sand and silt. In the Åre Formation the fine-grained MBF sediments have been more influenced by eogenetic siderite cementation compared to FF deposits. Siderite cement, in places, constitute more than 10% of the total rock volume and inferring eogenetic cementation, it would imply a reduction in the mechanical compactability of these sediments. Since the presence of organic matter seems to control the localization of the siderite cement, the amount of differential compaction will be reduced, thus decreasing the early compaction of the coaly and clayey beds. FF is more clay rich and only a few percent of siderite cement is present.

Another effect of cementation is where carbonate cements are laterally extensive and acts as a barrier for fluid flow.

6.2. Porosity reduction during burial

Studies of natural unconsolidated sands were conducted by Pryor (1973) on Holocene sand bodies measuring porosity, permeability and textural characteristics of sands from point bars, beaches and eolian sands. Point bar sands ranged in porosity from 17% to 42% with a mean of 41%. The detrital composition of the sandstones from the Heidrun area, arkosic to sub-arkosic, consists

of framework grains with moderate porosity preservation potential during burial in the mechanical compaction regime. Compared with hypothetical burial curves for claystone and sandstone at 2.5 km, the porosity of the arkosic sandstones of the Åre Formation would be relatively similar to the claystone in a mechanical compaction model, i.e. $\sim 20\%$ (Fig. 12). Åre sandstones display, however, an average of 27% porosity. A reason for the 10% higher value could be that secondary porosity, created by leaching of framework grains, may have greater preservation potential than primary porosity during mechanical compaction (Bjørlykke and Brendsdal, 1986).

16.3. Identification of cementation and compaction on wireline log data

In order to compare with properties in wells that lack cores, identification of cementation and compaction on wireline log data is a necessary task. Plotting porosity vs density (NPHI vs RHOB) from 6507/7-A-38 and 6507/7-A-27 reveals a facies dependent bundling of points (Fig. 13). The plot shows FCH sandstones to have a generally lower porosity value compared to SBF sandstones. FF and MBF seem to have the same mean porosity, whereas density values differ as FF has a slightly higher mean RHOB-value, reflecting a higher content of mudstone intervals. NPHI and GR-values for FCH and SBF sandstones display differences related to the observed detrital composition (feldspar, kaolinite). As discussed earlier in this paper, MBF seems to be more preferred for siderite cementation compared to FF inferring that MBF would be denser than FF, i.e. opposite of the observed trend. The siderite in MBF is associated with the presence of detrital organic matter and the effect of cementation on density (net increase) is therefore slightly reduced. In addition, MBF appears more heterogeneous, i.e. is sandier and includes more finely alternating sand/silt beds and laminae

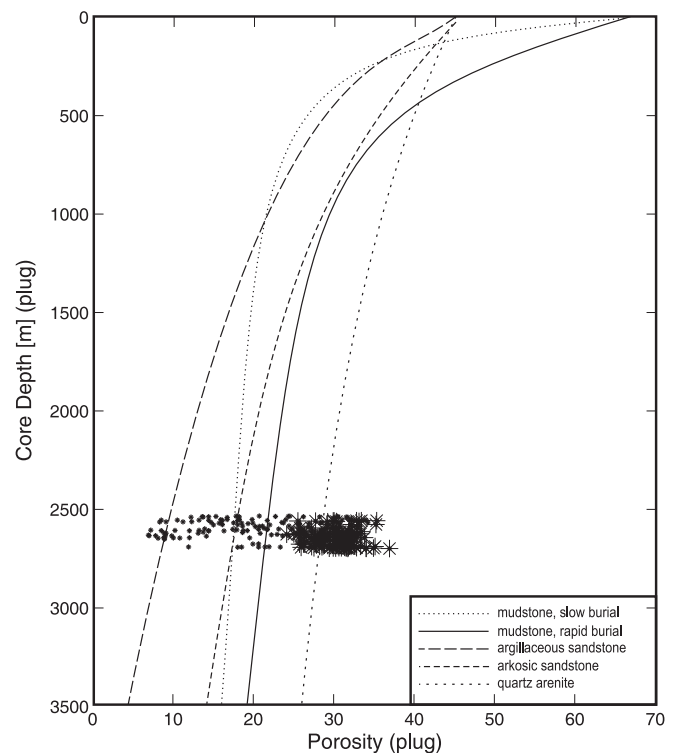


Fig. 12. Compaction curves for sandstones and mudstones of different composition (modified from Worden and Burley, 2003) and plug porosities from well 6507/7-A-38. Large symbols indicate clean, uncemented sandstone intervals, small symbols represents more mud-rich samples.

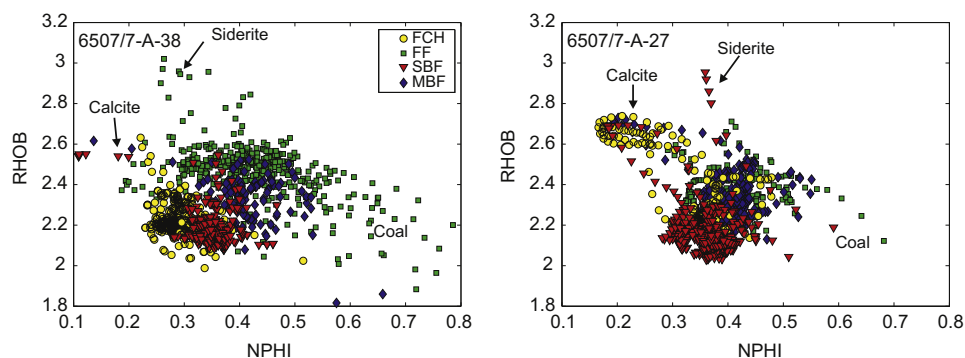


Fig. 13. Density (RHOB) vs porosity (NPHI) plot for FCH, FF and SBF/MBF from 6507/7-A-38 and 6507/7-A-27 indicating a relationship between depositional environment and cementation. Arrows indicate massively cemented zones. The high NPHI values represent coaly intervals. Cemented beds are identified as spikes on RHOB-NPHI-logs (high RHOB, low NPHI) (see arrows in Fig. 4) where the separation may relate to type of cement as a result of the density difference between calcite/ankerite (2.71 g/cm^3 , 2.86 g/cm^3) and siderite (3.89 g/cm^3), and to the presence of hydrogen-bearing minerals, such as kaolinite and mica, which are more abundant in siderite cemented beds.

compared to FF. This contributes to lower density and GR-values in MBF compared to FF. The presence of siderite (low GR) in the mudstones will also decrease the net GR value of the rock. If MBF is more cemented in the clayey parts of the unit, and include more frequent sandy beds than FF, then the compactability of MBF would be lower than that of FF, which infers that FF is more compacted compared to MBF. Depending on the thickness of the clay and sand units this difference in compactability may be as much as 20% ($V_{\text{shale}} = 0.5$ in MBF, 1 in FF).

6.4. Implication of cementation and compaction for sediment correlatability

Considering normal trends of porosity vs depth, the studied units from Heidrun are from depths where the average porosity of mudstone and arkosic sandstone would be rather similar ($\sim 20\%$). However, average porosities in sandstones from the Åre Formation display higher values ($\sim 27\%$). A reason for this may be due to the relatively late, rapid burial occurring during the last 3 million years as a result of deposition of 1.5–2 km of glacial sediments (c.f. Ottesen, 2006). At ~ 2.5 km burial depth average porosity values in mudstones are found to be around 18–20%. Assuming a $\sim 60\%$ initial porosity of clayey beds and $\sim 20\%$ porosity after compaction we can assume a minimum 40% volume reduction. For sandstones, assuming porosity is reduced from $\sim 40\%$ to 23% in FCH and 20% in SBF, there was a 20% and 17% volume reduction in FCH and SBF respectively, i.e. a 1:2 compaction ratio for sandstones vs mudstones (1 m thick sandstone will compact to 0.8 m whereas a 1 m thick mudstone will compact to 0.6 m). Siderite is the most abundant authigenic mineral in the Åre Formation. The effect of siderite on reservoir quality, however, is relatively limited as it is restricted to mm-scaled lamina of mica and organic debris. The effect on compactability of siderite cemented sediments, on the other hand, may be significant. The precipitation of eogenetic Sid I in fine-grained MBF deposits will reduce the compactability of these sediments during mechanical compaction. Due to the abundance of authigenic siderite observed in MBF, locally up to 10% of the bulk volume, and the more heterolithic nature (sandier), differential compaction between MBF and FF deposits may be as much as 20%. As authigenic siderite precipitated relatively early and predates other carbonate cements in the Åre Formation, differentiating between cement types on petrophysical log data is important when such data are used as input for decompaction routines. Backstripping exercises are dependent on timing of cement precipitation which will lead, if not corrected for, to overestimation of sediment compaction, especially in finer-grained sediments.

Differentiation between cements in petrophysical log data may also be useful for sequence stratigraphic interpretation if cement type is related to a specific event, i.e. flooding event, as illustrated earlier in this paper.

7. Conclusions

Diagenesis has altered the fluvial-deltaic sediments of the Åre Formation by porosity reducing, porosity enhancing and replacive reaction processes. Porosity reduction is due to mechanical compaction and precipitation of authigenic carbonate minerals e.g. siderite, Fe-dolomite, ankerite and calcite, and kaolinite and minor pyrite.

Porosity enhancing processes by leaching and dissolution of feldspar, in particular in the fluvial part of the succession, is common. Replacement of detrital grains by kaolinite and carbonate minerals is especially abundant in massively cemented beds.

Eogenetic carbonate precipitation is favored in the finer-grained sediments of MBF and FF facies associations. Authigenic kaolinite is common in all facies, but more abundant in fluvial FCH and FF sediments. Fe-dolomite can be related to the transition from fluvial to deltaic environment suggesting mixing-zone dolomitization, and a regional correlatable calcite cemented layer is related to a regional flooding event.

A paragenetic sequence for diagenesis of the Åre Formation in the Heidrun Field is suggested: Siderite and kaolinite are interpreted as eogenetic, predating any significant mechanical compaction. Fe-dolomite, ankerite and calcite formed post compactional bending of mica. The carbonate minerals display decreasing Fe from early to late authigenic cements.

The combination of abundant detrital minerals which can act as Fe-sources and high content of organic debris seems to have been favorable for siderite formation. Some siderite shapes also indicate sideritization of organic particles.

Evidence for mesogenetic precipitation for authigenic ankerite and calcite is the inclusion relationships to eogenetic minerals and presence of enclosed compactional bent mica grains in the cement.

Porosity is well preserved in channel and bay-fill sandstones, in absence of cementation, revealing a 17%–20% volume reduction for FCH and SBF respectively, during burial. A 40% porosity reduction in fine-grained sediments suggests that differential compaction between uncemented sandstone and mudstone has a ratio of up to 1:2.

The precipitation of eogenetic Sid I in fine-grained MBF deposits will reduce the compactability of these sediments during mechanical compaction. Due to the abundance of authigenic

siderite observed in MBF, locally up to 10% of the bulk volume, and the more heterolithic nature (sandier), differential compaction between MBF compared to FF deposits may be as much as 20%, lowering the sandstone – mudstone compaction ratio for these sediments.

Acknowledgments

Heidrun Unit (Statoil Petroleum AS, ConocoPhillips Skandinavia AS, Petoro AS, Eni Norge AS) is acknowledged for providing well data, rock samples and permission to publish these data from the Heidrun Field.

References

- Bensing, J., Mozley, P., Dunbar, N., 2005. Importance of clay in iron transport and sediment reddening: evidence from reduction features of the Abo Formation, New Mexico, U.S.A. *Journal of Sedimentary Research* 75, 562–571.
- Bjørlykke, K., 1983. Diagenetic reactions in sandstones. In: Parker, A., Sellwood, B. (Eds.), *Sediment Diagenesis*. Reidel Publications Co., pp. 169–213.
- Bjørlykke, K., 1984. Formation of secondary porosity: how important is it. In: McDonald, D., Surdam, R. (Eds.), *Clastic Diagenesis*. American Association of Petroleum Geologists Memoir, vol. 37, pp. 277–286.
- Bjørlykke, K., Aagaard, P., Dypvik, H., Hastings, D., Harper, A., 1986. Diagenesis and reservoir properties of Jurassic sandstones from the Haltenbanken area, offshore Mid-Norway. In: Spencer, A. (Ed.), *Habitat of Hydrocarbons on the Norwegian Continental Shelf*. Norwegian Petroleum Society. Graham and Trotman, pp. 275–286.
- Bjørlykke, K., Brendsdal, A., 1986. Diagenesis of the Brent sandstone in the Statfjord field, North Sea. In: Gautier, D. (Ed.), *Roles of Organic Matter in Sediment Diagenesis*. SEPM Special Publications, vol. 38, pp. 157–167.
- Bjørlykke, K., Ramm, M., Saigal, G., 1989. Sandstone diagenesis and porosity modification during basin evolution. *International Journal of Earth Sciences* 68, 1151–1171.
- Blystad, P., Brekke, H., Færseth, R., Larsen, B., Skogseid, J., Tærudbakken, B., 1995. Structural elements of the Norwegian continental shelf. Part II: the Norwegian Sea region. *Norwegian Petroleum Directorate Bulletin* 8, 45.
- Brekke, H., Sjulstad, H., Magnus, C., Williams, R., 2001. Sedimentary environments offshore Norway – an overview. In: Martinsen, O., Dreyer, T. (Eds.), *Sedimentary Environments Offshore Norway – Palaeozoic to Recent*. Norwegian Petroleum Society Special Publication, vol. 10, pp. 7–37.
- Bukovics, C., Shaw, N., Cartier, E., Ziegler, P., 1984. Structure and development of the Mid-Norway continental margin. In: Spencer, A. (Ed.), *Petroleum Geology of the North European Margin*. Norwegian Petroleum Society. Graham and Trotman, London, pp. 407–423.
- Bukovics, C., Ziegler, P., 1985. Tectonic development of the Mid-Norway continental margin. *Marine and Petroleum Geology* 2, 1–22.
- Burst, J., 1965. Subaqueously formed shrinkage cracks in clay. *Journal of Sedimentary Petrology* 35, 348–353.
- Carroll, D., 1958. Role of clay minerals in the transportation of iron. *Geochimica et Cosmochimica Acta* 14, 1–27.
- Clemmensen, L., Kent, D., Jenkins, F., 1998. A late triassic lake system in East Greenland: facies, depositional cycles and palaeoclimate. *Palaeogeography, Palaeoclimatology, Palaeoecology* 140 (1), 135–159.
- Curtis, C., 1987. Mineralogical consequences of organic matter degradation in sediments: inorganic/organic diagenesis. In: Leggett, J., Zuffa, G. (Eds.), *Marine Clastic Sedimentology*. Graham and Trotman, pp. 108–123.
- Curtis, C., Coleman, M., 1986. Controls on the precipitation of early diagenetic calcite, dolomite and siderite concretions in complex depositional sequences. In: Gautier, D. (Ed.), *Roles of Organic Matter in Sediment*. The Society of Economic Paleontologists and Mineralogists Special Publication, pp. 23–33.
- Curtis, C.D., Burns, R.G., Smith, J.V., 1977. Sedimentary geochemistry: environments and processes dominated by involvement of an aqueous phase [and discussion]. *Philosophical Transactions of the Royal Society of London. Series A, Mathematical and Physical Sciences* 286 (1336), 353–372.
- Dalland, A., Agedahl, H., Bomstad, K., Ofstad, K., 1988. The post-Triassic succession of the mid-Norwegian shelf. In: Dalland, A., Worsley, D., Ofstad, K. (Eds.), *A Lithostratigraphic Scheme for the Mesozoic and Cenozoic Succession Offshore Mid- and Northern Norway*, vol. 4. Norwegian Petroleum Directorate Bulletin, pp. 5–42.
- Djeran-Miagre, I., Tessier, D., Grunberger, D., Velde, B., Vasseur, G., 1998. Evolution of microstructures and of macroscopic properties of some clays during experimental compaction. *Marine and Petroleum Geology* 15, 109–128.
- Dooley, T., McCay, K., Pascoe, R., 2003. 3D analogue models of variable displacement extensional faults: applications to the Revfallet Fault system, offshore Mid-Norway. In: Nieuwland, D. (Ed.), *New Insights into Structural Interpretation and Modelling*. Geological Society, London, Special Publications, vol. 212, pp. 151–167.
- Doré, A., 1991. The structural foundation and evolution of Mesozoic seaways between Europe and the Arctic Sea. *Palaeogeography, Palaeoclimatology, Palaeoecology* 87, 441–492.
- Doré, A., Gage, M., 1987. Crestal alignments and sedimentary domains in the evolution of the North Sea, northeast Atlantic margin and the Barents Shelf. In: Brooks, J., Glennie, K. (Eds.), *Petroleum Geology of NW Europe*. Graham and Trotman, London, UK, pp. 1131–1148.
- Dutton, S., Diggs, T., 1990. History of quartz cementation in the lower cretaceous Travis peak formation, East Texas. *Journal of Sedimentary Petrology* 60 (2), 191–202.
- Ehrenberg, S., 1990. Relationship between diagenesis and reservoir quality in sandstones of the Garn Formation, Haltenbanken, Mid-Norwegian Continental Shelf. *The American Association of Petroleum Geologists Bulletin* 74, 1538–1558.
- Ehrenberg, S., 1993. Preservation of anomalously high porosity in deeply buried sandstones by grain-coating chlorite: examples from the Norwegian Continental Shelf. *The American Association of Petroleum Geologists Bulletin* 77, 1260–1286.
- Ehrenberg, S., Gjerstad, H., Hadler-Jacobsen, F., 1992. Smørbukkk field: a gas condensate fault trap in the Haltenbanken province, offshore Mid-Norway. In: Halbouty, M. (Ed.), *Giant Oil Fields of the Decade 1978–1988*. American Association of Petroleum Geologists Memoir, vol. 54, pp. 323–348.
- Gabrielsen, R., Færseth, R., Hamar, G., Ronnevik, H., 1984. Nomenclature of the main structural features on the Norwegian Continental Shelf north of the 62nd parallel. In: Spencer, A., Holter, E., Johnsen, S., Mork, A., Nysæther, E., Songstad, P., Spinnanger, A. (Eds.), *Petroleum Geology of the North European Margin*. Norwegian Petroleum Society, pp. 41–60.
- Gjelberg, J., Dreyer, T., Høie, A., Tjelland, T., Lilleng, T., 1987. Late jurassic to mid-jurassic sandbody development on the Barents and mid-Norwegian shelf. In: Brooks, J., Glennie, K. (Eds.), *Petroleum Geology of Northwest Europe*. Graham and Trotman, London, pp. 1105–1129.
- Hallam, A., 1984. Continental humid and arid zones during the Jurassic and Cretaceous. *Palaeogeography, Palaeoclimatology, Palaeoecology* 47, 195–223.
- Hemmens, P., Hole, A., Reid, B., Leach, P., Landrum, W., 1994. The Heidrun field. In: Aasen, J., Berg, E., Buller, A., Hjelmeland, O., Holt, R., Kleppe, J., Torsæter, O. (Eds.), *North Sea Oil and Gas Reservoirs III*. Kluwer Academic Publishers, Dordrecht, pp. 1–23.
- Hurst, V., Kunkle, A., 1985. Dehydroxylation, rehydroxylation, and stability of kaolinite. *Clays and Clay Minerals* 33, 1–14.
- Kantorowicz, J., Bryant, I., Dawans, J., 1987. Controls on geometry and distribution of carbonate cements in jurassic sandstones: bridport sands, southern England and the viking group, Troll field, Norway. In: Marshall, J. (Ed.), *Diagenesis of Sedimentary Sequences*. Geological Society, London, Special Publications, vol. 36, pp. 103–118.
- Kjærefjord, J., 1999. Bayfill successions in the lower jurassic Åre Formation, offshore Norway: sedimentology and heterogeneity based on subsurface data from the Heidrun field and analog data from the upper cretaceous Neslen Formation, eastern Book Cliffs, Utha. In: Hentz, T. (Ed.), *19th Annual Research Conference. Advanced Reservoir Characterization for the Twenty-First Century*. Gulf Coast Section and Society Economic Paleontologists and Mineralogists Foundation, Special Publication, pp. 149–157.
- Koch, J., Heum, O., 1995. Exploration trends of the Halten terrace. In: Hanslien, S. (Ed.), *Petroleum Exploration in Norway*. Norwegian Petroleum Society Special Publication, vol. 4, pp. 235–251.
- Koenig, R., 1986. Oil discovery in 6507; an initial look at the Heidrun Field. In: Spencer, A., Campbell, C., Hanslien, S., Nelson, P., Nysæther, E., Ormaasen, E. (Eds.), *Habitat of Hydrocarbons on the Norwegian Continental Shelf*. Norwegian Petroleum Society, pp. 307–311.
- Leary, S., Næss, A., Thrana, C., Brekken, M., Cullum, A., Gowland, S., Selnes, H., 2007. The Åre formation, Heidrun field, Norwegian sea. In: 25th International Association of Sedimentologists, Meeting of Sedimentologists, Patras, Greece. Poster.
- Mamet, B., Stemmerik, L., 2000. Carboniferous algal microflora, Kap Jungersen and Foldedal formations, Holm land and Amdrup land, eastern North Greenland. In: Stemmerik, L. (Ed.), *Palynology and Deposition in the Wandel Sea Basin, Eastern North Greenland*. Geology of Greenland Survey Bulletin, vol. 187, pp. 79–101.
- Martinius, A., Kaas, I., Næss, A., Helgesen, G., Kjærefjord, J., Leith, D., 2001. Sedimentology of the heterolithic and tide-dominated Tilje Formation (Early Jurassic, Halten Terrace, offshore Mid-Norway). In: Martinsen, O., Dreyer, T. (Eds.), *Sedimentary Environments Offshore Norway – Paleozoic to Recent*. Norwegian Petroleum Society Special Publication, vol. 10. Elsevier Science B.V., Amsterdam, pp. 103–144.
- Matsumoto, R., Iijima, A., 1981. Origin and diagenetic evolution of Ca-Mg-Fe carbonates in some coalfields of Japan. *Sedimentology* 28, 239–259.
- Mondol, N.H., Bjørlykke, K., Jahren, J., Høeg, K., 2007. Experimental mechanical compaction of clay mineral aggregates - changes in physical properties of mudstones during burial. *Marine and Petroleum Geology* 24 (5), 289–311.
- Morad, S., De Ros, L., Nystuen, J., Bergan, M., 1998. Carbonate diagenesis and porosity evolution in sheet-flood sandstones: evidence from the middle and lower Lunde members (Triassic) in the Snorre field, Norwegian North Sea. In: Morad, S. (Ed.), *Carbonate Cementation in Sandstones*. International Association of Sedimentologists Special Publications, vol. 26. Blackwell Scientific Publications, Oxford, UK, pp. 53–85.
- Mørk, M., Vigran, J., Smelror, M., Fjerdingsstad, V., Bøe, R., 2003. Mesozoic mudstone compositions and the role of kaolinite weathering – shallow cores in the Norwegian Sea (møre to Troms). *Norwegian Journal of Geology* 83, 61–78.

- Mørk, M.B.E., 2008. Detrital mineral controls on diagenetic textures in sandstones from the Åre Formation. In: 28th Nordic Geological Winter Meeting, Aalborg University, Department of Civil Engineering, Aalborg 33.
- Nadon, G.C., 1998. Magnitude and timing of peat-to-coal compaction. *Geology* 26 (8), 727–730.
- Nøttvedt, A., Gabrielsen, R., Steel, R., 1995. Tectonostratigraphy and sedimentary architecture of rift basins, with reference to the northern North Sea. *Marine and Petroleum Geology* 12, 881–901.
- Nygård, R., Gutierrez, M., Gautam, R., Høeg, K., 2004. Compaction behavior of argillaceous sediments as function of diagenesis. *Marine and Petroleum Geology* 21, 349–362.
- Olsen, T., Rosvoll, K., Kjærefjord, J., Arnesen, D., Sandsdalen, C., Jørgenvåg, S., Langlais, V., Sveta, K., 1999. Integrated reservoir characterization and uncertainty analysis, Heidrun field, Norway. In: Fleet, A., Boldy, S. (Eds.), *Petroleum Geology of Northwest Europe: Proceedings of the 5th Conference. GSL Miscellaneous Titles. Geological Society of London*, vol. 86, pp. 1209–1220.
- Ottesen, D., 2006. Ice-sheet Dynamics and Glacial Development of the Norwegian Continental Margin During the Last 3 Million Years. Dr.philos. Department of Earth Science, University of Bergen, Norway.
- Pearson, M., 1990. Clay mineral distribution and provenance in Mesozoic and Tertiary mudrocks of the Moray firth and northern North Sea. *Clay Minerals* 25, 519–541.
- Pettijohn, F., Potter, P.E., Siever, R., 1972. *Sand and Sandstone*. Springer-Verlag, Berlin-Heidelberg-New York.
- Pryor, W., 1973. Permeability-porosity patterns and variations in some Holocene sand bodies. *The American Association of Petroleum Geologists Bulletin* 57, 162–189.
- Ramm, M., 1992. Porosity-depth trends in reservoir sandstones: theoretical models related to Jurassic sandstones offshore Norway. *Marine and Petroleum Geology* 9, 553–567.
- Rieke, H., Chilingarian, G., 1974. *Compaction of Argillaceous Sediments, Developments in Sedimentology*, vol. 16. Elsevier, Amsterdam.
- Rossi, C., Marfil, R., Ramseyer, K., Permanyer, A., 2001. Facies-related diagenesis and multiphase siderite cementation and dissolution in the reservoir sandstones of the Khatatba Formation, Egypt's western desert. *Journal of Sedimentary Research* 71 (3), 459–472.
- Ryer, T.A., Lange, A.W., 1980. Thickness change involved in the peat-to-coal transformation for a bituminous coal of cretaceous age in central Utah. *Journal of Sedimentary Research* 50 (3), 987–992.
- Schmidt, W., 1992. Structure of the Mid-Norway Heidrun field and its regional implications. In: Larsen, R., Brekke, H., Larsen, B., Talleraas, E. (Eds.), *Structural and Tectonic Modelling and Its Application to Petroleum Geology*. Norwegian Petroleum Society Special Publication, vol. 1, pp. 381–395.
- Spencer, A., Birkeland, Ø., Koch, J.-O., 1993. Petroleum geology of the proven hydrocarbon basins, offshore Norway. *First Break* 11, 161–176.
- Storvoll, V., Bjørlykke, K., Karlsen, D., Saigal, G., 2002. Porosity preservation in reservoir sandstones due to grain-coating illite: a study of the Jurassic Garn Formation from the Kristin and Lavrans fields, offshore Mid-Norway. *Marine and Petroleum Geology* 19, 767–782.
- Sveta, K., 2001. Sedimentary facies in the fluvial-dominated åre n in the åre 1 member in the Heidrun field. In: Martinsen, O., Dreyer, T. (Eds.), *Sedimentary Environments Offshore Norway - Paleozoic to Recent*. Norwegian Petroleum Society Special Publication, vol. 10. Elsevier Science B.V., Amsterdam, pp. 87–102.
- Swiecicki, T., Gibbs, P., Farrow, G., Coward, M., 1998. A tectonostratigraphic framework for the Mid-Norway region. *Marine and Petroleum Geology*, 245–276.
- Taylor, K., Gawthorpe, R., Van Wagoner, J., 1995. Stratigraphic control on laterally persistent cementation, book cliffs, Utah. *Journal of the Geological Society* 152 (2), 225–228.
- Thrana, C., Brekken, M., Næss, A., Leary, S., Gowland, S., 2008. Revised reservoir characterization of the åre Fm., Heidrun field, Halten Terrace, Abstract, the 33rd IGC, Oslo, Norway. In: 33rd International Geological Congress, Oslo, Norway, Lillestrøm. Poster.
- Tugarova, M., Pchelina, T., Ustinov, N., Viskunova, K., 2008. Lithological and geochemical characteristics of Triassic sediments from the central part of the South Barents depression (Arkticheskaya-1 well). *Polar Research* 27, 495–501.
- Walderhaug, O., 1996. Kinetic modeling of quartz cementation and porosity loss in deeply buried sandstone reservoirs. *The American Association of Petroleum Geologists Bulletin* 80 (5), 731–745.
- Walderhaug, O., Bjørkum, P., Nadeau, P., Langnes, O., 2001. Quantitative modelling of basin subsidence caused by temperature-driven silica dissolution and reprecipitation. *Petroleum Geoscience* 7, 107–113.
- Whitley, P., 1992. The geology of Heidrun. A giant oil and gas field on the Mid-Norwegian shelf. In: Halbouty, M. (Ed.), *Giant Oil Fields of the Decade 1978–1988*. The American Association of Petroleum Geologists Memoirs, vol. 54, pp. 383–406.
- Worden, R., Burley, S., 2003. Sandstone diagenesis: the evolution of sand to stone. In: Burley, S., Worden, R. (Eds.), *Sandstone Diagenesis. Recent and Ancient*. Reprint Series 4 of the International Association of Sedimentologists. Blackwell Publishing, pp. 3–44.

Paper II

Reconstruction of Heterogeneous Reservoir Architecture based on Differential
Decompaction in Sequential Re-burial modelling

*Authors: Erik Hammer, Kristian Bjarnøe Brandsegg, Mai Britt E. Mørk and
Arve Næss*

Submitted: Petroleum Geoscience, pages 1-20

Reconstruction of Heterogeneous Reservoir Architecture based on Differential Decompaction in Sequential Re-burial modelling

Erik Hammer^{*,a}, Kristian Bjarnøe Brandsegg^{a,1}, Mai Britt E. Mørk^a, Arve Næss^b

^a*Department of Geology and Mineral Resources Engineering, Norwegian University of Science and Technology, N-7491, Norway*

^b*StatoilHydro, E&P Norway, Strandveien 4, N-7501 Stjørdal, Norway*

Abstract

A new and improved methodology for robust, high-resolution correlation of reservoir sandstones in highly compactable depositional sequences is proposed. Quantitative sequential re-burial modelling has been successfully applied on real data from seven wells covering the heterogeneous fluviodeltaic Åre Fm. in the Heidrun Field, offshore Mid-Norway. The methodology is based on ten interpreted lithofacies classes derived from core descriptions and wireline logs signatures, in addition to interpreted sequence stratigraphic surfaces, i.e. flooding surfaces. Analysis of decompacted sedimentary columns with emphasis on studies of shallow compaction effects, tied to uniquely calculated compaction curves, has revealed several new correlatable horizons within the Åre Fm., including three laterally extensive coals and several laterally correlatable fluvial sandstones, some of which extend the total width of the studied area. The results from the present study demonstrate the benefits of correcting for the effects of differential compaction in well-to-well correlation of heterogeneous reservoirs comprising highly compactable sediments. The methodology outlined here has widespread applicability to other stratigraphic successions and could potential help in the correlation of highly compacted sediments in the subsurface.

Key words: Re-burial, sequence stratigraphy, compaction curves, decompaction, porosity, correlation

1. Introduction

Depositional systems are generally thought of as a product of the interactions of three main allo-genic controls - basin floor subsidence, base-level change and sediment supply (Posamentier et al., 1988; Posamentier and Vail, 1988; Van Wagoner et al., 1990, 1988). In addition, local factors, such as climate, topography and sediment compaction, define major autogenic controls. Heterogeneities in the sedimentary architecture at many scales can affect reservoir performance by differential compaction. Subsidence analysis of wells and core sections based on decompaction of the sediment column (e.g. Bond and Kominz, 1984; Sclater and Christie, 1980; Van Hinte, 1978) is a standard

method for investigating sedimentary basins (Allen and Allen, 2005; Leeder, 1999; Miall, 1999). The restored sediment thicknesses based on the back-stripping technique (Sleep, 1971) allow for the calculation of sedimentation rate and basement subsidence, and is the standard method for basin reconstruction (Bond and Kominz, 1984). In this study we introduce backstripping as a tool also for reservoir scale reconstruction based on high resolution (cm scale) wireline- and core data. The correlatability of reservoir units in heterogeneous deposits can be improved by applying decompacted sedimentary columns in the correlation process and taking into account and correcting for the effect of differential compaction. Robust correlations are a fundamental prerequisite in refined reservoir models used as a decision tool in optimizing drainage solutions.

*Corresponding author: Tel.: +47 41501284.

Email address: Erik.Hammer@ntnu.no (Erik Hammer)

¹Current address: Exploro AS, Stiklestadveien 1, N-7041, Trondheim

2. Background; correlation challenges in fluvial deposits

The Åre Fm. (Dalland et al., 1988) in the Heidrun Field (Koenig, 1986) comprises strongly heterogeneous sediments deposited in a fluvial to lower delta plain environment (Pedersen et al., 1989; Gjølberg et al., 1987; Svela, 2001; Leary et al., 2007; Thrana et al., 2008). Due to the lateral and vertical heterogeneous nature and architecture of the deposits, including isolated channel fills and highly compactable lithologies (i.e. muds and coals), large reservoir correlation difficulties are encountered. A reservoir model also taking into account differential compaction was therefore desired in order to counter this effect and hence, increasing the correlatability of sandstone reservoir units. Based on the backstripping technique and using interpreted flooding surfaces as backstripping surfaces, high resolution petrophysical data, and interpreted core sections in the correlation process, we suggest that the effect of differential compaction can be accounted for by stepwise correlation on decompactified reservoir sections (Fig. 1).

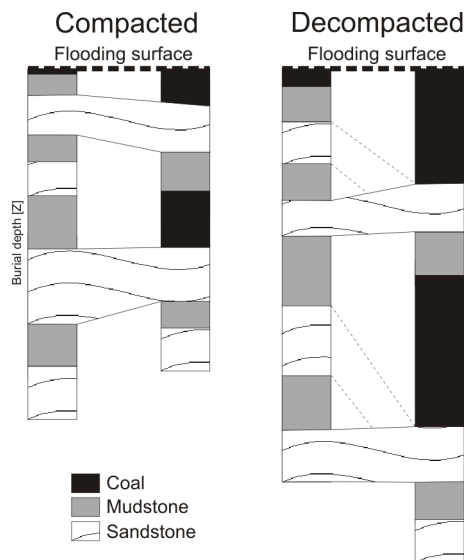


Figure 1: Sketch comparing correlation of two artificial lithological columns illustrating the effect of differential compaction. Correlation of reservoir sands in the columns presented to the left is very different from the decompactified columns presented to the right.

3. Backstripping calculation

To account for the effect of differential compaction, especially where considerable early differential compaction occurs, a correlation exercise performed on decompactified sediment columns is suggested. This challenge is solved by applying the technique of backstripping in a reservoir scale, although in this study a more precise definition would be reverse backstripping or sequential reburial (reloading). Backstripping, a technique developed by Sleep (1971), was first explored in detail by Watts and Ryan (1976). The technique is generally used to estimate tectonic subsidence by accounting for and removing the effect of other causes of subsidence, such as loading due to the sedimentary column (Bond and Kominz, 1984; Steckler and Watts, 1978), or in a basin in which the tectonic subsidence history is simple, allowing to model sea-level changes (e.g. Bond et al., 1989; Kominz and Pekar, 2001). Where tectonic subsidence can be estimated, the backstripping approach can be used to calculate palaeobathymetry and reconstruct the stratigraphy through time (Steckler et al., 1999, 1988). The process of reconstructing the development of a sedimentary column consists of several steps (Bond and Kominz, 1984). The procedure starts with the division of the stratigraphic column into increments, usually formations or groups, or as suggested here, at higher resolution, such as lithofacies, if stratigraphically correlatable surfaces are available, for which the thickness and age range can be accurately determined. Age is not considered here, except relative age, as the increments represent relatively small time periods (in the $\sim 100,000$ yrs range). These "time slices" are added to the basement one by one, calculating the original decompactified thickness and bulk density and placing its top at a depth below sea level corresponding to the average depth of water in which the unit was deposited (palaeobathymetry). The isostatic subsidence caused by the weight of this sediment can then be calculated, and the depth to the surface on which the sediment was deposited is calculated with only the weight of the water as the basement load. For fluvial deposits (as for the Åre Fm.), no water is present as overburden. The second unit is then added and adjusted accordingly. The thickness and bulk density of the first unit are adjusted in accordance with the depth of burial beneath the second unit, and so on up the column (Fig. 2). Age controlled stratigraphic sur-

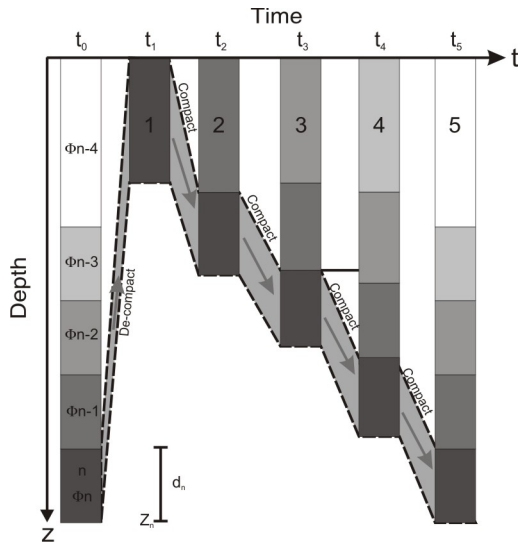


Figure 2: A conceptual sketch illustrating the backstripping procedure. Stepwise loading comprising progressive compaction beginning with decompaction of the lowermost unit (1) after removing the overburden (2-5). This is followed by a stepwise burial (compaction) in time steps (t_1 - t_5), determined by flooding surfaces, of each unit and subsequent reduction in porosity following calculated porosity-depth-trends for each interpreted lithofacies within each unit (modified from Bond and Kominz, 1984). t_0 corresponds to the present day scenario.

faces, such as sequence boundaries and flooding surfaces, are the ground pillar of backstripping. If available, high-resolution, biostratigraphic and/or chronostratigraphic markers are excellent surface markers to be applied in a backstripping reconstruction of a sedimentary basin. A study done by Morris et al. (2003) on interpreted sequence stratigraphy based on megaspore assemblages within the Åre Fm. in the Heidrun Field shows potential and could have been added and tested in our study. A simple model, where decompaction is a mechanical, non-reversible process, is here assumed, despite the results of Hammer et al. (2009) indicating some alteration of the grains due to diagenesis. These effects are however accordingly accounted for where they effect the compactability of the lithofacies class (see below). In a mechanical decompaction process initial porosity and compaction gradients for each lithology are necessary input data and discussed in turn below. We "restore" all the stratigraphic units in a sequence for each time step - decompacting the younger units and compacting the older ones. The calculations of the new depths for each step for each

unit can be expressed as:

$$Z_n = \sum_{i=1}^n d_i \quad (1)$$

where

$$d_i = d_n \left[\frac{\phi_i + S}{\phi_n + S} \right] \quad (2)$$

and

$$\phi_i = k + (\phi_0 + k)e^{-CZ_i} \quad (3)$$

Z_n is the calculated burial depth of the n 'th layer, d_n is the thickness of the n 'th layer at depth Z_n . ϕ_0 , ϕ_n and ϕ_i are initial porosity, primary porosity and porosity at depth Z_i , respectively. As shown in Fig. 3 secondary porosity, if present, must be subtracted from the porosity measurements. S is the solid grain fraction and is calculated by $s = 1 - \phi_0$ for each lithofacies class. ϕ_n is derived from compaction curves calculated for each lithofacies expressed by Eq.3 (Sclater and Christie, 1980) and are discussed in more detail below. C is a lithology-dependent constant calculated for each lithofacies class using Eq.3 with present burial depth, present burial porosities and initial porosities as input values. If no porosity data is available from the reservoir, C can, according to Ramm (1992), be estimated from least-square regression methods or, according to Wood (1989), be approximated from estimates of the initial porosity (ϕ_0) and the depth to half-porosity, $Z_{1/2}$. k is a correction constant for coal and equals 0.15 which is the lower limit for coal compaction. For other lithofacies classes $k = 0$. This correction is due to the rapid porosity decrease in coal where the thickness of coal (d_{coal}) would approach zero for relatively shallow burial depths (~ 100 m). The stepwise reconstruction of sedimentary units to the time of interest in the presented model is based on the reduction of porosity with burial depth. Numerous authors have published porosity-depth-curves for siliciclastic sediments (e.g. Athy, 1930; Baldwin and Butler, 1985; Gluyas and Cade, 1997; Hedberg, 1936; Houseknecht, 1987; Mondol et al., 2007; Paxton et al., 2002; Sclater and Christie, 1980; Velde, 1996; Wilson and McBride, 1988). Depth is, however, a poor indicator for compaction (Schmoker and Gautier, 1988), but acceptable for sediments not subjected to overpressure or to extensive chemical diagenesis. Normally pressured sediments, unaffected by diagenetic effects such as cementation and dissolution, display an exponential decrease

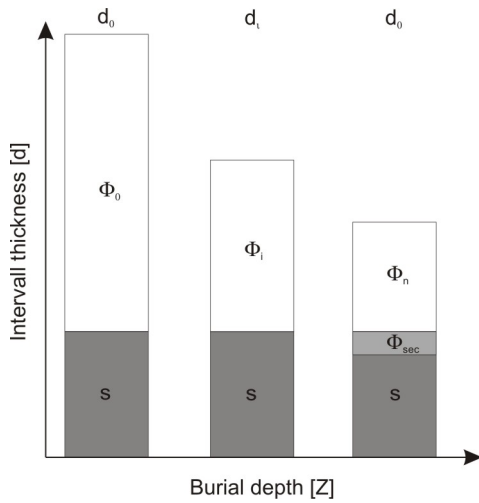


Figure 3: Sketch illustrating the interval thickness change (d) related to porosity changes with burial. Secondary porosity is not related to the mechanical reduction of pore-space and must be quantified and corrected for.

in porosity vs depth (Sclater and Christie, 1980). This relationship, first presented by Athy (1930), has later been modified by accounting for effective stress, time and temperature (Bjørlykke et al., 1989; Ramm and Bjørlykke, 1994; Schneider et al., 1996; Walderhaug, 1996; Walderhaug et al., 2001) assessing the effect of mechanical and chemical compaction. In the present case of the Åre Fm. in the Heidrun area with a burial depth of no more than $\sim 3000\text{m}$ and with most rapid burial during the last 3 million years (Ottesen, 2006), pure mechanical compaction is assumed, discarding the effect of chemical compactional processes. According to Hammer et al. (2009) diagenesis within the Åre Fm. in the Heidrun Field occurred locally during initial and late stages of burial. Early diagenesis resulted in variable dissolution of feldspar and mica grains from meteoric leaching in fluvial channel (FCH) or sandy bay fill (SBF) facies associations, and local early siderite precipitation in muddy bay fill (MBF) facies association. The leaching of labile grains amounts in some places up to 10% porosity units, with fluvial sandstones (FCH) being more affected than the marginal marine facies (SBF). Eogenetic siderite cement was found to represent on average 10% of the bulk volume of MBF sediments, although only a few samples are recorded from this facies association. These effects are eogenetic in origin, however, they are not considered to have influenced significantly on differential burial com-

paction, although it has local influence on porosity. Any effect of differential compaction would decrease in magnitude as the difference in compactability between SBF and MBF decrease. Secondary porosity may be accounted for by subtracting average values of secondary porosity from modal analysis, for the FCH and SBF sediments, respectively. For cemented layers the average volume fraction of cement is added to the average measured porosity e.g. in the MBF deposits. In many cases modification of porosity-depth trends are performed by replacing depth with effective stress that accounts for the effect of overpressure (e.g. Ungerer et al., 1990) and corrections using intergranular volume (IGV) values (e.g. Lander and Walderhaug, 1999). The use of IGV values from the sandstones of the Åre Fm. is disfavoured by the variable replacement of framework grains in cases of cementation (c.f. Hammer et al., 2009). In the fine-grained sediments, however, approximately 10% cement is corrected for in the MBF deposits. Regarding overpressure, minor pressure gradients have been identified across some flooding surfaces in the Heidrun Field, but probably not sufficient to contribute significantly to preservation of porosity.

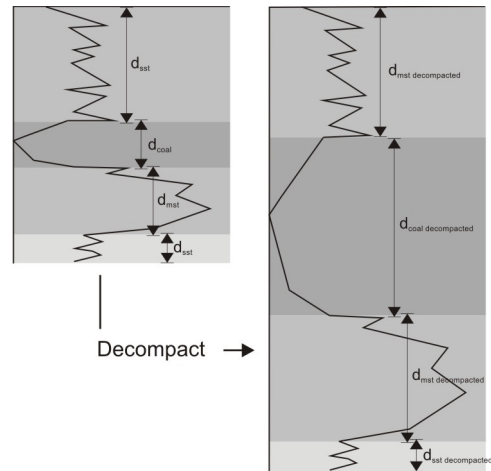


Figure 4: A conceptual sketch illustrating the principles of signal stretching. The sample interval is increased in relation to the added porosity due to decompaction whereas the sample value is retained.

4. Interactive, sample based model

The presented model is sample based, i.e. the backstripping calculation is performed for each sample in the database (15cm interval). In the

present study a sample is defined as the petrophysical sample recorded at 15cm intervals which have been manually interpreted and classified according to ten identified lithofacies classes for all the seven analyzed wells. This allows us to create an interactive dataset, where surfaces can be picked at any desired sample point and decompacted accordingly. This also allows us to tie the initial sample to petrophysical wireline log data values (gamma, density, neutron porosity etc.). These values are connected to the sample point through the backstripping procedure. As the length of the sample interval is modified according to the porosity variation vs depth function (Eq. 3), the wireline data remains constant for each sample. The signal signature is thereby stretched, but with measured values retained (Fig. 4). This method thereby allows for interpretation of decompacted depositional sequences between known surfaces and in uncored intervals. The backstripping modelling process is iterative and may be repeated using additional new identified surfaces as new backstripping surfaces.

5. Application

The applicability of our model has been tested on data from the Late Triassic - Early Jurassic Åre Fm. in the Heidrun Field, offshore Mid-Norway (Fig. 5). These sediments consist of heterogeneous, fluvial to lower delta plain (fluviodeltaic) deposits comprising fluvial and tidally influenced channel sands, floodplain fines, sandy and muddy bay fill deposits in addition to coal units. Some thin (~dm- to a few m) carbonate cemented intervals are also observed throughout the studied interval. The present study uses the Åre Fm. as a case study, as this has large reservoir sandstone correlation challenges. Having established an age model with correlation between wells based on a sequence stratigraphic framework (Leary et al., 2007; Thrana et al., 2009; Hammer, 2010), the thickness of the sediments up to surface level was reconstructed using the backstripping model (Eq. 1-3). Relative sea level changes and palaeobathymetric data have not been incorporated since the basin sediments are predominantly continental deposits.

5.1. Database

The primary data for the present study were obtained from petrophysical wireline logs; gamma ray (GR), density (RHOB) neutron density (NPHI)

sonic (DT) and resistivity (RT), as well as core sections from four wells (Wells II, III, IV and V) from the Heidrun Field. These data form the basis for facies interpretation and porosity vs depth calculations in addition to identifying suitable flooding surfaces used as backstripping horizons. Flooding surfaces are here considered to represent a relatively flat landscape making them excellent datums for sequential re-burial modelling. For the backstripping procedure in the present study, ten lithofacies classes are introduced (Table 1). These include five facies associations identified within the Åre Fm.; fluvial channel sand (FCH), floodplain fines (FF), tidally influenced distributary channel sand (TCH), sandy bay fill (SBF) and muddy bay fill (MBF), in addition to coal and coaly units (COAL). Cemented intervals are also classified, however, due to the limited amount and occurrence within sandy intervals, these are defined as FCH. Regarding the overburden (post-Åre Fm. deposits), the sediments have been classified as undifferentiated sandstone (Undiff.sst) or undifferentiated mudstone (Undiff.mst) using the parameters specified for FCH and FF, respectively. Fault zones, recognized in well I and V, are treated as incompressible rock ($\phi=0$) for the purpose of reconstructing the fault throws within the reservoir formation. Each identified fault is treated separately to take into account the respective throws. The calculation of faults is discussed further below.

5.2. Data preparation and input to decompaction calculations

As a prerequisite for facies interpretation on wireline logs, the continuous wireline logs first have to be segmented into discrete zones with similar properties (electrofacies (c.f. Serra and Abbott, 1982)) representing each of the identified lithofacies. These electrofacies constitute the elementary units of reference for inferring a correlation between wells and they are equivalent, but not identical to the lithofacies interpreted from core data. Log data are the result of indirect measurements of petrophysical responses to lithology, whereas lithofacies classification from cores are defined directly from the visible features of the rocks. Manual interpretation of facies from well logs and core data is a labor-intensive process that requires a considerable amount of time by an experienced log analyst (Doveton, 1994). For this reason, computerized numerical procedures have thus been introduced for pattern recognition in facies determination (Moline and Bahr, 1995; Bhatt

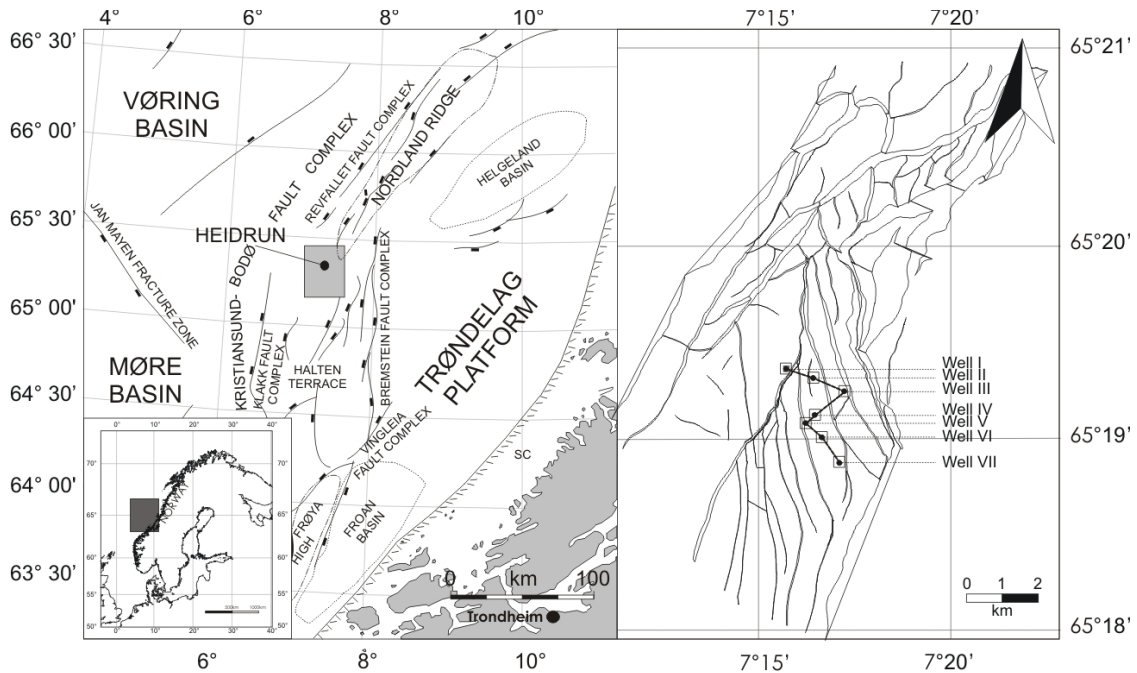


Figure 5: Left: The structural elements of the Mid-Norwegian continental shelf (modified from Gabrielsen et al. (1984); Koch and Heum (1995)) and the location of the Heidrun Field (shaded rectangle). Right: Top Åre reservoir structure (after Svella, 2001) and the location of studied wells and cross-section.

and Helle, 2002; Brandsegg et al., 2010). Facies interpretation from log data is influenced by rules that are difficult to represent by simple algorithms (e.g. tool variability, stratigraphic context, overlap of measurements, diagenetic effects etc.). For this reason, manual interpretation of combined log and core data is essential within the present study in order to achieve the necessary resolution in the model.

Scale dependent analysis of reservoir heterogeneity, spanning from micro- to meso scale (thin section to facies scale), utilizes the advantages of all approaches in determining a Representative Elements Scale (RES) for facies interpretation. RES is in this context applied as the 2D version of the 3D Representative Elementary Volume (REV) as first presented by Bear (1972). The REV notation is essential in the effective medium approximation, where a heterogeneous property field is replaced by a hypothetical homogeneous one (Nordahl and Ringrose, 2008). In the present study, RES is related to the ten interpreted lithofacies (meso) and their associated compactability (micro). RES is here the scale in which the property field is large enough to capture the representative amount of the heterogeneity (i.e. Bear, 1988). Meso- and micro-scale approaches

offer a more accurate representation, but requirements on computer resources (CPU-time) often become prohibitive for large-scale structures, such as reservoirs and basins.

5.3. Sandstone compaction (FCH, SBF, TCH, Undiff.sst)

The sandstones of the Åre Fm. are relatively loose and sometimes appear unconsolidated in core sections, despite a burial depth of up to 3000m. Average porosity values from plug data representing FCH, TCH and SBF are calculated to 29% (+/- 6%). Modal analysis reveal average secondary porosity amounting to 4% in FCH/TCH and 7% in SBF, although up to 10% secondary porosity (FCH) has been counted (Hammer et al., 2009). Hammer et al. (2009) concluded that only minor diagenesis has occurred in the sandstones, in most intervals limited to authigenic kaolinite precipitation due to meteoric flushing and subsequent feldspar dissolution, and eogenetic siderite cementation associated with thin (mm scale) mica and organic rich lamina. Massively carbonate cemented intervals occur in decimeter and up to a few meters thick zones in rare cases. However, these cemented intervals

Table 1: Calculated and measured values for the identified lithofacies classes included in the study

Lithofacies class	C-value	Initial porosity	Burial porosity (~ 2.5 km)
FCH/TCH/Undiff.sst	0.000188	40	25(29) ^a
SBF	0.000239	40	22(29) ^b
FF/Undiff.mst	0.000481	60	18
MBF	0.000232	50	28 ^c
COAL	0.001156	90	5
Fault	N/A	0	0
Seawater	N/A	100	100

^a4% average secondary porosity^b7% average secondary porosity^c10% average cement

are thought to have little influence on the calculations due to the limited occurrence and the timing as late diagenetic precipitation (Hammer et al., 2009). Backstripping procedures are dependent on the initial values of porosity for each identified lithofacies class to be able to calculate porosity reduction during burial. Variation in porosity is a function of sorting, grain shape, and depositional processes. Many authors have published porosity data on freshly deposited sands (c.f. Table 1 in Atkins and McBride, 1992), from field measurements on sands deposited in river pointbars, beaches and eolian dunes, and from sands deposited in laboratory experiments. These studies display average porosity values ranging from 39-49% for pointbars, 41-47% for beaches, 39-51% for eolian dunes, and 37-45% for laboratory experiments (Atkins and McBride, 1992). Based on these data 40% initial porosity is usually assumed for moderately to well sorted sandstones (e.g. Houseknecht, 1987; Wilson and McBride, 1988), however Ehrenberg (1989) argued that their value of 40% is an unnecessary oversimplification based on the correlation between the decrease in sorting and initial porosity as demonstrated by Beard and Weyl (1973). Nevertheless, in this study 40% initial porosity is applied for the moderately to well sorted Åre Fm. reservoir sandstones.

5.4. Fine-grained sediment compaction (FF, MBF, Undiff.mst)

Concerning argillaceous sediments, a wide range of porosity-depth trends are published in Mondol et al. (2007). Sediments comparable to the muddy siltstones of the Åre Fm. at burial depth porosities similar to reservoir depth display values of about 18% and average initial porosity values of

$\sim 60\%$. Some of these authors present initial porosities lower than 60%, which is explained by the presence of sand that reduces initial porosities. The siltstones in the fluvial part of the Åre Fm. (FF) are observed to be relatively free of sand, whereas the sediments comprising MBF deposits are more heterogeneous including both more muddy and more sandy successions. The MBF are also found to be more preferable for eogenetic siderite cementation, amounting up to 10% in some samples (Hammer et al., 2009). Initial porosity is here set at 60% for FF, whereas MBF is defined lower ($\sim 50\%$) and with more preserved burial porosity ($\sim 28\%$) due to the early stage siderite cements compared to FF (18%).

5.5. Coal compaction

Peat-to-coal ratios are defined as the ratio of thickness before compaction to thickness after compaction (e.g. Ryer and Lange, 1980). Based on a comparison between the thickness of vertical aggraded channel fills and the underlying peat deposit, a peat-to-coal ratio of 6:1 (i.e. a 83,3% volume reduction) is applied for the coals in the Åre Fm. The coals of the Åre Fm. are interpreted as high volatile bituminous coals (TOCs varying from 20% to 50% in the true coals) (Leith, T.L. pers.comm. 2009), which are reported to have a porosity of $\sim 5\%$ (Rodrigues and Lemos de Sousa, 2002). The peat-to-coal ratio and a present burial porosity of 5% reveals an initial porosity value of 90% when assuming predominantly mechanical compaction has taken place during burial. This peat-to-coal ratio has been calculated by assuming that peat compaction created the accumulation space for the channel sand. This has previously been proposed by Rajchl and Ulicný (2005) for the

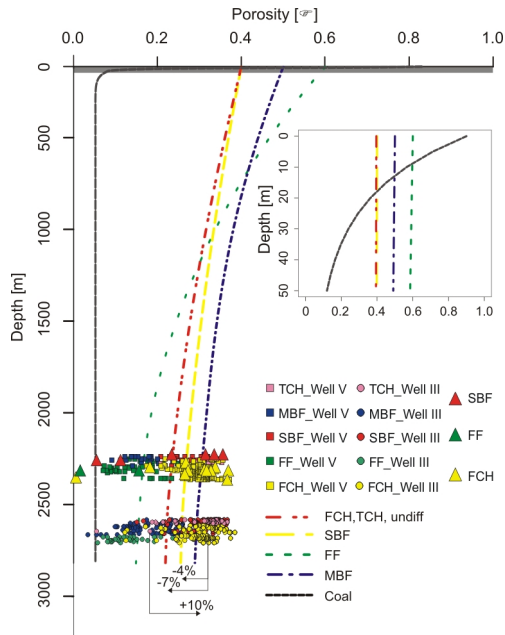


Figure 6: Compaction curves calculated for each of the main interpreted lithofacies. The calculations are based on initial and burial porosities from published and measured (plug and modal analyses) data, respectively. Note that burial porosities for curve calculations have been corrected for diagenetic effects and therefore do not match the measured porosities directly. Plug porosities from Well III and V are plotted in small symbols, porosity from modal analyses from well V are plotted in large symbols. Inset figure displays compaction trends of the first 50m of burial. At present the Åre Fm. in the Heidrun Field is interpreted to be at maximum burial depth between 2200-2900m. See Fig.5 for location of wells III and V.

Neogene, Most Basin, Czech Republic. Using the decompacted thickness of the sand as a measure for the original peat thickness and comparing this result to the present thickness of the coal provides an initial peat-to-coal ratio. This can, however, lead to an overestimation of the ratio based on the fact that the channel can and may have eroded parts of the underlying peat. The coal zone also displays a large variability in composition, from mudprone organic rich intervals to pure coals, and this must be taken into consideration when relating the decompacted thickness of the coal to the decompacted thickness of the sand. Concerning the timing of peat-to-coal compaction, a large part of the volume reduction is thought to occur shortly after burial, i.e. within the first meters or tens of meters of burial (Nadon, 1998) as indicated from Eq. 3 for low C-values. Based on these observations, compaction of peat is in this study represented by an

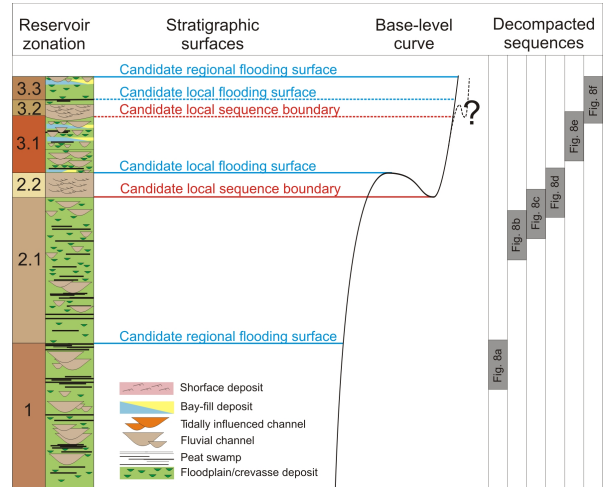


Figure 7: Statoil's revised reservoir zonation scheme modified from (Thrana et al., 2009). Interpreted flooding surfaces used in the present study as backstripping horizons as well as base-level changes interpreted for the selected Åre interval are displayed. Stippled lines indicates local (field-wide) surfaces, whereas continuous lines are correlatable in a larger area, i.e. to neighbouring fields. Interval coverage of presented decompacted sequences (c.f. Figs. 8 a to h) are displayed on the right.

exponential decrease of porosity down to a cut-off value of about 5% related to the peat-to-coal-ratio of 6:1. In the following sections the coals are termed peat where they are discussed in the context of decompacted deposits and coals for compacted intervals. Porosity-depth-curves for different lithology composition are presented in Fig. 6.

6. Interpretation of a decompacted reservoir

In this section a modified sequence stratigraphic interpretation, as compared to the model presented by Thrana et al. (2009) of the Åre Fm., is suggested based on correlations of six decompacted reservoir cross-sections (Fig. 8a-f), corresponding to time steps selected at known correlatable surfaces (flooding surfaces). The reconstructed units are presented in 50m thick interpreted decompacted sections representing the upper part of the decompacted sequence. The stretched wireline log data are also shown for inter-well comparison of gamma ray (GR) and neutron-density (NPHI-RHOB) log signatures. Interpretation on decompacted reservoir architecture reveals additional (inter-zonal) correlations of lithofacies, which are not part of the current sequence stratigraphic model enabling a re-

finned sequence stratigraphy of the Åre Fm., Heidrun Field.

6.1. The Åre Fm. reservoir zonation

The Åre Fm. is about 300-500m thick and has been subdivided into seven reservoir zones (Fig.7). The present study focuses on the lower fluvial dominated/fluvial influenced part of the stratigraphy, i.e. Åre 1 to Åre 3. This interval contains abundant, highly compactable sediments (FF and coals) which are thought to have influenced reservoir architecture significantly during burial due to differential compaction. Åre 1-2.2 are interpreted as entirely fluvial deposits comprising fluvial channel sands, flood plain fines and crevasses. Åre 3 is a transition zone from fluvial to deltaic environment, including sediments deposited in distributary delta channels and interdistributary bay areas. The studied interval is terminated by a regionally interpreted flooding event at top Åre 3.3.

6.2. Åre 1 and 2

Wells I, II, III, V and VI penetrate into the Åre 2.1 interval, whereas wells I, III and V also penetrate into Åre 1.

Due to the heterogeneous nature of the Åre 1-2.1 reservoir zones, correlation of channel sandstone bodies is difficult on wireline log data. However, one coal zone has been mapped on seismic and correlated in all the wells penetrating this lower Åre interval, representing the top Åre 1 coal marker. The zone ranges from a >15m relatively pure peat deposit overlying a >20m interbedded sequence of FF and peat in Well I, to a thick unit (several 10s of meters) of interbedded mudstones and peats, including a thin FCH sand deposit, in Well III (Fig. 8(a)). In Well V the sequence is dominated by ~10m peats and thicker fluvial sandstones. By applying this flooding surface in our model, a lower channel feature appears as correlatable between wells.

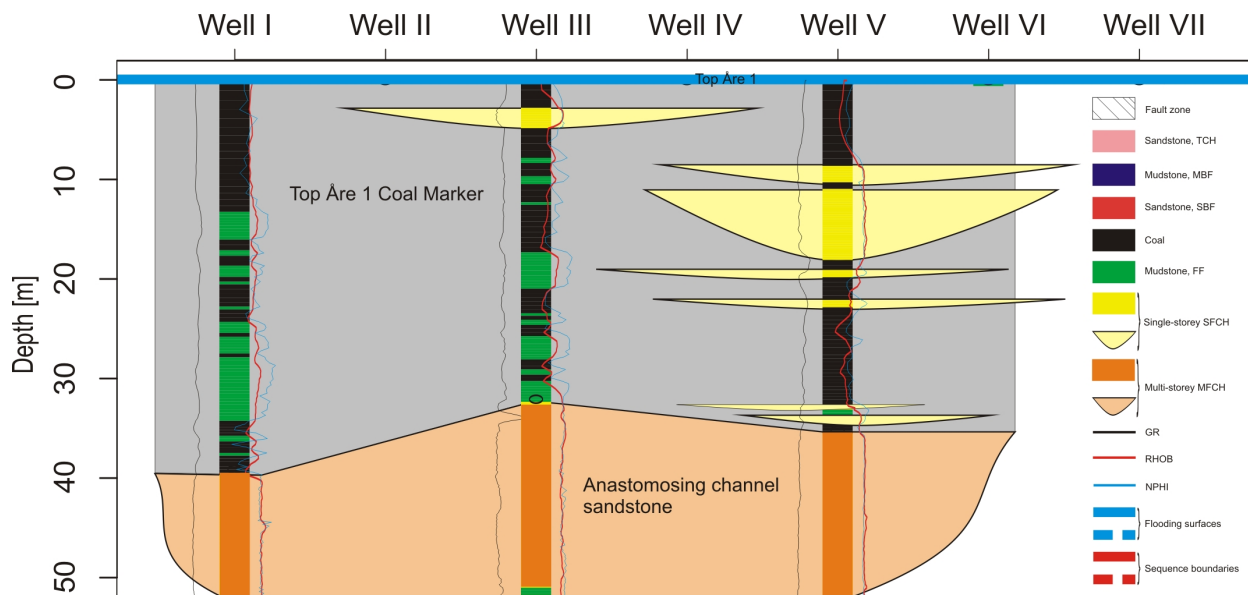
The sandstones comprise up to ~30m thick, vertical aggraded, fluvial channel sandstones underlain by a thick coal rich unit (Fig. 9). Svela (2001) interpreted these channel sandstone deposits as incised valley fill, suggesting a relative sea level fall prior to or during deposition. However, based on the presence of these thick underlying peat deposits, a factor of compaction controlling sand deposition must have occurred and that autogenic rather than allogenic factors dominated during the deposition at this time. These peats, when compacted, created

accommodation space for the channel sands to be deposited (i.e. Rajchl and Ulicný, 2005), i.e. autogenic controlled channel sand deposition, promoting vertical accretion in an anastomosing channel environment.

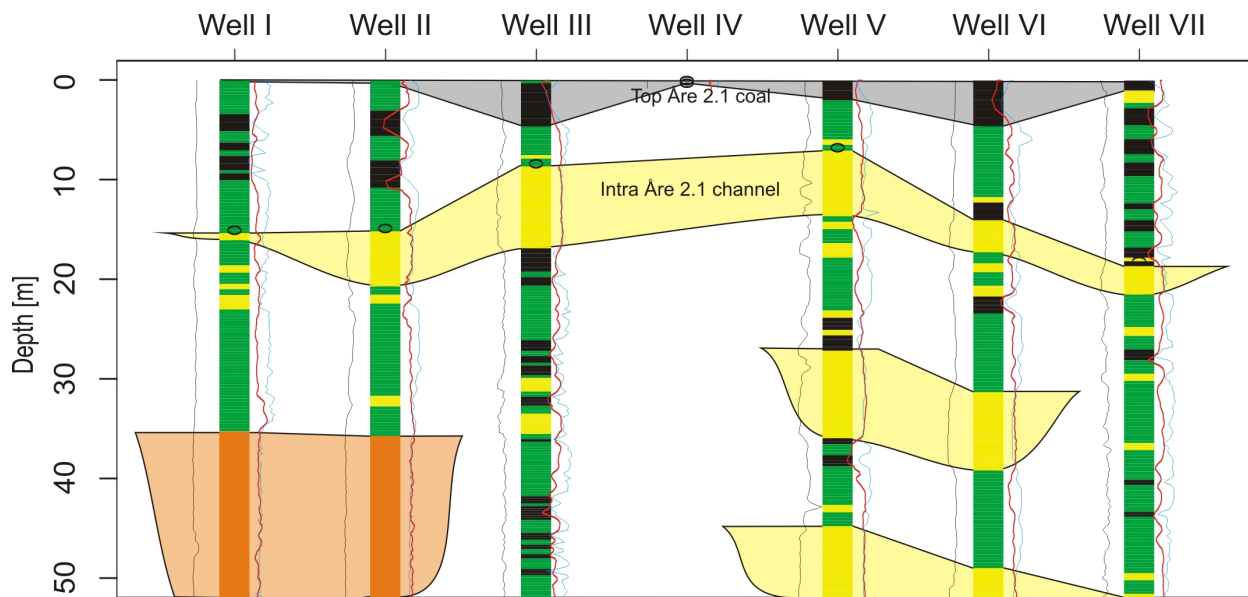
Above the Åre 1, sedimentation changes from the thick, multi-storey channel sandstones, to deposition dominated by single storey channels. An increase in correlatable channel sandstones is observed from the decompacted cross-section in Figs. 8(b) and 8(c), although the thickness of the sandstones are observed to decrease. The cause for this change in sandstone geometry may be related to the base level fall interpreted for the overlying Åre 2.2 incised valley (see below). If a base level fall occurred at that time, then the underlying top Åre 2.1 sediments may represent late highstand deposition which would explain the presence of increased abundance of laterally extensive channel sandstones.

A zone rich in peat deposits occurs in the uppermost part of Åre 2.1, which is correlated in the studied wells. The zone is in a way similar, although thinner, compared to the coal zone occurring in Åre 1 (i.e. Fig. 8(c)). This could suggest that this zone represents a short period of increased base level rise and may therefore be interpreted as a local flooding surface. However, the zone is hard to correlate, especially in the bounding wells (well I and VII) and therefore not added as a flooding surface in Fig 7. Applying this surface as a backstripping surface reveals a possible correlation of three single storey channel sandstone bodies (i.e. well Fig. 8(b)) of which the uppermost unit is correlated across the entire cross-section. These correlatable units are not part of the Thrana et al. (2009) sequence stratigraphic model for the Åre Fm. We do not conclude that these horizons are true sequence stratigraphic surfaces, on the contrary, they are probably not. Nevertheless, they correspond to, at least local, base level variations and their associated reservoir sandstones show potential as possible reservoir flow units if they are correlatable.

In the uppermost part of the Åre 2, a new significant channel feature appears, representing laterally and vertically amalgamated braided river deposits corresponding to the Åre 2.2 reservoir zone (i.e Fig. 8(c)). The unit is up to 15m thick in the studied wells and comprises individual channel sands on average 2-8m thick. This feature has been interpreted as an incised valley fill by Svela (2001); Leary et al. (2007); Thrana et al. (2009) suggesting a base level fall during/prior to deposition. A

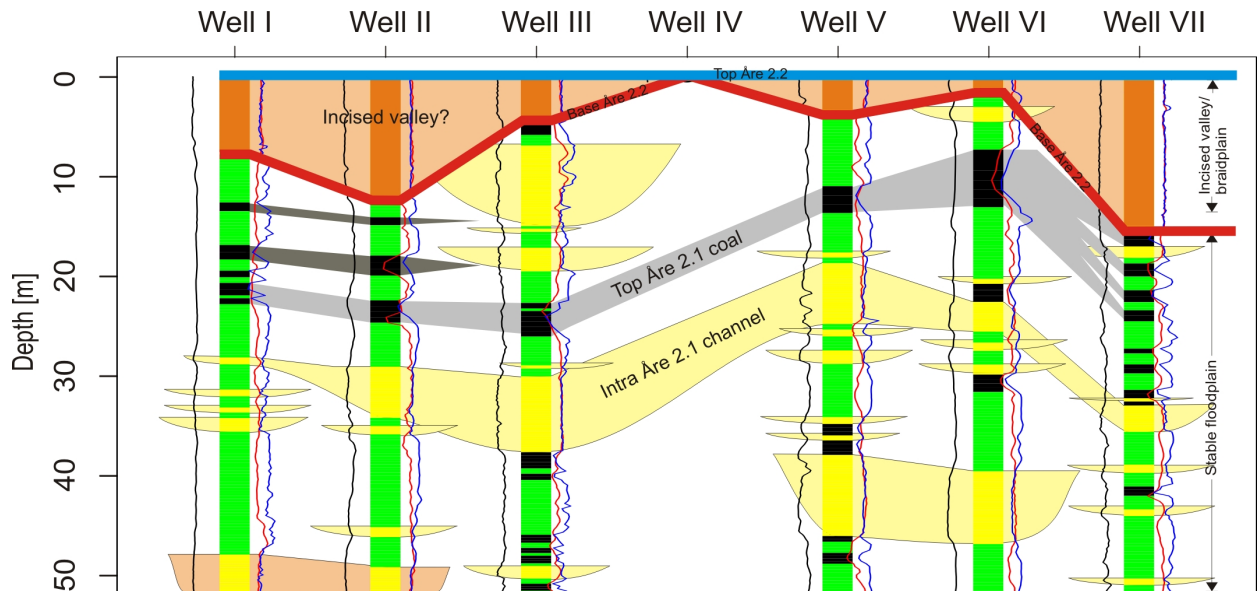


(a) Cross-section 1 comprising the Top Åre 1 Coal Marker. A correlation of MFCH deposits in wells I, III and V is suggested. The cross-section is interpreted as parallel to palaeoflow direction (south east) as these sandstones are suggested to represent anastomosing channel deposits indicating limited channel widths. See Fig. 5 for well locations.

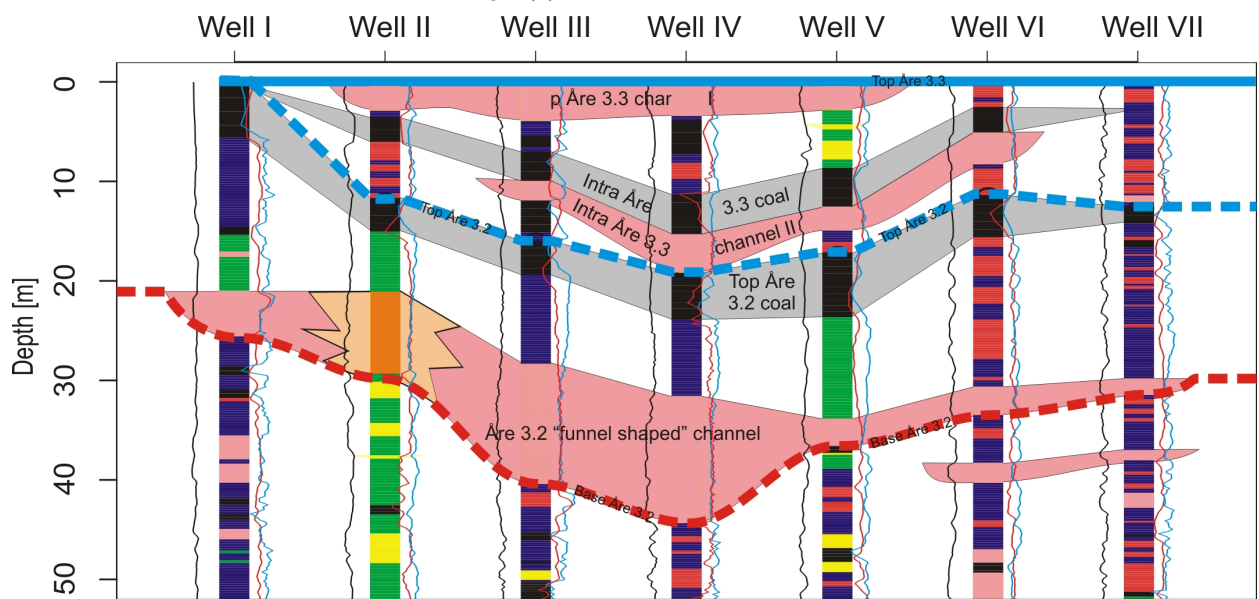


(b) Cross-section 2 showing 50m decompacted reservoir underlying the top Åre 2.1 coal. Three possible correlatable FCH sandstones and one correlated anastomosing FCH sandstone are suggested. In particular the uppermost channel sandstone (Intra Åre 2.1 channel) seems to have a lateral continuity extending all six wells penetrating this interval.

Figure 8: continued

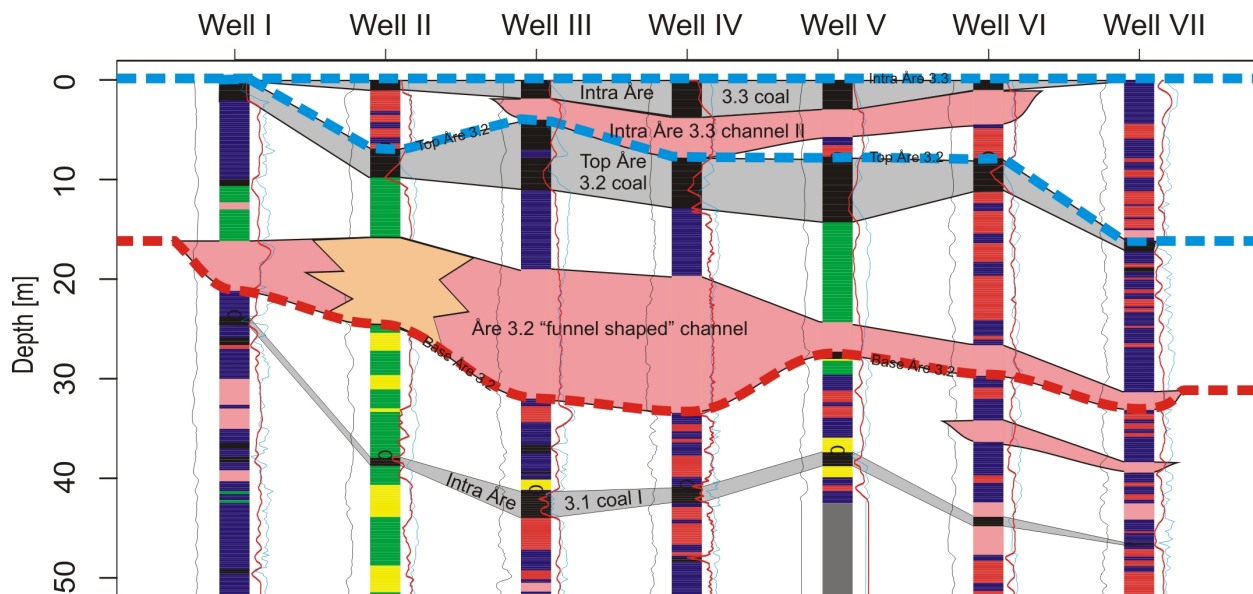


(c) Cross-section 3 showing 50m decompacted reservoir underlying the top Åre 2.2 incised valley fill. The valley fill displays large thickness variations across the studied area (total and partly faulted out in wells IV and V, respectively)). Underlying this channel are the correlatable units discussed in Fig. 8(b).

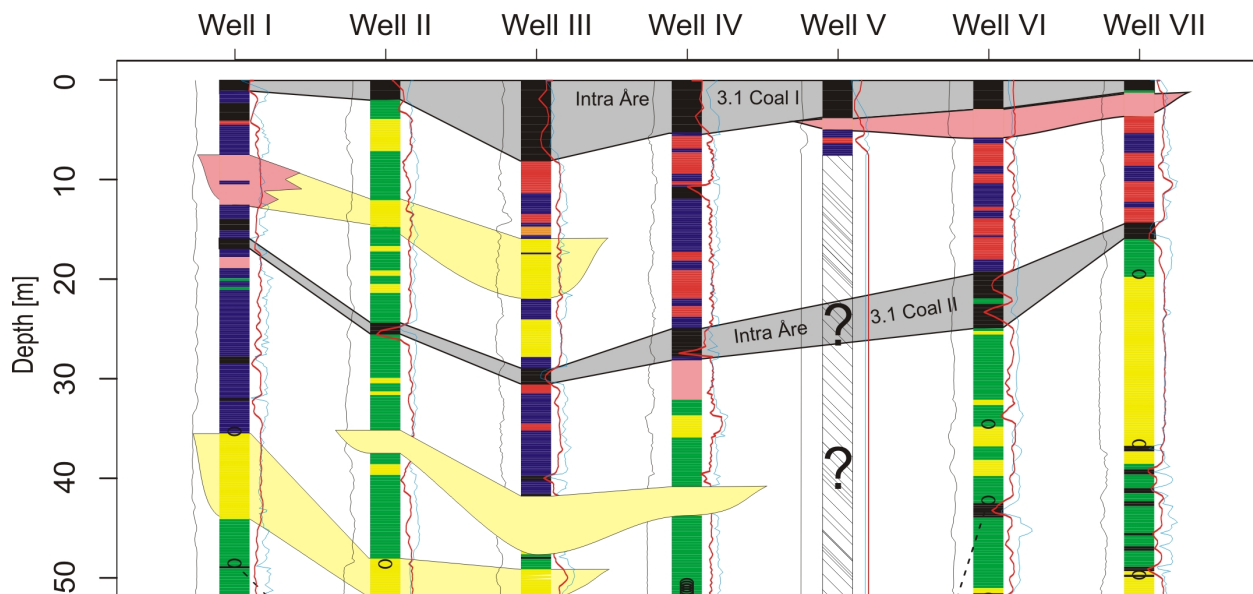


(d) Cross-section 4 showing 50m section of decompacted reservoir underlying the top Åre 3.3 flooding surface. The section suggest five correlatable units; Åre 3.2 "funnel shaped" channel sand, Intra- and top Åre 3.3 channel sandstones top Åre 3.2 coal and intra Åre 3.3 coal. See text for discussion.

Figure 8: continued



(e) Cross-section 5 showing 50m decompactified reservoir underlying the intra Åre 3.3 coal. A possible correlatable coal is suggested in the lower part of the cross-section; intra Åre 3.1 coal.



(f) Cross-section 6 showing 50m decompactified reservoir underlying the intra Åre 3.1 coal suggests several correlatable channel sandstones in addition to intra Åre 3.1 coal II approximately 20 m below the intra Åre 3.1 coal I.

Figure 8: Reconstructed cross-sections of 50m decompactified intervals from Wells I-VII. Key sedimentary units are interpreted. See Fig. 8(a) for legend and Fig. 5 for location of wells.

sequence boundary is therefore interpreted at the channel base. As the valley filled with sediments, the constraint on the river by the valley topography was suspended, enabling channel accretions onto the interfluvial, consequently significantly decreasing the channel width to floodplain width ratio. The rate of base-level increased, changing the controlling factors from predominantly allogenic to autogenic and, thus river style. The upper boundary of this unit is therefore interpreted as a flooding surface, marking a level of change in fluvial style in the sediments, from braided back to single story, meandering type deposits.

6.3. Åre 3

The unit comprises sediments dominated by floodplain fines and single storey channel sands (some showing evidence of tidal influence) and bay fill deposits including both SBF and MBF. Marine influence, represented by SBF, MBF and TCH deposits, increase upwards. A tendency of more abundant and thicker fluvially derived sediments is observed in the central parts of the cross-section (Figs. 8(d) and 9), within zones Åre 3.2 to 3.3. Tidal influence increases upwards in the Åre 3 stratigraphy and towards the southeast, possibly indicating a retrogradational palaeocoastline in the southeast as earlier proposed.

A significant channel feature, up to ~20m thick, with a distinctive fining-upwards profile ("funnel shaped" on combined neutron porosity (NPHI)-density (RHOB) logs) capped with coal, is striking within this interval and is correlatable in all the studied wells. This channel thins towards the southeast and northwest. In areas where the main channel sandstone is thin (only a few m) as in Wells I, V, VI and VII, the channel termination phase is observed to comprise more abundant ~m scale sandstone units (crevasse channel) deposits. This could indicate that the palaeo channel developed along preferred courses, represented by the thicker channel sandstone units, such as in wells II, III and IV, and that the sand rich termination phase above represents an area close to these main channels, which are subjected to steady influx of crevasse sands during floods. This may also be suggested for the Top and Intra Åre 3.3 channel, although thinner as compared to the Åre 3.2 unit. In addition, the laterally correlatable coals representing Top Åre 3.2 and Intra Åre 3.3 appear thicker in the central parts of the cross-section which may suggest that the coals controlled the preferred course of the

channels and subsequent channel sand deposition. The Åre 3.2 channel succession is always capped by coal in the studied wells which is interpreted to represent a local flooding surface.

Below this channel another coal interval appears and may possibly represent a local (not necessarily field-wide) flooding surface, probably originating from autogenic delta lobe switching (e.g. Emery and Myers, 1996). Using this surface as datum enables correlation of a third coal interval and two suggested correlatable channel sandstones (Fig. 8(e) and 8(f)). Although these correlations are uncertain, the stacking pattern reveals a reservoir architecture dominated by single storey channel deposits where some might be correlatable between wells. The upper boundary of Åre 3.2 is represented by up to a few m thick peat (now coal) deposits. This unit has been identified and correlated in central parts of the Heidrun Field (i.e. Fig. 8(d)) and is here interpreted as a local candidate flooding surface .

The central parts of the Åre 3.3 unit are sandier compared to the marginal parts, comprising relatively thin, possibly laterally extensive, single storey fluvial channel sands (i.e. Fig. 8(d), 8(e) and 8(f)). A peat interval a few meters thick occurring in the middle part of the unit appears similar to the top Åre 3.2 coal and thinning towards the southeast. The lobate shape of this Åre 3.3 succession, as seen in cross-section, is somewhat distorted by a fault in well I (not seen on cross-section). Nevertheless, a depositional environment controlled by delta lobe switching is suggested as the main controlling factor during deposition, based on the geometries and stacking pattern of the facies associations, where compaction of peat to coal may have played an important part.

Compared to fluvially originated peat swamps, coals deposited in interdistributary bays are thought to have a greater lateral distribution. These coals may have extended the total width of the bay, suggested by Kjærefjord (1999) to be 2-7 km wide in the Heidrun field, which is sufficient for good well-to-well correlatability with the current well spacing (<~1 km). A regionally correlatable, well defined bay fill succession defines the upper boundary of this unit and is interpreted as a candidate flooding surface by Leary et al. (2007). It has a distinct signature on wireline logs and is correlatable throughout the Heidrun field.

The Åre 3 reservoir zone shows sediments deposited in a transgressive environment as fluvial de-

posits below are gradually replaced by marine influenced bay fills and distributary channel sandstones. The unit is relatively heterogeneous, dominated by thin beds of sand, silt and coal interpreted to be deposited in the transition zone between a fluvial and marine influenced delta plain environment, including fluvial channel sands, crevasses, lacustrine muds, paleosols and bay fill sediments.

A reservoir architecture interpretation of the Åre 1 to Åre 3 based on published and identified correlatable surfaces from this study is presented in Fig. 9.

7. Discussion

As noted previously, backstripping, *sensu sticto*, is traditionally applied for basin reconstruction and therefore not directly applicable to reservoir scale reconstruction. Presented here is a reservoir reconstruction taking into account effects of differential compaction on intra-reservoir scale. Estimation of decompacted reservoir lithofacies classes using the backstripping approach on high resolution petrophysical data and interpreted flooding surfaces has shown to increase the correlatability of heterogeneous reservoirs by considering and removing the effect of differential compaction. This is in particular the case where highly compactable sediments, such as coals and muds, are present, such as in the lower Åre Fm in the Heidrun Field.

The presented model suggest several correlations of depositional units between known correlatable surfaces. No proof of actual connectivity exists, such as by pressure support indications etc. However, as the palaeo flow direction is fairly certain, indicating channel orientation towards the southeast, in addition to relatively closed spaced wells (<~1km apart)(i.e. Fig. 5), correlations performed on decompacted reservoir architecture seems fairly valid, especially for the upper most part (<50m) of decompacted cross-sections.

Improvements regarding reservoir unit correlations are suggested within Åre 1, 2.1 and 3 reservoir zones. Especially for Åre 3, several additional interpreted horizons are identified, which enable a refined interpretation of the depositional environment for this reservoir zone compared to the interpretation of Thrana et al. (2009).

As discussed earlier, a relationship between channel sand deposition and compaction of peat-to-coal is suggested for some of the vertically aggraded

channel sandstone successions. This is exemplified by the significant channel features in Åre 1, occurring in wells I, III and V, interpreted to represent anastomosing channel deposits. Anastomosing rivers comprise relatively narrow features with a low width-to-depth ratio (c.f. Nadon, 1994). With a well spacing of up to a kilometer apart, a correlation of the Åre 1 channel sandstone suggests that the cross-section is oriented along the palaeoflow direction, i.e. towards the southeast. This is supported by provenance studies of Early Jurassic rocks in the Heidrun Field, where Morton et al. (2009) found that the fluvial parts of Åre have been sourced from a westerly source area. In addition, Thrana et al. (2009) also concluded with a southeastern palaeoflow direction based on lateral facies shifts within the Åre 1-2.1 zones.

The intra Åre 2.1 channel sandstone (i.e. 8(c)) is suggested correlatable in all the studied wells. However, as the shape of the unit (in cross-section) seems to follow the base of the Åre 2.2 incised valley fill, one could argue that if the Åre 2.2 is truly an incised valley, less correlation between the shapes of the underlying 2.1 channel compared to the base of the valley should be expected. This is, on the other hand, no evidence of either one or the other because the thickness of the Åre 2.2 in the studied wells are small (up to ~10 m) and no conclusion is made.

As suggested from the decompacted sections in Figs. 8(d), 8(e) and 8(f) an autogenic signature due to delta lobe switching is revealed within the Åre 3.3 reservoir zone. The lateral distribution and vertical stacking of facies associations within this zone suggests delta lobe switching was active in the study area during deposition. The thickening of the reservoir units towards the center of the cross-sections and thinning towards the southeast seems to correlate well with the thickness of the top Åre 3.2 and intra Åre 3.3 coals. A relationship is therefore suggested between compaction of peat and deposition of sand. In addition, as the Åre 3.2 funnel-shaped channel also follow this trend of thickening towards the central parts of the cross-section, the weight of this sand may have created a focus point for subsidence in this area, evidently resulting in the peat distribution seen above.

The correlatable channel sandstones corresponding to intra and top Åre 3.3 may comprise the proximal part of individual prograding delta lobes, whereas the coals represents abandonment. As seen from the cross-sections a possible lateral shift to-

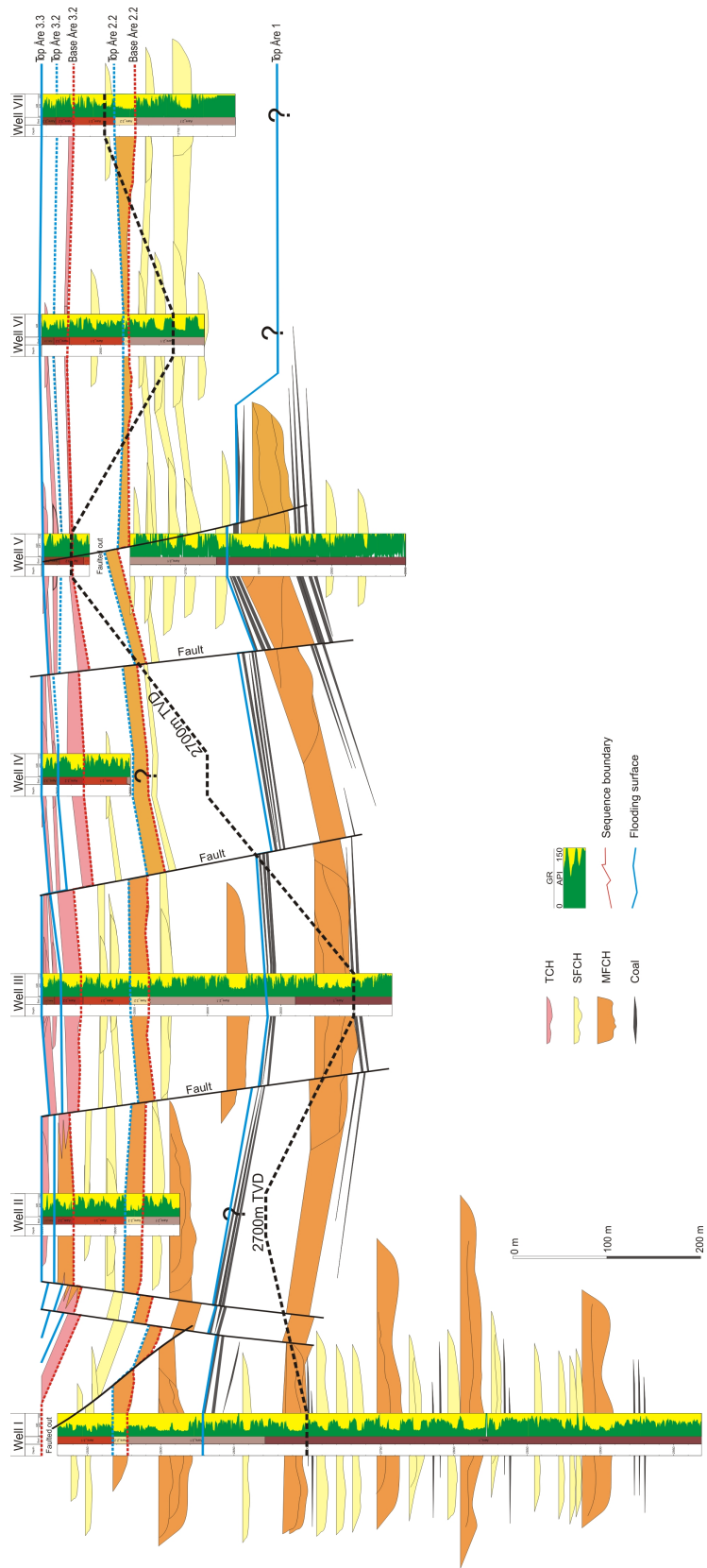


Figure 9: Interpreted cross-section of the seven studied wells displaying suggestive correlatable units within the studied Aie interval (Aie 1-3.3). Newly available correlatable units enable identification of correlatable channel sandstone units within top Aie 1, Top 2.1, Intra Aie 3.3 and top Aie 3.3, in addition to several coal zones (See Figs. 8(a) to 8(f)).

wards the northwest of the main delta depocenter is inferred by the more westerly oriented top Åre 3.3 channel compared to the intra Åre 3.3 channel where the underlying top Åre 3.2 and intra Åre 3.3 coals controlled the preferred course of the channels and subsequent channel sand deposition.

The effect of differential compaction on correlatability is accounted for by correcting for the compactability of interpreted lithofacies classes by differential decompaction and by applying flooding surfaces as backstripping surfaces in a sequence stratigraphic backstripping exercise.

The methodology was successfully tested on the fluviodeltaic Åre Fm. in the Heidrun Field, where several new correlatable channel sandstones within the Åre Fm. are recognized. These correlations would be important for reservoir property modelling and drainage strategies, especially for the studied central area of the Heidrun Field.

In addition to magnitude, timing of compaction is equally important, especially for coal rich fluvial deposits as the bulk of volume reduction in peat deposits occurs in the earliest phases of burial (first few meters) (Nadon, 1998). As observed in the Åre Fm. fluvial succession, several types of fluvial channel deposits occur. Single storey channel sands dominate of which some are correlatable between wells. Anastomosing channel sands are present in the lowermost unit and occur regularly above thick peat deposits (e.g. Fig. 8(a)). The presence of the underlying peat, in addition to the lower lateral extent of these units as compared to the upper Åre 2.2 sand, suggests that these sands are vertical accreted channel deposits where the compaction of peat created the accommodation for sand deposition. The unit Åre 2.2 sand, on the other hand, is regional, laterally correlatable over a 2km distance within the study area and varies in thickness from 3-34m, with a typical thickness of 10-15m. The unit is thinning towards the southeast and west with greatest thickness in the northwest. However, in some wells (i.e. Well V) the unit is missing due to normal faulting related to consecutive divergent tectonic activity in the study area (c.f. Fig. 5).

Due to tectonic activity, several faults have been interpreted in the studied wells, represented by missing sections in cross-section with length equal to the interpreted missing sediment thickness (compacted). The unit thicknesses in the reconstructed reservoir seem fairly uniform in un-faulted parts, increasing in thickness where faults are present. Keeping in mind that the cross-section represents

partly decompacted sediments and that the thickening due to fault reconstruction would increase further during burial, leads us to imply an overestimation of the fault throws in the Åre Fm. This overestimation may be as much as 20m in the largest faults which is a significant amount, especially when vertical thicknesses of the reservoir sands in the fluvial part of the Åre Fm. usually are below this value. The basis for calculation of compactabil-

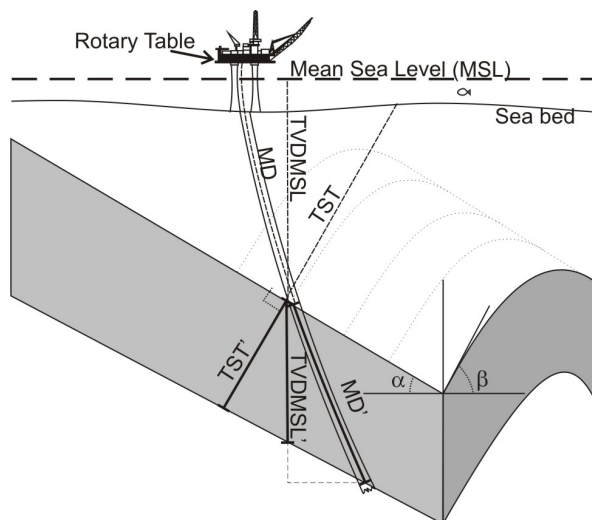


Figure 10: Sketched definitions of TST, TVDMSL and MD. TST is calculated based on TVD and the azimuth (α) and the dip angle (β). Thickness of the selected reservoir unit is MD', TVDMSL' or TST'. For vertical wells, TVDMSL'=TST=MD'. For wells with reservoir dip in the same direction as well dip: TST<TVDMSL', for opposite dips, TST>TVDMSL'. Note MD measured from rotary table, TVDMSL from mean sea level (MSL) and TST from sea bed.

ity and compaction rate for the lithofacies classes used in this study is porosity and rate of porosity change with depth. A basic requirement was therefore to discriminate between the different lithofacies classes. Due to long distance between source and receiver of some of the wireline logging tools, unprecise petrophysical signature recording of specific geologic layers may occur. However, as the Heidrun Field is a mature hydrocarbon area, multiple relatively closed spaced wells, some of which are cored, are available. This creates the opportunity of reducing this bias effect by applying sedimentological log interpretations from core section in the lithofacies class interpretation process.

The lithofacies classes are derived from observations and interpretations of cores tied to specific wireline signatures. However, when core data is

unavailable, methods such as principal component analysis (PCA) may be used by combining separate PCs derived from different lithological intervals to detect higher order heterogeneities that corresponds to small scale lithological variations within the lithofacies classes (c.f. Brandsegg et al., 2010).

Porosity variation vs depth is in the present study defined as an exponential decrease in porosity with depth (c.f. Eq. 3), where the degree of decrease is dependent on the facies association classification and the depositional (initial) porosity of the sediments. It has been widely argued that the exponential porosity-depth relationship does not fit shallower depth data particularly well (Falvey and Middleton, 1981; Falvey and Deighton, 1982). Falvey and Middleton (1981) proposed an alternative relationship by assuming incremental change in porosity is proportional to change in load. However, no explanatory reason is given for this improvement. However, the Sclater and Christie (1980) model has been successfully applied to calculate land subsidence rates due to early compaction in the coastal areas of the Netherlands (c.f. Kooi, 2000).

Exponential decrease in porosity vs depth may on the other hand be an oversimplification as errors are introduced due to e.g. overpressure (as discussed above) and diagenesis (cementation, dissolution), which may modify the pore space in the rock. These errors may be small for each effect; however the sum could be significant and influence the correlatability of the reservoir. It is therefore important to investigate the presence of diagenesis (e.g. Hammer et al., 2009) and overpressure before a backstripping routine is applied. Secondly, the determination of initial porosity is based on published values for different lithologies (c.f. Beard and Weyl, 1973). The initial porosity of the sand and silt of the Åre Fm. is not known, however, values are estimated based on comparison with published data and grain size, sorting, angularity and sand purity in the sandy deposits of the Åre Fm. Mudstones are on the other hand a larger source of error as these calculations are entirely dependent on published porosity-depth-curves. Third, coal compaction is determined by peat-to-coal ratios and published burial porosities. Coals may vary significantly from well to well and from interval to interval. This is exemplified in the text with coals varying from true "coal" to coaly units interbedded with sand and silt, which would reduce the compactability of the unit. However, as the calculations are based on direct indicators for peat-to-coal-compaction and the coals in the Åre

Fm. are generally a mixture of coal, silt and sand, the presented values seems fairly valid.

In an optimal backstripping routine it is customary to use the true stratigraphic thickness (TST) to avoid errors due to inclined reservoir units caused by folding, faulting etc. (Fig. 10). The tilt on the stratal units from the studied interval in the Heidrun Field due to the tectonic history of this region (Blystad et al., 1995; Brekke et al., 2001; Bukovics et al., 1984; Bukovics and Ziegler, 1985; Dooley et al., 2003; Doré, 1991; Gjelberg et al., 1987; Schmidt, 1992; Swiecicki et al., 1998), should be accounted for and is traditionally included by using true stratigraphic thickness (TST) during backstripping. We are however using true vertical depth mean sea level (TVDMSL) thicknesses. The wells used in this study are near vertical wells and the difference between TST and TVDMSL is small (2% in average, reaching a maximum of 6% in Well IV). TVDMSL is also used because it is measured continuously throughout the well which is a necessary criteria in a sample based model, as compared to TST thickness which is only measured for each reservoir zone. To investigate the intra zone architecture we are therefore compelled to use TVDMSL data. A third argument is that TST is a calculated thickness based on angle of dip and azimuth of the layers. Small errors in these values can lead to significant miscalculations of the TST thickness.

A major advantage in the presented model is the sample based decompaction routine. Any selected sample point (15cm interval) can be used as a potential datum (backstripping surface) and decompacted accordingly. This allows for a more interactive role for the user in the decompaction process. The petrophysical parameter values are retained from the original sample values making lithological interpretation between identified surfaces and in uncored wells possible at any desired level. New correlatable surfaces identified after decompaction can be used and implemented in the model and a new backstripping is modelled using the previous and the new surfaces as datums. This process is then repeated for any new surfaces identified to increase the correlation resolution after each iteration. In the present study each sample has been assigned, by observation and interpretation of core and wireline logs, to a specific lithofacies (1-9). This gives us the possibility to work with resolutions far beyond that of traditional backstripping. By using these available high resolution data in the backstripping process, we are able to reconstruct the

reservoir architecture, as regards to decompacted facies distributions. This will potentially increase the productivity of such reservoirs by increasing the understanding of reservoir sand connectivity.

7.1. Recommendations

The technique described in this study can be applied to refine reservoir models, based on correlation of decompacted sediments, and implemented in a process-based modeling tool (e.g Nordahl et al., 2005). Simulation of permeability distribution and fluid flow by such modeling tools, and comparing the results to real production data has the potential of optimizing production and increasing recoverable reserves by enhanced hydrocarbon flow prediction. It would also be beneficial to test this methodology on other fluviodeltaic deposits with less faults and other depositional environments in general, to test the robustness of our quantitative, sequential re-burial modelling tool.

8. Conclusion

A method for sequence stratigraphic backstripping in heterogeneous fluviodeltaic deposits is proposed which explicitly models stepwise deposition at intra-reservoir scale using lithofacies classes derived from wireline logs and core data.

Differential decompaction is calculated based on porosity change vs. burial depth for each identified lithofacies class and incorporated in the backstripping model. The presented model is sample based and measured values of petrophysical parameters are kept constant while relating the sample thickness change to changes in porosity with burial depth (decompaction). This enables interpretation and correlation of depositional units between known correlatable surfaces and different depositional scenarios can be evaluated. In particular, this can be valuable in reservoirs comprising highly compactable sediments, such as coals.

The effect of differential compaction on correlatability is accounted for by correcting for the compactability of interpreted lithofacies classes by differential decompaction and by applying flooding surfaces as backstripping surfaces in a sequence stratigraphic backstripping exercise.

The methodology was successfully tested on the fluviodeltaic Åre Fm. in the Heidrun Field, where several new correlatable channel sandstones within the Åre Fm. are recognized. These correlations

would be important for reservoir property modelling and drainage strategies, especially for the studied central area of the Heidrun Field.

Improving the reservoir sequence stratigraphic resolution increases the robustness of the Åre geomodel and has the potential as a decision making tool for hydrocarbon production optimization. This would also benefit HC volume calculations of reservoir sections which are an important part of field economics.

9. Acknowledgements

Heidrun Unit (Statoil Petroleum AS, ConocoPhillips Skandinavia AS, Petoro AS, Eni Norge AS) is acknowledged for providing well data, rock samples and permission to publish these data from the Heidrun Field.

References

- Allen, P., Allen, J., 2005. Basin Analysis. Blackwell Scientific Publications, Oxford.
- Athy, L., 1930. Density, porosity and compaction of sedimentary rocks. The American Association of Petroleum Geologists Bulletin 31, 241–287.
- Atkins, John, E., McBride, Earle, F., 1992. Porosity and packing of Holocene river, dune, and beach sands. The American Association of Petroleum Geologists Bulletin 76 (3), 339–355.
- Baldwin, B., Butler, C., 1985. Compaction curves. The American Association of Petroleum Geologists Bulletin 69 (4), 622–626.
- Bear, J., 1972. Dynamics of fluids in porous media. American Elsevier Publishing Company, New York.
- Bear, J., 1988. Dynamics of fluids in porous media. Dover Publications, Dover, New York.
- Beard, D. C., Weyl, P. K., 1973. Influence of texture on porosity and permeability of unconsolidated sand. The American Association of Petroleum Geologists Bulletin 57, 349–369.
- Bhatt, A., Helle, H. B., 2002. Determination of facies from well logs using modular neural networks. Petroleum Geoscience 8 (3), 217–228.
- Bjørlykke, K., Ramm, M., Saigal, G., 1989. Sandstone diagenesis and porosity modification during basin evolution. Geologische Rundschau 68, 1151–1171.
- Blystad, P., Brekke, H., Færseth, R., Larsen, B., Skogseid, J., Tærudbakken, B., 1995. Structural elements of the Norwegian continental shelf. Part II: the Norwegian Sea region. Norwegian Petroleum Directorate Bulletin (No 8), 45.
- Bond, G., Kominz, M., 1984. Construction of tectonic subsidence curves for the early Paleozoic miogeocline, southern Canadian Rocky Mountains: implications for subsidence mechanisms, age of breakup, and crustal thinning. Geological Society of America Bulletin 95, 155–173.
- Bond, G., Kominz, M., Steckler, M., Grotzinger, J., 1989. Role of thermal subsidence, flexure, and eustasy in the

- evolution of early Paleozoic passive-margin carbonate platforms. In: Crevello, P., Wilson, J., Sarg, J., Read, J. (Eds.), *Controls on Carbonate Platform and Basin Development*. Vol. 44. SEPM Special Publication, pp. 40–61.
- Brandsegg, K. B., Hammer, E., Sinding-Larsen, R., 2010. A Comparison of Unstructured and Structured Principal Component Analyses and their Interpretation. *Natural Resources Research* 19 (1), 45–62.
- Brekke, H., Sjulstad, H., Magnus, C., Williams, R., 2001. Sedimentary environments offshore Norway - an overview. In: Martinsen, O., Dreyer, T. (Eds.), *Sedimentary Environments Offshore Norway - Palaeozoic to Recent*. Vol. 10. Norwegian Petroleum Society Special Publication, pp. 7–37.
- Bukovics, C., Shaw, N., Cartier, E., Ziegler, P., 1984. Structure and development of the Mid-Norway continental margin. In: Spencer, A., Holter, E., Johnsen, S., Mørk, A., Nysæther, E., Songstad, P., Spinnanger, Å. (Eds.), *Petroleum Geology of the North European Margin*. Norwegian Petroleum Society, Graham and Trotman, London, pp. 407–423.
- Bukovics, C., Ziegler, P., 1985. Tectonic development of the Mid-Norway continental margin. *Marine and Petroleum Geology* 2, 1–22.
- Dalland, A., Augedahl, H., Bomstad, K., Ofstad, K., 1988. The post-Triassic succession of the Mid-Norwegian Shelf. In: Dalland, A., Worsley, D., Ofstad, K. (Eds.), *A lithostratigraphic scheme for the Mesozoic and Cenozoic succession offshore mid - and northern Norway*. Vol. 4 of Norwegian Petroleum Directorate Bulletin. pp. 5–42.
- Dooley, T., McCay, K., Pascoe, R., 2003. 3d analogue models of variable displacement extensional faults: applications to the Revfallet Fault system, offshore Mid-Norway. In: Nieuwland, D. (Ed.), *New Insights into Structural Interpretation and Modelling*. Vol. 212 of Geological Society, London, Special Publications. pp. 151–167.
- Doré, A., 1991. The structural foundation and evolution of Mesozoic seaways between Europe and the Arctic Sea. *Palaeogeography, Palaeoclimatology, Palaeoecology* 87, 441–492.
- Doveton, J., 1994. Geologic log analysis using computer methods. Vol. 2 of AAPG Computer Applications in Geology. American Association of Petroleum Geologists, Tulsa, OK.
- Ehrenberg, S., 1989. Assessing the relative importance of compaction processes and cementation to reduction of porosity in sandstones; discussion; compaction and porosity evolution of Pliocene sandstones, Ventura Basin, California; discussion. *The American Association of Petroleum Geologists Bulletin* 73 (10), 1274–1276.
- Emery, D., Myers, K. J., 1996. *Sequence stratigraphy*. Blackwell Science Ltd.
- Falvey, D., Deighton, I., 1982. Recent advances in burial and thermal geohistory analysis. *Journal of Australian Petroleum Exploration Association* 22, 65–81.
- Falvey, D., Middleton, M., 1981. Passive continental margins: evidence for a prebreakup deep crustal metamorphic subsidence mechanism. In: *Colloquium in Geology of Continental Margins (C3, Paris, 7-17 July, 1980)*. No. 4 (supplement) in *Oceanologica Acta*. pp. 103–114.
- Gabrielsen, R., Færseth, R., Hamar, G., Rønnevik, H., 1984. Nomenclature of the main structural features on the Norwegian Continental Shelf north of the 62nd parallel. In: Spencer, A., Holter, E., Johnsen, S., Mørk, A., Nysæther, E., Songstad, P., Spinnanger, Å. (Eds.), *Petroleum Geology of the North European Margin*. Norwegian Petroleum Society, pp. 41–60.
- Gjelberg, J., Dreyer, T., Høie, A., Tjelland, T., Lilleng, T., 1987. Late Jurassic to Mid-Jurassic sandbody development on the Barents and Mid-Norwegian shelf. In: Brooks, J., Glennie, K. (Eds.), *Petroleum Geology of Northwest Europe*. Graham and Trotman, London, pp. 1105–1129.
- Gluyas, J., Cade, C., 1997. Prediction of porosity in compacted sands. In: Kupecz, J., Gluyas, J., Bloch, S. (Eds.), *Reservoir quality prediction in sandstones and carbonates*. Vol. 69 of American Association of Petroleum Geologists Memoir. pp. 19–28.
- Hammer, E., 2010. Sedimentological correlation of heterogeneous reservoir rocks: Effects of lithology, differential compaction and diagenetic processes. Doctoral, Norwegian University of Science and Technology.
- Hammer, E., Mørk, M., Næss, A., 2009. Facies control on the distribution of diagenesis and compaction in fluviodeltaic deposits. *Marine and Petroleum Geology*.
- Hedberg, H., 1936. Gravitational compaction of clays and shales. *American Journal of Science* 31 (184), 241–287.
- Houseknecht, D. W., 1987. Assessing the relative importance of compaction processes and cementation to reduction of porosity in sandstones. *The American Association of Petroleum Geologists Bulletin* 71 (6), 633–642.
- Kjærefjord, J., 1999. Bayfill successions in the Lower Jurassic Åre Formation, offshore Norway: sedimentology and heterogeneity based on subsurface data from the Heidrun Field and analog data from the Upper Cretaceous Neslen Formation, eastern Book Cliffs, Utah. In: Hentz, T. (Ed.), *19th Annual Research Conference. Advanced reservoir characterization for the Twenty-First Century*. Gulf Coast Section and Society Economic Paleontologists and Mineralogists Foundation, Special Publication. pp. 149–157.
- Koch, J., Heum, O., 1995. Exploration trends of the Halten Terrace. In: Hanslien, S. (Ed.), *Petroleum Exploration in Norway*. Vol. 4 of Norwegian Petroleum Society Special publication. pp. 235–251.
- Koenig, R., 1986. Oil discovery in 6507; an initial look at the Heidrun Field. In: Spencer, A., Holter, E., Campbell, C., Hanslien, S., Nelson, P., Nysæther, E., Ormaasen, E. (Eds.), *Habitat of Hydrocarbons on the Norwegian Continental Shelf*. Norwegian Petroleum Society, pp. 307–311.
- Kominz, M. A., Pekar, S. F., 2001. Oligocene eustasy from two-dimensional sequence stratigraphic backstripping. *Geological Society of America Bulletin* 113 (3), 291–304.
- Kooi, H., 2000. Land subsidence due to compaction in the coastal area of The Netherlands: the role of lateral fluid flow and constraints from well-log data. *Global and Planetary Change* 27, 207–222.
- Lander, R. H., Walderhaug, O., 1999. Predicting porosity through simulating sandstone compaction and quartz cementation. *The American Association of Petroleum Geologists Bulletin* 83 (3), 433–449.
- Leary, S., Næss, A., Thrana, C., Brekken, M., Cullum, A., Gowland, S., Selnes, H., 2007. The Åre Formation, Heidrun Field, Norwegian Sea. In: *25th International Association of Sedimentologists, Meeting of Sedimentologists, Patras, Greece*. Poster.
- Leeder, M., 1999. *Sedimentology and sedimentary basins*. Blackwell Scientific Publications, Oxford.
- Miall, A., 1999. *Principles of sedimentary basin analysis*.

- Springer, Berlin.
- Moline, G. R., Bahr, J. M., 1995. Estimating spatial distributions of heterogeneous subsurface characteristics by regionalized classification of electrofacies. *Mathematical Geology* 27 (1), 3–22.
- Mondol, N. H., Bjørlykke, K., Jahren, J., Høeg, K., 2007. Experimental mechanical compaction of clay mineral aggregates - Changes in physical properties of mudstones during burial. *Marine and Petroleum Geology* 24(5), 289–311.
- Morris, P., Cullum, A., Pearce, M., Batten, D., 2003. Megaspore assemblages from the Åre Formation (Rhaetian–Pliensbachian) offshore Mid-Norway, and their value as field and regional stratigraphical markers. *Journal of Micropalaeontology* 28, 161–181.
- Morton, A., Hallsworth, C., Strogon, D., Whitman, A., Fanning, M., 2009. Evolution of provenance in the NE Atlantic rift: The Early-Middle Jurassic succession in the Heidrun Field, Halten Terrace, offshore Mid-Norway. *Marine and petroleum geology* 26, 1100–1117.
- Nadon, G. C., 1994. The genesis and recognition of anastomosed fluvial deposits: Data from the St. Mary River Formation, Southwestern Alberta, Canada. *Journal of Sedimentary Research, Section B: Stratigraphy and Global Studies* 64B (4), 451–463.
- Nadon, G. C., 1998. Magnitude and timing of peat-to-coal compaction. *Geology* 26 (8), 727–730.
- Nordahl, K., Ringrose, P. S., 2008. Identifying the representative elementary volume for permeability in heterolithic deposits using numerical rock models. *Mathematical Geosciences* 40, 753–771.
- Nordahl, K., Ringrose, P. S., Wen, R. J., 2005. Petrophysical characterization of a heterolithic tidal reservoir interval using a process-based modelling tool. *Petroleum Geoscience* 11 (1), 17–28.
- Ottesen, D., 2006. Ice-sheet dynamics and glacial development of the Norwegian continental margin during the last 3 million years. Dr.philos, Department of Earth Science, University of Bergen, Norway.
- Paxton, S., Szabo, J., Ajdukiewicz, J., Klimentidis, R., 2002. Construction of an intergranular volume compaction curve for evaluating and predicting compaction and porosity loss in rigid-grain sandstone reservoirs. *The American Association of Petroleum Geologists Bulletin* 86, 2047–2067.
- Pedersen, T., Harms, J., Harris, N., Mitchell, R., Tooby, K., 1989. The role of correlation in generating the Heidrun Field geologic model. In: Collinson, J. (Ed.), *Correlation in hydrocarbon exploration*. Norwegian Petroleum Society, Springer, pp. 327–338.
- Posamentier, H., Jervy, M., Vail, P., 1988. Eustatic controls on clastic deposition, I. conceptual framework. In: Wilgus, C., Hastings, B., Ross, C., Posamentier, H., Van Wagoner, J., Kendall, C. (Eds.), *Sea-Level changes: an integrated approach*. Vol. 42 of Society of Economic Palaeontologists and Mineralogists Special Publication. Society of Economic Paleontologists, Mineralogists, pp. 109–124.
- Posamentier, H., Vail, P., 1988. Eustatic controls on clastic deposition, II. Sequence and systems tract models. In: Wilgus, C., Hastings, B., Ross, C., Posamentier, H., Van Wagoner, J., Kendall, C. (Eds.), *Sea-Level Changes: An Integrated Approach*. Vol. 42 of Society of Economic Palaeontologists and Mineralogists Special Publication. Society of Economic Paleontologists, Mineralogists, pp. 125–154.
- Rajchl, M., Ulicný, D., 2005. Depositional record of an avulsive fluvial system controlled by peat compaction (Neogene, Most Basin, Czech Republic). *Sedimentology* 52, 601–625.
- Ramm, M., 1992. Porosity-depth trends in reservoir sandstones: theoretical models related to Jurassic sandstones offshore Norway. *Marine and Petroleum geology* 9, 553–567.
- Ramm, M., Bjørlykke, K., 1994. Porosity depth trends in reservoir sandstones - Assessing the quantitative effects of varying pore-pressure, temperature history and mineralogy, Norwegian shelf data. *Clay Minerals* 29, 475–490.
- Rodrigues, C., Lemos de Sousa, M., 2002. The measurement of coal porosity with different gases. *International Journal of Coal Geology* 48, 245–251.
- Ryer, T. A., Lange, A. W., 1980. Thickness change involved in the peat-to-coal transformation for a bituminous coal of Cretaceous age in central Utah. *Journal of Sedimentary Research* 50 (3), 987–992.
- Schmidt, W., 1992. Structure of the Mid-Norway Heidrun Field and its regional implications. In: Larsen, R., Brekke, H., Larsen, B., Talleraas, E. (Eds.), *Structural and Tectonic Modelling and its Application to Petroleum Geology*. Vol. 1 of Norwegian Petroleum Society Special Publication. pp. 381–395.
- Schmoker, J. W., Gautier, D. L., 1988. Sandstone porosity as a function of thermal maturity. *Geology* 16 (11), 1007–1010.
- Schneider, F., Potdevin, J., Wolf, S., Faille, I., 1996. Mechanical and chemical compaction model for sedimentary basin simulators. *Tectonophysics* 263, 307–317.
- Sclater, J., Christie, P., 1980. Continental stretching: an explanation of the post Mid-Cretaceous subsidence of the Central North Sea basin. *Journal of Geophysical Research* 85, 3711–3739.
- Serra, O., Abbott, H., 1982. The contribution of logging data to sedimentology and stratigraphy. *Society of Petroleum Engineers journal* 22 (1), 117–131.
- Sleep, N. H., 1971. Thermal effects of the formation of Atlantic continental margins by continental break-up. *Geophysical Journal International* 24 (4), 325–350.
- Steckler, M., Watts, A., 1978. Subsidence of the Atlantic-type continental margin off New York. *Earth and Planetary Science Letters* 41, 1–13.
- Steckler, M., Watts, A., Thorne, J., 1988. Subsidence and basin modeling at the U.S. Atlantic passive margin. In: Sheridan, R., Grow, J. (Eds.), *The Atlantic Continental Margin*. The Geology of North America. Vol. I-2. U.S. Geological Society of America, Boulder, CO, pp. 399–416.
- Steckler, M. S., Mountain, G. S., Miller, K. G., Christie-Blick, N., 1999. Reconstruction of Tertiary progradation and clinoform development on the New Jersey passive margin by 2D backstripping. *Marine Geology* 154, 399–420.
- Svela, K., 2001. Sedimentary facies in the fluvial-dominated Åre Formation as seen in the Åre 1 Member in the Heidrun Field. In: Martinsen, O., Dreyer, T. (Eds.), *Sedimentary Environments Offshore Norway - Paleozoic to Recent*. Vol. 10 of Norwegian Petroleum Society Special Publication. Elsevier Science B.V., Amsterdam, pp. 87–102.
- Swiecicki, T., Gibbs, P., Farrow, G., Coward, M., 1998. A tectonostratigraphic framework for the Mid-Norway region. *Marine and Petroleum Geology*, 245–276.

- Thrana, C., Brekken, M., Næss, A., Leary, S., Gowland, S., 2008. Revised reservoir characterization of the Åre Fm., Heidrun Field, Halten Terrace, Abstract, the 33rd IGC, Oslo, Norway. In: 33rd International Geological Congress, Oslo, Norway. Poster.
- Thrana, C., Brekken, M., Næss, A., Leary, S., Gowland, S., 2009. Milking the goat: revised reservoir characterization of the Åre Formation, Heidrun Field, offshore Mid-Norway. In: Search and Discovery Article # 20069 (2009). Adapted from oral presentation at AAPG International Conference and Exhibition, Cape Town, South Africa, October 26-29, 2008.
- Ungerer, P., Burrus, J., Doligez, B., Chenet, P. Y., Bessis, F., 1990. Basin evaluation by integrated two-dimensional modeling of heat transfer, fluid flow, hydrocarbon generation, and migration. *The American Association of Petroleum Geologists Bulletin* 74 (3), 309–335.
- Van Hinte, J., 1978. Geohistory analysis-application of micropaleontology in exploration geology. *The American Association of Petroleum Geologists Bulletin* 62, 201–222.
- Van Wagoner, J. C., Mitchum, R. M., Campion, K. M., Rahmanian, V. D., 1990. Siliciclastic sequence stratigraphy in well logs, cores, and outcrops: concepts for high-resolution correlation of time and facies. Vol. 7 of American Association of Petroleum Geologists, *Methods in Exploration series*. The American Association of Petroleum Geologists, Tulsa, OK (USA).
- Van Wagoner, L., Posamentier, H., Mitchum, R., Vail, P., Sarg, J., Loutit, T., Hardenbol, J., 1988. An overview of the fundamentals of sequence stratigraphy and key definitions. In: Wilgus, C., Hastings, B., Ross, C., Posamentier, H., Van Wagoner, J., Kendall, C. (Eds.), *Sea-Level Changes: An Integrated Approach*. Vol. 42 of Society of Economic Palaeontologists and Mineralogists Special Publication. Society of Economic Paleontologists, Mineralogists, pp. 39–45.
- Velde, B., 1996. Compaction trends of clay-rich deep sea sediments. *Marine Geology* 133, 193–201.
- Walderhaug, O., 1996. Kinetic modeling of quartz cementation and porosity loss in deeply buried sandstone reservoirs. *The American Association of Petroleum Geologists Bulletin* 80 (5), 731–745.
- Walderhaug, O., Bjørkum, P., Nadeau, P., Langnes, O., 2001. Quantitative modelling of basin subsidence caused by temperature-driven silica dissolution and reprecipitation. *Petroleum Geoscience* 7, 107–113.
- Watts, A. B., Ryan, W. B. F., 1976. Flexure of the lithosphere and continental margin basins. *Tectonophysics* 36, 25–44.
- Wilson, J. C., McBride, E. F., 1988. Compaction and porosity evolution of Pliocene sandstones, Ventura Basin, California. *The American Association of Petroleum Geologists Bulletin* 72 (6), 664–681.
- Wood, J., 1989. Modelling the effect of compaction and reprecipitation/dissolution on porosity. In: Hutcheon, I. (Ed.), *Short Course in Burial Diagenesis*. No. 15. Mineralogical Association of Canada, pp. 311–362.

Paper III

A comparison of unstructured and structured principal component analyses and their interpretation

Authors: Kristian Bjarnøe Brandsegg, Erik Hammer, Richard Sinding-Larsen

Published: Natural Resources Research, Vol. 19, No. 1, pages 45-62

Is not included due to copyright

Part IV

Appendices

A Conference Contributions

HAMMER E., MØRK, M.B.E. AND NÆSS, A. 2008. Facies controls on the distribution of diagenesis and compaction in fluviodeltaic deposits. Oral presentation. 33rd International Geological Congress, Oslo, Norway, Aug. 6-14th.

HAMMER E., MØRK, M.B.E. AND NÆSS, A. 2008. Facies controls on the distribution of diagenesis in fluviodeltaic deposits. Poster. 33rd International Geological Congress, Oslo, Norway, Aug. 6-14th.

HAMMER E., MØRK, M.B.E. AND NÆSS, A. 2007 Correlation of Heterolithic Sediments of the upper Triassic/lower Jurassic Åre Formation, Heidrun Field Offshore Mid-Norway. NGF Vinterkonferansen 2007, Stavanger, Norway. NGF abstracts and proceedings 2007. Volume 1, p. 36.

HAMMER E., NÆSS, A. AND MØRK, M.B.E. 2007. Correlation of Heterolithic Sediments and the Role of Differential Compaction from the Åre Formation in the Heidrun Field. Abstract. AAPG Annual Convention and Exhibition, Long Beach, CA, USA, p.15.

BRANDSEGG, K.B., HAMMER, E. AND SINDING-LARSEN, R. 2008. Refined Lithological classification through multivariate analysis. Poster. 33rd International Geological

Congress, Oslo, Norway, Aug. 6-14th.

BRANDSEGG, K.B., HAMMER, E. AND SINDING-LARSEN, R. 2008. Lateral correlation of cemented zones using structured multivariate analysis. Poster. 33rd International Geological Congress, Oslo, Norway, Aug. 6-14th.

BRANDSEGG, K.B., HAMMER, E. AND SINDING-LARSEN, R. 2008. Quantifying fluvial sandstone heterogeneity by using multivariate analysis. NGF abstracts and proceedings 2008. Volume 1, pp. 1-9.

BRANDSEGG, K.B., HAMMER, E. AND SINDING-LARSEN, R. 2007. Refined Lithological Classification through Structured Multivariate Analysis. In: Proceedings of IAMG'07: Geomathematics and GIS Analysis of Resources, Environment and Hazards. China: State Key Laboratory of Geological Processes and Mineral Resources (GPMR), China University of Geosciences 2007. pp. 679-683.

BRANDSEGG, K.B., HAMMER, E. AND SINDING-LARSEN, R. 2007. Facies identification from well logs of a fluvial deposit using multivariate pattern recognition. Poster. NGF Vinterkonferansen 2007, Stavanger, Norway.

B Methods and Material

Methods

This chapter describes the different methods and techniques used in this thesis. Some data not included in the papers are also enclosed.

Material and data

Petrophysical wireline data from fourteen wells have been used. Of these fourteen wells, four have been cored and subjected to sedimentological interpretation. 53 rock samples from wells 4, 5 and 10 have been collected and studied. Petrographic thin-sections are made from each sample with blue impregnation resin to facilitate the identification of porosity. XRD and SEM micro-probe analysis were carried out at the Department of Geology and Mineral Resources Engineering to investigate mineral compositions. Petrophysical wireline log data from all wells has been made available by Statoil and subjected to calculations and interpretations in many scales throughout the work.

Core data

Sedimentological core description has been done based on detailed logging of cores from well wells 2, 4, 5 and 10 covering in total 448m of the Åre Fm. These interpretations were used as reference for petrophysical wireline log interpretation of lithology and sedimentary facies associations. The sedimentological logging was carried out on a 1:50 scale and later

reduced to 1:200 for petrophysical wireline log comparison reasons. Wireline log signature for each interpreted facies association was determined and used as a basis for correlation between wells. Core photos of the entire cored section of well 5 well are available at www.npd.no.

Table 2: Well and core coverage of the Åre Fm., Heidrun Field. Wells in **bold** have been subjected to detailed core studies.

Well name	Log coverage, zone	Core coverage, zone	Core coverage, m	Faults
Well 1	7.2 - 1	7.2 - 5.3		Yes
Well 2	7.2 - 2.1	6.2 - 4.1	92	Yes
Well 3	7.2 - 1	4.4 - 2.1		Yes
Well 4	7.2 - 3.1	7.2 - 4.3	133	No
Well 5	7.2 - 1	7.2 + 5.1 - 1	186	Yes
Well 6	7.2 - 2.1	None		No
Well 7	7.2 - 2.1	None		No
Well 8	7.2 - 2.1	None		No
Well 9	7.2 - 2.1	7.1 - 2.2		Yes
Well 10	7.2 - 1	4.2 - 3.1	46	No
Well 11	7.2 - 1	None		No
Well 12	3.1 - 1	2.2 - 1		No
Well 13	7.2 - 2.1	None		No
Well 14	7.2 - 2.1	7.2 - 5.3		No

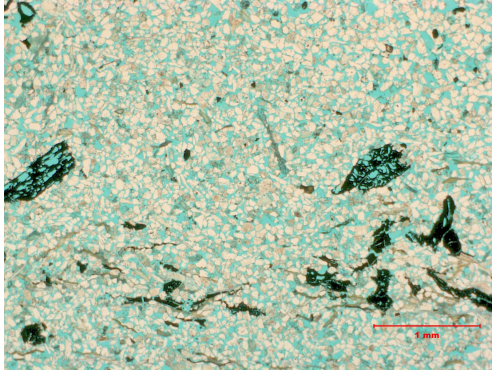
Optical Microscopy

The optical microscopy investigations (polarized and crossed polars) were carried out on a Nikon Eclipse E600 microscope equipped with a two mega pixels SPOT Insight IN320 color digital camera from Diagnostic Instruments Inc. connected directly to a PC for real-time image capture and enhancement using SPOT software. Polished thin

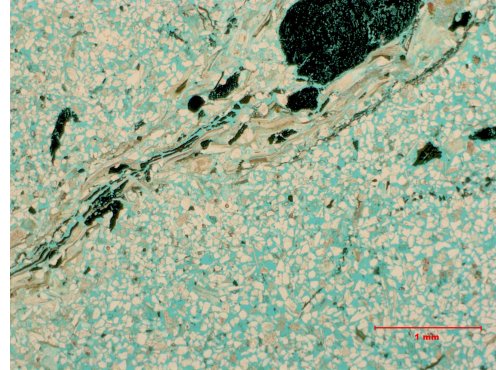
sections were prepared at the Department of Geology and Mineral Resources Engineering, NTNU as standard 28x48mm sections, approx. 30µm thick and impregnated with a blue impregnation resin to facilitate the identification of porosity. Samples were subject to modal analysis by point counting using 300 points pr. thin section. Results are presented in Table 3. Snapshots taken in polarized light (2,5x magnification) from samples from well 5 are presented in Fig. 24 and clearly illustrate the petrographic heterogeneity of the sampled intervals.

Table 3: Modal analysis of samples from wells 4 and 5

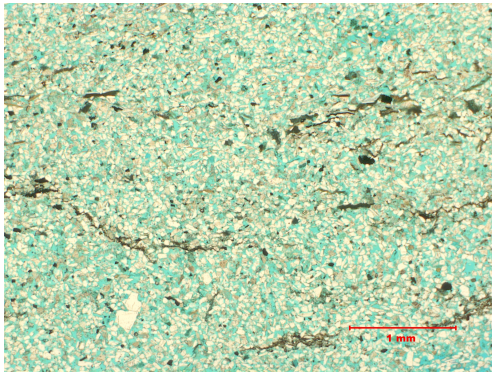
Well	Depth	Qtz	Sum			Alterred						Carb		Sum			Grain size			
			Fsp	Kfs	Plg	Fsp	Mic	Rt	ClyGm	Cal/Ank	Carb	Sid	Org	QCm	Opq	Por		Zone	Facies	
Well 4	2751.71	31.00	27.00	n/a	n/a	n/a	2.00	2.00	3.60	3.60	0.60	0.00	0.00	0.00	3.00	0.00	27.60	Are 5.1	MBF	F
Well 4	2769.74	24.60	27.00	n/a	n/a	n/a	2.30	2.30	4.00	4.00	0.30	0.00	0.00	0.00	3.60	0.00	35.60	Are 4.4	SBF	VF
Well 4	2769.78	30.00	21.60	n/a	n/a	n/a	1.70	1.70	3.60	3.60	0.70	0.00	0.00	0.00	5.00	0.00	30.60	Are 4.4	SBF	VF
Well 4	2771.07	37.60	17.70	n/a	n/a	n/a	2.70	2.70	7.60	7.60	0.00	0.00	0.00	0.00	3.70	0.00	26.70	Are 4.4	SBF	F
Well 4	2771.12	42.30	12.90	n/a	n/a	n/a	1.70	1.70	7.30	7.30	0.00	0.00	0.00	0.00	5.30	0.00	26.00	Are 4.4	SBF	M
Well 4	2772.3	45.30	17.60	n/a	n/a	n/a	2.30	2.30	6.60	6.60	1.00	0.00	0.00	2.30	0.00	0.00	19.30	Are 4.4	FCH	C
Well 4	2776.77	25.60	27.00	n/a	n/a	n/a	4.60	4.60	5.00	5.00	0.70	0.00	0.00	0.00	0.60	0.00	33.60	Are 4.4	SBF	C
Well 5	2671.78A	47.30	12.00	0.33	0.67	0.67	2.30	2.30	3.00	3.00	0.00	0.00	0.30	0.30	0.00	0.30	31.30	Are 4.4	SBF	F
Well 5	2671.78B	41.60	9.60	0.33	0.66	0.66	3.00	3.00	6.60	6.60	0.00	0.30	1.00	1.30	0.00	1.30	35.30	Are 4.4	SBF	F
Well 5	2671.78B	32.00	5.00	0.67	0.00	0.00	7.30	7.30	1.30	1.30	0.00	29.00	1.00	0.00	0.00	0.00	23.30	Are 4.4	SBF	F
Well 5	2673.63	40.60	14.30	0.33	0.33	0.33	1.60	1.60	6.60	6.60	0.00	1.00	0.00	0.00	0.00	0.30	33.30	Are 4.4	SBF	VF
Well 5	2716.96	45.50	1.00	0.25	0.00	0.75	1.50	1.50	0.20	0.20	38.00	0.00	0.00	0.00	0.00	0.00	11.20	Are 3.3	SBF	M
Well 5	2717.25	46.00	1.20	0.72	0.24	0.24	0.70	0.70	3.20	3.20	41.20	0.00	0.00	0.00	0.00	0.00	5.50	Are 3.3	SBF	M
Well 5	2730.44	38.00	8.00	3.00	0.00	5.00	4.60	4.60	15.30	15.30	0.00	2.60	0.30	0.00	0.00	0.00	26.60	Are 3.3	CCH	C
Well 5	2765.78	43.60	5.30	0.00	0.00	0.33	5.30	5.30	2.30	2.30	0.00	0.30	9.00	0.00	0.00	0.00	33.60	Are 2.1	FCH	C
Well 5	2765.78	22.00	2.60	0.65	0.98	0.98	11.30	11.30	6.60	6.60	0.00	35.30	3.60	0.00	0.00	0.00	18.00	Are 2.1	FCH	M
Well 5	2778.62	51.00	2.00	0.67	0.33	1.00	2.00	2.00	7.60	7.60	0.00	1.00	1.00	0.00	0.00	0.30	31.00	Are 2.1	FCH	C
Well 5	2787.00	23.20	10.00	0.00	0.00	10.00	5.20	5.20	18.00	18.00	0.00	17.00	9.70	0.00	0.50	15.50	Are 2.1	FF	F	
Well 5	2791.30B	43.30	4.60	0.00	0.00	4.60	3.60	3.60	7.00	7.00	0.00	1.00	0.00	0.00	0.00	0.00	36.60	Are 2.1	FCH	C
Well 5	2791.30B	48.60	2.60	0.19	0.37	2.04	1.30	1.30	9.00	9.00	0.00	1.60	1.30	0.00	0.00	0.00	32.60	Are 2.1	FCH	C
Well 5	2791.31A	47.30	3.60	0.33	0.00	3.27	2.60	2.60	9.30	9.30	0.00	0.60	0.00	0.00	0.00	0.00	31.60	Are 2.1	FCH	C
Well 5	2791.31A	49.30	7.60	1.65	3.30	2.64	3.60	3.60	10.00	10.00	0.00	0.90	0.00	0.00	0.00	0.00	27.00	Are 2.2	FCH	C
Well 5	2800.80	14.70	0.50	0.25	0.00	0.25	1.20	1.20	0.00	0.00	0.00	80.20	1.20	0.00	0.00	0.00	1.50	Are 2.1	FF	VF
Well 5	2812.40	51.70	5.70	0.00	0.17	3.83	0.20	0.20	5.40	5.40	0.00	5.20	0.00	0.00	0.00	2.00	26.20	Are 1	LEV	M
Well 5	2814.70	36.70	4.00	0.00	0.00	4.00	0.50	0.50	0.00	0.00	0.00	0.70	0.00	0.00	0.00	56.50	Are 1	FCH	n/a	
Well 5	2835.40	48.00	5.20	1.98	0.25	2.97	2.00	2.00	5.00	5.00	0.00	0.20	0.00	0.00	0.00	0.00	36.50	Are 1	FCH	C
Well 5	2852.20	47.70	7.00	2.50	0.00	4.50	0.00	0.00	3.00	3.00	0.00	0.20	0.00	0.00	0.00	0.70	35.50	Are 1	FCH	C
Well 10	3539.58	52.00	9.70	n/a	n/a	n/a	2.60	2.60	3.70	3.70	3.00	0.00	0.00	0.00	0.70	0.00	26.30	Are 4.2	FCH	M
Well 10	3541.51	37.70	7.90	n/a	n/a	n/a	1.70	1.70	5.00	5.00	34.70	0.00	0.00	0.00	2.30	0.00	5.30	Are 4.2	FCH	M
Well 10	3541.74	34.00	10.60	n/a	n/a	n/a	0.30	0.30	2.70	2.70	46.70	0.00	0.00	1.00	0.00	0.00	2.00	Are 4.2	FCH	M
Well 10	3542.51	21.60	12.60	n/a	n/a	n/a	4.30	4.30	7.60	7.60	49.00	0.00	0.00	0.60	0.00	0.00	2.70	Are 4.2	FCH	M
Well 10	3557.85	27.30	14.90	n/a	n/a	n/a	1.70	1.70	6.80	6.80	9.60	0.00	4.00	3.00	0.00	0.00	28.00	Are 4.1	FCH	VF
Well 10	3571.5	42.70	9.60	n/a	n/a	n/a	0.70	0.70	7.70	7.70	11.30	0.00	0.00	0.00	2.30	0.00	20.70	Are 3.3	FCH	M-VC
Well 10	3580.47	33.15	14.45	n/a	n/a	n/a	5.00	5.00	6.30	6.30	20.80	0.00	0.00	2.50	0.00	0.00	16.15	Are 3.3	FCH	F
Well 10	3578.68	17.70	23.70	n/a	n/a	n/a	12.30	12.30	8.70	8.70	8.30	0.00	0.00	1.60	0.00	0.00	1.00	Are 3.3	CCH	VF-C
Well 10	3579.39	27.00	22.00	n/a	n/a	n/a	4.60	4.60	4.70	4.70	4.70	0.00	5.30	2.70	0.00	0.00	24.70	Are 3.3	CCH	silt
Well 10	3584.29	28.90	19.20	n/a	n/a	n/a	17.00	17.00	15.00	15.00	10.00	0.00	2.00	2.00	0.00	0.00	3.30	Are 3.2	CCH	F
Well 10	3553.81	21.00	32.90	n/a	n/a	n/a	8.70	8.70	6.50	6.50	0.30	0.00	5.30	2.70	0.00	0.00	17.30	Are 4.1	SBF	VF
Well 10	3554.85	32.30	22.90	n/a	n/a	n/a	1.30	1.30	3.80	3.80	0.30	0.00	0.00	2.00	0.00	0.00	32.70	Are 4.1	SBF	VF
Well 10	3556.87	24.90	23.30	n/a	n/a	n/a	8.00	8.00	7.00	7.00	16.30	0.00	3.00	2.70	0.00	0.00	12.60	Are 4.1	SBF	VF



(a) SBF 2671,78A m



(b) SBF 2671,78b m



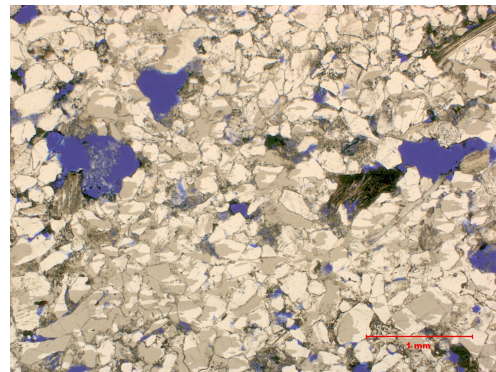
(c) SBF 2673,63 m



(d) SBF 2693,30 m

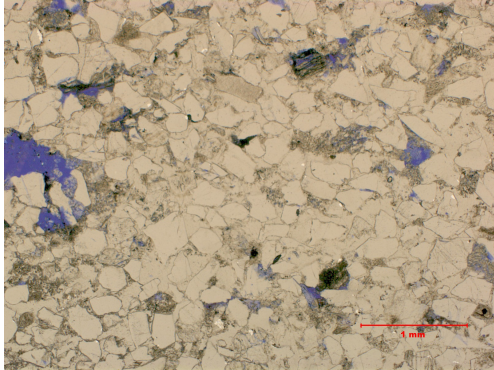


(e) SBF 2705,50 m. Siderite cemented

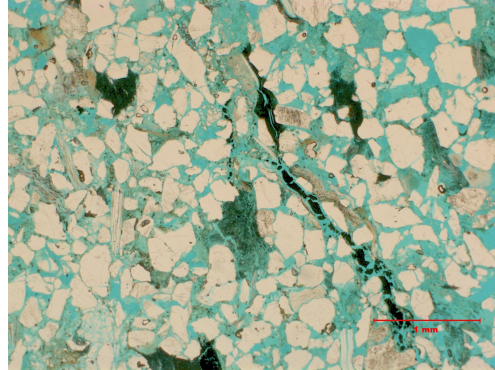


(f) SBF 2716,96 m. Calcite cemented

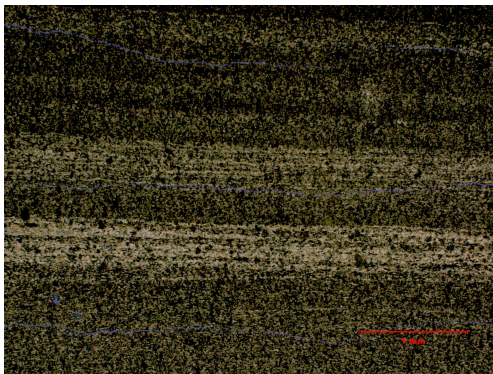
Figure 24: continued



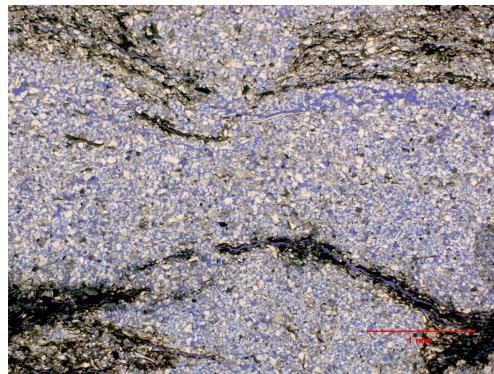
(g) SBF 2717,25 m. Calcite cemented



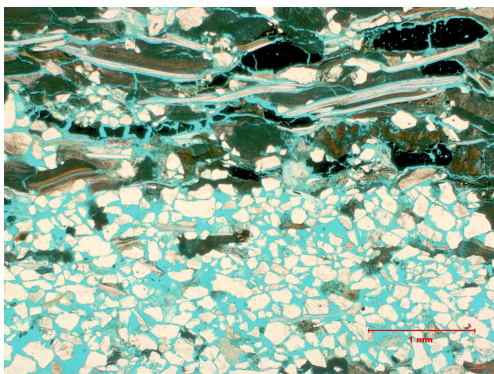
(h) CCH 2730,44 m



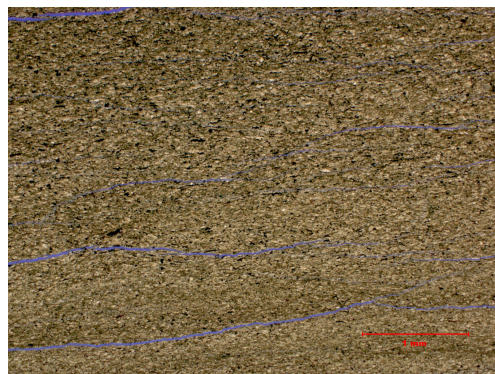
(i) MBF 2737,60 m. Flooding surface



(j) SBF 2746,80 m. Synaeresis

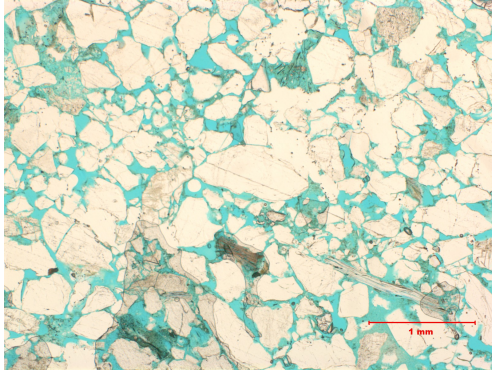


(k) FCH 2765,78 m. Single-storey



(l) FF 2774,50 m

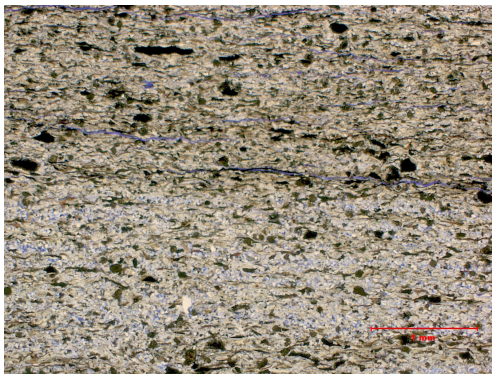
Figure 24: continued



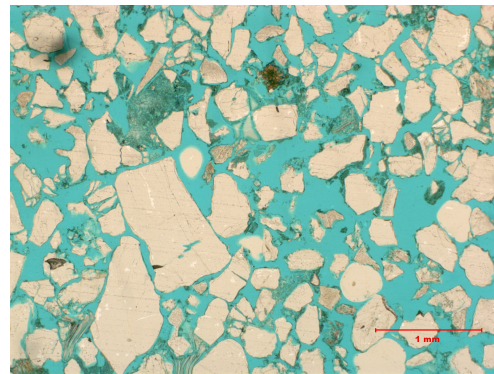
(m) FCH 2778,62 m. Single-storey



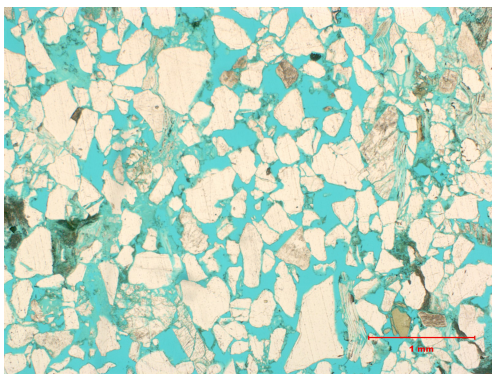
(n) FF 2785,00 m



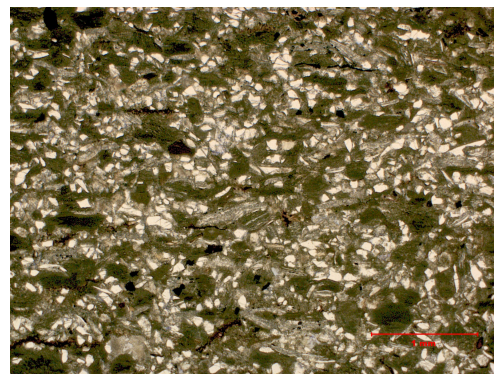
(o) FF 2787,00 m. Gamma spike



(p) FCH 2791,30B m. Single-storey

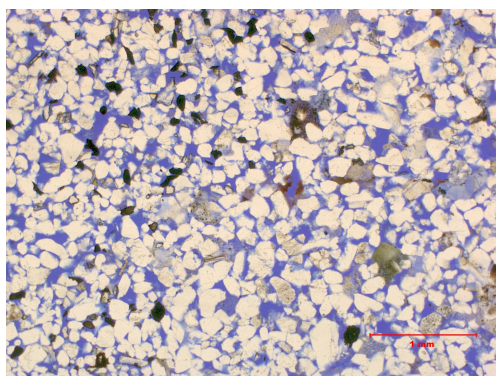


(q) FCH 2791,31A m. Single-storey

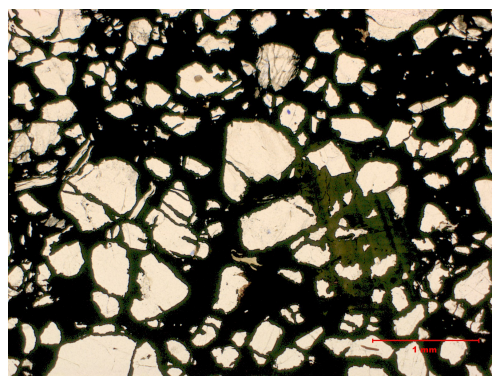


(r) FF 2800,80 m. Siderite cemented

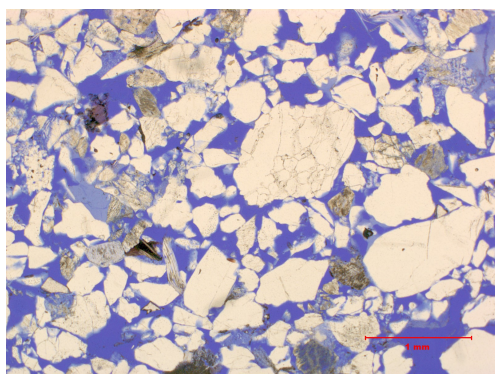
Figure 24: continued



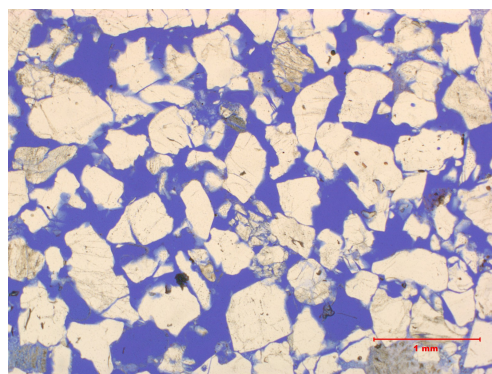
(s) LEV 2812,40 m



(t) FCH 2814,70 m. Pyrite nodule



(u) FCH 2835,40 m. Multi-storey



(v) FCH 2852,20 m. Multi-storey

Figure 24: Optical micrographs (2,5x magnification) of thin-sections from identified facies associations from well 5 displaying cemented intervals, diagenetic effects, grain-size, shape etc. Photos by Erik Hammer.

Scanning Electron Microscopy

SEM electron backscatter image (SEM BEI) analysis in combination with micro-probe analysis and X-ray mapping of elements were performed with the JXA-8500F Hyperprobe JOEL Electron Probe Micro Analyzer (EPMA) equipment at the Department of Materials Science and Engineering NTNU. Mineral chemical analyses were performed using the mineral standards presented in Table 4. The samples (polished thin-sections) were coated with carbon before the analysis. Cement compositions are presented as Ca, Mg, Fe-fractions in Table (Table 24)

Table 4: Standards for cement mineral/chemical identification by EPMA

Element (oxide)	Mineral Standard	Wt%	Element (oxide)	Mineral Standard	Wt%
Al_2O_3	Garnet	20.6	BaO	BaF2	87.46
Na_2O	Albite	11.46	MnO	Garnet	40.31
S	FeS_2	53.41	TiO_2	Sphene	37.80
C	C	100	La	LaB_6	68.17
FeO	Hematite	89.98	Zr	Zr	100
SiO_2	Wollastonite	51.72	Ce	CeAl2	72.20
MgO	Dolomite	21.86	P_2O_5	Apatite	40.93
CaO	Dolomite	30.41	ThO_2	Cal-std ^a	n/a
K_2O	Orthoclase	15.41			

^ameans virtual std used

Table 5: Proportions of Ca, Mg and Fe in carbonate cement calculated from SEM Microprobe analysis. Samples from wells 5 and 10.

Well and date	Sample nr.	Ca	Fe+Mn	Mg	Facies	Cement	Note	Saturation	Zonation
Well 5 30jan2008									
	5.1	96.9	2.7	0.3	FF	Calcite		W	Åre 2.1
	5.2	47.7	14.7	37.6	FF	Ankerite		W	Åre 2.1
	5.3	2.9	96.8	0.3	FF	Sid I		W	Åre 2.1
	5.4	2.7	97.0	0.3	FF	Sid I		W	Åre 2.1
	5.5	97.8	1.8	0.4	FF	Calcite		W	Åre 2.1
	9.1	5.4	94.1	0.3	MBF	Sid I		W	Åre 3.1
	9.3	0.8	99.0	0.2	MBF	Sid I		W	Åre 3.1
	9.4	5.7	94.0	0.3	MBF	Sid I		W	Åre 3.1
	10.1	97.5	2.3	0.2	SBF	Calcite		W	Åre 4.1
	10.2	8.8	71.5	19.7	SBF	Sid II		W	Åre 4.1
	10.3	1.4	98.2	0.4	SBF	Sid I		W	Åre 4.1
	11.1	97.6	1.8	0.6	SBF	Calcite		W	Åre 4.1
Well 5 16nov2007									
	2.1	4.8	82.7	12.5	FCH	Sid II		W	Åre 2.1
	2.2	3.2	83.4	13.3	FCH	Sid II		W	Åre 2.1
	6.1	8.4	76.3	15.3	FCH	Sid II		W	Åre 2.1
	6.5	6.3	74.3	19.3	FCH	Sid II		W	Åre 2.1
Well 5 26-27mar2008									
	2765.78-1	1.9	96.7	1.3	FCH	Sid I		W	Åre 2.1
	2765.78-2	0.4	99.1	0.5	FCH	Sid I		W	Åre 2.1
	2765.78-3	8.8	65.9	25.3	FCH	Sid II		W	Åre 2.1
	2765.78-4	2.0	97.3	0.7	FCH	Sid I		W	Åre 2.1
	2765.78-5	5.0	69.7	25.3	FCH	Sid II		W	Åre 2.1
	4.1.1	0.7	98.9	0.4	FF	Sid I		W	Åre 2.1
	5.1.1	97.1	2.1	0.9	FF	Calcite		W	Åre 2.1
	5.1.2	2.7	96.9	0.4	FF	Sid I		W	Åre 2.1
	5.1.4	2.5	95.4	2.1	FF	Sid I		W	Åre 2.1
	5.3.1	49.9	13.0	37.1	FF	Ankerite		W	Åre 2.1
	5.3.2	97.0	2.2	0.8	FF	Calcite		W	Åre 2.1
	5.3.3	2.4	97.2	0.4	FF	Sid I		W	Åre 2.1
	5.3.4	92.1	5.5	2.4	FF	Calcite		W	Åre 2.1
	6.1.1	9.1	80.1	10.8	FF	Sid II		W	Åre 2.1
	6.1.2	21.6	73.9	4.4	FF	Sid II		W	Åre 2.1
	9.1.1	5.4	94.0	0.7	MBF	Sid I		W	Åre 3.1
	9.1.2	3.6	96.1	0.3	MBF	Sid I		W	Åre 3.1
	9.1.3	4.0	94.5	1.5	MBF	Sid I		W	Åre 3.1
	10.1.1	6.6	82.4	11.0	SBF	Sid II	Mg-rich	W	Åre 3.3
	10.1.2	5.9	74.7	19.4	SBF	Sid II		W	Åre 3.3
	10.1.3	95.4	3.7	0.9	SBF	Calcite		W	Åre 3.3
	10.2.1	2.5	94.7	2.8	SBF	Sid I		W	Åre 3.3
	10.2.2	6.2	76.0	17.8	SBF	Sid II	Mg-rich	W	Åre 3.3
	10.2.3	95.2	3.9	0.9	SBF	Calcite		W	Åre 3.3
	11.1	95.0	4.1	0.9	SBF	Calcite		W	Åre 3.3
	11.2	2.8	96.2	1.0	SBF	Sid I		W	Åre 3.3
	11.3	4.8	73.3	21.9	SBF	Sid II	Mg-rich	W	Åre 3.3
	12.1.1	57.0	27.1	16.0	SBF	Ankerite		W	Åre 4.2
	12.1.2	2.2	63.3	34.5	SBF	Sid II	Mg-rich	W	Åre 4.2

to be continued on next page

Table 24 continued

Well and date	Sample nr.	Ca	Fe+Mn	Mg	Facies	Cement	Note	Saturation	Zonation
	12.1.3	1.2	82.2	16.6	SBF	Sid II	Mg-rich	W	Åre 4.2
	12.2.1	98.0	1.4	0.6	SBF	Calcite		W	Åre 4.2
	12.2.2	3.0	96.2	0.8	SBF	Sid I		W	Åre 4.2
	12.2.3	7.8	90.7	1.5	SBF	Sid I		W	Åre 4.2
	12.3.1	93.9	4.2	1.9	SBF	Calcite		W	Åre 4.2
	13.1.1	5.9	93.8	0.3	SBF	Sid I		W	Åre 4.2
	13.2.1	0.9	97.3	1.8	SBF	Sid I		W	Åre 4.2
	13.4.1	1.0	98.1	0.9	SBF	Sid I		W	Åre 4.2
	Well 10 3542m								
	1	57.1	21.4	21.5	FCH	Ankerite		O	Åre 4.2
	2	50.8	8.1	41.1	FCH	Fe-Dolomite		O	Åre 4.2
	3	49.3	18.2	32.5	FCH	Ankerite		O	Åre 4.2
	4	12.8	77.1	10.0	FCH	Sid II		O	Åre 4.2
	5	58.6	20.5	20.9	FCH	Ankerite		O	Åre 4.2
	6	57.7	5.7	36.6	FCH	Fe-Dolomite		O	Åre 4.2
	7	58.7	16.4	24.9	FCH	Ankerite		O	Åre 4.2
	8	3.8	90.9	5.3	FCH	Sid I		O	Åre 4.2
	9	8.7	67.5	23.8	FCH	Sid II	Mg-rich	O	Åre 4.2
	10	12.5	68.6	18.8	FCH	Sid II	Mg-rich	O	Åre 4.2
	11	13.6	65.9	20.5	FCH	Sid II	Mg-rich	O	Åre 4.2
	12	12.2	67.2	20.7	FCH	Sid II	Mg-rich	O	Åre 4.2
	13	5.6	91.9	2.5	FCH	Sid I		O	Åre 4.2
	15	52.6	3.3	44.1	FCH	Fe-Dolomite		O	Åre 4.1
	16	57.7	15.8	26.5	FCH	Ankerite		O	Åre 4.1
	17	12.7	64.6	22.7	FCH	Sid II	Mg-rich	O	Åre 4.1
	18	9.9	65.8	24.3	FCH	Sid II	Mg-rich	O	Åre 4.1
	19	4.2	94.1	1.7	FCH	Sid I		O	Åre 4.1
Well 10 3571m									
	20	53.6	16.5	29.9	FCH	Ankerite		O	Åre 4.1
	21	56.9	15.8	27.3	FCH	Ankerite		O	Åre 4.1
	22	54.0	15.1	30.9	FCH	Ankerite		O	Åre 4.1
	23	3.4	93.8	2.9	FCH	Sid I		O	Åre 4.1
	24	6.9	63.7	29.4	FCH	Sid II	Mg-rich	O	Åre 4.1
Well 10 3541m									
	1	56.2	22.3	21.1	FCH	Ankerite		O	Åre 4.2
	2	52.0	19.4	28.1	FCH	Ankerite		O	Åre 4.2
	3	3.8	75.4	20.0	FCH	Sid II	Mg-rich	O	Åre 4.2
	4	5.1	71.2	23.1	FCH	Sid II	Mg-rich	O	Åre 4.2
	5	57.3	23.4	18.6	FCH	Ankerite		O	Åre 4.2
	6	11.1	62.9	25.4	FCH	Sid II	Mg-rich	O	Åre 4.2
	7	56.7	22.6	20.2	FCH	Ankerite		O	Åre 4.2
	8	10.4	64.6	24.4	FCH	Sid II	Mg-rich	O	Åre 4.2
	9	6.3	62.2	30.9	FCH	Sid II	Mg-rich	O	Åre 4.2
	10	5.4	62.4	31.6	FCH	Sid II	Mg-rich	O	Åre 4.2
	11	11.0	63.0	27.0	FCH	Sid II	Mg-rich	O	Åre 4.2
	12	59.0	16.0	25.0	FCH	Ankerite		O	Åre 4.2
	13	55.0	21.0	24.0	FCH	Ankerite		O	Åre 4.2
Well 10 3556m									
	25	1.5	97.7	0.8	SBF	Sid I		O	Åre 4.1
Well 5 20aug2008									
	5.1.1	2.0	96.8	1.2	FF	Sid I		W	Åre 2.1

to be continued on next page

Table 24 continued

Well and date	Sample nr.	Ca	Fe+Mn	Mg	Facies	Cement	Note	Saturation	Zonation
	5.1.2	1.1	98.5	0.4	FF	Sid I		W	Åre 2.1
	5.1.3	1.6	97.9	0.4	FF	Sid I		W	Åre 2.1
	5.1.4	1.1	98.8	0.1	FF	Sid I		W	Åre 2.1
	5.1.5	1.4	97.6	1.0	FF	Sid I		W	Åre 2.1
	5.1.6	1.4	97.6	1.0	FF	Sid I		W	Åre 2.1
	5.1.7	95.6	3.9	0.5	FF	Calcite		W	Åre 2.1
	5.1.8	11.9	65.7	22.4	FF	Sid II	Mg-rich	W	Åre 2.1
	5.1.9	95.8	3.3	0.9	FF	Calcite		W	Åre 2.1
	5.1.10	3.2	96.1	0.7	FF	Sid I		W	Åre 2.1
	5.1.11	66.6	15.5	18.0	FF	Ankerite		W	Åre 2.1
	5.1.12	97.4	1.4	1.2	FF	Calcite		W	Åre 2.1
	5.1.13	1.2	98.3	0.5	FF	Sid I		W	Åre 2.1
	5.2.1	2.3	96.4	1.3	FF	Sid I		W	Åre 2.1
	5.2.2	98.5	1.2	0.3	FF	Calcite		W	Åre 2.1
	5.2.3	59.6	18.3	22.1	FF	Ankerite		W	Åre 2.1
	5.2.4	98.2	1.3	0.4	FF	Calcite		W	Åre 2.1
	5.2.5	56.9	15.3	27.8	FF	Ankerite		W	Åre 2.1
	5.2.6	67.8	32.2	0.0	FF	Calcite	Fe-rich	W	Åre 2.1
	5.2.7	1.4	98.3	0.4	FF	Sid I		W	Åre 2.1
	5.2.8	1.2	98.5	0.3	FF	Sid I		W	Åre 2.1
	5.2.9	2.7	95.0	2.3	FF	Sid I		W	Åre 2.1
	5.2.10	1.5	97.7	0.8	FF	Sid I		W	Åre 2.1
	5.3.1	95.5	3.1	1.4	FF	Calcite		W	Åre 2.1
	5.3.2	97.7	2.0	0.3	FF	Calcite		W	Åre 2.1
	5.3.3	59.8	17.5	22.7	FF	Ankerite		W	Åre 2.1
	5.3.4	3.2	96.1	0.7	FF	Sid I		W	Åre 2.1
	5.3.5	88.8	10.7	0.6	FF	Calcite		W	Åre 2.1
	5.3.6	93.5	5.5	1.0	FF	Calcite		W	Åre 2.1
	5.3.7	1.7	97.8	0.3	FF	Sid I		W	Åre 2.1
	9.1.1	4.9	95.0	0.1	MBF	Sid I		W	Åre 3.3
	9.1.2	4.9	94.8	0.4	MBF	Sid I		W	Åre 3.3
	9.1.3	3.5	95.3	1.2	MBF	Sid I		W	Åre 3.3
	9.1.4	2.0	97.9	0.1	MBF	Sid I		W	Åre 3.3
	9.1.5	3.8	95.3	0.8	MBF	Sid I		W	Åre 3.3
	9.1.6	4.8	94.3	0.9	MBF	Sid I		W	Åre 3.3
Well 5 28aug2008									
	12.1.1	6.5	93.0	0.5	SBF	Sid I		W	Åre 4.2
	12.1.2	1.3	98.6	0.2	SBF	Sid I		W	Åre 4.2
	12.1.3	4.0	95.6	0.4	SBF	Sid I		W	Åre 4.2
	12.1.4	5.5	94.2	0.3	SBF	Sid I		W	Åre 4.2
	12.1.5	53.4	42.6	4.0	SBF	Ankerite		W	Åre 4.2
	12.1.6	4.0	95.4	0.5	SBF	Sid I		W	Åre 4.2
	12.1.7	8.7	88.8	2.5	SBF	Sid I		W	Åre 4.2
	12.1.8	96.7	2.5	0.9	SBF	Calcite		W	Åre 4.2
	12.1.10	6.3	92.2	1.4	SBF	Sid I		W	Åre 4.2
	12.2.1	6.8	91.6	1.6	SBF	Sid I		W	Åre 4.2
	12.2.2	6.7	91.3	2.0	SBF	Sid I		W	Åre 4.2
	12.2.3	97.2	2.7	0.1	SBF	Calcite		W	Åre 4.2
	12.2.4	3.0	96.7	0.3	SBF	Sid I		W	Åre 4.2
	12.2.5	96.6	3.1	0.3	SBF	Calcite		W	Åre 4.2
	12.2.6	94.6	4.1	1.3	SBF	Calcite		W	Åre 4.2

to be continued on next page

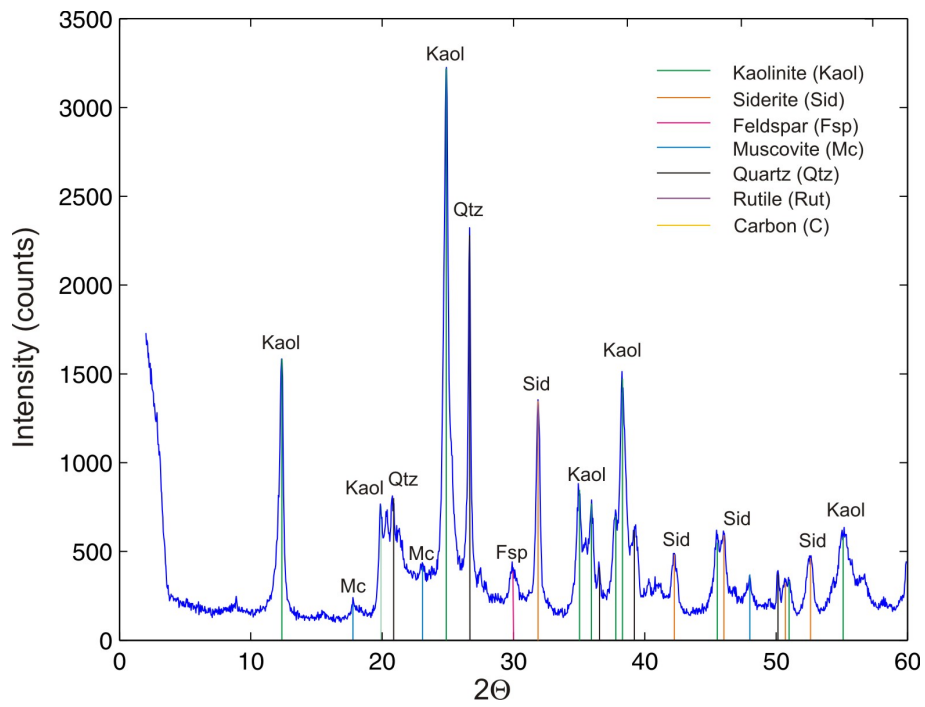
Table 24 continued

Well and date	Sample nr.	Ca	Fe+Mn	Mg	Facies	Cement	Note	Saturation	Zonation
	12.2.7	94.2	5.1	0.8	SBF	Calcite		W	Åre 4.2
	12.3.1	5.5	92.7	1.8	SBF	Sid I		W	Åre 4.2
	12.3.2	51.9	31.1	17.0	SBF	Ankerite		W	Åre 4.2
	12.3.3	1.2	88.1	10.8	SBF	Sid II		W	Åre 4.2
	12.3.4	94.6	4.8	0.6	SBF	Calcite		W	Åre 4.2
	13.1.1	1.9	97.7	0.4	SBF	Sid I		W	Åre 4.2
	13.1.2	0.8	99.2	0.0	SBF	Sid I		W	Åre 4.2
	13.1.3	5.0	94.9	0.2	SBF	Sid I		W	Åre 4.2
	13.1.4	1.3	98.2	0.5	SBF	Sid I		W	Åre 4.2
	13.2.2	4.2	95.5	0.3	SBF	Sid I		W	Åre 4.2
	13.2.3	2.4	97.5	0.1	SBF	Sid I		W	Åre 4.2
	13.2.4	3.3	95.9	0.8	SBF	Sid I		W	Åre 4.2
	2765,78.1.1	1.4	98.3	0.3	FCH	Sid I		W	Åre 2.1
	2765,78.1.2	1.9	97.6	0.5	FCH	Sid I		W	Åre 2.1
	2765,78.1.3	1.4	98.0	0.6	FCH	Sid I		W	Åre 2.1
	2765,78.1.4	1.1	98.7	0.2	FCH	Sid I		W	Åre 2.1
	2765,78.1.5	2.3	96.3	1.4	FCH	Sid I		W	Åre 2.1
	2765,78.2.1	0.3	99.4	0.3	FCH	Sid I		W	Åre 2.1
	2765,78.2.2	1.1	98.2	0.8	FCH	Sid I		W	Åre 2.1
	2765,78.2.3	0.6	98.8	0.6	FCH	Sid I		W	Åre 2.1
	2791,30B.1	0.6	99.2	0.1	FCH	Sid I		W	Åre 2.1
	2791,30B.2	0.8	99.1	0.1	FCH	Sid I		W	Åre 2.1
	2791,30B.3	4.0	83.3	12.6	FCH	Sid II		W	Åre 2.1
	2791,30B.4	4.0	83.7	12.4	FCH	Sid II		W	Åre 2.1
	2791,30B.5	1.0	98.6	0.3	FCH	Sid I		W	Åre 2.1
	2791,30B.6	1.1	98.8	0.1	FCH	Sid I		W	Åre 2.1
	2791,30B.7	2.9	85.2	11.9	FCH	Sid II		W	Åre 2.1

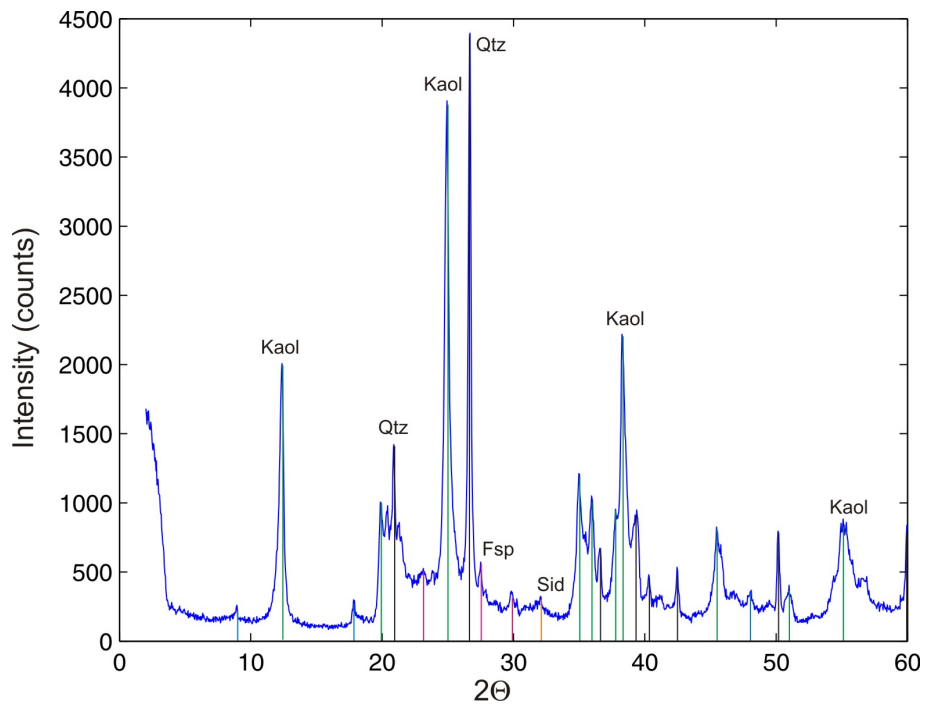
End of table

X-ray Diffraction (XRD)

Nineteen samples from wells 5 and 10 have been subject to XRD analysis on a Phillips PW XRD to identify mineralogical composition and to investigate clay types. Eleven crushed bulk analysis were done in addition to eight separated clay-size particle fraction ($<2\mu\text{m}$) analysis following the procedure of Gibbs et al. (1971). Examples of mp and wr analysis of selected samples are presented in Fig. 25.

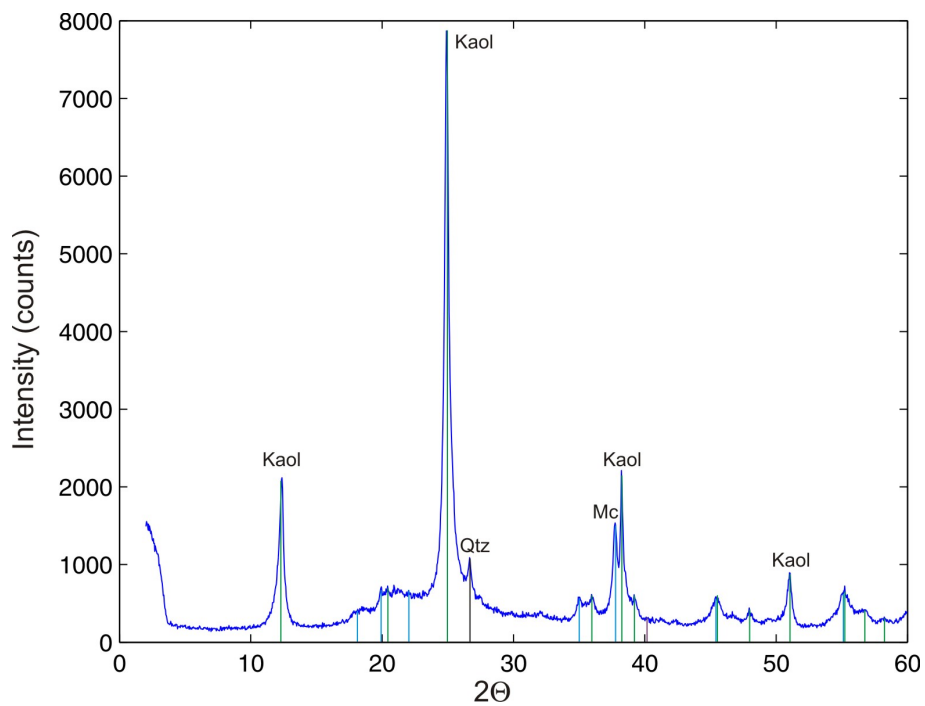


(a) Well 10 3566,37m MBF, 270049wr

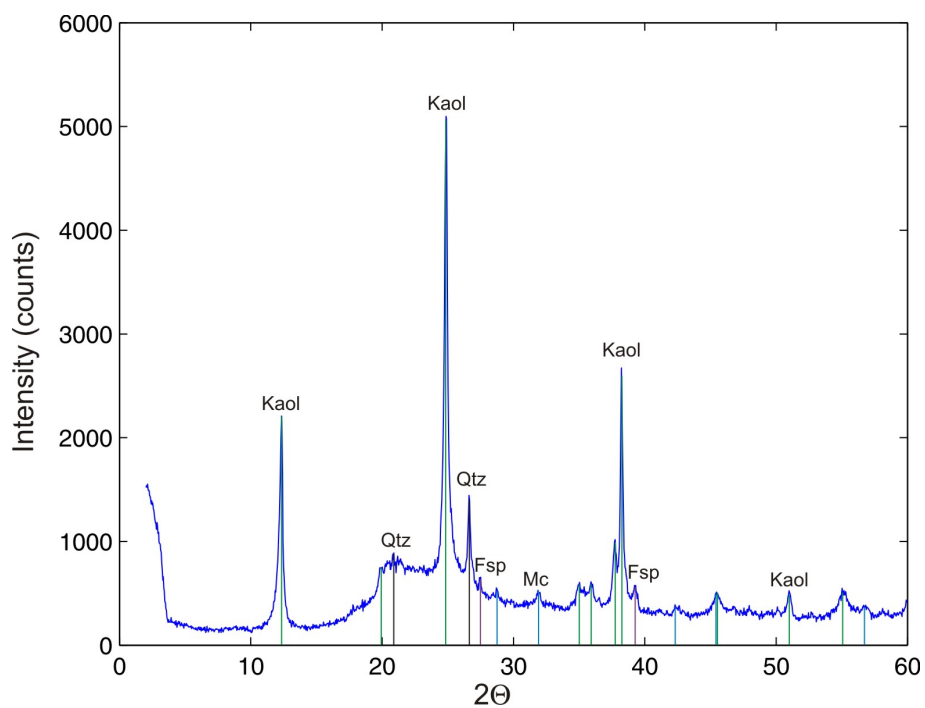


(b) Well 10 3582,84m FF, 270046wr

Figure 25: XRD Diffractograms. wr = whole rock, mp = millipore.

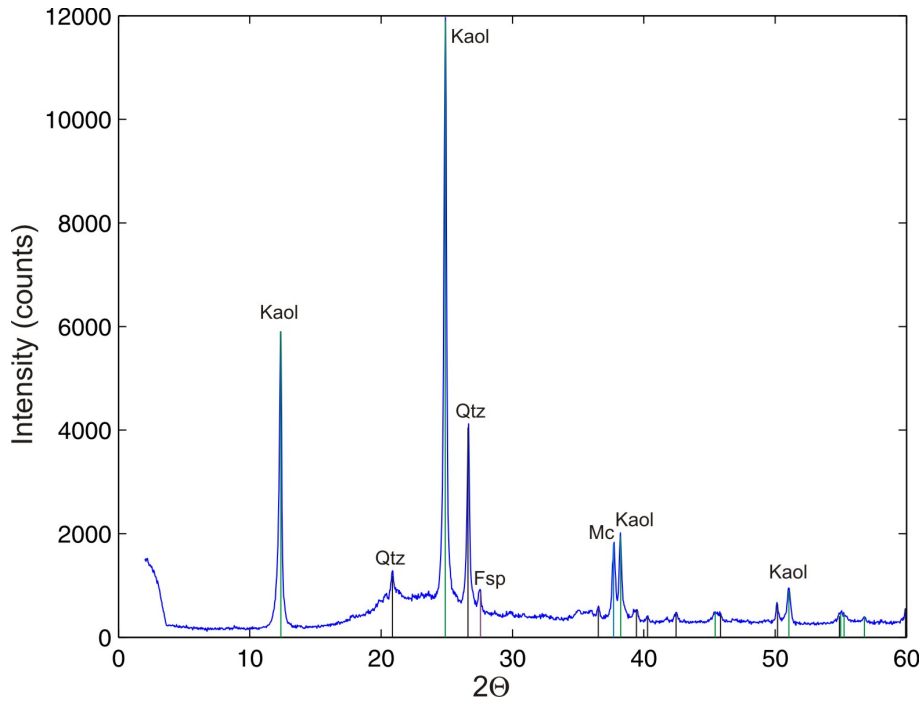


(c) Well 5 2778,62m FCH, 270601mp

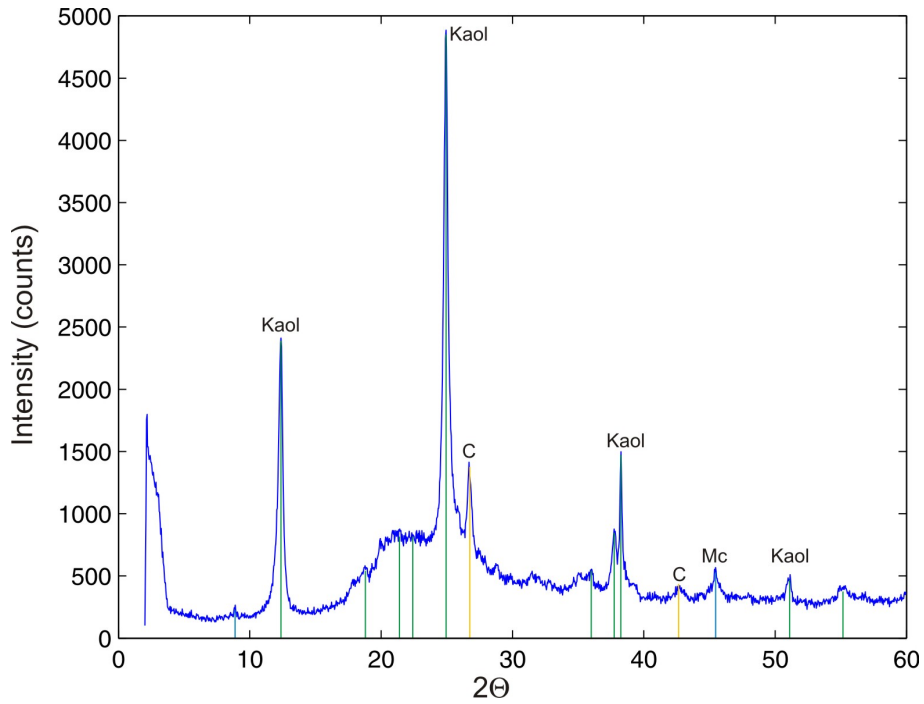


(d) Well 5 2730,44m CCH, 270603mp

Figure 25: continued

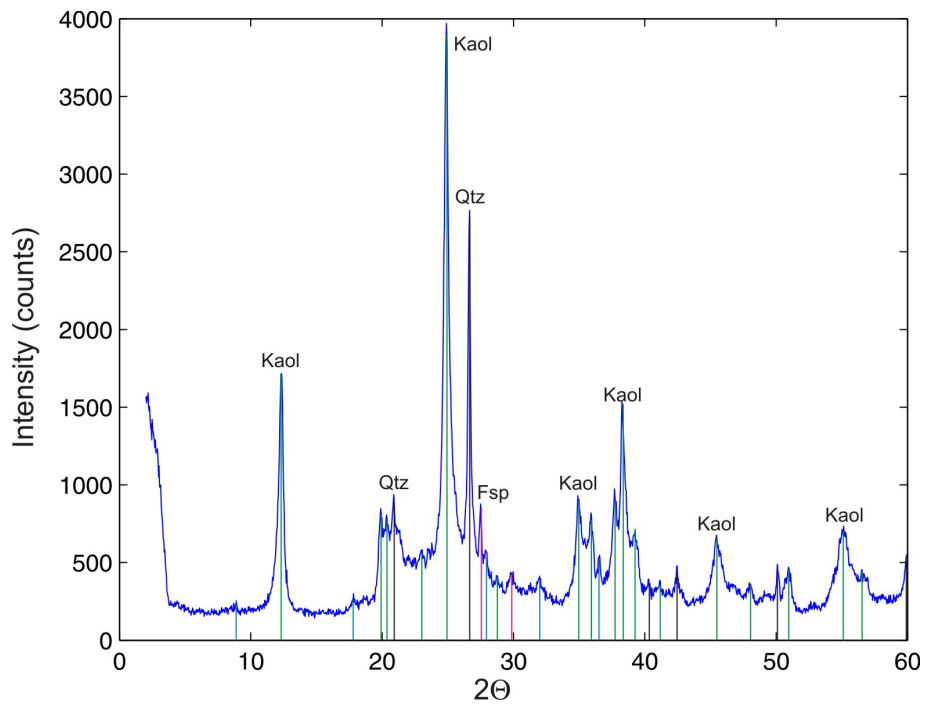


(e) Well 5 2671,78Am SBF, 270607mp



(f) Well 5 2696,20m MBF, 280109mp

Figure 25: continued



(g) Well 5 2696,20m MBF, 280109wr

Figure 25: continued

Petrophysical wireline logs

The main data in this study came from wireline data from fourteen wells covering the central parts of the Heidrun Field. These data has been made available by the courtesy of Statoil and partners for this study and include standard measured parameters (Table 6). Landmarks OpenWorks and Stratworks software is used for wireline log signature investigation and correlation exercises.

In addition to the various petrophysical data used, various depth types are also used for different purposes (See Table 7). These data form the basis for the correlation performed in this thesis.

Table 6: Well Logs and measured properties

Petrophysical Log	Property measured	Units
Density (RHOB)	Bulk density (electron density)	g/cm ³
Neutron (NPHI)	Hydrogen density	Per cent porosity
Gamma ray (GR)	Natural radioactivity (K, Th, U)	API
Resistivity (RT)	Resistivity to electric current	ohm.m
Sonic (DT)	Two-way travel time (twt), V_p	μ s/ft
Permeability (KLOGH)	KLOGH is calculated from the density log (RHOB) ^a	mD

^abased on Chillingar's equation (Chillingar, 1964)

Table 7: Well depth and thickness definitions

Abbreviation	Name	Definition
TVDMSL	True Vertical Depth	Vertical depth, calculated from the well trajectory logs, relative to a "geographical" reference, generally mean sea level (MSL) (TVDSS, for sub-sea)
TVDT	TVD Thickness	Bed thickness calculated by subtracting the TVDMSL values of the bed top and bottom (note that this thickness is far from being "true") ^a
TVT	True Vertical Thickness	Vertical thickness, measured vertically through the wellbore entry point
TST	True Stratigraphic Thickness	Thickness calculated perpendicular to the bed. The TST is the closest to the "geological" thickness
MD	Drilled Thickness	Bed length measured along the well

^aTVDMSL = TST for horizontal layers